# CHAPTER 3
# TRANSPORT OF GRAVEL AND SEDIMENT MIXTURES

## 3.1 FLUVIAL PHENOMENA ASSOCIATED WITH SEDIMENT MIXTURES

When ASCE Manual No. 54, "Sedimentation Engineering," was first published in 1975, the subject of the transport and sorting of heterogeneous sediments with wide grain size distributions was still in its infancy. This was particularly true in the case of bed-load transport. The method of Einstein (1950) was one of the few available at the time capable of computing the entire grain size distribution of particles in bed-load transport, but this capability had not been extensively tested against either laboratory or field data. Since that time there has been a flowering of research on the subject of the selective (or non-selective) transport of sediment mixtures. A brief attempt to summarize this research in a useful form is provided here.

A river supplied with a wide range of grain sizes has the opportunity to sort them. While the grain size distribution found on the bed of rivers is never uniform, the range of sizes tends to be particularly broad in the case of rivers with beds consisting of a mixture of gravel and sand. These streams are termed "gravel-bed streams" if the mean or median size of the bed material is in the gravel range; otherwise they are termed "sand-bed streams." The river can sort its gravel and sand in the streamwise, lateral and vertical directions, giving rise in each case to a characteristic morphology. Summaries of these morphologies are given in Whiting (1996) and Powell (1998); Parker (1992) provides a mechanistic basis for their study.

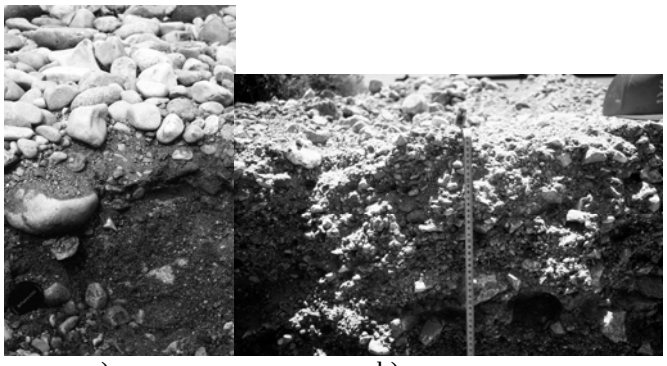

a) b)

Figure 3.1 Contrasts in surface armoring between a) the River Wharfe, UK, a perennial stream with a low sediment supply (left) and b) the Nahal Yatir, Israel, an ephemeral stream with a high rate of sediment supply (right). From Powell (1998).

Sorting phenomena range from very small scale to very large scale. In many gravel-bed rivers the bed is vertically stratified, with a coarse armor layer on the surface. This coarse layer acts to limit the supply of fine material from the subsurface to the bed-load at high flow. Some gravel-bed streams, however, show no stratification in the vertical. An example of each type is shown in Figure 3.1. The difference between the two is that the image on the left pertains to a perennial stream with low sediment supply and moderate floods, whereas the image on the right pertains to an ephemeral stream with a high sediment supply and violent floods.

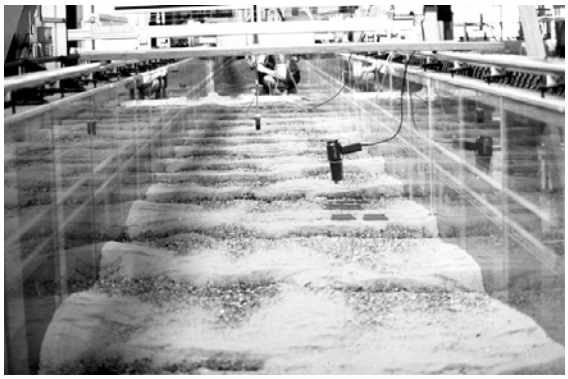

Figure 3.2 Sediment sorting in the presence of a dune field. Flow was from top to bottom. Image courtesy A. Blom.

If the flow is of sufficient strength bedforms such as dunes can form in gravel-bed streams (e.g. Dinehart, 1992). Dunes are the most common bedform in sand-bed streams. Depending on the strength of the flow the parent grain size distribution can interact with the bedforms to induce strong vertical and streamwise sorting, with coarser material accumulating preferentially in dune troughs. This is illustrated in Figure 3.2. Note that the transition from lower-regime plane bed to dunes, which is illustrated in Figure 2.19 thus engenders a reversal of vertical sorting, with a coarse layer at the top of the bed in the former case and near the base of the dunes in the latter case.

Under conditions of weak transport the dunes devolve into bed-load sheets, which are rhythmic waves expressing downstream variation predominantly in terms of alternating zones of fine and coarse sediment rather than elevation variation (Figure 3.3). Both dunes and bed-load sheets result in a bed-load transport that strongly pulsates in terms of both total rate and characteristic grain size.

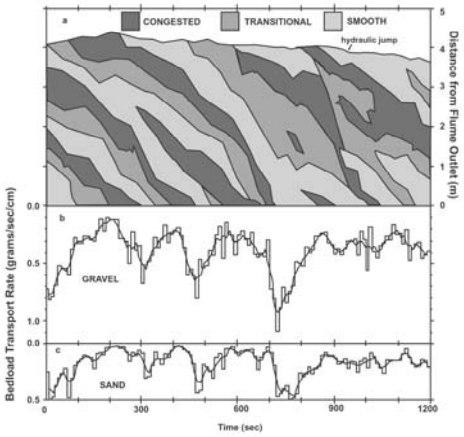


Figure 3.3 Pulsations associated with experimental bedload sheets composed of a mixture of sand and gravel. a) Alternating arrangement of three bed states. b) Fluctuation in gravel transport rate. c) Fluctuation in sand transport rate. From Iseya and Ikeda (1987).

When bars and bends form in rivers they interact with the sediment to produce sorting morphologies at larger scale. Figure 3.4 shows a mildly sinuous reach of the Ooi River, Japan. It is readily apparent that bar heads tend to be coarser, whereas bar tails tend to be finer. Similar patterns can be observed in the bars of braided streams.

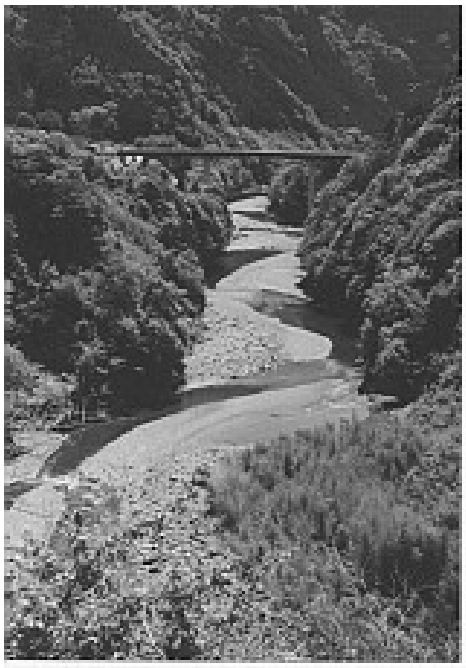

Figure 3.4 View of the Ooi River, Japan, showing sorting of gravel and sand on bars. From Ikeda (2001).

At sufficiently steep slopes bars give way to pool-riffle sequences, which are bar-like undulations in bed elevation and grain size that are for the most part expressed in the streamwise rather than the lateral direction. As opposed to dunes and some bars, pool-riffle patterns usually show little tendency to migrate downstream. At even steeper slopes, which support flow that is supercritical in the Froude sense during floods, the bed devolves into a well-defined step-pool pattern. Each step is defined by what might be described as a boulder jam, as seen in Figure 3.5; the pools between steps contain much finer material.

A lake or reservoir interrupts the downstream transport of sediment. As a result, the river bed often aggrades upstream of the dam and degrades downstream. Figure 3.6 shows the aggradational deposit upstream of a sediment retention dam on the North Fork Toutle River, Washington, USA. Over the 10 km upstream of the dam, characteristic bed sediment size shows a pronounced pattern of downstream fining, declining from about 7.4 mm to 0.4 mm. This downstream fining appears to be abetted by the tendency of the bed to devolve into local patches or lanes of finer and coarser sediment. Figure 3.7 illustrates two such patches on the North Fork Toutle River. An extreme limiting case of such local segregation is the formation of roughness "streaks," "stripes" or "ribbons," which consist of vertical lanes of alternating coarse and fine material, with a high transport rate of the latter relative to the former. These streaks are shown in Figure 3.8.

Figure 3.5 Step-pool topography in the Hiyamizu River, Japan. Image courtesy K. Hasegawa

Downstream of a dam, on the other hand, the bed often both degrades and coarsens in response to the cutoff of sediment, eventually forming a static or nearly static armor which inhibits further bed erosion. An image of the static armor downstream of the Lewiston Dam on the Trinity River, California, USA is shown in Figure 3.9. The static armor is partially covered by mobile, pea-sized gravel from a tributary entering downstream of the dam.

Sorting appears at the largest scale in terms of the tendency for characteristic grain size to become finer over 10's or 100's of km. This large-scale downstream fining

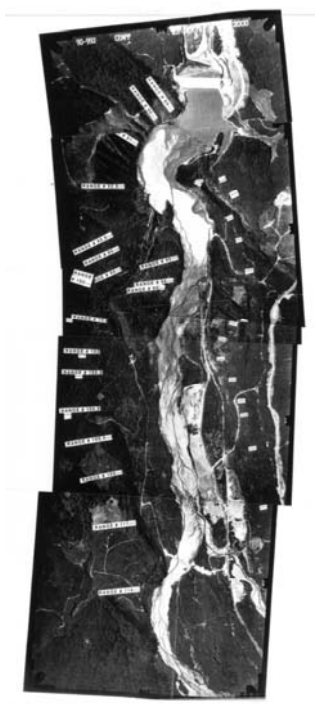

Figure 3.6 View of sedimentation upstream of a sediment retention dam on the North Fork Toutle River, Washington, USA. Flow is from bottom to top. From Seal and Paola (1995).

a) b)

Figure 3.7 Sorted sediment patches on the North Fork Toutle River, Washington, USA: a) coarse patch on fine sediment; b) fine patch on coarse sediment. From Paola and Seal (1995).

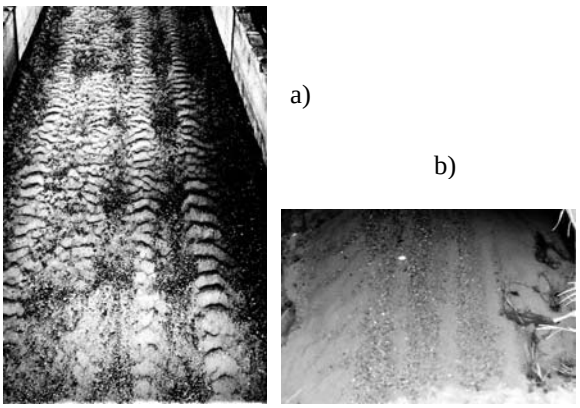

a)

b)

Figure 3.8 Streaks of sorted sediment in a) a laboratory flume (from Günter, 1971; courtesy A. Müller), and b) a river (image courtesy T. Tsujimoto).

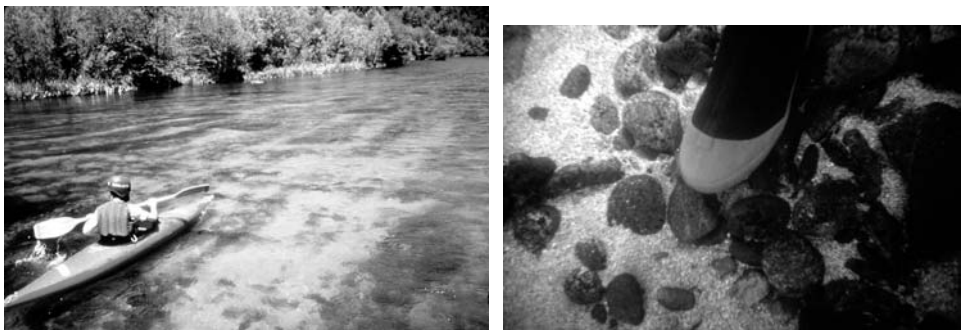

a) b)

Figure 3.9 Coarse static armor (dark grains) with a partial coverage of finer, mobile sediment (light grains) on the bed of the Trinity River, California, USA. The coarse grains are rendered immobile by the presence of the Lewiston Dam upstream. Image courtesy A. Bartha. a) View of the river. b) Closeup of the bed.

is typically associated with a long profile of the river that is concave upward. A famous example, that of the Kinu River, Japan is shown in Figure 3.10. This river not only displays downstream fining, but also a relatively abrupt transition from gravel-bed to sand-bed. Downstream fining is observed strongly along the gravel-bed reach, and rather more weakly along the sand-bed reach.

Abrupt gravel-sand transitions are quite common in the field, and are associated with the tendency for grain sizes in the range of pea gravel to be relatively scarce in

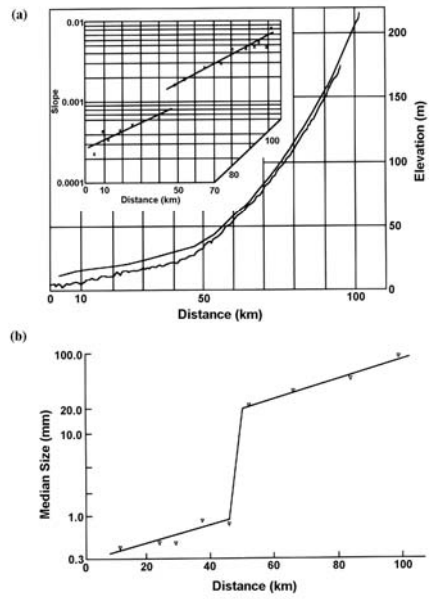


Figure 3.10 a) Long profile and b) downstream change in grain size of the Kinu River, Japan, illustrating downstream fining and a gravel-sand transition. Redrafted from an original in Yatsu (1955).

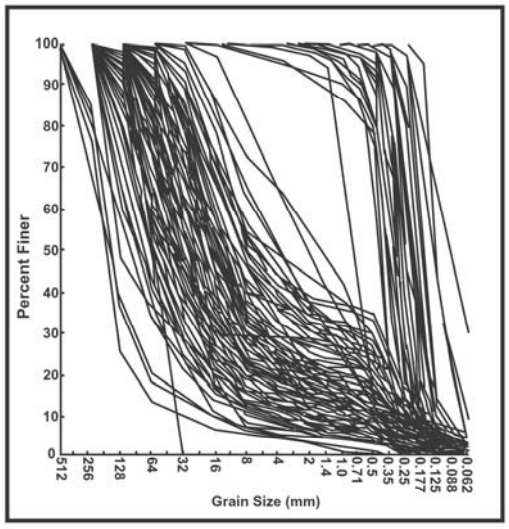


Figure 3.11 Grain size distribution of 174 samples of bed sediment from rivers in Alberta, Canada. From Shaw and Kellerhals (1982).

rivers. This tendency is common but by no means universal. An example of this tendency is shown in Figure 3.11, which shows the bed material grain size distributions of 174 river reaches in Alberta, Canada (Shaw and Kellerhals, 1982). Note that the sand-bed streams (median size in the sand range) contain very little gravel. The gravel-bed streams (median size in the gravel range) often contain a substantial amount of sand, but very little material between 1 and 8 mm.

Transient sorting can be induced by a pulse of sediment introduced into a river from a debris flow or landslide. An example illustrating a landslide that flowed into and blocked the Navarro River, California, USA is shown in Figure 3.12. Such inflows often contain copious amounts of material that is much finer than the ambient bed material. They can also contain some material that is much coarser than the ambient bed material. Grain size sorting plays a key role in the process by which rivers "digest" such sediment inputs.

Figure 3.12 View of a landslide that blocked the Navarro River, California., USA in 1995. Image courtesy T. Lisle.

Most sediment sorting in rivers is accomplished by the differential transport of different sizes. In the case of heavy minerals (placers) however, increased specific gravity replaces the role of increased size. The issue is of some interest in

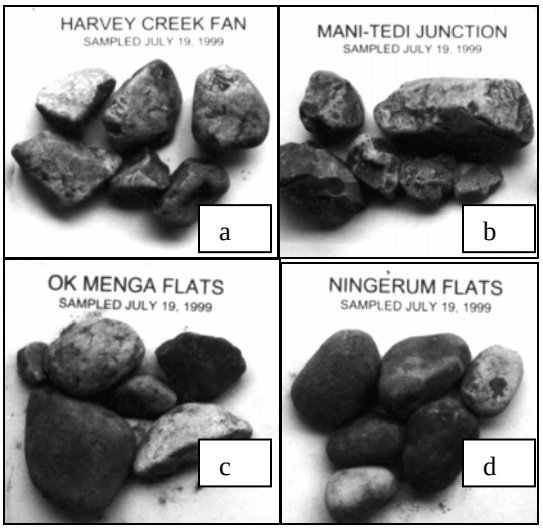


Figure 3.13 Four sediment samples from the Ok Tedi River system, Papua New Guinea.
a) 1 km downstream of the Southern Dumps of the Ok Tedi Mine, and after having passed over a high waterfall, in the Harvey Creek debris flow fan as it enters the Ok Mani;
b) 8 km downstream, at the fluvial fan of the Ok Mani where it enters the Ok Tedi;
c) 27 km downstream on the Ok Tedi near the junction with the Ok Menga; and
d) 90 km downstream on the Ok Tedi at Ningerum Flats.
Note that the grains become progressively rounder as the distance from the source increases.

regard to the extraction of placer gold from rivers. It may appear to be intuitively obvious that finer grains are more mobile than coarser grains of the same specific density. This is usually but not always the case.

In addition to selective transport, however, rivers have the opportunity to create finer grains from coarser grains. This is sometimes accomplished by shattering of grains, but is more commonly associated with a gradual abrasion and rounding of stones, yielding silt and some sand as a result. Abrasion can thus be a contributor to downstream fining. Figure 3.13 illustrates the effect of abrasion in gradually rounding grains downstream from their source.

The main focus of this chapter is on transport of mixed sizes and concomitant sorting in bed-load-dominated rivers. In the field, this usually means gravel-bed rivers. Some (typically small) sand-bed streams, such as Muddy Creek (Dietrich and Whiting, 1999) also satisfy this criterion. Near the end of the chapter, however, suspension-dominated rivers, i.e. most sand-bed streams, are considered as well.

Figure 3.14 Evidence of channel degradation on the Mad River, California under the Highway 101 bridge.

## 3.2 ENGINEERING RELEVANCE

Various aspects of grain sorting are of relevance to river engineering design, habitat maintenance and restoration of river ecosystems. First and foremost among these is gravel extraction, or mining from rivers for concrete aggregate and other construction purposes. The word "gravel" is used loosely in regard to gravel mining, and includes sand as well. The mining of fluvial gravels is particularly common in the western part of the United States. Gravel mining without appropriate constraints can lead to severe bed degradation downstream, with the resulting failure of bridges, exposure of buried pipelines etc. (Galay, 1983). The Mad River, California, USA has been heavily utilized for gravel

extraction. The effect on bed elevation at the bridge piers where Highway 101 crosses the river is readily apparent in Figure 3.14. Gravel extraction was taking place on the day the photo was taken. Engineering models of the erosion, transport and deposition of heterogeneous gravels have an important role to play in determining how much gravel can be safely extracted without adverse effects.

A common practice in many western rivers is "bar scalping," by which high-quality material is locally stripped from the surface of bars. This is done on the supposition that the river will eventually replace the mined gravel with material of similar competence. Anadromous fish such as salmon, however, are rather particular about the gravels in which they choose to build redds (egg nests) (Reiser, 1998). If the bed material is too coarse the fish cannot excavate a redd. If the bed is too fine, and in particular if it contains too much sand and silt, the fish will avoid it, instinctively knowing that the eggs will be suffocated and poisoned by inability for groundwater flow to carry away excreta. The Ooi river of Figure 3.4 might be a good candidate for bar scalping in the United States, but in Japan gravel extraction from most rivers has been banned in order to control bed degradation. This degradation is not only a product of gravel mining in previous times, but also due to the fact that intensive sediment control works (e.g. sabou dams) in the upstream reaches of Japanese rivers have dramatically reduced the sediment supply.

Spawning grounds can also be damaged or destroyed by the activities of agriculture or forestry. Road building due to forest harvesting in particular can, if not done appropriately, cause massive inputs of sand and finer material to a stream that is intrinsically gravel-bed. This finer material is usually transient, being washed downstream by successive floods. If the bed happens to be buried in "fines," however, just before spawning, fish recruitment can drop drastically (e.g. Reiser, 1998).

The installation of a dam on a river typically blocks the downstream delivery of all but the finest sediment, creating a pattern of bed aggradation upstream. The dam raises base level, i.e. the downstream water surface elevation to which the river upstream must adjust, forcing upstream-migrating deposition. This deposition is most intense near the delta at the upstream end of the reservoir. As a result, the effect is to intensify the upward concavity of the long profile of the bed upstream of the dam. The more sharply declining bed slope intensifies selective transport of fine material, setting up strong local downstream fining. This is what has taken place in the reservoir of the North Fork Toutle River, Washington, USA illustrated in Figure 3.6.

This downstream fining has a beneficial effect in terms of engineering that should be taken into consideration when designing dams. The aggradation induced by dams can require the leveeing of towns upstream of the dam. Sorting, however, tends to concentrate the aggradation toward the downstream end of the reach in question. Indeed, Leopold et al. (1964) have observed that the upstream aggradation driven by a dam never extends infinitely far upstream, no matter how much time has passed. Part of the reason for this is the tendency for the main stem and tributaries farther upstream in the drainage basin to absorb the effect of the dam. This is because sediment sizes which deposit in the

backwater zone of the dam can be carried without deposition by steeper main stem and tributaries upstream.

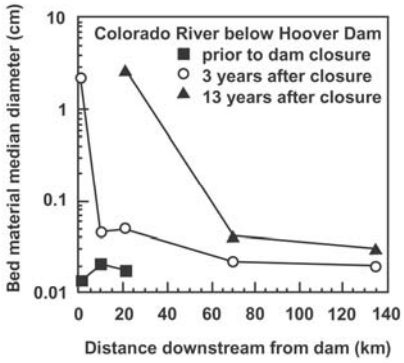


Figure 3.15 Bed surface median grain size downstream of Hoover Dam on the Colorado River before and after closure. From Williams and Wolman (1984).

An extreme case of this tendency for sorting to damp upstream effects is often seen on gravel-bed streams, many of which carry loads of sand that are far in excess of the corresponding loads of gravel, yet the bed surface consists for the most part of gravel, with sand partially or completely filling the interstices. In analogy to the mud washload of sand-bed rivers, this sand load on a gravel-bed stream is called "throughput load" if it interacts only passively with the bed, i.e. simply filling the pores of a gravel deposit. Sand can be carried as throughput load over a gravel bed when the rate of sand input necessary to drown the bed in sand is higher than the prevailing sand input. In gravel-bed rivers, the disparity between the two becomes increasingly large with increasing bed slope. The threshold for major sand deposition is crossed as bed slope declines. As a result, the sandy deposit caused by a dam migrates upstream only so far as the stream becomes sufficiently steep to prevent it from covering the bed completely.

The dam in Figure 3.6 was installed as a debris control measure in the wake of the Mount St. Helens eruption in 1980. Such dams play an important role in disaster mitigation. At the time of Figure 3.6 the dam was nearly full. Understanding the process of filling requires an understanding of the transport of sediment mixtures.

The cutoff of sediment at a dam often induces bed degradation, as the river mines itself to replace the lost load. Bed degradation rarely continues unabated. Even small amounts of coarse, erosion resistant material in the substrate tend to concentrate on the bed surface as the bed degrades, eventually limiting the process through the formation of a static armor. An example of the time evolution of bed armoring is given in Figure 3.15 (Williams and Wolman, 1984) for the Colorado River downstream of Hoover Dam.

It would be a mistake, however, to believe that the installation of a dam universally causes bed degradation downstream. As illustrated in Figure 2.26, bank-full flows in gravel-bed rivers often correspond to conditions that are not greatly higher than that needed to mobilize the gravel. When dams are operated for flood control, so as to cut off the flood peaks needed to mobilize the gravel, the river can lose most of the capacity to move gravel. As a result, downstream of the first tributary the river bed aggrades, as the sediment from the tributaries reaches a main stem that is no longer competent to transport it. This process has been documented in e.g. the Peace River, Canada, downstream of the W. A. C. Bennett Dam (Kellerhals and Gill, 1973).

The Trinity River, California, USA downstream of the Lewiston Dam provides a type example of the downstream effects of a dam (Kondolf and Wilcock, 1996). This dam not only cuts off the sediment, but also maintains a constant flow that is well below bank-full flow. From the dam to the first major tributary downstream not only is the gravel not replenished, but the lack of flows necessary to mobilize it have allowed the interstices of the gravel to become filled with debris that is not cleaned out by floods (Figure 3.9). This lack of renewal not only degrades the gravel bars as spawning habitat, but leads to a general decline in the ecological productivity of the system. The first tributary brings in a substantial quantity of corn-sized grains of weathered granite that partially fill the pores of the gravel and further degrade habitat. The loss of flood flows has also caused channel narrowing associated with the encroachment of alders as well as humans, the latter being lulled by the lack of flood flows. The renewal of such a stream requires at the least controlled flood releases from the dam. How much, and how long must be determined at least partially in terms of the mobility of the various sizes of sediment in the bed (Wilcock et al, 1996).

Dam removal has become quite popular in recent years, the main motivating factor being habitat improvement and stream restoration. A lack of understanding of the transport mechanics of heterogeneous sediments has often led to the complete excavation of the deposit behind the dam, even when the sediment is uncontaminated. This lack of understanding is a relative one; the techniques necessary to evaluate the fate of both coarse and fine sediments released from a dam, and thus whether or not removal is necessary, are available, but have not usually been put into practice. Fortunately, however, a description of one version of the technology is provided as an Appendix to this manual (Cui and Wilcox, this volume, Appendix A). Developments in the area of river restoration can be found in Hay (1998) and Hotchkiss and Glade (2000).

a) b) c)

Figure 3.16 a) View of waste rock dump site at the Ok Tedi Mine, Papua New Guinea. b) View of the gravel-bed Ok Tedi downstream of the mine. The channel bed has aggraded and widened in response to disposal of mine sediment. c) View of the sand-bed Fly River downstream of its confluence with the Ok Tedi. Aggradation of bed sediment has exacerbated both flooding and the overbank deposition of fine sediment, resulting in the loss of riparian forest.

The disposal of mine waste into a river can lead to massive bed aggradation. This aggradation is almost invariably associated with a pattern of downstream fining. The Ok

Tedi copper/gold mine in Papua New Guinea is a case in point (Parker et al., 1996; Dietrich et al., 1999). Throughout much of the latter 1990s' the mine disposed some 40 Mt/year of waste rock and 30 Mt/year of tailings into a river system characterized by a steep gravel-bed reach with a fairly sharp transition to a sand-bed reach (Figure 3.16). The extreme overloading of the system has caused massive channel and floodplain deposition, as well as a major modification in the pattern of downstream fining. Input sizes range from boulders to silt. The coarse material contains several mineral types, some of which are highly subject to abrasion. The effect of wear on the coarser grains is illustrated in Figure 3.13; the degree of overloading makes it highly likely that all grains in the image originated from the mine. Any numerical model designed to track the fate of the sediment, the evolution of the river profile and the design of countermeasures must account for downstream fining, abrasion of several rock types and overbank deposition of finer material. Cui and Parker (1999) describe such a model. Part of the model was adapted for studying the effects of dam removal (Cui and Wilcox, this volume, Appendix A).

The above examples represent a subset of the engineering problems requiring a description of the selective transport of heterogeneous sediments. Other examples include woody debris in rivers, flow augmentation by diversion, the effect of extreme floods, the fate of contaminated sediments from mines and industrial sites, avulsion on alluvial fans and the competence of riprap placed on or in an alluvial bed to resist scour.

## 3.3 GRAIN SIZE DISTRIBUTIONS

### 3.3.1 Definitions and Continuous Formulation

The sedimentological phi scale introduced in Chapter 2 has the disadvantage that grain size decreases as the value of $\phi$ increases. With this in mind, the alternative $\psi$ scale is introduced (Parker and Andrews, 1985); where $D$ denotes grain size in mm

$$\psi = \frac{ln(D)}{ln(2)}, \quad D = 2^{\psi} \tag{3.1a,b}$$

Thus $\psi = -\phi$. Let $p(\psi)$ denote the probability density by weight of a sample associated with size $\psi$, and $p_f(\psi)$ denote the associated probability distribution. Then by definition,

$$\int_{-\infty}^{\infty} p(\psi)d\psi = 1, \quad p_f(\psi) = \int_{-\infty}^{\psi} p(\psi)d\psi \tag{3.2a,b}$$

Thus $p_f(\psi)$ denotes the fraction of the sample that is finer than size $\psi$. Let $x$ denote some percentage, say 50%, and $\psi_x$ denote the grain size on the $\psi$ scale such that $x$ percent of the sample is finer. It then follows that

$$p_f(\psi_x) = \frac{x}{100} \tag{3.3}$$

The corresponding grain size in mm $D_x$ is given from (3.1b) as

$$D_x = 2^{\psi_x} \tag{3.4}$$

A value $x$ = 50 yields the median grain size $D_{50}$; the value $x$ = 90 yields the value $D_{90}$ such that 90 percent of the sample is finer, a value commonly used in the computation of the roughness associated with skin friction (grain roughness).

The arithmetic mean $\psi_m$ and arithmetic standard deviation $\sigma_m$ of the grain size distribution are given as

$$\psi_m = \int \psi p(\psi) d\psi \,, \quad \sigma^2 = \int (\psi - \psi_m)^2 \, p(\psi) d\psi \tag{3.5a,b}$$

The corresponding geometric mean $D_g$ and geometric standard deviation $\sigma_g$ are then given as

$$D_g = 2^{\psi_m} \,, \quad \sigma_g = 2^{\sigma} \tag{3.6a,b}$$

Sediment samples with values of $\sigma_g$ in excess of 1.6 are said to be poorly sorted (Chapter 5, this volume). Poorly sorted sediment provides grist for the mill of the river as it sorts it spatially over the planform and in the vertical.

A grain size distribution is said to be unimodal if the density $p(\psi)$ displays a single peak and bimodal if it displays two peaks. The grain size densities and distributions associated with unimodal and bimodal distributions are illustrated in Figures 3.17a,b. Comparing Figures 3.11 and 3.17a,b, it is seen that the sediment samples from the sand-bed streams of the former diagram, i.e. those for which $D_{50}$ is in the sand size are unimodal, and those from the gravel-bed streams of the former diagram, i.e. those for which $D_{50}$ is in the gravel range, are bimodal, with peaks in the sand and gravel range and a paucity in the pea gravel range (2 – 8 mm). It is not accurate to say that the sediment in all sand-bed streams is unimodal and the sediment in all gravel-bed streams is bimodal, but this tendency is observed.

The simplest realistic analytical forms for the probability density and distribution of grain sizes is the log-normal form (normal distribution of the logarithm of grain size) i.e.

$$p(\psi) = \frac{\mathbf{1}}{\sqrt{\mathbf{2}\pi}\,\sigma} exp\left( - \frac{(\psi - \psi_m)^2}{\mathbf{2}\sigma^2} \right)$$
$$p_f(\psi) = \frac{\mathbf{1}}{\sqrt{\mathbf{2}\pi}\,\sigma} \int_{-\infty}^{\psi} exp\left( - \frac{(\psi' - \psi_m)^2}{\mathbf{2}\sigma^2} \right) d\psi' \tag{3.7a.b}$$

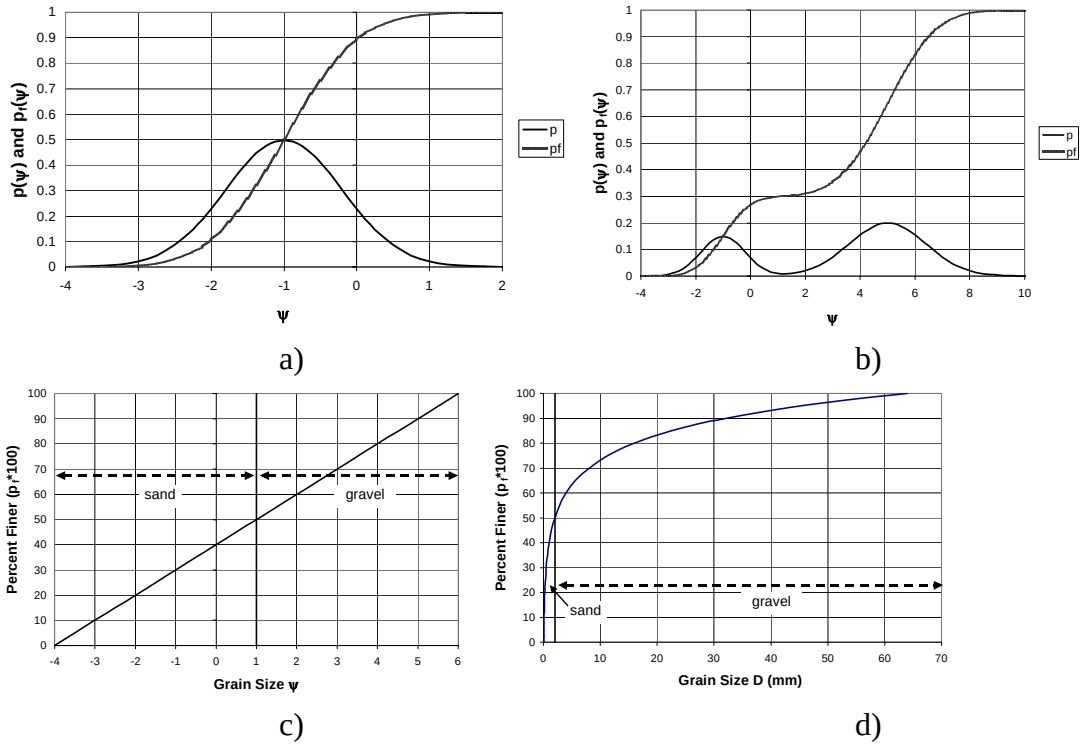


Figure 3.17 a) Diagram illustrating the probability density and distribution functions of a unimodal sediment sample. b) Diagram illustrating the probability density and distribution functions of a bimodal sediment sample. c) Plot of probability distribution function for a sand-gravel mix with constant content density as percent finer versus logarithmic grain size $\psi$. d) Plot of the same probability distribution function versus $D$ in mm on a linear scale.

Eq. (3.7a) describes a symmetric, unimodal probability density that often provides a reasonable fit for samples from sand-bed streams, but rarely does so in the case of gravel-bed streams. (The size densities of gravel-bed streams with a bimodal mix of sand and gravel can sometimes be approximated as the weighted sum of two log-normal densities.)

In the case of a sediment sample that is log-normally distributed, it can be shown that the mean size $\psi_m$ and the standard deviation $\sigma$ are given by the relations

$$\psi_m = \frac{1}{2}(\psi_{84} + \Psi_{16}), \quad \sigma = \frac{1}{2}(\psi_{84} - \Psi_{16}) \tag{3.8a,b}$$

The corresponding geometric mean and geometric standard deviation are

$$D_g = \sqrt{D_{84} D_{16}}, \quad \sigma_g = \sqrt{\frac{D_{84}}{D_{16}}} \tag{3.9a,b}$$

It should be emphasized, however, that Eqs. (3.9a,b) are not generally accurate when the distribution cannot be approximated as log-normal, in which case $D_g$ and $\sigma_g$ must be computed from Eqs. (3.5) and (3.6).

The necessity of using a logarithmic scale when treating the grain size distributions of poorly sorted river sediments cannot be overemphasized. Consider a size distribution that is 1/2 sand (0.0625 mm – 2 mm) and 1/2 gravel (2 mm – 64 mm), uniformly distributed over all sizes. A plot of the distribution versus the logarithmic scale $\psi$ (equivalent to a logarithmic scale for $D$) is given in Figure 3.17c; the corresponding plot using a linear scale for $D$ is given in Figure 3.17d. Figure 3.17c clearly reflects the fact that half of the sample is sand and half is gravel, whereas in the case of Figure 3.17d the sand is squeezed into a tiny range on the left-hand size of the graph. The use of statistics based on $D$ rather than any logarithmic scale for $D$ (such as $\psi$) implies the computation of an arithmetic mean grain size $D_m$, given as

$$D_m = \int Dp(D)dD \tag{3.10}$$

rather than the geometric mean grain size $D_g$ given from Eqs. (3.5a) and (3.6a). In the case of the distribution of Figures 3.17c and 3.17d, the two differ substantially; $D_g$ is equal to 2 mm, reflecting the fact that the sample is half sand and half gravel, whereas $D_m$ is 9.25 mm, reflecting a strong bias toward the coarse material

These comments notwithstanding, at least three bed-load transport relations for mixtures discussed below in Section 3.7, i.e. Ashida and Michiue (1972), Tsujimoto (1991; 1999) and Hunziker and Jaeggi (2002) define and use $D_m$ rather than $D_g$.

### 3.3.2 Discretization of the Grain Size Distribution

While grain size density and distribution are continuous concepts, they must be discretized in order to handle data from rivers. Let the size range within which a sediment sample has content be divided into $n$ intervals bounded by $n + 1$ grain sizes $\psi_i$, $i = 1..n+1$. The following definitions are made; for $i = 1..n$ ordered in increasing size,

$$\overline{\psi}_i = \frac{1}{2}(\psi_i + \psi_{i+1}), \quad p_i = p_f(\psi_{i+1}) - p_f(\psi_i), \quad \Delta\psi_i = \psi_{i+1} - \psi_i \tag{3.11a,b,c}$$

Note that by definition

$$\sum_{i=1}^{n} p_i = 1 \tag{3.12a}$$

The discretized versions of Eqs. (3.5a,b) and (3.10) are then

$$\psi_m = \sum_{i=1}^{n} \overline{\psi}_i p_i \ , \quad \sigma^2 = \sum_{i=1}^{n} (\overline{\psi}_i - \psi_m)^2 p_i \ , \quad D_m = \sum_{i=1}^{n} D_i p_i \qquad (3.12b,c,d)$$

The following notations are used to characterize sediment size distributions. Gravel-bed rivers often show some degree of armoring (coarsening) of the sediment at the surface of the bed compared to the substrate below, so it is useful to distinguish between the two. The fractions in the surface layer of the bed are denoted as $F_i$; the median size, geometric mean size, arithmetic standard deviation, geometric standard deviation and arithmetic mean size of the surface sediment are denoted as $D_{50}$, $D_g$, $\sigma$, $\sigma_g$ and $D_m$, respectively. The fractions within the substrate at elevation $z$ are denoted as $f_i(z)$. The fractions averaged over a relatively thick layer of substrate just below the surface layer are denoted as $\bar{f}_i$; the corresponding median size, geometric mean size, arithmetic standard deviation, geometric standard deviation and arithmetic mean size of the substrate sediment are denoted as $D_{u50}$, $D_{ug}$, $\sigma_u$, $\sigma_{ug}$ and $D_{um}$, respectively. The fractions in the bed-load transport are denoted as $f_{bi}$.

### 3.3.3 Sampling of Bed Sediments

The subject of the sampling of river bed sediments is treated in depth in Chapter 5 of this volume as well as Bunte and Abt (2001), and so only a short summary is given here. There are two basic types of sediment samples in the field. The first of these is the bulk sample, according to which a large amount of sediment is removed in bulk from the bed. Church et al. (1987) provide rigorous criteria for accurate sampling. They indicate that each bulk sample should be sufficiently large such that the largest stone in the sample is not more than 1% of the total sample weight. They also provide guidelines for the areal distribution of bulk samples. A careful areal distribution of samples is often necessary because wherever the sediment is poorly sorted, the distribution itself is likely to vary from place to place.

The second kind of sample is the Wolman point count sample. Such a sample can be obtained by defining a grid on the bed and sampling those particles at each node of the grid (Wolman, 1954). Alternatively, the bed can be paced according to a conceptual grid, and 100 or more grains exposed on the surface may be sampled randomly near e.g. the toe of one's shoe (preferably with one's eyes shut). Such a sample is biased toward the coarse grains in two ways. Firstly, the method is usually appropriate only for gravel-sized grains; it is very difficult to pick up single sand grains. Secondly, even those grains that are sampled are systematically biased toward coarser sizes if analyzed in terms of percent finer by weight, as demonstrated in Kellerhals and Bray (1971).

Kellerhals and Bray (1971) have suggested a simple equivalency by which a Wolman sample analyzed in terms of percent finer by number of grains is a good approximation to a bulk sample of the same parent material analyzed by weight. This approximate conversion has generally stood the test of time with only minor modifications; see Chapter 5 of this volume, Diplas and Sutherland (1988) and Fripp and Diplas (1993) for more details. The equivalency only holds, however, when the bulk

sample has been truncated so as to exclude sizes that are too small to sample by means of the Wolman technique.

Useful variations on these two techniques have been proposed. In the freeze-core technique, a hollow rod is pounded into the bed and liquid carbon dioxide is introduced into the rod. The evaporation of the carbon dioxide causes the sediment adjacent to the rod to freeze to it. The sample is obtained by hoisting the rod out. Freeze-core sampling has the advantage of obtaining a sample with minimal disturbance. It is however, biased toward the coarser sizes around the edge of the sample. Rood and Church (1994) describe a modified freeze-core technique based on a frozen barrel that helps overcome this disadvantage.

A second technique may be called the Klingeman surface sample (Klingeman et al., 1979). In this case a circle is placed over the bed surface. The circle should have a radius that is at least 10 times the largest stone exposed on the surface. This stone is then removed, and all the sediment is removed to the deepest level exposed by the stone. This method has the advantage of sampling not only the coarse grains on the bed surface, but also those finer grains, including sand, that would be exposed by the removal of the coarse grains. In addition, Klingeman samples can be obtained in deep gravel-bed rivers with the use of a cylindrical "cookie cutter" with a serrated bottom that can be worked into the bed by divers. The stilling of the flow in the cylinder helps prevent the loss of the finer part of the sample as it is collected by divers.

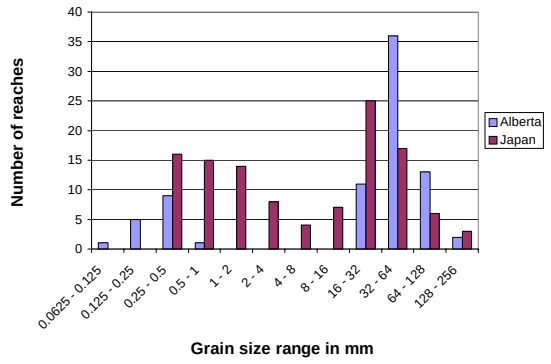


Figure 3.18 Plot of number of reaches for which characteristic grain size is within the specified grain size range for streams in Alberta, Canada and Japan.

In general the Wolman surface sample best serves to characterize the grain roughness offered by the bed surface, whereas the Klingeman surface sample best characterizes the material immediately available for transport under flow conditions sufficient to mobilize the larger surface grains. As a result, Klingeman samples are often used to characterize the grain size distribution of the active layer, i.e. the bed layer that exchanges directly with the bed-load, in gravel-bed streams.

## 3.4 DIMENSIONLESS BANK-FULL RELATIONS FOR GRAVEL-BED AND SAND-BED STREAMS

Alluvial rivers can be broadly divided into two types, i.e sand-bed streams, for which surface median size $D_{50}$ falls in the range 0.0625 – 2 mm, and gravel-bed streams, for which $2 < D_{50} < 256$ mm. Here cobbles and gravel are grouped together for simplicity. The dividing line between the two is not arbitrary; streams with a

characteristic size between 2 and 16 mm (pea gravel) are relatively rare. This is illustrated below using two sets of data. One set pertains to 78 river reaches in Alberta, Canada contained in Kellerhals et al. (1972). The other set is a combination of two sets pertaining to a total of 115 reaches in the Japanese archipelago (Yamamoto, 1994; Fujita et al., 1998; K. Fujita kindly provided the full data set). In Figure 3.18 the number of river reaches in each set with a characteristic grain size falling with each specified grain size range is plotted. The two sets are not completely comparable; whereas (surface) $D_{50}$ is used in the Alberta data, the Japanese data are based on size $D_{bulk60}$, where the subscript "*bulk*" denotes bulk. The difference between the two is likely to be appreciable only for gravel-bed streams, for which surface median size $D_{50}$ can be more than twice the substrate median size $D_{u50}$, and thus substantially larger than $D_{bulk60}$.

In the case of the Alberta streams the division between sand-bed and gravel-bed streams is complete; there are no streams in the set with values of $D_{50}$ between 1 and 16 mm. In the case of the Japanese streams every size range is represented, but there is a clear paucity of streams with $D_{bulk60}$ between 2 and 16 mm, with the lowest number of reaches in the range 4 – 8 mm.

Modeling of the transport of sediment mixtures in rivers requires some feel for how the rivers behave. Alluvial rivers tend to construct their channel geometries and floodplains in consistent ways. This geometry can be characterized in terms of bank-full characteristics, where bank-full conditions are attained when the river is just beginning to spill out of its channel and onto its floodplain. Bank-full conditions can be most easily defined in terms of a rating curve of stage $\xi$ (water surface elevation) versus flow discharge $Q$. When the flow is confined within the channel, stage increases relatively rapidly with discharge. As stage increases the water spills out onto the floodplain, so that even substantial increases in discharge beyond bank-full discharge $Q_{bf}$ yield much smaller increases in stage. A plot of $\xi$ versus $Q$ allows the determination of $Q_{bf}$ as shown in Figure 3.19.

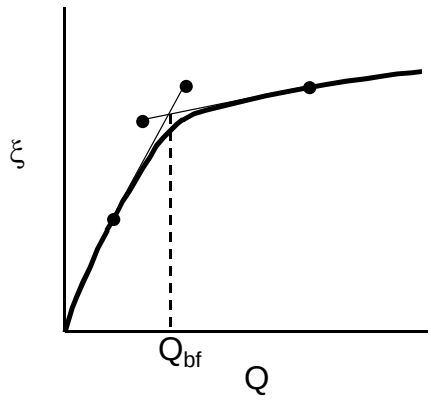

Figure 3.19 Diagram illustrating the definition of bank-full discharge in terms of the stage-discharge ($\xi$ - $Q$) relation.

At any given point along the river an average down-channel bed slope $S$ can be defined. Once bank-full discharge $Q_{bf}$ is identified the bank-full channel width $B_{bf}$ and average depth $H_{bf}$ can be determined from cross-sectional shape. Bank-full flow velocity $U_{bf}$ is given from continuity as

$$U_{bf} = \frac{Q_{bf}}{B_{bf} H_{bf}} \tag{3.13}$$

A characteristic bank-full boundary shear stress $\tau_{bbf}$ and shear velocity $u_{*bf}$ can be estimated from the depth-slope product rule for normal (steady, uniform) flow in open channels;

$$\tau_{bbf} = \rho g H_{bf} S \ , \quad u_{*bf} = \sqrt{\frac{\tau_{bbf}}{\rho}} = \sqrt{g H_{bf} S} \tag{3.14a,b}$$

where $\rho$ denotes water density. It is useful to define two dimensionless friction coefficients $C_{fbf}$ and $Cz_{bf}$ as

$$C_{fbf} = \frac{\tau_{bbf}}{\rho U_{bf}^2} = \frac{g H_{bf} S}{U_{bf}^2} \ , \quad Cz_{bf} = \frac{U_{bf}}{u_{*bf}} = C_{fbf}^{-1/2} \tag{3.15a,b}$$

The friction coefficient $C_{fbf}$ is of the standard form used in the study of fluid mechanics, and is precisely equal to the corresponding D'arcy-Weisbach friction coefficient divided by 8. The parameter $Cz_{bf}$ may be called a dimensionless Chezy resistance coefficient, because between Eqs. (3.14b) and (3.15b) it is found that

$$U_{bf} = Cz_{bf} \sqrt{g H_{bf} S} \tag{3.16}$$

i.e a form of the Chezy relation for flow velocity.

The friction coefficients $C_{fbf}$ and $Cz_{bf}$ are examples of dimensionless numbers. In the study of natural phenomena a dimensional number such as bank-full depth may vary greatly from site to site, whereas an appropriately defined dimensionless counterpart can allow the extraction of more universal characteristics. Alluvial rivers are no exception in this regard.

In order to implement a dimensionless characterization of the bank-full characteristics of alluvial streams, the following dimensionless parameters are defined;

$$\hat{Q} = \frac{Q_{bf}}{\sqrt{g D_{50}}\, D_{50}^2} \ , \quad \hat{B} = \frac{B_{bf}}{D_{50}} \ , \quad \hat{H} = \frac{H_{bf}}{D_{50}} \ , \quad Fr_{bf} = \frac{U_{bf}}{\sqrt{g H_{bf}}}$$
$$\tau^*_{bf\,50} = \frac{\tau_{bbf}}{\rho R g D_{50}} \ , \quad Re_{p50} = \frac{\sqrt{R g D_{50}}\, D_{50}}{\nu} \ , \quad R = \frac{\rho_s}{\rho} - 1 \tag{3.17a-g}$$

where $\rho_s$ denotes the density of the sediment. That is, $\hat{Q}$ denotes dimensionless bank-full discharge, $\hat{B}$ denotes dimensionless bank-full width, $\hat{H}$ denotes dimensionless bank-full depth, $Fr_{bf}$ denotes dimensionless bank-full Froude number, $\tau_{bf50}{}^*$ denotes the bank-full Shields number and $Re_{p50}$ is a version of the particle Reynolds number introduced in Chapter 2, but here based on the surface median size $D_{50}$. Note that between Eqs. (3.14a), (3.16), and (3.17d,e) it is found that

$$C_{fbf} = Fr_{bf}^{-2} S \ , \quad Cz_{bf} = \frac{Fr_{bf}}{\sqrt{S}} \ , \quad \tau^*_{bf\,50} = \frac{H_{bf} S}{R D_{50}} \tag{3.18a,b,c}$$

Two simple limiting cases are considered so as to characterize alluvial rivers in a simple but clear way. One case consists of alluvial sand-bed streams (0.0625 mm < $D_{50}$ < 2 mm) that are further restricted to have values of $D_{50}$ not larger than 0.5 mm. Such streams are almost invariably suspension-dominated in terms of how the river bed interacts with the sediment it carries. Another limiting case consists of alluvial gravel-bed streams with $D_{50}$ > 25 mm. (Here cobble-bed streams are included in the classification of gravel-bed streams for simplicity.) Such streams are almost invariably bed-load-dominated in terms of the interaction between river bed and sediment load. Most sand-bed streams transport much more mud (silt and clay) than sand, and many gravel-bed streams transport much more sand than gravel, but in both cases the finer fraction often interacts only weakly with the bed.

The restriction to these two limiting cases in terms of grain size does not mean that streams with values of $D_{50}$ between 0.5 mm and 25 mm do not exist; their existence is demonstrated in Figure 3.18. Rather, the difference between the two limiting cases helps characterize the difference between bed-load-dominated and suspension-dominated rivers.

The data base for the relations presented here pertains to a) three sets of gravel-bed streams, one from Alberta, Canada, one from Wales, UK and one from Idaho, USA and b) a set of both single-channel and multiple-channel sand-bed streams from various locations. The three sets for gravel-bed streams are given in Parker et al. (2003). The sand-bed set was extracted from the much larger data base of Church and Rood (1983).

Figure 3.20 shows $\hat{H}$ versus $\hat{Q}$. The gravel-bed and sand-bed streams each form coherent and very similar trends in the case of depth. The following regressions are obtained;

$$\hat{H} = \begin{cases} 0.368 \hat{Q}^{0.405} \ , \ gravel-bed \\ 3.01 \hat{Q}^{0.321} \ , \ sand-bed \end{cases} \tag{3.19}$$

In Figure 3.21 $\hat{B}$ is plotted versus $\hat{Q}$. Again each data set defines a coherent trend, but there is a somewhat greater discrimination between the sand-bed and gravel-bed case in the case of width. The regressions are

$$\hat{B} = \begin{cases} 4.87 \hat{Q}^{0.461} \ , \ gravel-bed \\ 0.274 \ \hat{Q}^{0.565} \ , \ sand-bed \end{cases} \tag{3.20}$$

In Figure 3.22 $S$ is plotted against $\hat{Q}$. Here the scatter is much larger, and the discrimination between sand-bed and gravel-bed streams stronger. There is a reason for the scatter in slope. Rivers can construct their own cross-sectional geometry in relatively short geomorphic time. Changing the slope of the long profile of a river requires much more time, however. The characteristic time scale is so large that it can be on the order of the tectonism (uplift or subsidence) that ultimately drives landscape evolution. As a result, there is a general trend for $S$ to decrease with $\hat{Q}$, but not a precise one. The regression relations are

$$S = \begin{cases} 0.0976\hat{Q}^{-0.341} \, , gravel-bed \\ 6.42\hat{Q}^{-0.397} \, , sand-bed \end{cases} \tag{3.21}$$

Figure 3.23 shows bank-full Shields number $\tau_{bf50}^{*}$ versus $\hat{Q}$. Again, there is a strong discrimination between sand-bed and gravel-bed streams, but little variation with $\hat{Q}$ The trends can be reasonably approximated in terms of average values of $\tau_{bf50}^{*}$;

$$\tau_{bf\,50}^{*} \approx \begin{cases} 0.049 \, , gravel-bed \\ 1.86 \, , sand-bed \end{cases} \tag{3.22}$$

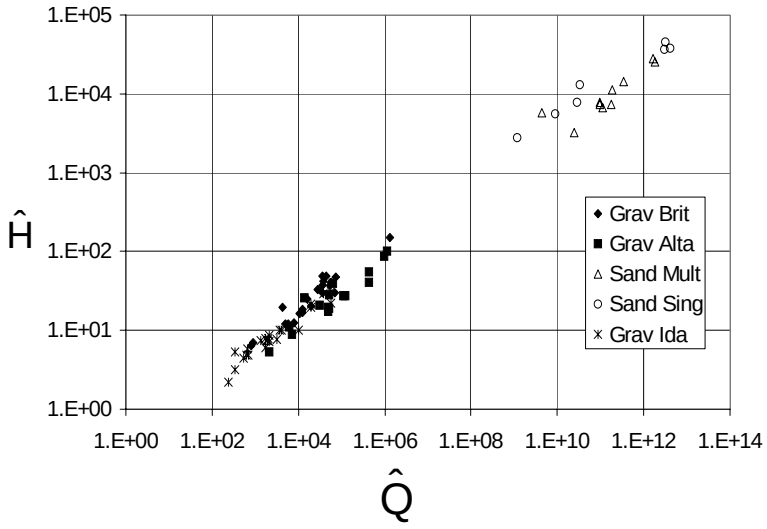


Figure 3.20 Dimensionless bank-full depth $\hat{H}$ versus dimensionless bank-full discharge $\hat{Q}$.

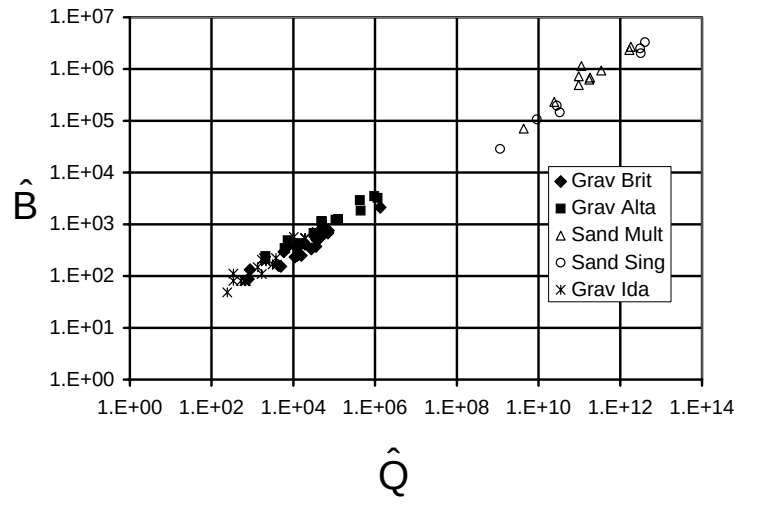


Figure 3.21 Dimensionless bank-full width $\hat{B}$ versus dimensionless bank-full discharge $\hat{Q}$.

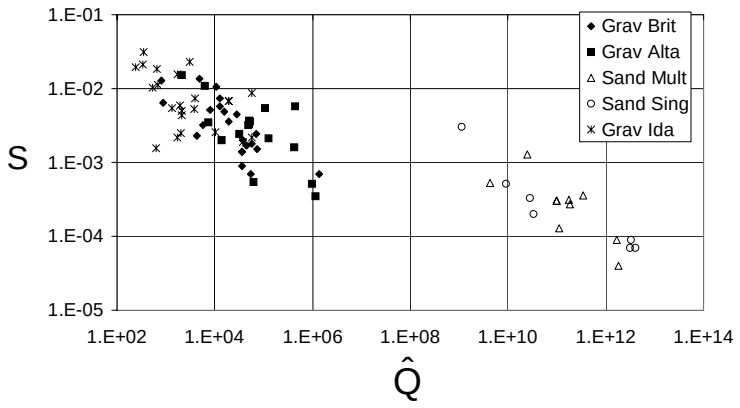


Figure 3.22 Channel bed slope *S* versus dimensionless bank-full discharge $\hat{Q}$.

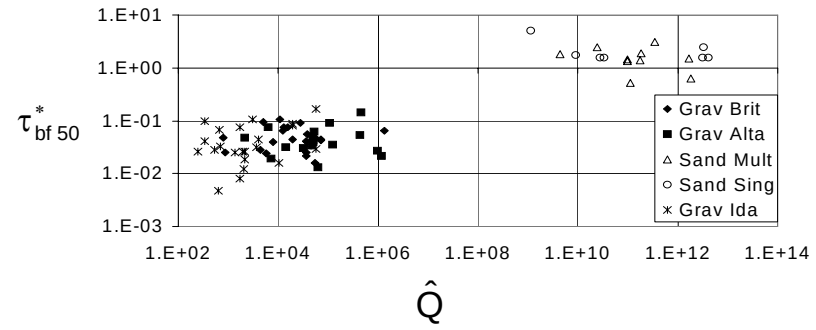


Figure 3.23 Dimensionless Shields number $\tau_{bf50}{}^*$ based on bank-full flow and $D_{50}$ versus dimensionless bank-full discharge $\hat{Q}$.

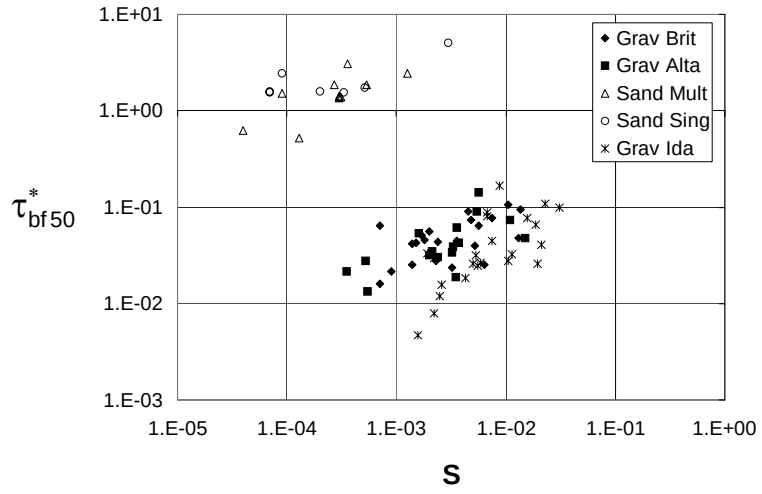


Figure 3.24 Dimensionless Shields number $\tau_{bf50}^*$ based on bank-full flow and $D_{50}$ versus channel bed slope $S$.

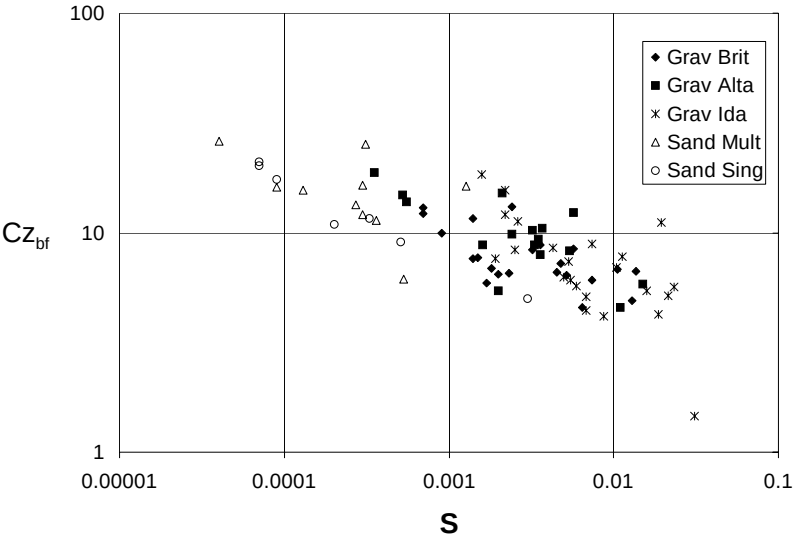


Figure 3.25 Dimensionless Chezy friction coefficient $Cz_{bf}$ versus channel bed slope $S$.

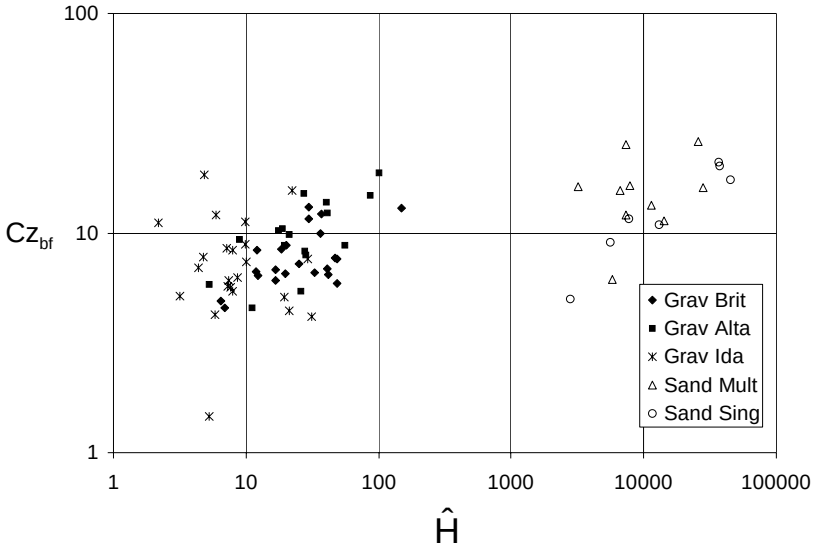


Figure 3.26 Dimensionless Chezy friction coefficient $Cz_{bf}$ versus dimensionless depth $\hat{H}$.

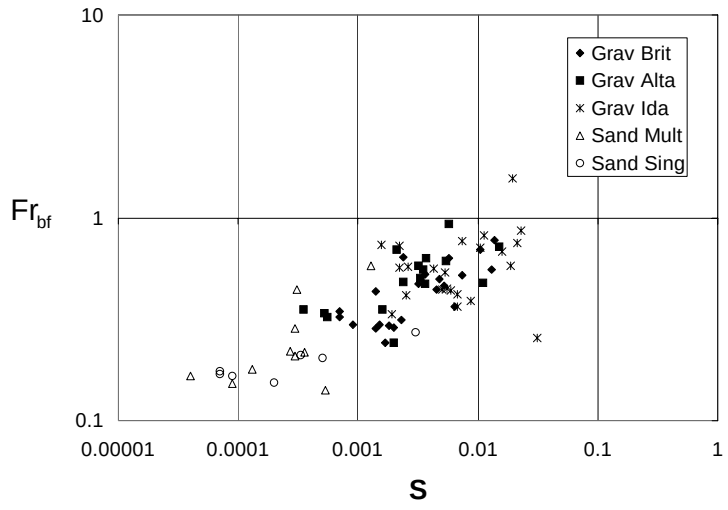


Figure 3.27 Froude number at bank-full flow $Fr_{bf}$ versus channel bed slope $S$.

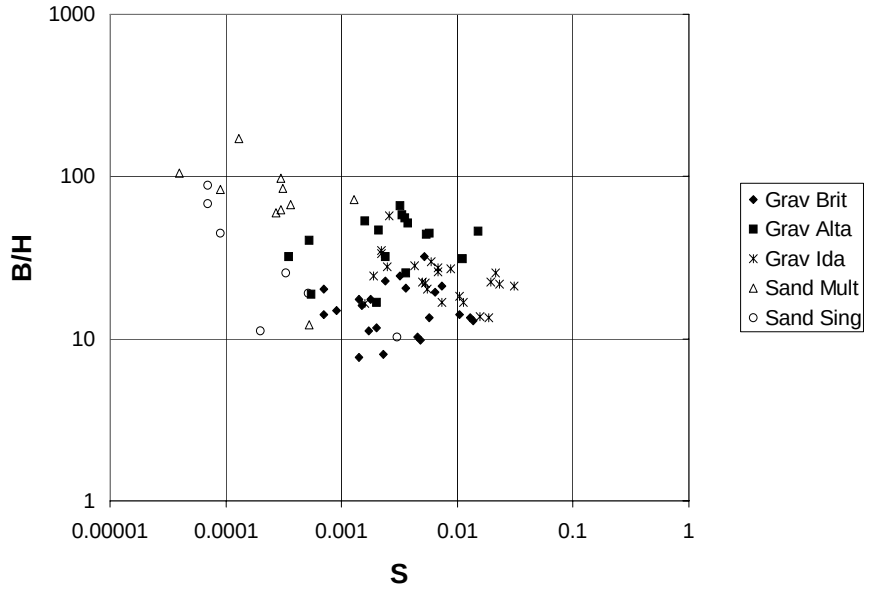


Figure 3.28 Bank-full width-depth ratio *B/H* versus channel bed slope *S*.

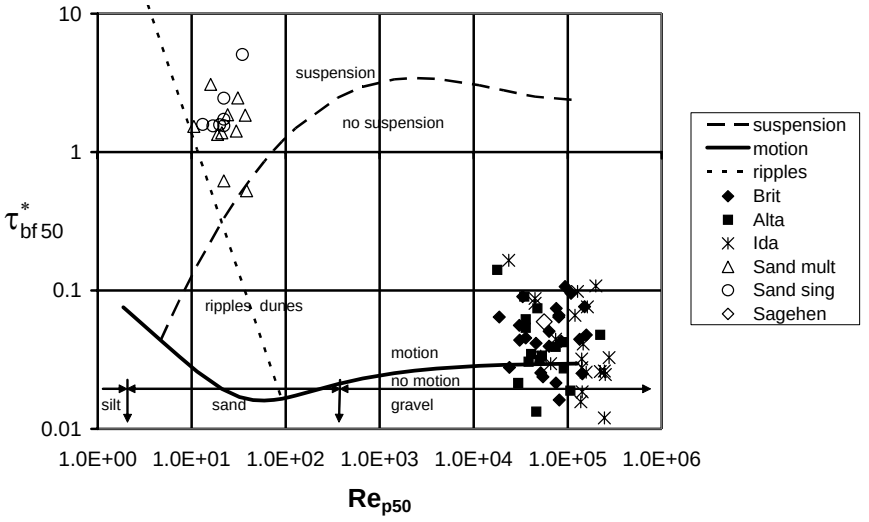


Figure 3.29 Dimensionless Shields stress based on bank-full flow $\tau_{bf50}^{*}$ versus particle Reynolds $Re_{p50}$ number based on $D_{50}$. Also included is a point from Sagehen Creek, California, USA.

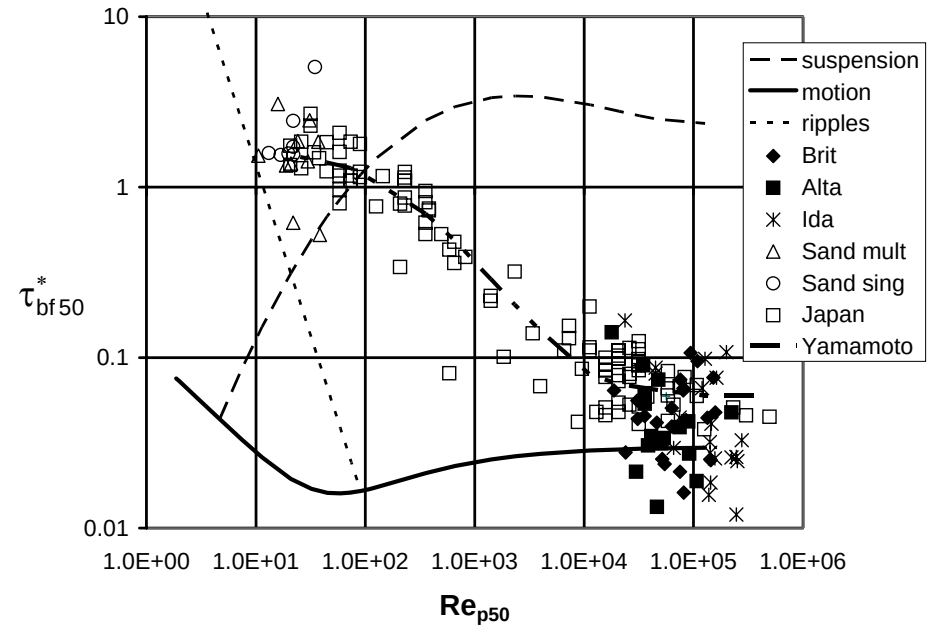


Figure 3.30 Extended version of Figure 3.29 including data from Japanese streams and the empirical regime relation of Yamamoto (1994).

Figure 3.23 shows a considerable amount of scatter. There are at least two reasons for this. The fine component of the load (mud in the case of sand-bed streams and sand in the case of gravel-bed streams) may either not be present in the bed (sand-bed streams) or may interact only passively with the bed (sand simply filling the pores of gravel-bed streams). This finer material is, however, available to build up the floodplain. As result, bank-full depth $H_{bf}$ in particular can vary in ways that are not captured with the use of a single bed surface median size $D_{50}$. In addition, some gravel-bed streams contain relict gravel on their beds that was emplaced during a regime of higher flows. In such streams a finer gravel may move over the bed without completely covering the relict material. As a result the median size $D_{50}$ may be too large to reflect the present mobility of the stream. These caveats notwithstanding, the estimates of Eq. (3.22) are useful for characterizing the two limiting cases. A bank-full Shields number on the order of 1.86, i.e. the average value for the sand-bed streams in Figure 3.23, describes a suspension-dominated river, whereas a bank-full Shields number on the order of 0.049, i.e. the average value for the gravel-bed streams in Figure 3.23, describes a bed-load-dominated system, as illustrated in Figure 2.26.

Figure 3.24 shows a plot of $\tau_{bf50}^*$ versus $S$. Again the sand-bed and gravel-bed streams plot in different regimes, but in each case $\tau_{bf50}^*$ shows a weak tendency to increase with increasing slope $S$.

Figure 3.25 shows the dimensionless Chezy number $Cz_{bf}$ versus $S$. Except for one outlier the values of $Cz_{bf}$ range between 4 and 26, and $Cz_{bf}$ decreases noticeably with

increasing *S*. There is little discrimination between sand-bed streams and gravel-bed streams in terms of the trend, but values for sand-bed streams, ranging from 9 to 26 excluding one outlier, are generally somewhat higher than for gravel-bed streams, which range from 4 to 19 excluding one outlier. Thus sand-bed streams tend to have somewhat lower bank-full friction coefficients $C_{fbf}$ than gravel-bed streams (0.0015 – 0.012 versus 0.003 – 0.06). Figure 3.26 shows $Cz_{bf}$ plotted against $\hat{H}$. The scatter is large, and the two types plot in very different regions. The fact that the values of $Cz_{bf}$ are not that greatly different between the two cases even with vastly different values of $\hat{H}$ indicates that grain roughness, which is often dominant for gravel-bed streams, may be relatively unimportant in most sand-bed streams, with bedforms taking over that role.

Figure 3.27 shows a plot of $Fr_{bf}$ versus S. With the exception of one point, all the bank-full flows are in the Froude-subcritical regime. This does not mean that supercritical flow does not occur in rivers. It does, however, tend to be restricted to floods in very steep rivers with a step-pool topography, a class of stream that is not represented in Figure 3.27. Within the scatter of the data, the two stream types define a common trend, but with sand-bed streams usually having lower bank-full Froude numbers. More specifically, sand-bed streams have values of $Fr_{bf}$ ranging from 0.14 to 0.58 and gravel-bed stream having values ranging from 0.24 – 0.93 (excluding one supercritical outlier).

Figure 3.28 shows the bank-full width-depth ratio (aspect ratio) $B_{bf}/H_{bf}$ versus bed slope *S*. In general the aspect ratio tends to be between 10 and 100, with the sand-bed streams tending toward somewhat larger values than the gravel-bed streams.

Figure 3.29 shows the bank-full Shields number $\tau_{bf50}^{*}$ against particle Reynolds number $Re_{p50}$, which is a surrogate for grain size $D_{50}$. A slightly different version of the diagram was presented as Figure 2.12 of Chapter 2, where the basis for the various regimes was explained. The only essential difference between the two figures is that Brownlie's (1981) relation for the onset of motion is used in Figure 2.26, whereas a modified version, in which the predicted critical Shields number is halved, is used in Figure 3.29 (and also Figure 3.30). (This modified relation is presented and explained below in Section 3.7.1). The strong tendency for the size $D_{50}$ to move as bed-load in gravel-bed streams and as suspended load in sand-bed streams is clear. In addition, at bank-full stage the Shields numbers of sand-bed rivers are typically about 50 times the critical Shields number at the threshold of motion, whereas the corresponding value for the gravel-bed streams is only about 1.6. These differences provide the basis for the exposition of grain size-specific sediment transport relations for heterogeneous sediment given below. Also included in Figure 3.29 is a single point for Sagehen Creek, California, USA (Andrews and Erman, 1986). Sagehen Creek is explained in more detail in Section 3.11.3.

Figure 3.30 addresses the issue of streams with values of $D_{50}$ between 0.5 mm and 25 mm. The added data are from the two sets of Japanese streams described above in regard to Figure 3.18. As noted above, $D_{bulk60}$ rather than surface median size $D_{50}$ was used to characterize the bed material of the Japanese streams. In addition, self-formed

bank-full discharge is not as clearly defined in the heavily engineered Japanese streams as in streams in other parts of the world, and as a result a mean annual peak flood flow was used as the basis for the computation of Shields number in the diagram. This notwithstanding, the plot shows a concentration of sand-bed and gravel-bed streams within and adjacent to the two limiting cases described here, along with a lesser but still substantial number of transitional streams. The solid line in the figure is due to Yamamoto (1994). It should be remembered that such transitional streams are not unique to Japan; see Kleinhans (2002) for a description of such streams in Europe.

A final discriminator between sand-bed and gravel-bed streams is embodied in Figure 2.11. It is seen in that figure that gravel-bed rivers tend to have grain size distributions that are substantially wider than sand-bed streams. This fact, combined with the fact that in Figure 3.29 the gravel-bed streams tend to cluster close to the threshold condition at bank-full conditions whereas the sand-bed streams plot well above it, renders grain sorting of heterogeneous sediment rather more intense in gravel-bed streams than sand-bed streams. The difference is, of course, relative; sand-bed rivers also sort their sediment.

## 3.5 THE ACTIVE LAYER CONCEPT

### 3.5.1 The Role of Fluctuations in Bed Elevation during Sediment Transport

The transport of bed material load in a river is always accompanied by fluctuations in bed elevation. Fluctuations occur at a variety of scales, including the scour and fill of river bends, pool-riffles and bank-attached bars through a flood hydrograph, as well as the migration of free bars, dunes and ripples and their interaction. At the finest scale, even in the absence of clearly defined bedforms, bed elevation fluctuations are observed at the scale of the surface size $D_{90}$ of the bed material. That is, coarse clusters form and break up, the removal of a coarse grain creates a hole in which finer grains are captured, coarse grains are buried by local scour of the finer grains around them etc. Fluctuations in bed elevation are typically linked to fluctuations in the rate of sediment transport. In the case of dunes in a bed-load-dominated regime, for example, the probability density of bed-load fluctuations can often be accurately estimated from the probability density of bed elevation through considerations of bedform migration (Hamamori, 1962; Hubbell, 1987; Ribberink, 1987; Kuhnle and Southard, 1988; Gomez et al., 1989).

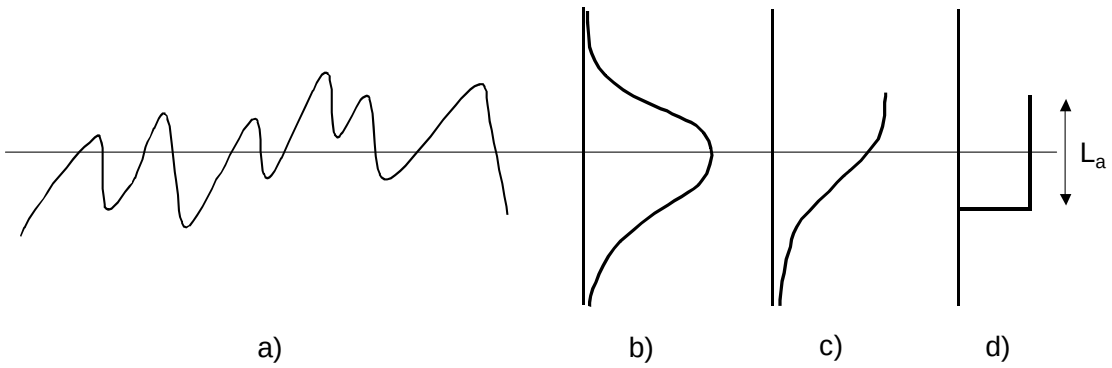


Figure 3.31 Definition diagram showing a) the spatial variation of bed elevation at a given time or temporal variation of bed elevation at a given location;
b) the probability density of bed elevation;
c) the probability of entrainment per unit time of a grain as a function of elevation in the bed; and
d) the approximation of c) embodied in the active layer approximation.

These bed fluctuations are an interesting feature of the transport of uniform or well sorted sediments, but are essential to the understanding of the transport of sediment mixtures. If the possibility of leaching of fine grains through the bed sediment by groundwater flow is neglected for the sake of argument, in order for a grain in the bed to be entrained into motion it must be exposed at least momentarily at the bed surface. The higher the elevation of the grain, the higher is the probability per unit time that it is entrained. Deeply buried grains have minimal probability of entrainment because the probability that the bed will locally be at that elevation must decline with depth. Figure 3.31 schematizes a) the instantaneous bed profile, b) the associated probability density of bed elevation and c) the probability per unit time of entrainment of a grain as a function of elevation.

The simplest reasonable approximation of the curve c) is as a step function, according to which the probability of erosion of a grain per unit time is a constant value in an "exchange", "active" or "surface" layer of thickness $L_a$ near the bed surface, and is vanishing below this layer. That is, all the bed fluctuations are assumed to be concentrated in a well-mixed layer of finite thickness $L_a$. This approximation, which is shown as d) in Figure 3.31, is the essence of the active layer formulation for the Exner equation of the conservation of bed sediment mass for mixtures. It was first introduced in a landmark paper by Hirano (1971), and is outlined below. The extension to continuous variation in the vertical direction is briefly introduced in Section 3.15.2.

### 3.5.2 The Formulation of Hirano

Consider the bed of Figure 3.32. Let the fractions $p_i$ in the size distribution in the active or surface layer be denoted as $F_i$; here it is assumed that the fractions have been averaged over fluctuations. Note that $F_i$ might be functions of time $t$, streamwise coordinate $s$ and transverse coordinate $n$, but may not be functions of the upward normal coordinate $z$ because the surface layer is assumed to be perfectly mixed by the fluctuations. The size fractions in the substrate are denoted as $f_i$, where in general $f_i$ can be functions of $s$, $n$ and $z$, so defining the stratigraphy of the deposit, but cannot be functions of $t$ because they are assumed to be below the level of bed fluctuations.

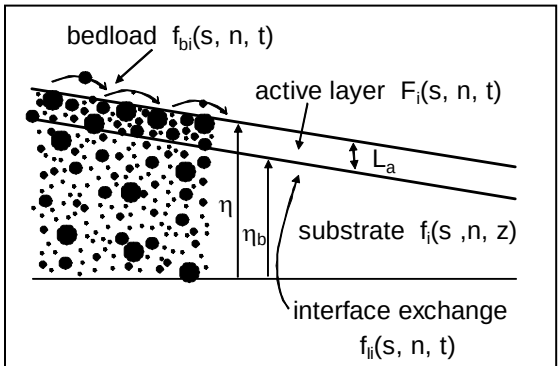

Figure 3.32 Definition diagram for the active layer concept.

Now consider one-dimensional transport of bed-load in the $s$ direction. Let $q_i$ denote the volume rate of bed-load transport of sediment in the *ith* grain size range per unit width normal to the flow. In the case of 1-D bed-load transport of sediment mixtures, Eq. (**2.XX**) generalizes to

$$(1-\lambda_p)\left[ f_{Ii}\frac{\partial \eta_b}{\partial t}+\frac{\partial}{\partial t}(L_a F_i)\right]=-\frac{\partial q_i}{\partial s} \tag{3.23}$$

In the above relation $f_{Ii}$ denotes the size fractions of the material exchanged between the surface layer and the substrate as the bed aggrades or degrades. In addition, $\eta_b$ denotes the elevation of the bottom of the surface layer, so that bed elevation $\eta$ is given as

$$\eta=\eta_b+L_a \tag{3.24}$$

Note that $\eta$ and $\eta_b$ correspond to averages over bed elevation fluctuations. Eq. (3.23) may be summed over all grain sizes, yielding in conjunction with Eq. (3.24) the 1-D version of Eq. (**2.XX**) in the absence of suspended load;

$$(1-\lambda_p)\frac{\partial \eta}{\partial t} = -\frac{\partial q_T}{\partial s} \tag{3.25}$$

where

$$q_T = \sum_{i=1}^{n} q_i \tag{3.26}$$

The four equations given above yield the following relation for the time evolution of the active layer;

$$(1-\lambda_p)\left[\frac{\partial}{\partial t}(L_a F_i) - f_{Ii}\frac{\partial L_a}{\partial t}\right] = -\left(\frac{\partial q_i}{\partial s} - f_{Ii}\frac{\partial q_T}{\partial s}\right) \tag{3.27}$$

Denoting the fractions in the bed-load as $f_{bi}$, it is seen from Eq. (3.26) that

$$f_{bi} = \frac{q_i}{\sum_{i=1}^{n} q_i} \tag{3.28}$$

A full derivation of Eq. (3.23) and the associated forms (3.25) and (3.27) can be found in Parker and Sutherland (1990) and Parker et al. (2000). Once appropriate forms for $q_i$, $L_a$ and $f_{Ii}$ are specified, Eq. (3.25) can be used to compute the time change in bed elevation due to net deposition or erosion, and Eq. (3.27) can be used to compute the time change in the composition in the surface layer of the bed.

### 3.5.3 Active Layer Thickness and Interfacial Exchange Fractions

There is a degree of arbitrariness in the specification of the active surface layer thickness $L_a$. In the absence of bedforms, $L_a$ can be thought to scale with a characteristic large size of the surface such as $D_{90}$ or $D_\sigma$, where $D_\sigma$ is defined as

$$D_\sigma = D_g \sigma_g \tag{3.29}$$

Note that $D_\sigma$ corresponds to $D_{84}$ for a log-normal distribution. Thus e.g.

$$L_a = n_a D_{90} \tag{3.30}$$

where $n_a$ is an order-one parameter that requires calibration in the absence of a probability distribution of bed fluctuations. The Klingeman sampling method discussed above implicitly assumes that $n_a$ is unity. When bedforms such as dunes and bars are present, and when the time scales of interest are large enough for the bed above the troughs to be thoroughly mixed by these bedforms, $L_a$ must scale with bedform height.

In the case of meander bends, $L_a$ must scale with some measure of the amplitude of scour and fill, and the time scales must be restricted to those larger than one corresponding to the passage of enough floods to completely rework the sediment within this amplitude. A compendium of expressions for $L_a$ used by various researchers in numerical models of bed elevation variation and sorting due to the transport of mixtures can be found in Kelsey (1996).

The interfacial exchange fractions $f_{Ii}$ describe the mean size distribution of the sediment that is exchanged between the surface layer and the substrate as the bed aggrades or degrades. When the bed degrades, substrate is transferred to the active layer, so that

$$f_{Ii} = f_i(z)\big|_{z=\eta_b} \quad for \quad \frac{\partial \eta_b}{\partial t} < 0 \tag{3.31}$$

In the original formulation of Hirano (1971), surface material was transferred to the substrate during bed aggradation. Subsequent research has suggested that the material transferred is a weighted mixture of bed-load and surface material, so that

$$f_{Ii} = aF_i + (1-a) f_{bi} \quad for \quad \frac{\partial \eta_b}{\partial t} > 0 \tag{3.32}$$

This form was first suggested by Hoey and Ferguson (1994); Toro-Escobar et al. (1996) used a set of large-scale experiments on downstream fining of gravel-sand mixtures to evaluate *a* for at least one case.

### 3.5.4 Further Generalizations and Alternate Formulations

Eq. (3.23) is easily generalized to include a) channel width variation in a 1-D formulation, b) transverse as well as streamwise variation in a 2-D formulation, c) suspended sediment as well as bed-load sediment and d) abrasion. All these cases are discussed later in this chapter. Abrasion may be included in a variety of ways. Here it is assumed that the product of abrasion is silt or fine sand that then moves as throughput load. As a result, abrasion is assumed to represent a net loss of bed material. Where $A_i$ denotes the net loss per unit time per unit bed area of clast volume in the *ith* grain size range due to abrasion, Eq. (3.23) generalizes to

$$(1-\lambda_p)\left[ f_{Ii} \frac{\partial \eta_b}{\partial t} + \frac{\partial}{\partial t}(L_a F_i) \right] = -\frac{\partial q_i}{\partial s} - A_i \tag{3.33}$$

The issue of abrasion will be treated in more detail below in Section 3.9.

The use of Eq. (3.23) or some close variant thereof has increasingly become the standard in the implementation of the active layer formulation. Some researchers, however, have used *ad hoc* formulations that are similar in nature but cannot be expressed in the compact analytical formulation given above. Examples of these *ad hoc*

formulations can be found in Borah et al. (1982), Park and Jain (1987), Copeland and Thomas (1992) and Belleudy and SOGREAH (2000). In many such treatments the active layer is implemented only to the extent necessary to describe the evolution of a static armor as the sediment supply is cut off.

As will be shown in Section 3.11, Eq. (3.27) can be used to describe the evolution of bed armoring. When the supply of sediment to a river with a mix of sediment sizes is cut off, the bed coarsens to eventually form a static armor, i.e. a surface layer containing material so coarse that it can no longer be removed and the bed can no longer degrade. The same formulation can also be used to describe a mobile armor, in which case a coarse surface layer is maintained even when all sizes are mobile. It will be demonstrated that there is a smooth progression from the unarmored state to a mobile armor, and then to a static armor as river stage decreases.

As can be seen by comparing cases c) and d) in Figure 3.31, the active layer formulation is the simplest formulation capable of describing the change in bed composition due to the selective transport of sediment mixtures. Recently progress has been made by Parker et al. (2000) in moving from the simplified case d) to the real case c). This work is described briefly in Section 3.15 below.

### 3.5.5 Entrainment Formulation

Before closing this chapter, an alternative active layer formulation for the Exner equation of sediment conservation of mixtures deserves mention. Bed-load particles typically roll, slide or saltate intermittently without being substantially supported by turbulence. Einstein (1950) introduced the concepts of a pickup rate and a step length for bed-load particles. Tsujimoto and Motohashi (1990) and Tsujimoto (1991, 1999) have pursued these concepts. Here the pickup rate is described in terms of a bed-load volume entrainment rate per unit time per unit bed area for the *ith* grain size range $E_{bi.}$ The probability density that a grain in size range *i* moves a distance *s* in one step is denoted as $P_{si}(s)$. The mean step length $L_{si}$ for the *ith* grain size range is thus given as

$$L_{si} = \int_0^\infty s P_{si}(s)\,ds \tag{3.34}$$

The volume rate of deposition of particles in the *ith* size range from the bed-load per unit time per unit bed area is given as $D_{bi}$, where

$$D_{bi} = \int_0^\infty E_{bi}(s - s')P_{si}(s')\,ds' \tag{3.35}$$

The entrainment form of Eq. (3.23) is thus

$$(1-\lambda_p)\left[ f_{Ii}\frac{\partial \eta_b}{\partial t} + \frac{\partial}{\partial t}(L_a F_i) \right] = D_{bi} - E_{bi} = \int_0^\infty E_{bi}(s - s')P_{si}(s')\,ds' - E_{bi} \tag{3.36}$$

The bed-load transport rate $q_i$ can be computed as

$$q_i = \int_0^\infty E_{bi}(s - s') \int_{s'}^\infty P_{si}(s'') ds'' ds' \tag{3.37}$$

With a little algebra it can be demonstrated between Eqs. (3.35) and (3.37) that

$$D_{bi} - E_{bi} = -\frac{\partial q_i}{\partial x} \tag{3.38}$$

so demonstrating the equivalency between Eqs. (3.23) and (3.36).

This equivalency applies, however, only to the treatment of sediment conservation. In the transport formulation of Eq. (3.23) it is necessary to specify $q_i$ as a function of the flow and surface layer characteristics; in the entrainment formulation of Eq. (3.36) it is necessary to specify $E_{bi}$ and $P_{si}$ as functions of the flow and surface layer characteristics. At small time and length scales the predictions of the two methods may be different. At scales that are large compared to the step length and associated step time, the predictions will be nearly the same if the bed-load and entrainment formulations are related by Eq. (3.37).

The above model can be simplified by assuming the step length $L_{si}$ to be specified deterministically rather than in terms of a probability function. The versions of Eqs. (3.35), (3.36) and (3.37) simplified in this manner are, respectively,

$$D_{bi} = E_{bi}(s - L_{si}) \tag{3.39}$$

$$(1 - \lambda_p)\left[ f_{Ii} \frac{\partial \eta_b}{\partial t} + \frac{\partial}{\partial t}(L_a F_i) \right] = D_{bi} - E_{bi} \tag{3.40}$$

$$q_i = \int_0^{L_{si}} E_{bi}(s - s') ds' \tag{3.41}$$

## 3.6 GENERAL FORMULATION FOR BED-LOAD TRANSPORT OF MIXTURES.

### 3.6.1 Surface-based formulation

If material within a given size range is not present in the bed surface then it cannot be entrained into the bed-load. To account for this it is appropriate to define a volume bed-load transport rate $q_{Ui}$ per unit time, per unit width and per unit fraction content in the surface layer, and a corresponding bed-load entrainment rate $E_{Ubi}$ such that

$$q_{Ui} = \frac{q_i}{F_i}, \quad E_{Ubi} = \frac{E_{bi}}{F_i} \tag{3.42a,b}$$

Thus, for example, even if a given model predicts that $q_{Ui} > 0$, implying that the flow is competent to move material in the *ith* grain size range, if $F_i = 0$ then that size range is unavailable for participation in bed-load transport. The model thus must predict a value of $q_i$ of zero. Such a treatment defines a "surface-based" formulation for bed-load transport. A "substrate-based" formulation will also be defined below.

### 3.6.2 Dimensional Analysis for Bed-load Transport of Mixtures

In general the unit bed-load transport rate $q_{Ui}$ can be expected to be a function of not more than two hydraulic parameters, here denoted as $X_1$ and $X_2$, and also water density $\rho$, sediment material density $\rho_s$, water viscosity $\nu$, gravitational acceleration $g$, grain sizes $D_i$ and other parameters based on the first, second, third… moments of the surface grain size distribution, here denotes as $m_1$, $m_2$, $m_3$… (Parker and Anderson, 1977). Thus

$$q_{Ui} = \frac{q_i}{F_i} = fn( X_1, X_2, \rho_s, \rho, \nu, g, D_i, m_1, m_2 \ldots ) \tag{3.43}$$

Here the moment series is truncated at second moment, $m_1$ is equated with the surface size $D_g$ (based on the first moment of $F_i$) and $m_2$ is equated with the surface arithmetic standard deviation $\sigma$ (square root of second moment of $F_i$). In a theory with the highest local accuracy $X_1$ and $X_2$ must be parameters that are most closely tied to bed-load. In a formulation to be applied to locally quasi-equilibrium flows at a macroscopic scale, however, the precise choice of these parameters is less critical. They can be chosen from, e.g. depth-averaged flow velocity $U$, flow depth $h$, water discharge per unit width $q_w$, bed or energy slope $S$, boundary shear stress $\tau_b$ etc. Customarily one of the hydraulic parameters plays a primary role in sediment transport and the other one (or other ones) play a secondary role. Here it is assumed that $X_1$ is the primary hydraulic parameter. In addition, many researchers have used $D_{50}$ rather than $D_g$ as the parameter of choice for characteristic surface grain size.

Some researchers, e.g. Einstein (1950), have included more than two hydraulic parameters their formulation of Eq. (3.43). For the case of locally quasi-equilibrium transport, however, the constraints of fluid mass and momentum balance as well as a formulation for hydraulic resistance allow the ultimate elimination of the extra hydraulic parameters.

Eq. (3.43) truncated at the second moment constitutes a relation between ten dimensioned parameters. The principles of dimensional analysis allow the reduction of this relation to an equivalent dimensionless one involving seven parameters. Defining

$$R = \frac{\rho_s}{\rho} - 1 , \quad q_i^* = \frac{q_i}{F_i \sqrt{RgD_i}\, D_i} , \quad Re_{pg} = \frac{\sqrt{RgD_g}\, D_g}{\nu} \tag{3.44a,b,c}$$

then Eq. (3.43) can be recast as

$$q_i^* = T_b\left( \hat{X}_1, \hat{X}_2, \frac{D_i}{D_g}, \sigma, Re_{pg}, R \right) \tag{3.45a}$$

In the above relation $T_b$ denotes a dimensionless bed-load transport function, $\hat{X}_1$ and $\hat{X}_2$ are dimensionless versions of $X_1$ and $X_2$, $q_i^*$ denotes a grain size specific Einstein number, $R$ denotes the submerged specific gravity of the sediment (near 1.65 for the most common natural sediments in rivers) and $Re_{pg}$ denotes an explicit particle Reynolds number. Note that $\hat{X}_1$ and $\hat{X}_2$ may contain the parameter $D_i$ and thus be grain-size specific.

Many but not all researchers have assumed the existence of a critical or threshold value of the primary dimensionless hydraulic parameter $\hat{X}_{1c}$, which may in turn depend on $D_i/D_g$, $\sigma$, $Re_p$ and $R$, below which sediment transport vanishes. In this way (3.45a) is amended to

$$q_i^* = T_b\left( \hat{X}_1 - \hat{X}_{1c}, \hat{X}_2, \frac{D_i}{D_g}, \sigma, Re_{pg}, R \right) \tag{3.45b}$$

Nearly all dimensionless formulations for the bed-load transport of sediment mixtures can be cast into the form of Eq. (3.45) (but sometimes with extra dimensionless hydraulic parameters). Researchers such as Fernandez Luque and van Beek (1976) have studied bed-load transport rates for a variety of values of $R$ and found no discernible independent effect as long as $R$ is incorporated into the primary dimensionless hydraulic parameter (e.g. the Shields number). As a result it is dropped here. Although there are many possible choices for $\hat{X}_1$ and $\hat{X}_2$, for the sake of illustration $\hat{X}_2$ is dropped and $\hat{X}_1$ is set equal to a Shields number $\tau_{si}^*$ based on the shear stress associated with skin friction $\tau_{bs}$ and grain size $D_i$;

$$\tau_{si}^* = \frac{\tau_{bs}}{\rho R g D_i} = \frac{u_{*s}^2}{R g D_i} \tag{3.46}$$

where

$$u_{*s} = \sqrt{\frac{\tau_{bs}}{\rho}} \tag{3.47}$$

denotes the shear velocity associated with skin friction. The (partial) justification for the use of the Shields number is that it has become the standard primary dimensionless hydraulic parameter in many recent bed-load formulations. The (partial) justification for dropping the second dimensionless hydraulic parameter refers to the fact that the removal of the form drag from the boundary shear stress used in Eq. (3.46) eliminates other

parameters that would enter into the bed-load transport relation through the relation for hydraulic resistance. (See Chapter 2 for a discussion of these relations, and the decomposition of boundary shear stress into skin friction and form drag components.) With these assumptions Eq. (3.45a) becomes

$$q_i^* = T_b\left(\tau_{si}^*, \frac{D_i}{D_g}, \sigma, Re_{pg}\right) \tag{3.48}$$

The flow is hydraulically rough during events that transport gravel in gravel-bed streams and many laboratory flumes. For such flows the particle Reynolds number $Re_{pg}$ can be dropped. In the case of flow in sand-bed streams, however, it generally cannot be dropped. The reader should also be reminded that $D_g$ can be replaced with $D_{50}$ in the above formulation with no loss of generality.

A form equivalent to Eq. (3.48) can be obtained by dividing both sides of the equation by $(\tau_{si}^*)^{3/2}$, in which case it reduces to

$$W_i^* = \hat{T}_b\left(\tau_{si}^*, \frac{D_i}{D_g}, \sigma, Re_{pg}\right) \tag{3.49}$$

where

$$W_i^* = \frac{Rgq_i}{F_i u_{*s}^3} = \frac{q_i^*}{\left(\tau_{si}^*\right)^{3/2}}, \quad \hat{T}_b = \frac{T_b}{\left(\tau_{si}^*\right)^{3/2}} \tag{3.50a,b}$$

The advantage of Eq. 3.49 is that it places all the effect of variation of grain sizes $D_i$ and $D_g$ on the right-hand side of the equation, so simplifying the job of identifying selective transport.

### 3.6.3 Critical or Reference Condition for the Onset of Significant Transport

Eqs. (3.48) and (3.49) provides a basis for studying not only bed-load transport itself, but also the beginning of transport of sediment mixtures. Before proceeding with this, however, one must wrestle with the meaning of "beginning of transport." In Chapter 2, the transport equation (2.95) of Meyer-Peter and Müller (1948) contains a critical condition for the onset of bed-load transport, whereas the Einstein (1950) relation (2.99) does not. This leads one to ask whether or not there really is a threshold condition for the onset of motion.

The answer is yes and no. Fortunately, however, this answer is not a complicated as one might think. In a classical set of experiments, Paintal (1971) ran flows over an erodible bed at conditions that were well below established critical conditions for the onset of bed-load transport. After weeks or months of patient waiting, some sediment was invariably collected at the downsteam end of the flume. In addition, this data could

be organized into a sensible transport relation satisfying the following relation at very low transport rates;

$$q^* = 6.5x10^{18}\left(\tau^*\right)^{16}, \quad W^* = 6.5x10^{18}\left(\tau^*\right)^{14.5} \qquad (3.51a,b)$$

where $\tau^*$ and $q^*$ are defined in Eqs. (2.56) and (2.91) and and $W^*$ is obtained by dividing $q^*$ by $(\tau^*)^{3/2}$. The implication is that there is no "absolute" threshold of motion in the statistical sense.

This notwithstanding, Paintal's work allows for the definition of an "effective" threshold of motion, below which the sediment transport rate is so low that the resulting morphodynamic change of the bed is negligible over most or all time periods of interest. The definition is made meaningful by the high exponent in Eq. (3.51), which guarantees that in the regime of very low bed-load transport rates large changes in $q^*$ lead to only small changes in $\tau^*$. Both the "absolute" and "effective" approaches are pursued here in order to better summarize the available data.

In the "absolute" approach, $q_i^*$ is set equal to zero in Eq. (3.48) or $W_i^*$ is set equal to zero in Eq. (3.49), resulting in the following relation for the critical Shields number $\tau_{sci}^*$ for the *ith* grain size;

$$\tau_{sci}^* = F_c\left(\frac{D_i}{D_g}, \sigma, Re_{pg}\right) \qquad (3.52)$$

(Here the subscript "*sci*" denotes "skin, critical, *i*th grain size). In the "effective" approach, flow conditions are determined for a very low but measurable reference value of bed-load transport. Parker et al. (1982a), for example suggested the reference dimensionless transport rate

$$W_r^* = 0.002 \qquad (3.53)$$

based on field data from Oak Creek, Oregon, USA. Setting $W_i^*$ equal to $W_r^*$ in Eq. (3.49) and solving for the associated reference Shields number $\tau_{ssri}^*$, it is found that

$$\tau_{ssri}^* = F_r\left(\frac{D_i}{D_g}, W_r^*, \sigma, Re_{pg}\right) \qquad (3.54)$$

(Here the subscript "*ssri*" denotes "skin, surface-based, reference, *i*th grain size). Eqs. (3.52) and (3.54) are very similar. The latter equation has the advantage of referring to a small but measurable transport rate. It is very hard to accurately measure zero sediment transport rate. Based on the high exponent in Eq. (3.52b) of Paintal (1971), it can be expected that the values of $\tau_{ssri}^*$ depend only weakly on the choice of $W_r^*$ as long as it is sufficiently small.

Eqs. (3.52) or (3.54) can be further reduced by evaluating it for $D_i = D_g$ and dividing the result into the original equation, yielding the respective forms

$$\frac{\tau^*_{sci}}{\tau^*_{scg}} = \frac{F_c\left(\frac{D_i}{D_g}, \sigma, Re_{pg}\right)}{F_c\left(1, \sigma, Re_{pg}\right)}, \quad \frac{\tau^*_{ssri}}{\tau^*_{ssrg}} = \frac{F_r\left(\frac{D_i}{D_g}, \sigma, Re_{pg}\right)}{F_r\left(1, \sigma, Re_{pg}\right)} \qquad (3.55a,b)$$

(The parameter $W_r^*$ is suppressed in Eq. (3.55b) because in any given formulation its value must be specified and held constant subsequently.) It is commonly assumed that the critical or reference Shields number $\tau_{scg}^*$ or $\tau_{ssrg}^*$ (or equivalent forms using the surface size $D_{50}$ instead of $D_g$) depends only on $Re_{pg}$, and the ratios on the left-hand sides of Eqs. (3.55a,b) depend only on $D_i/D_g$ (or $D_i/D_{50}$);

$$\frac{\tau^*_{sci}}{\tau^*_{scg}(Re_{pg})} = F_{hc}\left(\frac{D_i}{D_g}\right), \quad \frac{\tau^*_{ssri}}{\tau^*_{ssrg}(Re_{pg})} = F_{hr}\left(\frac{D_i}{D_g}\right) \qquad (3.56a,b)$$

where the functions $F_{hc}$ and $F_{hr}$ above differ from those in Eq. (3.55a,b).

### 3.6.4 Similarity Hypothesis

The bed-load transport rate $q_i^*$ in Eq. (3.48) or alternatively $W_i^*$ in Eq. (3.49) is assumed to be a function of, among other parameters, the ratio $D_i/D_g$ The shape of the bed-load curve defined as $q_i^*$ versus $\tau_{si}^*$, or alternatively $W_i^*$ versus $\tau_{si}^*$ may thus differ from grain size to grain size in a mixture. It may be, however, that the curve for each value of $D_i/D_g$ can be collapsed into a single curve, greatly simplifying the analysis. Similarity analysis can be used to test this hypothesis.

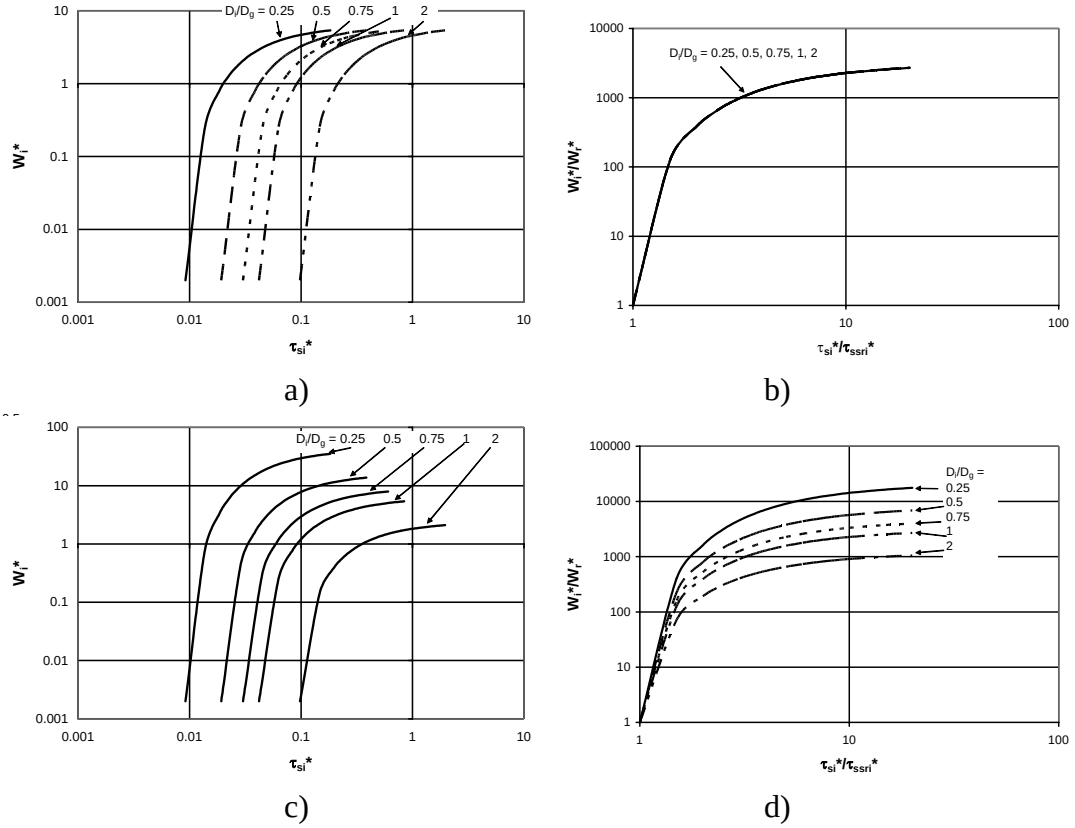


Figure 3.33 Plots illustrating the use of similarity.
a) Plot of $W_i^*$ versus $\tau_{si}^*$ for a case for which similarity collapse is realized.
b) Similarity plot of the data of the figure to the left which results in a perfect collapse.
c) Plot of $W_i^*$ versus $\tau_{si}^*$ for a case for which similarity collapse is not realized.
d) Similarity plot of the data of the figure to the left does not results in a collapse.

Here a similarity analysis is pursued in the context of Eq. (3.49) as an example. In Figures 3.33a and 3.33c $W_i^*$ is plotted against $\tau_{si}^*$ for $n$ = 5 values of $D_i/D_g$ based on two sets of synthetic data. The solid lines shown in the figures can be taken to be fits to data points. A standard value $W_r^*$ of 0.002 used to define the reference parameters $\tau_{ssri}^*$ in accordance with Eq. (3.54). The ratio $W_i^*/W_r^*$ is then plotted against $\tau_{si}^*/\tau_{ssri}^*$, so defining a total of $n$ curves, one for each value of $i$. Note that by definition every curve passes through the point $(W_i^*/W_r^*,\ \tau_{si}^*/\tau_{ssri}^*) = (1, 1)$. If the curves in fact coincide for all values of $\tau_{si}^*/\tau_{ssri}^*$ and every value of $i$, a similarity collapse is realized according to which

$$\frac{W_i^*}{W_r^*} = G_{sim}\left(\frac{\tau_{si}^*}{\tau_{ssri}^*}\right) \tag{3.57}$$

where $G_{sim}$ is a similarity collapse function which is independent of grain size. The synthetic data of Figure 3.33a do in fact yield the similarity collapse of Figure 3.33b.

The synthetic data of Figure 3.33c, however, do not collapse into a single line, as shown in Figure 3.33d.

Figures 3.33a and 3.33b thus show a case for which a similarity collapse to a common function is realized; Figures 3.33c and 3.33d show one for which it is not realized. Even in the event that similarity is realized, the parameters $D_i/D_g$, $\sigma$ and $Re_{pg}$ do not necessarily become unimportant; rather, it follows that $\tau_{ssri}^*$ itself may be a function of these parameters. A further similarity collapse, if successful, allows this relation to be reduced to the form

$$\frac{\tau_{ssri}^*}{\tau_{ssrg}^*(Re_{pg},\sigma)} = F_{hr}\left(\frac{D_i}{D_g}\right) \tag{3.58}$$

i.e. a hiding function similar to Eq. (3.56b).

Parker et al. (1982a), Parker and Klingeman (1982), Parker (1990a), Wilcock and McArdell (1993), Wilcock (1997a) and Wilcock and Crowe (2003) have pursued approximate similarity collapses of the above type based on both surface and substrate. They have invariably found that a better approximation to a collapse of the data is realized using the parameter $W_i^*$ than $q_{bi}^*$, largely because $W_i^*$ does not contain grain size $D_i$ in its definition by Eq. (3.50a).

### 3.6.4 Hiding Functions

Equations (3.55), (3.56) and (3.58) may be termed hiding functions. The reason for this relates to the seminal work of Egiazaroff (1965), who derived a relation of the above form from considerations of the forces acting on grains exposed on a bed containing a mixture of grain sizes. In Egiazaroff's simple but cogent model, larger grains are harder to move because they are heavier. Larger grains are, on the other hand, easier to move because they tend to protrude more into the flow, so feeling a higher drag. (Hence the terminology "hiding," in that the finer grains are sheltered from the full brunt of the flow by the protrusion of the coarser grains.) The net result of these two effects is a modest bias toward lesser mobility for coarser grains. The reduced mobility of coarser grains in a mixture turns out, then, to be much more subdued than what would be expected based on weight alone. Egiazaroff's version of (3.56), along with others, are introduced in the Section 3.7.

The dimensioned values of the critical (reference) boundary shear stresses based on skin friction (and surface content in the case of reference values) $\tau_{bsci}$ and $\tau_{bscg}$ ($\tau_{bssri}$ and $\tau_{bssrg}$) associated with sizes $D_i$ and $D_g$, respectively, are given from the relations

$$\tau_{bsci} = \rho RgD_i\tau_{sci}^* \;,\quad \tau_{bscg} = \rho RgD_g\tau_{scg}^*$$
$$\tau_{bssri} = \rho RgD_i\tau_{ssri}^* \;,\quad \tau_{bssrg} = \rho RgD_g\tau_{ssrg}^* \tag{3.59a,b,c,d}$$

Between Eqs. (3.56) and (3.59) it is found that

$$\frac{\tau_{bsci}}{\tau_{bscg}} = F_{rhc}\left(\frac{D_i}{D_g}\right) \equiv \frac{D_i}{D_g} F_{hc}\left(\frac{D_i}{D_g}\right)$$
$$\frac{\tau_{bssri}}{\tau_{bssrg}} = F_{rhr}\left(\frac{D_i}{D_c}\right) \equiv \frac{D_i}{D_g} F_{hr}\left(\frac{D_i}{D_g}\right) \qquad (3.60a,b)$$

The above equations may be termed reduced hiding functions.

### 3.6.5 Size-independence and Equal-threshold Limiting Cases

Two limiting cases are of interest here. In one limit $F_{hc}$ (or $F_{hr}$) is equal to unity, in which case Eqs. (3.56a,b), and (3.60a,b) devolve to

$$\frac{\tau^*_{sci}}{\tau^*_{scg}(Re_{pg})} = 1, \quad \frac{\tau^*_{ssri}}{\tau^*_{ssrg}(Re_{pg})} = 1, \qquad \frac{\tau_{bsci}}{\tau_{bscg}} = \frac{D_i}{D_g}, \quad \frac{\tau_{bssri}}{\tau_{bssrg}} = \frac{D_i}{D_g} \qquad (3.61a,b,c,d)$$

This case corresponds to the absence of hiding. Each grain has a critical (reference) Shields number that is the same, regardless of size. A grain of given size $D$ within a mixture has exactly the same mobility as it would have if the bed were composed entirely of size $D$. Thus each grain acts independently of its neighbors of differing size. The dimensioned critical (reference) shear stress needed to move a grain of size $D$ within a mixture increases linearly with size $D$. If this size-independence (hiding-free) scenario were to hold, the initiation of (significant) transport of sediment mixtures would be highly selective based on grain size.

In the second limiting case $F_{hc}$ ($F_{hr}$) is equated to $(D_i/D_g)^{-1}$, in which case Eqs. (3.56a,b) and (3.58a,b) devolve to

$$\frac{\tau^*_{sci}}{\tau^*_{scg}(Re_{pg})} = \left(\frac{D_i}{D_g}\right)^{-1}, \quad \frac{\tau^*_{ssri}}{\tau^*_{ssrg}(Re_{pg})} = \left(\frac{D_i}{D_g}\right)^{-1}, \qquad \frac{\tau_{bsci}}{\tau_{bscg}} = 1, \quad \frac{\tau_{bssri}}{\tau_{bssrg}} = 1 \qquad (3.62a,b,c,d)$$

In this limiting case the effect of the mixture has been to equalize the threshold for (significant) motion, so that all grains are mobilized at the same absolute boundary shear stress.

In the next chapter it will be shown that sediment mixtures behave somewhere in between the size-independence and equal-threshold scenarios, but are biased more toward the latter than the former.

### 3.6.6 Substrate-based Formulation

A surface-based formulation is necessary in order to develop a local predictor of bed-load transport. Gross, overall predictions can be made, however, using a substrate-based formulation. Let $\bar{f}_i$ denote the volume fraction of material the *i*th grain size range averaged over a relatively thick layer of substrate, proceeding downward from the surface-substrate interface. The substrate-based forms corresponding to Eqs. (3.44b), (3.48), (3.49), (3.50a), (3.56) and (3.60) are

$$q_{ui}^* = \frac{q_i}{\bar{f}_i \sqrt{RgD_i}\, D_i} \tag{3.63}$$

$$q_{ui}^* = T_{ub}\left( \tau_{si}^*, \frac{D_i}{D_{ug}}, \sigma_u, Re_{pug} \right) \tag{3.64}$$

$$W_{ui}^* = \hat{T}_{ub}\left( \tau_{si}^*, \frac{D_i}{D_{ug}}, \sigma_u, Re_{pug} \right) \tag{3.65}$$

$$W_{ui}^* = \frac{Rgq_i}{\bar{f}_i u_{*s}^3} \tag{3.646}$$

$$\frac{\tau_{suci}^*}{\tau_{sucg}^*(Re_{pug})} = F_{uhc}\left( \frac{D_i}{D_{ug}} \right), \quad \frac{\tau_{suri}^*}{\tau_{surg}^*(Re_{pug})} = F_{uhr}\left( \frac{D_i}{D_{ug}} \right) \tag{3.67a,b}$$

$$\frac{\tau_{bsuci}}{\tau_{bsucg}} = F_{urhc}\left( \frac{D_i}{D_{ug}} \right) \equiv \frac{D_i}{D_{ug}} F_{uhc}\left( \frac{D_i}{D_{ug}} \right)$$

$$\frac{\tau_{bsuri}}{\tau_{bsurg}} = F_{urhr}\left( \frac{D_i}{D_{ug}} \right) \equiv \frac{D_i}{D_{ug}} F_{ur}\left( \frac{D_i}{D_{ug}} \right) \tag{3.68a,b}$$

where the subscript "*u*" everywhere denotes "under", i.e. substrate (as "*s*" has already been used for surface) and the parameter $Re_{pug}$ is obtained from Eq. (3.44c) with the transformation $D_g \rightarrow D_{ug}$, where $D_{ug}$ ($D_{u50}$) refers to substrate values based on $\bar{f}_i$. It is useful to remind the reader that $D_g$ ($D_{50}$) refers to surface mean (median) sizes based on $F_i$. The same limiting cases of grain-independent and equal-threshold behavior can be defined based on a substrate formulation with the use of Eqs. (3.67) and (3.68).

### 3.6.7 Surface-based Formulation for Entrainment

A parallel development is possible for the entrainment formulation. Here the case of deterministic step lengths $L_{si}$ in a surface-based formulation is considered for simplicity. In analogy to Eq. (3.44b), the dimensionless entrainment rate $E_i^*$ and step length $L_{si}^*$ are defined as

$$E_i^* = \frac{E_i}{\sqrt{RgD_i}}, \quad L_{si}^* = \frac{L_{si}}{D_i} \tag{3.69a,b}$$

The analogs of Eq. (3.48) are

$$E_i^* = T_{be}\left(\tau_{si}^*, \frac{D_i}{D_g}, \sigma, Re_{pg}\right), \quad L_{si}^* = T_{bl}\left(\tau_{si}^*, \frac{D_i}{D_g}, \sigma, Re_{pg}\right) \qquad (3.70a,b)$$

Eq. (3.70a) can be used to develop threshold (reference) conditions for the onset of (significant) entrainment into bed-load that are analogous to Eqs. (3.56) and (3.60).

## 3.7 RELATIONS FOR HIDING AND BED-LOAD TRANSPORT OF MIXTURES

### 3.7.1 Relations for Threshold of Motion and Hiding

The classical relation for the threshold of motion of uniform sediment is that of Shields (1936). In terms of the notation presented above, the relation predicts the critical Shields number $\tau_{scg}^*$ (or $\tau_{sc50}^*$) as a function of explicit particle Reynolds number $Re_{pg}$ or $Re_{p50}$. Brownlie (1981) fitted a convenient analytical function to this curve. In general, however, the Shields curve tends to overpredict the critical Shields number. For example, in the limit of hydraulically rough flows ($Re_{pg} \rightarrow \infty$) the predicted value of $\tau_{scg}^*$ is near 0.06. This criterion incorrectly indicates, however, that most gravel-bed streams would be unable to move a surface mean or median size particle even at bank-full flow, as demonstrated below. Neill (1968) has suggested a revised value of 0.03, which appears to have stood the test of time (e.g. in the case of Oak Creek, Oregon, California as analysed by Milhous, 1973 and Parker and Klingeman, 1982; and in the case of the Nahal Eshtemoa, Israel, as analyzed by Powell et al., 2001). Adjusting the Brownlie relation by multiplying the right-hand side by one-half to obtain this limit, the following curve is obtained;

$$\tau_{scg}^* = \frac{1}{2}\left[0.22\ Re_{pg}^{-0.6} + 0.06 \cdot 10^{\left(-7.7\, Re_{pg}^{-0.6}\right)}\right] \qquad (3.71)$$

The appropriate grain size to use in Eq. (3.71) is a surface value $D_g$ or $D_{50}$. In the case of field gravel-bed rivers in particular, the bed tends to be armored at low flow, so that the corresponding substrate $D_{ug}$ or $D_{u50}$ can usually be expected to be below the corresponding surface value, by a multiplicative factor ranging from 0.25 to 1 (e.g. Dietrich et al., 1989). As a result the value of $\tau_{sucg}^*$ based on $D_{ug}$ tends to be higher than $\tau_{scg}^*$ by a factor of 1 to 4.

Buffington and Montgomery (1997) conducted a review of eight decades of incipient motion data, with special reference to gravel-bed rivers. Their data base includes both experimental and field data. Their analysis was done in terms of $D_{50}$ rather than $D_g$. They went to some effort to ensure the removal of form drag from most of the estimates of shear stress used in their treatment. In addition, they performed a service to the community in publishing their entire data set. They found that the data generally followed the overall shape of the Shields curve. Eq. (3.71) forms an approximate lower bound for the data for $Re_{pg} > 100$ ($D_g >$ 0.85 mm for $R = 1.65$ and $\nu = 1\text{x}10^{-6}$ m$^2$/s). A subset of their data base is compared with Eq. (3.71) in Figure 3.34. Also included in the figure are a) the original form of the Brownlie fit to the Shields curve and b) points based on bank-full flow and surface $D_{50}$ (measured at low flow) for the three sets of gravel-bed streams introduced in Section 3.3 above. Most (but not all) of these streams can be expected to be competent to move the surface $D_{50}$ size at bank-full flow.

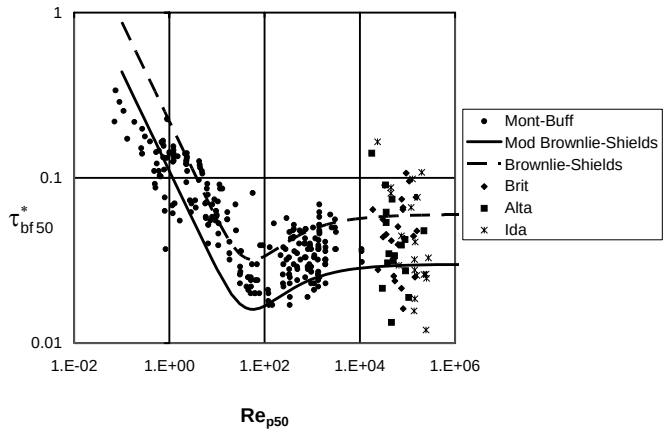


Figure 3.34 Plot of critical Shields number versus particle Reynolds number showing a) the Brownlie (1981) fit to the original Shields (1936) curve, b) the modified Brownlie fit of Eq. (3.71), c) the data of Buffington and Montgomery (1997) pertaining to $\tau_{cv50m}{}^*$ and d) the gravel-bed rivers of Figure 3.29.

The large scatter in Figure 3.34 is a problem, as noted by Buffington and Montgomery (1997). This notwithstanding, Eq. (3.71) would appear to be an appropriate estimator of at least a lower bound on $\tau_{scg}{}^*$ or the corresponding $\tau_{sc50}{}^*$ based on $D_{50}$ in streams with values of $D_g$ or $D_{50}$ in excess of 1 mm. The original form the the Brownlie fit to the Shields curve is seen to overpredict the critical Shields number for the great majority of the data from Buffington and Montgomery (1997), and to render most of the gravel-bed streams therein incapable of transporting their mean or median surface size at bank-full flow.

Several researchers have presented derivations of the Shields diagram from basic principles. In the case of uniform sediment, the work of Ikeda (1982) and Wiberg and Smith (1987) stand out. The latter work also provides an extension to sediment mixtures, and thus implicitly determines a hiding function similar to that of Egiazaroff (1965).

The first researcher to suggest a form for a hiding function for sediment mixtures was Einstein (1950). This work is remarkable in that it provides a complete, physically based implementation of the dimensional analysis presented above. Unfortunately the work was so far ahead of its time that little data was available to test the hiding function. Further analysis (e.g. Misri et al., 1984) has shown that the Einstein hiding function is a poor approximation of the data.

The first hiding function which was found to be a reasonable approximation of at least some data for heterogeneous sediments is the surface-based relation of Egiazaroff (1965). Egiazaroff provides a simplified derivation from basic principles so as to include both the effect of increasing grain weight in reducing mobility, and increasing protrusion of larger grains in increasing mobility, within a mixture.

$$\frac{\tau^*_{sci}}{\tau^*_{scg}} = F_{hc}\left(\frac{D_i}{D_g}\right) = \left[\frac{log(19)}{log\left(19\frac{D_i}{D_g}\right)}\right]^2$$

$$\frac{\tau_{bsci}}{\tau_{bscg}} = F_{rhc}\left(\frac{D_i}{D_g}\right) = \frac{D_i}{D_g}\left[\frac{log(19)}{log\left(19\frac{D_i}{D_g}\right)}\right]^2 \qquad (3.72a,b)$$

(In point of fact Egiazaroff used $D_m$, defined by Eq. (3.10), rather than $D_g$, so perpetuating a misconception that has continued to this day, i.e. that $D_m$ rather than $D_g$ is the appropriate size with which to characterize sediment mixtures.) The Egiazaroff hiding function is illustrated in Figure 3.35a, along with the limiting cases of size-independence (no hiding) and equal-threshold. The corresponding reduced hiding function is shown in Figure 3.35b, along with the limiting cases.

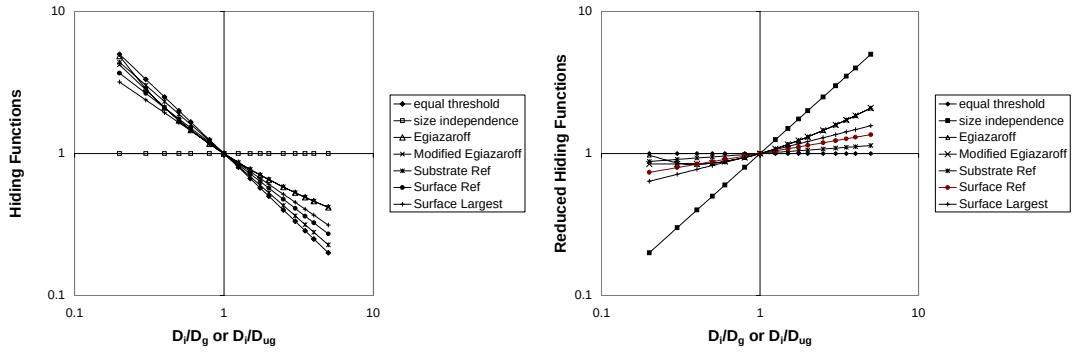


a) b)

Figure 3.35 Plots of a) hiding function obtained from Egiazaroff relation, the modified Egiazaroff relation, the condition of size-independence, the condition of equal-threshold, and the power relations of Eqs. (3.74a,b) using $\gamma_{subref} = 0.81$, $\gamma_{surfref} = 0.90$ and $\gamma_{surflarg} = 0.72$; and
b) reduced hiding functions corresponding to a) above.

Figure 3.35b is of particular interest. The Egiazaroff hiding function clearly plots between the case of size-independence and equal-threshold. It is clearly closer, however,

to the latter case, indicating that the structure of sediment mixtures works in the direction of equalizing the threshold shear stress required for the motion of all grains. This equalization cannot extend, however, all the way to very coarse, rare grains, and as a result the largest deviation from equal-threshold is for the coarsest grains in a mix.

Ashida and Michiue (1972) noted one curious feature in Figure 3.35b; sizes such that $D_i/D_g < 0.04$ become progressively harder to move with decreasing grain size. With this in mind, they suggested the following *ad-hoc* modification;

$$\frac{\tau^*_{sci}}{\tau^*_{scg}} = F_{hc}\left(\frac{D_i}{D_g}\right) = 0.843\left(\frac{D_i}{D_g}\right)^{-1} \quad for \; \frac{D_i}{D_g} \le 0.4$$
$$\frac{\tau_{bsci}}{\tau_{bscg}} = F_{rhc}\left(\frac{D_i}{D_g}\right) = 0.843 \; for \; \frac{D_i}{D_g} \le 0.4 \qquad (3.73a,b)$$

This modified form has been used by many subsequent researchers.

Parker et al. (1982a) and Parker and Klingeman (1982) introduced the concept of power relations for hiding functions. In particular, they deduced the following surface-based forms for reference (rather than critical) conditions using $D_{50}$;

$$\frac{\tau^*_{ssri}}{\tau^*_{ssr50}} = F_{hr}\left(\frac{D_i}{D_{50}}\right) = \left(\frac{D_i}{D_{50}}\right)^{-\gamma}$$
$$\frac{\tau_{bssri}}{\tau_{bssr50}} = F_{rhr}\left(\frac{D_i}{D_{50}}\right) = \left(\frac{D_i}{D_{50}}\right)^{1-\gamma} \qquad (3.74a,b)$$

as well as corresponding substrate-based forms. Here a value of $\gamma$ of 0 corresponds to size-independence and a value of 1 corresponds to equal-threshold conditions.

Parker et al. (1982a) found a substrate-based value of $\gamma$ of 0.982 for Oak Creek, Oregon, USA, i.e. very near equal-threshold conditions. Parker (1990a) deduced a surface-based value for the same stream of 0.905. Parker and Klingeman (1982) interpreted the difference between these two numbers in terms of a mobile-bed armor, as discussed in Section 3.10.

Values of $\gamma$ have been investigated in a number of rivers and laboratory flumes. Buffington and Montgomery (1997) and Powell (1998) provide summaries of these relations. Computations have proceeded using the reference concentration method, in which a measured bed-load data are used to interpolate or extrapolate values of reference Shields number, and also by determining the coarsest grain captured in a bed-load sample for a given flow. Discussion of the difference between the two methods can be found in Komar (1987), Wilcock (1988) and Shih and Komar (1990). The reported values of $\gamma$ are summarized for field streams in Table 3.1.

Table 3.1. Values of γ Measured for Various Gravel-bed Streams

| STREAM | AUTHORS | $D_{50}$ | γ |
|---|---|---|---|
| | | | |
| *SURFACE-BASED REFERENCE METHOD* | | | |
| Oak Creek, Oregon, USA | Parker (1990a) | 54 | 0.90 |
| Allt Dubhaig, Scotland | Ashworth and Ferguson (1989) | 50 | 0.65 |
| Goodwin Creek, Mississippi, USA | Kuhnle (1992) | 11.7 | 0.81 |
| Allt Dubhaig, Scotland | Wathen et al. (1995) | 21 | 0.90 |
| Sunwapta River, Canada | Ashworth et al. (1992) | 24 | 0.79 |
| *AVERAGED SURFACE-BASED REFERENCE* | | | 0.81 |
| | | | |
| *SUBSTRATE-BASED REFERENCE METHOD* | | | |
| Oak Creek, Oregon, USA | Parker et al. (1982a) | 20 | 0.98 |
| Goodwin Creek, Mississippi, USA | Kuhnle (1992) | 8.3 | 0.81 |
| *AVERAGED SUBSTRATE-BASED REFERENCE* | | | 0.90 |
| | | | |
| *SURFACE-BASED LARGEST GRAIN METHOD* | | | |
| Sage Hen Creek, California, USA | Andrews (1983) and Andrews and Erman (1986) | 58 | 1.07 |
| Oak Creek, Oregon, USA | Komar (1987) and Komar and Carling (1991) | 63 | 0.43 – 0.64 |
| Great Egglesthorpe Beck, UK | Komar (1987) and Komar and Carling (1991) | 62 | 0.64 = - 0.82 |
| Sunwapta River, Canada | Ashworth et al. (1992) | 21 | 0.69 |
| *AVERAGED SURFACE BASED LARGEST GRAIN* | | | 0.72 |

Table 3.1 can be summarized as follows. Substrate-based values of γ based on the reference method average to $\gamma_{subref} = 0.90$, and are closest to the equal-threshold condition. Surface-based values based on the reference method average to $\gamma_{surfref} = 0.81$, and surface-based values using the method of largest clast average to $\gamma_{surflarg} = 0.72$. The resulting hiding functions are shown in Figure 3.34. In all cases the trend is far more toward equal-threshold conditions rather than size-independence conditions. In all cases,

however, there is at least a residual tendency toward selecting the finer sizes in mobilizing sediment mixtures. Surface-based values of the exponent $\gamma$ are smaller than substrate-based values.

As pointed out above, a simple power form for the hiding function cannot in general be correct. In particular, both the hiding function and the reduced hiding function can be expected to be concave-upward. On the one hand rare, large clasts must be rendered difficult to move, causing the hiding function to curve upward as relative grain size increases. On the other hand the influence of grain size on mobility can be expected to diminish as relative grain size decreases, causing the hiding function to curve upward with decreasing grain size. The hiding functions of Egiazaroff (1965) and Proffitt and Sutherland (1983) have this property; in the former case it can be readily seen in Figures 3.35a and 3.35b. Misri et al. (1984) have demonstrated the same behavior for their experimental data. Wilcock and Southard (1988) demonstrated it for their own data, as well as the experimental data of Day (1980) and Parker et al. (1982b) and the field data for Oak Creek due to Milhous (1973). The hiding function of Wilcock and Crowe (2003) also shows this property, as is discussed below in Section 3.7.9.

### 3.7.2 Calculation of Boundary Shear Stress and Other Flow Parameters

Bed-load transport is driven by the hydraulics of the flow. As noted in Section 3.6.2, at least one hydraulic parameter, such as boundary shear stress $\tau_b$ or depth-averaged flow velocity $U$ invariably appears in bed-load transport relations. Boundary shear stress is often quantified in terms of shear velocity $u_*$, where

$$u_* = \sqrt{\frac{\tau_b}{\rho}} \tag{3.75a}$$

Depth- or cross-sectionally averaged flow velocity $U$ is related to shear velocity in terms of a dimensionless friction coefficient $C_f$, or an equivalent dimensionless Chezy coefficient $Cz$, where

$$Cz = \frac{U}{u_*}, \quad C_f = \frac{\tau_b}{\rho U^2} = Cz^{-2} \tag{3.75b,c}$$

Forms for these parameters were introduced for bank-full flow as Eqs. (3.15a,b) in Section 3.4.

The boundary shear stress acting on the bed of a river can be a mixture of skin friction $\tau_{bs}$ and form drag $\tau_{bf}$, as discussed in Chapter 2. In the case of flow over a hydraulic rough granular bed in the absence of form drag friction relations of the following type are often used;

$$Cz = 2.5 ln\left(11\frac{H}{k_s}\right), \quad Cz = 8.1\left(\frac{H}{k_s}\right)^{1/6} \tag{3.75d,e}$$

where $H$ denotes flow depth and $k_s$ denotes roughness height. Eqs. (3.75d) and (3.75e) are similar; the former is a logarithmic form due to Keulegan (1938) and the latter is a Manning-Strickler form due to Parker (1991a). Many variations on these forms can be found in literature. Roughness height $k_s$ is often related to the surface size $D_{90}$ as follows;

$$k_s = n_k D_{90} \tag{3.75f}$$

where $n_k$ has been estimated to range between 2 and 3.5 for granular beds (Kamphuis, 1974; Hey, 1979).

Many predictive relations for bed-load transport require boundary shear stress as an input parameter. The simplest formulation for calculating boundary shear stress, or shear velocity is based on the assumption of 1D normal (steady, uniform equilibrium) flow in a wide rectangular channel;

$$\tau_b = \rho g H S \ , \quad u_* = \sqrt{gHS} \tag{3.76a,b}$$

where $H$ and $S$ denote flow depth and bed slope. Where flow velocity is required for a sediment transport calculation, it can then be computed from Eqs (3.75) and (3.76).

Two questions arise at this point. Is form drag negligible in gravel-bed rivers? Can the flow field be accurately computed from the assumption of 1D normal flow? The latter query is approached first. Many gravel-bed rivers are small and steep, with very flashy hydrographs. For such streams Eq. (3.76) may be inadequate to model boundary shear stress. The next level of complication is the use of the 1D shallow-water St. Venant equations to predict the flow field. The 1D equations of momentum balance takes the form

$$\frac{\partial H}{\partial t} + \frac{\partial UH}{\partial s} = 0 \ , \quad \frac{\partial U}{\partial t} + U\frac{\partial U}{\partial s} = -g\frac{\partial H}{\partial s} + gS - \frac{C_f U^2}{H} \tag{3.76c,d}$$

Thes equations, coupled with the resistance formulations of Eqs. (3.75d,e) allow for the computation of $\tau_b$ or $u_*$, $U$, $H$ and other hydraulic parameters that might serve as inputs to sediment transport equations as functions of streamwise distance $s$ and time $t$. In some cases Eqs. (3.76c,d) can be simplified to their backwater forms by neglecting the time derivatives. In other cases even a 1D unstready, nonuniform approach may be insufficient, and the local input parameters to a sediment transport equation may require estimation with a 2D model. A case in point is a resolution of the 2D sediment transport field in a river bend. The issue is discussed in more detail in Section 3.13.2.

As for the former question, form drag in sand-bed streams is of sufficient importance to merit extensive attention, as seen in Chapter 2. A number of methods are available to extract out only the term $\tau_{bs}$ due to skin friction from the total boundary shear stress $\tau_s$ for such streams.

As noted in Section 3.6.2, it is explicitly or implicitly assumed in most shear stress-based formulations of bed-load transport that only the portion of the shear stress due to skin friction actually drives sediment transport, so that $\tau_{bs}$ rather than $\tau_b$ should appear as input to the computation. The problem with gravel-bed streams, however, is that once obvious effects such as debris jams and major channel irregularities have been discounted, the residual form drag due to e.g. bars has only been poorly quantified to date. Parker and Peterson (1980) have argued that form drag associated with bars in gravel-bed rivers is negligible at flows high enough to transport significant gravel loads. Hey (1989) has argued otherwise, and Millar (1999) has presented further evidence suggesting that form drag can be significant in some gravel-bed streams. A generally-validated predictive method allowing a boundary shear stress decomposition into skin friction and form drag, however, is no yet available.

The reader is thus offered two caveats concerning the transport relations presented below.

- While the indicated input parameter in the text is $\tau_{bs}$, in point of fact the user will most often have to equate this to $\tau_b$ because the information for a shear stress decomposition is lacking.
- In addition, much of the data analysis used to estimate boundary shear stress and other parameters in developing the relations presented below is based on the assumption of normal flow, which in fact may not been an accurate approximation to the actual flows in question. This is particularly true of the field data.

The scatter seen between the predictions of the various relations must be viewed in light of these two sources of error.

### 3.7.3 Relation of Einstein

Considerations of dimensional analysis yielded bed-load transport relations of the type of Eqs. (3.48) and (3.49). The conversion of these forms into predictive relations has typically required the folding of parameters together by means of an explicit or implicit similarity hypothesis. Einstein (1950) was the first to execute such an analysis for the bed-load transport of mixtures. The relation cannot be considered appropriate for the purposes of calculation due to the gross inaccuracies in the hiding function. As a result the relation is not covered in detail here. (The form for a single grain size is given in Chapter 2.) This notwithstanding, subsequent researchers have owed a debt to Einstein for pointing the path toward the progress that has been realized to date.

### 3.7.4 Relation of Ashida and Michiue

The relation of Ashida and Michiue (1972) is the first bed-load transport relation for mixtures with a thorough test against against data. The data pertain exclusively to experiments. Although the authors did not specify their relation as surface-based because the concept did not exist at the time, it is here treated as such.

In Eq. (3.49) the parameters $Re_{pg}$ and $\sigma$ are dropped, $D_m$ is used rather than $D_g$ (so that $g \rightarrow m$ in the subscripts) and the dependence on $D_i/D_m$ is folded into a hiding relation for critical stress. The relation thus takes the form

$$q_i^* = 17\left(\tau_{si}^* - \tau_{sci}^*\right)\left(\sqrt{\tau_{si}^*} - \sqrt{\tau_{sci}^*}\right) \tag{3.77a}$$

where

$$\frac{\tau_{sci}^*}{\tau_{scm}^*} = F_{hc}\left(\frac{D_i}{D_m}\right) = \begin{cases} 0.843\left(\dfrac{D_i}{D_m}\right)^{-1} & for \dfrac{D_i}{D_m} \le 0.4 \\ \left[\dfrac{log(19)}{log\left(19\dfrac{D_i}{D_m}\right)}\right]^2 & for \dfrac{D_i}{D_m} > 0.4 \end{cases} \tag{3.77b}$$

i.e. the modified Egiazaroff relation. Note that in the above relation $D_m$ denotes a mean surface grain size calculated in accordance with the arithmetic rule of Eq. (3.10) rather than the geometric rule of Eqs. (3.5a) and (3.6a). This treatment of grain statistics appears to be a legacy of Egiazaroff (1965), who likely did not perceive clearly the difference between $D_g$ and $D_m$. Ashida and Michiue recommend the following value for $\tau_{scm}^*$;

$$\tau_{scm}^* = 0.05 \tag{3.77c}$$

Shear stress is based on skin friction. Ashida and Michiue provide their own method for removing form drag. The data base used to develop the relation consists mostly of experiments with a sand bed, but experiments using pea gravel were also a significant component. The relation, however, is difficult to apply to many natural gravel-bed streams due to the high value of $\tau_{scm}^*$. In particular, the average value of the bank-full Shields number $\tau_{bf50}^*$ based on surface median size in the gravel-bed streams of Figure 3.23 is only 0.049.

Calculations with the relation of Ashida and Michiue proceed as follows. The grain sizes and fractions ($D_i$, $F_i$) of the surface layer, submerged specific gravity of the sediment $R$ and shear velocity associated with skin friction $u_{*s}$ must be specified. The surface mean grain size $D_m$ is computed with Eq. (3.12d) (in which $p_i \rightarrow F_i$), the Shields

numbers $\tau_{si}^*$ are computed with Eqs. (3.46) and (3.47), and the critical Shields numbers $\tau_{sci}^*$ are computed from Eqs. (3.77b,c). The Einstein numbers $q_i^*$ are then computed from Eq. (3.77a), and the volume transport rates per unit width $q_i$ from Eq. (3.44b). The total bed-load transport rate per unit width $q_T$ and fraction bed-load in the $i$th grain size range $f_{bi}$ are then computed from Eqs. (3.26) and (3.28).

### 3.7.5 Substrate-based Relation of Parker, Klingeman and McLean and Derivative Formulations

The substrate-based relation of Parker et al (1982a) is based solely on field data, mostly from Oak Creek (Milhous, 1973) but also from the Elbow River, Canada (Hollingshead, 1971) and several other streams. The shear stresses were computed from depth-slope products, and it was assumed that form drag at gravel-transporting flows was negligible. This assumption was made based on visual observation of the channel of Oak Creek at low flow, which is not particular sinuous and contains only very subdued bars. In retrospect, however, the assumption may not be entirely accurate. The relations are developed with the aid of an approximate substrate-based similarity collapse similar to the one introduced in Section 3.6.4.

The relation applies only to gravel transport. A bulk sample of substrate in a relatively thick layer immediately below the surface layer is used to characterize the fractions $\bar{f}_i$ All sand must be extracted out of the substrate size distribution, and the resulting gravel distribution renormalized so that $\bar{f}_i$ sums to unity before applying the relation.

The relevant characteristic grain size in the relation is substrate median size $D_{u50}$. It does not contain a critical shear stress, but rather uses a reference value $W_r^*$ of 0.002 in order to determine reference Shields numbers $\tau_{suri}^*$. The hiding relation was found to be

$$\frac{\tau_{suri}^*}{\tau_{sur50}^*} = F_{uhr}\left(\frac{D_i}{D_{u50}}\right) = \left(\frac{D_i}{D_{u50}}\right)^{-0.98} \tag{3.78a}$$

where

$$\tau_{sur50}^* = 0.0876 \tag{3.78b}$$

The transport relation is obtained from an approximate similarity collapse of the data. Thus $Re_{pg}$ and $\sigma$ are dropped from Eq. (3.49), and the parameter $D_i/D_{u50}$ is folded into the reference Shields numbers, resulting in the relation

$$W_{ui}^* = \frac{Rgq_i}{\bar{f}_i u_{*s}^3} = G_u(\phi), \quad \phi = \frac{\tau_{si}^*}{\tau_{suri}^*} \tag{3.78c,d}$$

where

$$G_u(\phi) = \begin{cases} 0.0025 exp\left[14.2(\phi-1) - 9.28(\phi-1)^2\right] & for \quad 0.95 < \phi < 1.65 \\ 11.2\left(1 - \dfrac{0.822}{\phi}\right)^{4.5} & for \quad \phi > 1.65 \end{cases} \tag{3.78e}$$

The alternative for $\phi > 1.65$ in Eq. (3.76d) is based on the Parker (1978b) approximation of the Einstein (1950) relation for uniform sediment.

Calculations with the above relation proceed as follows. The grain sizes and fractions ($D_i$, $\bar{f}_i$) of the substrate layer, submerged specific gravity of the sediment $R$ and shear velocity associated with skin friction $u_{*s}$ must be specified. The substrate median grain size $D_{u50}$ is computed from by interpolation from the fractions finer. The Shields numbers $\tau_{si}^*$ are computed with Eqs. (3.46) and (3.47), and the reference Shields numbers $\tau_{suri}^*$ are computed from Eqs. (3.78a,b). The values of $W_{ui}^*$ and $q_i$ are then obtained from Eqs. (3.78c,d,e). The total bed-load transport rate per unit width $q_T$ and fraction bed-load in the $i$th grain size range $f_{bi}$ are then computed from Eqs. (3.26) and (3.28).

Eqs. (3.78a) and (3.78b) engender a remarkable simplification that merits note. Replacing the exponent – 0.98 in Eq. (3.74a) with – 1, corresponding to the equal-threshold condition and substituting into Eq. (3.78c), it is found that grain size $D_i$ exactly cancels out, resulting in the relation

$$\phi = \frac{\tau_{si}^*}{\tau_{suri}^*} = \frac{\tau_{su50}^*}{\tau_{sur50}^*} \tag{3.78f}$$

$$\tau_{su50}^* = \frac{\tau_{bs}}{\rho R g D_{u50}} \tag{3.78g}$$

As a result, (3.78c) becomes

$$q_i = \bar{f}_i \frac{u_{*s}^3}{Rg} G_u\left(\frac{\tau_{su50}^*}{\tau_{sur50}^*}\right) \tag{3.78h}$$

Since $G_u$ has been rendered independent of $D_i$, it is quickly verified from Eqs. (3.28) and (3.78g) that

$$f_{bi} = \bar{f}_i \tag{3.78i}$$

That is, all sizes in the substrate are represented in the same proportion in the bed-load. This defines an extreme case of substrate-based equal mobility.

Parker et al. (1982a) went on to demonstrate that perfect substrate-based equal mobility is not in fact satisfied because the similarity collapse of Eq. (3.78c) is not

perfect. Lower flood flows are biased toward finer gravel, and higher flood flows are biased toward coarser gravel. This notwithstanding, substrate-based equal mobility is approximately satisfied in terms of the annual yield of gravel.

Parker et al. (1982a) extended their treatment to include deviation from perfect similarity. The resulting substrate-based transport relation contains three gravel size ranges, and correctly predicts the tendency for median bed-load gravel size to increase with increasing stage. Parker and Klingeman (1982) extended this three-size treatment to a surface-based model. Diplas (1987) further refined the work with a detailed analysis of deviation from similarity, resulting in a model that can clearly define the degree of transport selectivity in Oak Creek. Bakke et al. (1999) have used the basic model of Parker and Klingeman (1982) to develop a modified predictor allowing for efficient site-specific calibration.

### 3.7.6 Surface-based Relation of Parker

A substrate-based bed-load transport relation can be used for gross predictions of sediment transport. In a local sense, however, it is surface material that directly exchanges sediment with the bed-load. As a result, it is not obvious how to implement the active layer formulation of Section 3.5 with a substrate-based bed-load formulation. This renders numerical modeling of bed level variation and sorting difficult. In addition, it will be demonstrated in Section 3.10 that the grain size distribution of the surface layer varies dynamically with flow conditions.

With this in mind, Parker (1990a) reanalyzed the Oak Creek data to determine a surface-based bed-load transport formula. Again, all sand must be excluded from the surface grain size distribution and the fractions $F_i$ renormalized to sum to unity before applying the model. The reasons for the exclusion of sand are a) during flood flows capable of moving the gravel the sand may be suspended and carried as throughput load, with little interaction with the bed other than a passive filling of gravel pores, and b) many rivers (although not Oak Creek) are strongly bimodal, with a paucity of pea gravel, so defining a natural cutoff size for gravel. The model takes the form

$$W_i^* = \frac{Rgq_i}{F_i u_{*s}^3} = 0.00218 G(\phi) \tag{3.79a}$$

where

$$\phi = \omega\phi_{sgo}\left(\frac{D_i}{D_g}\right)^{-0.0951} \quad , \quad \phi_{sgo} = \frac{\tau^*_{sg}}{\tau^*_{ssrg}} \, , \quad \tau^*_{sg} = \frac{\tau_{bs}}{\rho RgD_g} \, , \quad \tau^*_{ssrg} = 0.0386$$

$$G(\phi) = \begin{cases} 5474\left(1 - \dfrac{0.853}{\phi}\right)^{4.5} & for\ \phi > 1.59 \\ exp\left[14.2(\phi - 1) - 9.28(\phi - 1)^2\right] & for\ 1 \le \phi \le 1.59 \\ \phi^{14.2} & for\ \phi < 1 \end{cases} \qquad (3.79b\text{-}g)$$

$$\omega = 1 + \frac{\sigma}{\sigma_O(\phi_{sgo})}\left[\omega_O(\phi_{sgo}) - 1\right]$$

Finally the functions $\sigma_O(\phi_{sgo})$ and $\omega_O(\phi_{sgo})$ are specified in Figure 3.36. Tables for these functions are given in Parker (1990b), along with a DOS implementation of the above method, ACRONYM1.

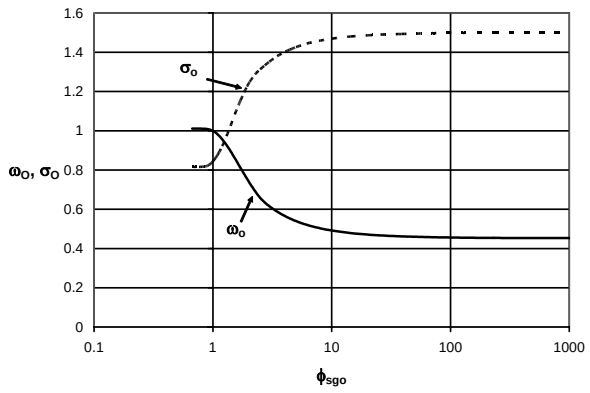


Figure 3.36 Plots of the functions $\sigma_O(\phi_{sgo})$ and $\omega_O(\phi_{sgo})$ for the Parker (1990a) relation.

Observations of the state of the bed surface of Oak Creek during floods transporting bed-load were not possible (Milhous, 1973). As a result, the above equation is not based on direct measurements of the composition of the surface layer during floods. Rather, the variation in $F_i$ as a function of stage was inferred in the derivation of the relation. When applied to Oak Creek with a varying gravel bed-load transport rate and a constant gravel bed-load grain size distribution, the model predicts a tendency for the surface layer to become finer with increasing stage, eventually approaching the composition of the substrate. That is, the model predicts that at very high stages the bed should be unarmored. This is exactly what is observed in some ephemeral streams subject to violent floods such as the Nahal Eshtemoa (Powell et al., 2001). The issue is explored in more detail in Section 3.11.3. Some debate about this result remains, however, because in point of fact the gravel bed-load grain size distribution becomes coarser with stage in Oak Creek.

Calculations with the above relation proceed as follows. The grain sizes and fractions ($D_i$, $F_i$) of the surface layer (from which the sand has been excluded), submerged specific gravity of the sediment $R$ and shear velocity associated with skin friction $u_{*s}$ must be specified. The surface geometric grain size $D_g$ and arithmetic standard deviation $\sigma$ are computed from Eqs. (3.6a), (3.12b) and (3.12c) with the transformation $p_i \rightarrow F_i$. The Shields number $\tau_{sg}^*$ are computed with Eqs. (3.79d) and (3.47). The values of $W_i^*$ and $q_i$ are then obtained from Eqs. (3.79a) with the aid of Eqs.

(3.79b,e,f,g). The total bed-load transport rate per unit width $q_T$ and fraction bed-load in the $i$th grain size range $f_{bi}$ are then computed from Eqs. (3.26) and (3.28).

### 3.7.7 Surface-based Entrainment Relation of Tsujimoto

In a bed-load entrainment model of type specified in Eqs. (3.39) – (3.41) it is necessary to specify expressions for $E_i$ and $L_{si}$ along the lines of Eqs. (3.70a,b). Tsujimoto and Motohashi (1990) and Tsujimoto (1991, 1999) have developed such forms;

$$E_i^* = 0.02\tau_{si}^*\left(1-0.7\frac{\tau_{sci}^*}{\tau_{si}^*}\right)^3 \tag{3.80a}$$

$$\frac{\tau_{sci}^*}{\tau_{scm}^*} = F_{hc}\left(\frac{D_i}{D_m}\right) = \begin{cases} 0.843\left(\dfrac{D_i}{D_m}\right)^{-1} & for\ \dfrac{D_i}{D_m} \le 0.4 \\ \left[\dfrac{log(19)}{log\left(19\dfrac{D_i}{D_m}\right)}\right]^2 & for\ \dfrac{D_i}{D_m} > 0.4 \end{cases} \tag{3.80b,c}$$

$$L_{si}^* = L_{so}^* \tag{3.80d}$$

In the above relations the arithmetic mean grain size $D_m$ is specified by the arithmetic rule of Eq. (3.10) rather than the geometric rule of Eqs. (3.5a) and (3.6a). The hiding function is the same one as used by Ashida and Michiue (1972), i.e. the modified Egiazaroff (1965) relation. The critical Shields number $\tau_{scm}^*$ is in general a function of $Re_{pm}$ that appears to be specified in Nakagawa et al. (1982), but takes the value 0.05 in the limit of large $Re_{pm}$, i.e. the same limit as Ashida and Michiue (1972). In addition, Tsujimoto (1990) rather vaguely specifies $L_{so}^*$ as "almost constant" among grain sizes and taking a value between 10 and 30, i.e. "smaller…than the value for uniform size material (80 – 250)."

In the case of bed-load transport that can be approximated as quasi-uniform at the scale of the step length, Eq. (3.41), the definitions of Eqs. (3.70a,b) and the above relations yield the following expression for bed-load transport rate;

$$q_i^* = E_i^* L_{si}^* = 0.02 L_{so}^* \tau_{si}^*\left(1-0.7\frac{\tau_{sci}^*}{\tau_{si}^*}\right)^3 \tag{3.80e}$$

The main reason for including this relation is the illustration of a bed-load transport relation obtained from considerations of entrainment into bed-load. The

equation itself is not of sufficient generality to recommend it as a general method for calculating bed-load transport in gravel-bed streams.

### 3.7.8 Surface-based Relation of Hunziker and Jaeggi

The surface-based relation of Hunziker and Jaeggi (2002) represents a generalization of the relation of Meyer-Peter and Müller (1948). It was developed in order to obtain a description of both static and mobile armoring in rivers. The experiments on mobile armoring reported in Suzuki and Kato (1991) and Suzuki and Hano (1992) were used to help develop and verify the model. The formulation is expressed as

$$q_i^* = 5\left(\frac{D_i}{D_m}\right)^{-3/2}\left[\left(\frac{D_i}{D_m}\right)^{-\alpha}\left(\tau_{sm}^* - \tau_{scm}^*\right)\right]^{1.5}$$

$$\tau_{sm}^* = \frac{\tau_{bs}}{\rho R g D_m}, \quad \tau_{scm}^* = \tau_{scmo}^*\left(\frac{D_{um}}{D_m}\right)^{0.33}, \quad \tau_{scmo}^* = 0.05 \qquad \text{(3.81a-e)}$$

$$\alpha = 0.011\left(\tau_{sm}^*\right)^{-1.5} - 0.3$$

where $D_m$ and $D_{um}$ refer to mean surface and substrate sizes, respectively, computed from the arithmetic rule of Eq. (3.10) rather than the geometric rule of Eqs. (3.5a) and (3.6a).

Calculations with the relation of Ashida and Michiue proceed as follows. The grain sizes and fractions ($D_i$, $F_i$, $\bar{f}_i$) of the surface and immediate substrate layers, submerged specific gravity of the sediment $R$ and shear velocity associated with skin friction $u_{*s}$ must be specified. The surface and substrate mean grain sizes $D_m$, respectively are computed from Eq. (3.12d) with the respective transformations $p_i \rightarrow F_i$ and $p_i \rightarrow \bar{f}_i$. The Shields number $\tau_{sm}^*$ is computed with Eqs. (3.81b) and (3.47), and the Einstein numbers $q_i^*$ are then computed from Eq. (3.81a) with the aid of Eqs. (3.81c,d,e). The volume transport rates per unit width $q_i$ are obtained from Eq. (3.44b). The total bed-load transport rate per unit width $q_T$ and fraction bed-load in the $i$th grain size range $f_{bi}$ are then computed from Eqs. (3.26) and (3.28).

### 3.7.9 Two-fraction Relation of Wilcock and Kenworthy

A unique set of experiments on the transport of sand-gravel mixtures in a recirculating flume (Wilcock et al., 2001) has allowed for a quantification of the interplay between the sand and gravel components of a mixture undergoing bed-load transport. The experiments, in which sand content in the bulk material varies from 6.2% to 34%, reveal a degree of interaction that was not foreseen by e.g. Parker (1990a), in whose relation the sand is excluded from the surface grain size distribution before computing the gravel bed-load transport.

Consider a sediment mixture undergoing bed-load transport in, for example, a sediment feed flume. Now increase the feed rate of a range of the finest grain sizes undergoing bed-load transport without changing the feed rate of the coarser sizes. The increased feed of finer sizes has the effect of lowering $D_{50}$, and so increases the Shields number $\tau_{s50}^*$, given as

$$\tau_{s50}^* = \frac{\tau_{sb}}{\rho R g D_{50}} \tag{3.82}$$

The result is an increased mobility of all sizes. The model of Parker (1990a) can capture this effect when fine gravel is added, but it is unable to capture it when sand is added because the sand is explicitly excluded from the grain size distribution.

Wilcock et al. (2001) have demonstrated that the addition of sand results in an effect that is stronger than that embodied in the increase of $\tau_{s50}^*$ through decreased $D_{50}$. In particular, the addition of sand can dramatically lower the reference Shield stress for gravel. This effect was first described in Wilcock (1998a). (Recall that a reference Shields number is a surrogate for critical Shields number).

Wilcock and Kenworthy (2002) captured this effect in terms of a two-fraction model such that grain size $D_1$ characterizes the sand and size $D_2$ characterizes the gravel. The model was developed with both the laboratory data reported in Wilcock et al. (2001) and field data from the East Fork River, Wyoming, USA (Emmett et al., 1980), Goodwin Creek, Mississippi, USA (Kuhne, 1992), Jacoby Creek, California, USA (Lisle, 1989) and Oak Creek, Oregon, USA (Milhous, 1973). Their model is presented in both surface-based and substrate-based form. Only the surface-based form is presented here; the reader is referred to the original reference for the substrate-based form.

$$W_i^* = \frac{R g q_i}{F_i u_{*s}^3} = G(\phi), \quad \phi = \frac{\tau_{si}^*}{\tau_{ssri}^*} = \frac{\tau_{bs}}{\tau_{bssri}}$$

$$G = \begin{cases} 0.002\phi^{7.5} & for\ \phi < \phi' \\ A\left(1 - \dfrac{\chi}{\phi^{0.25}}\right)^{4.5} & for\ \phi \geq \phi' \end{cases} \tag{3.83a-d}$$

$$\tau_{ssri}^* = \tau_{ssri,max}^* - \frac{\tau_{ssri,max}^* - \tau_{ssri,sand}^*}{1 + exp(-kF_1)}$$

Recall here that $i = 1$ corresponds to sand and $i = 2$ corresponds to gravel; thus $F_1$ and $F_2$ correspond to the content of sand and gravel, respectively, in the surface layer. in the surface layer. The form of $G$ has a steep dependence on $\phi$ for low stage, in the manner of Paintal (1971), and incorporates a modified form of the Parker (1978b) approximation to the Einstein (1950) relation for higher stage. In the above relations,

$$A=\begin{cases}70\,, & laboratory\\ 115\,, & field\end{cases}\,,\quad \chi=\begin{cases}0.908\,, & laboratory\\ 0.923\,, & field\end{cases}\,,\quad \phi'=\begin{cases}1.19\,, & laboratory\\ 1.27\,, & field\end{cases}$$

$$\tau^*_{ssr1,max}=\tau^*_{ssr2,max}\frac{D_2}{D_1}\,,\quad \tau^*_{ssr2,max}=0.061$$
$$\tau^*_{ssr1,sand}=0.065\,,\quad \tau^*_{ssr2,sand}=0.011\,,\quad k=20 \qquad \text{(3.83e-l)}$$

It is Eq. (3.83d) that plays the key role of increasing the mobility of gravel as sand content is increased.

Note that in Eqs. (3.83e-g) the constants in the relations differ between laboratory and field. There is a reason why the same underlying sediment transport relation might be expressed somewhat differently in the field as compared to the laboratory, even though the underlying physics is identical. This issue is discussed in more detail in Section 3.7.15.

In order to apply the above formulation, it is necessary to specify the characteristic grain sizes $D_1$ for the sand portion and $D_2$ for the gravel portion of the surface layer, the fractions $F_1$ and $F_2$ of sand and gravel, respectively in the surface layer, the submerged specific gravity of the sediment $R$ and shear velocity associated with skin friction $u_{*s}$. The Shields numbers $\tau_{si}^*$ are computed with Eqs. (3.46) and (3.47), and the parameters $\tau_{ssri}^*$ are evaluated from Eq. (3.83d) with the aid of Eqs. (3.83e-l). The parameters $W_i^*$ and $q_i$ are obtained from Eqs. (3.83a,b,c). The total bed-load transport rate per unit width $q_T$ and fraction bed-load in the $i$th grain size range $f_{bi}$ are then computed from Eqs. (3.26) and (3.28).

### 3.7.10 Surface-based Relation of Wilcock and Crowe

The surface-based relation of Wilcock and Crowe (2003) generalizes the two-grain method of Wilcock and Kenworthy (2002) to an arbitrary number of grain size ranges of both gravel and sand. That is, not only is the sand not excluded from the method, but it plays an important role in determining the gravel transport rate. A reference value $W_r^*$ of 0.002 was used to determine the reference stresses. The relation can be stated as

$$W_i^*=\frac{Rgq_i}{F_i u_{*s}^3}=G(\phi)$$

$$G = \begin{cases} 0.002\phi^{7.5} & for\ \phi < 1.35 \\ 14\left(1 - \dfrac{0.894}{\phi^{0.5}}\right)^{4.5} & for\ \phi \geq 1.35 \end{cases}$$

$$\phi = \frac{\tau^*_{sg}}{\tau^*_{ssrg}}\left(\frac{D_i}{D_g}\right)^{-b} \qquad \text{(3.84a-e)}$$

$$\tau^*_{ssrg} = 0.021 + 0.015 exp(-14F_s)$$

$$b = \frac{0.69}{1 + exp(1.5 - D_i / D_g)}$$

where $\tau_{sg}^*$ is given by Eq. (3.79d) and $F_s$ denotes the fraction of the material of the surface layer that is sand.

The essential role of sand is to depress the reference Shields number $\tau_{ssrg}^*$ via Eq. (3.84d). This in turn increases the mobility of all sizes, including gravel. The experiments of Wilcock et al. (2001), which were used to develop the above relation, clearly show that the addition of sand to a sand-gravel mix in a sediment-recirculating flume can increase the transport rate of gravel, in some cases substantially. Cui et al. (2003b) have confirmed this effect in an experimental study of sediment pulses in gravel-bed rivers using a sediment-feed flume.

The surface-based relation of Wilcock and Crowe (2003) has not yet been tested against field data. A notable aspect of the experiments used to develop the relation is the fact that the surface size distribution was measured immediately after a flow event, before substantial reworking could take place. In this sense, the relation is truly a surface-based relation. In point of fact the armor layer showed little variability in grain size distribution with stage over the range of the experiments.

Calculations with the above relation proceed as follows. The grain sizes and fractions ($D_i$, $F_i$) of the surface layer, submerged specific gravity of the sediment $R$ and shear velocity associated with skin friction $u_{*s}$ must be specified. The surface geometric mean size $D_g$ is computed from the fractions finer in the surface material and $\tau_{sg}^*$ is evaluated from Eqs. (3.82) (but with $D_{50} \rightarrow D_g$ therein) and (3.47). The fraction $F_s$ of the surface material that is sand is computed from the fractions $F_i$. The values of $W_i^*$ and $q_i$ are then obtained from Eqs.(3.84a) with the aid of Eqs. (3.84b,c,d,e). The total bed-load transport rate per unit width $q_T$ and fraction bed-load in the $i$th grain size range $f_{bi}$ are then computed from Eqs. (3.26) and (3.28).

### 3.7.11 Relation of Wu, Wang and Jia

The bed-load transport relation of Wu et al. (2000) was developed using data from one set of experiments using poorly sorted sand (Samaga et al., 1986), three sets of experiments using poorly sorted gravel (Liu, 1986; Kuhnle, 1993 and Wilcock and McArdell, 1993) and five gravel-bed streams in the United States (Williams and Rosgen,

1989). The model appears to be substrate-based, but the authors nowhere make a distinction between surface and substrate. The reference stress method was used to develop a hiding function. The relation can be expressed in the form

$$W_{ui}^* = \frac{Rgq_i}{\bar{f}_i u_{*s}^3} = 0.0053 \frac{1}{\left(\tau_{si}^*\right)^{3/2}} \left( \frac{\tau_{si}^*}{\tau_{suri}^*} - 1 \right)^{2.2}$$

$$\tau_{suri}^* = \tau_{suro}^* \left( \frac{p_{ei}}{p_{hi}} \right)^{-0.6} , \quad \tau_{suro}^* = 0.03 \qquad \text{(3.85a-e)}$$

$$p_{ei} = \sum_{j=1}^{N} \bar{f}_j \frac{D_i}{D_i + D_j} , \quad p_{hi} = \sum_{j=1}^{N} \bar{f}_j \frac{D_j}{D_i + D_j}$$

The authors also suggested a framework for removing form drag from the boundary shear stress based on adjusted Manning's *n*, but they do not specify how to implement it.

Wu et al. attempted to verify their bed-load relation in two ways. First, they compared the predictions of their relation in the limiting case of uniform sediment against 1859 sets of data from the compendium of Brownlie (1981), obtaining excellent agreement. The paper does not state, however, how many of the data refer to gravel. Second, they compared predictions for mixtures against laboratory and field data, all of which pertain to sand-bed streams. Again, excellent agreement is reported. The method awaits an independent test against a field gravel-bed stream.

Calculations with the above relation proceed as follows. The grain sizes and fractions ($D_i$, $\bar{f}_i$) of the substrate layer, submerged specific gravity of the sediment $R$ and shear velocity associated with skin friction $u_{*s}$ must be specified. The parameters $p_{ei}$ and $p_{hi}$ are computed from Eqs. (3.85d,e). The values of $\tau_{suri}^*$ are computed from Eqs. (3.85b,c). The values of $W_i^*$ and $q_i$ are then obtained from Eqs.(3.85a).

### 3.7.12 Relation of Powell, Reid and Laronne

The bed-load relation of Powell et al. (2001, 2003)) is solely based on field data from the Nahal Eshtemoa, an ephemeral stream in Israel subject to occasional violent floods. The streambed is virtually unarmored when the channel is dry. As a result it is not possible to use the data to discriminate between a surface-based and a substrate-based model. This notwithstanding, the model is treated as a surface-based formulation here.

The transport relation is based on the Parker (1978b) approximation to the Einstein (1950) relation. It is assumed that all material below 2 mm is removed and the grain size distribution renormalized so that it sums to unity before applying the model, which takes the form

$$W_i^* = \frac{Rgq_i}{F_i u_{*s}^3} = 11.2\left(1-\frac{1}{\phi}\right)^{4.5}, \quad \phi = \frac{\tau_{si}^*}{\tau_{sci}^*}$$
$$\frac{\tau_{sci}^*}{\tau_{sc50}^*} = F_{hc}\left(\frac{D_i}{D_{50}}\right) = \left(\frac{D_i}{D_{50}}\right)^{-0.74}, \quad \tau_{sc50}^* = \frac{\tau_{bsc}}{\rho RgD_{50}} = 0.03 \qquad (3.86a\text{-}d)$$

Eq. (3.86b) can be reduced with Eq. (3.86c) to yield

$$\phi = \frac{\tau_{s50}^*}{\tau_{sc50}^*}\left(\frac{D_i}{D_{50}}\right)^{-0.26} \qquad (3.86e)$$

While the model was not verified with data under conditions of mobile-bed armoring, it appears to have all the characteristics necessary to predict it.

Calculations with the above relation proceed as follows. The grain sizes and fractions ($D_i$, $F_i$) of the surface layer (from which the sand has been excluded), submerged specific gravity of the sediment $R$ and shear velocity associated with skin friction $u_{*s}$ must be specified. The surface median size $D_{50}$ is computed from the fractions finer in the surface material. The Shields numbers $\tau_{si}^*$ are computed with Eqs. (3.46) and (3.47). The values of $W_i^*$ and $q_i$ are then computed from Eq. (3.86a) with the aid of Eqs. (3.86b,c,d). The total bed-load transport rate per unit width $q_T$ and fraction bed-load in the $i$th grain size range $f_{bi}$ are then computed from Eqs. (3.26) and (3.28).

### 3.7.13 Relation of Ackers and White Extended with Proffitt and Sutherland's Hiding Function

The total bed material load predictor of Ackers and White (1973) has already been introduced in Chapter 2. It is based on a characteristic grain size $D$ of the bed material, and is not designed to compute the grain size distribution of the transported sediment. In point of fact very little of the data used to develop this relation was in the range of gravel-bed rivers. This notwithstanding, it has been found to be a good predictor of bed material load in both the laboratory and the field (Brownlie, 1981). Several efforts have been made to provide it with a hiding function that would allow generalization to sediment mixtures, including those of Day (1980), Ackers and White (1980), White and Day (1982) and Proffitt and Sutherland (1983). These reformulations were made with gravel-bed rivers specifically in mind. The hiding function due to Proffitt and Sutherland is presented here.

The reader is referred back to Eqs. (2.242a-l). The original relation of Ackers and White can be written as

$$q^* = C\frac{U}{\sqrt{RgD}}\left(\frac{U}{u_*}\right)^n\left(\frac{F_{gr}}{A}-1\right)^m \qquad (3.87a)$$

where the parameter $F_{gr}$ is a parameter specified as Eq. (2.242b) and requiring known values of $u_* u_{*s}$, $R$ and $D_{50}$ for its computation. In the above form the Einstein number $q^*$ is related to the transport parameter $G_{gr}$ of the original relation as

$$G_{gr} = \left( \frac{U}{\sqrt{RgD}} \right)^{-1} \left( \frac{U}{u_*} \right)^{-n} q^* \tag{3.87b}$$

In Eq. (3.87a) $F_{gr}$ is the primary dimensionless parameter driving sediment transport and $A$ is the value of $F_{gr}$ at the threshold of motion. These parameters are defined in Eqs. (2.242a-l); the parameter $F_{gr}$ contains an exponent $n$. The parameters $A$, $C$, $n$ and $m$ are all dependent on a dimensionless grain size $D_{gr}$, where in terms of the notation of this chapter

$$D_{gr} = Re_{p50}^{2/3} = \left( \frac{\sqrt{RgD_{50}}\, D_{50}}{\nu} \right)^{2/3} \tag{3.87c}$$

The generalization to mixtures is here treated as surface-based; it proceeds as follows. Eq. (3.87a) is amended to

$$q_{bmi}^* = C_i \frac{U}{\sqrt{RgD_i}} \left( \frac{U}{u_*} \right)^{n_i} \left( \frac{F_{gri}}{A_{ai}} - 1 \right)^{m_i} \tag{3.87d}$$

where

$$q_{bmi}^* = \frac{q_{bmi}}{F_i \sqrt{RgD_i}\, D_i}, \quad u_* = \sqrt{\frac{\tau_b}{\rho}} \tag{3.87e,f}$$

In the above relations $\tau_b$ denotes boundary shear stress at the bed and $u_*$ denotes shear velocity (total values, not skin friction only), and $q_{bmi}$ denotes the total volume bed material transport rate (bed-load plus bed material suspended load) per unit width per unit time. The parameters $F_{gri}$, $A_i$, $C_i$, $n_i$ and $m_i$ are all computed as in the original relation, but with the transformation $D_{50} \rightarrow D_i$. The adjusted value $A_{ai}$ embodying the hiding function is given as

$$\frac{A_{ai}}{A_i} = \begin{cases} \dfrac{1}{1.3} \ for \ \dfrac{D_i}{D_u} > 3.7 \\ \dfrac{1}{0.53 log\left(D_i / D_u\right) + 1} \ for \ 0.075 < \dfrac{D_i}{D_u} < 3.7 \\ \dfrac{1}{0.4} \ for \ \dfrac{D_i}{D_u} < 0.075 \end{cases} \tag{3.87g}$$

In addition, $D_u$ is computed from the relation

$$\frac{D_u}{D_{50}} = f_u(\tau^*_{50}), \quad \tau^*_{50} = \frac{\tau_b}{\sqrt{RgD_{50}}} \tag{3.87h,i}$$

given graphically in Figure 3.37a

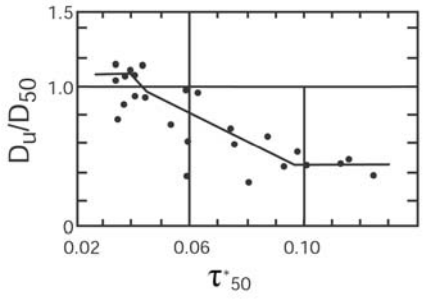


Figure 3.37 Plot of $D_u/D_{50}$ as a function of $\tau_{50}^*$ for the hiding function of Proffitt and Sutherland (1983) as applied to the sediment transport relation of Ackers and White (1973).

The original relation of Ackers and White (1973) was developed using the same data base as was used for the hydraulic resistance relation of White, Paris and Bettess (1980). It thus may be inferred that the relations should be used a pair, and that this also holds for the extension to mixtures.

In applying the above relation the grain sizes and surface layer fractions ($D_i$, $F_i$), cross-sectionally averaged flow velocity $U$, shear velocites $u_*$ and $u_{*S}$ the submerged specific gravity of the sediment $R$ and the kinematic viscosity of water $\nu$ must be specified. The surface median size $D_{50}$ is computed from the grain size distribution of the surface layer, and $\tau_{50}^*$ and $D_u$ are computed from Eqs. (3.87f,h,i). The parameters $n_i$, $m_i$, $F_{gri}$, $A_i$ and $C_i$ are all computed from the relations in Chapter 2, but with the transformation $D_{50} \rightarrow D_i$. The values of $A_{ai}$ are computed from Eq. (3.87g). The values of $q^*_{bmi}$ and $q_{bmi}$ are then computed from Eqs. (3.87d,e).

### 3.7.14 Other Bed-load Transport Relations for Mixtures

The relations given above represent only a sample of those available in the literature that describe the bed-load transport of sediment mixtures. Some others are listed below.

Proffitt and Sutherland (1983) generalized the Paintal (1971) transport relation to mixtures by developing a hiding relation, and used it to study the development of static armor. Misri et al. (1984) developed a new relation for bed-load transport for uniform material, and generalized it to mixtures using their own set of experimental data. The analysis clearly illustrates the failure of the Einstein (1950) hiding function. The only reason their relation is not presented in detail here is because the data used to develop the hiding function for mixtures are all restricted to the range of very coarse sand and pea gravel. Samaga et al. (1986) extended and corrected the model of Misri et al. (1984), this time including data from several rivers.

The Yang (1973) total bed material transport relation presented in Chapter 2 was developed for the prediction of sediment transport in sand-bed streams, and uses only a single sediment size. Yang (1984) extended this relation for gravel, again using only a single sediment size. Yang and Wan (1991) further extend these relations to allow for grain-size specific calculations of bed material transport of sediment mixtures, including gravel. These methods are summarized in Yang (1996).

Bridge and Bennett (1992) developed a Bagnold-type stream power formulation for the bed-load transport of mixtures. The model is notable in that it pays attention to differences in shape and density as well as size. Belleudy and SOGREAH (2000) adapted the bed material load predictor of Engelund and Hansen (1967) to mixtures in order to study bed-load transport. Their treatment of hiding had not yet been published at the time of writing of this chapter. Kleinhans and van Rijn (2002) generalized the bed-load transport relations of Meyer-Peter and Müller (1948) and van Rijn (1984) to mixtures. The generalization incorporates a stochastic sub-model in order to increase the accuracy of predictions near the threshold of motion. In addition to the hiding function of Egiazaroff (1965), the model also contains an empirical "hindrance" factor to account for the difficulty of movement of finer grains over and through a bed of coarser grains.

One relation that does not specifically pertain to mixtures merits mention here. Smart and Jaeggi (1983) and Smart (1984) have developed a bed-load transport relation specifically designed for channels with steep slopes, i.e. in excess of 3%. The data used to develop the relation were also used to show that the Meyer-Peter and Müller (1948) relation, for example, seriously underestimates the bed-load transport rate at such slopes. Their predictor yields only transport rates and not size distributions. This notwithstanding, many of the experiments used to develop it were performed with poorly sorted sediment. The issue of grain size distribution is of interest because Solari and Parker (2000) have documented and explained a reversal in mobility, with coarse grains rendered more mobile than fine grains in a mixture, at slopes exceeding about 2%.

Carson and Griffiths (1987) summarize several bed-load transport formulations and apply them to gravel-bed streams in New Zealand. Useful data on gravel transport for several streams in that country are presented. The treatment does not, however, focus on grain-size specific transport.

### 3.7.15 Sample Applications of Bed-load Relations

The results of sample calculations applied to a hypothetical gravel-bed river are presented here in order to illustrate the predictions of several of the relations presented above. The grain size distributions of the surface and substrate are presented in Figure 3.38a. The geometric mean size $D_g$, arithmetic mean size $D_m$, median size $D_{50}$, geometric standard deviation $\sigma_g$ and sand fraction $F_s$ of the surface material are given by the respective values 22.3 mm, 46.0 mm, 36.6 mm, 4.93 and 0.16; the corresponding values for the substrate $D_{ug}$, $D_{um}$, $D_{u50}$, $\sigma_{ug}$ and $F_{us}$ are, respectively, 10.9 mm, 33.1 mm, 21.0 mm, 5.22 and 0.28. Also shown in Figure 3.38a is the renormalized grain size

distribution of the surface with the sand removed, resulting in the respective values of $D_g$, $D_{50}$ and $\sigma_g$ of 40.7 mm, 45.3 mm and 2.36.

Calculations are performed for the relations of Ashida and Michiue (1972), Parker (1990a), Powell et al. (2001), Hunziker and Jaeggi (2002) and Wilcock and Crowe (2003), all of which are applied as surface-based relations. In applying the relations of Parker (1990a) and Powell et al. (2001) the sand has been excluded from the surface grain size distribution, and only the bed-load transport rates of the gravel sizes are calculated. In the other cases, bed-load transport rates of sand are predicted as well.

The hydraulic parameter entering into the calculations is the boundary shear stress due to skin friction $\tau_{bs}$, or alternatively the shear velocity due to skin friction $u_{*s}$ defined by Eq. (3.47). The range of values of $u_{*s}$ considered is 0.15 ~ 0.40 m/s, corresponding to a range of Shields numbers $\tau_{s50}^*$ based on surface median grain size of the surface material (sand included) of 0.038 ~ 0.270, where according to Eqs. (3.82) and (3.47)

$$\tau_{s50}^* = \frac{u_{*s}^2}{RgD_{50}} \tag{3.88}$$

Each model is used to compute a) the total volume gravel bed-load transport rate per unit width $q_G$ (summed over all gravel sizes; sand excluded), b) the geometric mean size of the gravel portion of the bed-load $D_{Gg}$ and c) the geometric standard deviation of the gravel portion of the bed-load $\sigma_{Gg}$. In addition, in all cases except the Parker (1990a) and Powell et al. (2001) relations, which exclude sand from the calculation, the fraction $f_{bG}$ of the bed-load consisting of gravel is computed.

The results are shown in Figures 3.38b~e. In Figure 3.38b it is seen that the predictions for $q_G$ fall well within an order of magnitude at all but the lowest shear velocities. The relations of Ashida and Michiue (1972) and Hunziker and Jaeggi (2002) predict vanishing transport rate for values of $u_{*s}$ below a value between 0.175 and 0.20 m/s due to the presence of relatively high critical Shields numbers in the formulations. At the highest transport rates the difference between the predicted values of $q_G$ is less than a factor of two.

The predictions for $D_{Gg}$ in Figure 3.38c are also quite similar. In all cases the gravel bed-load becomes coarser with increasing friction velocity, and the degree of coarsening levels off at the highest values of friction velocity. The relations of Hunziker and Jaeggi (2002) and Powell et al. (2001) show the strongest tendency for the gravel bed-load to coarsen with friction velocity, and the relation of Wilcock and Crowe (2003) shows the least tendency. Figure 3.38d indicates that the predicted values of $\sigma_{Gg}$ nearly all fall between 2 and 3, with a tendency for $\sigma_{Gg}$ to decrease with increasing friction velocity through most or all of the calculated range of $u_{*s}$ for all relations except Ashida and Michiue (1972).

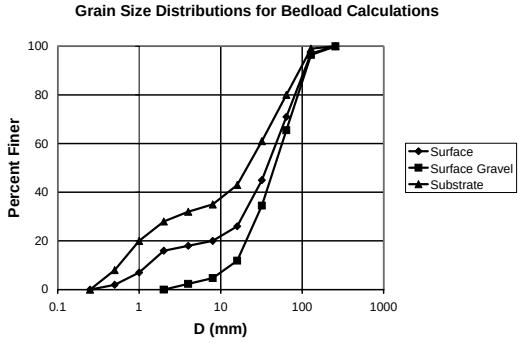


a)

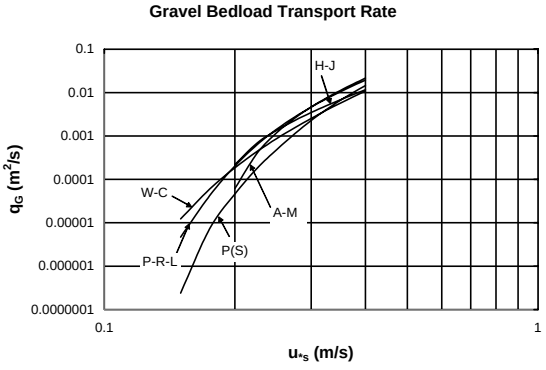


b)

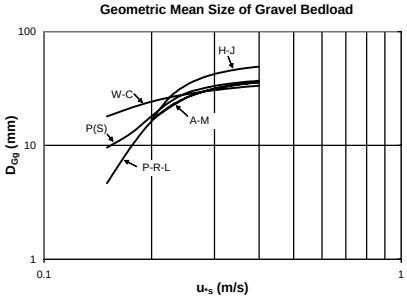


c)

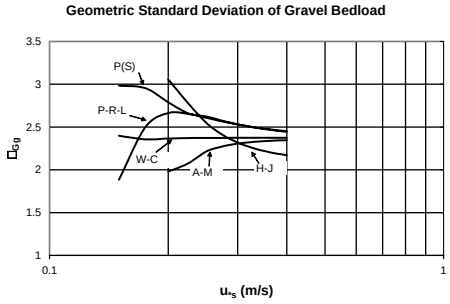


d)

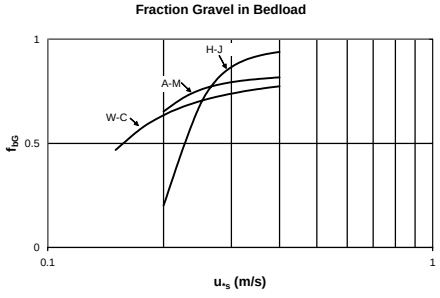


e)

Figure 3.38 Predictions of bedload transport using the relations of Ashida and Michiue (1972) (A-M), Parker (1990a) (P(S)), Powell et al. (2001) (P-R-L), Hunziker and Jaeggi (2002) (H-J) and Wilcock and Crowe (2003) (W-C). a) Grain size distributions for bedload calculations, b) total volume gravel bedload transport rate, c) geometric mean size of gravel bedload, d) geometric standard deviation of gravel bedload, and e) fraction of gravel in bedload (the rest being sand).

The most variation among the predictions is in the relation between fraction gravel in the bed-load $f_{bG}$ and $u_{*S}$ of Figure 3.38e. This is likely because the tendency for sand in gravel-bed streams to go into suspension rather easily makes the prediction of the bed-load transport of sand rather inaccurate. Note in this regard that the fraction of sand in the bed-load is given as $1 - f_{bG}$. This comment notwithstanding, for values of $u_{*S}$ above 0.25 m/s the bed-load transport is predicted to be predominantly gravel for all four relations in the figure.

Some further discussion of Figure 3.38b is warranted. It is encouraging to see that the predictions of the relations of Ashida and Michiue (1972), Hunziker and Jaeggi (2002) and Wilcock and Crowe (2003), all of which are based on laboratory data, are for the most part bracketed by the field-based relation of Powell et al. (2001) as an upper bound and the field-based relation of Parker (1990a) as a lower bound. This lends confidence to the concept of applying the results of laboratory studies of gravel transport to field-scale rivers.

These comments notwithstanding, the predictions of the Parker (1990a) relation and that of Powell et al. (2001), both of which are based on field data, do show substantial differences. Some of the possible reasons for these differences, as well as avenues for reducing them in the future, are discussed in Section 3.7.18.

### 3.7.16 Topographic Variability, Patchiness and Partial Transport

Rivers are not flumes; they are considerably more complex. Flumes are valuable tools for the study of sediment transport, but results based on flume data are not directly transferable to the field without accounting for the spatial and temporal variability characteristic of the field. A vivid example of this is provided by the bed material load (bed-load plus suspended load) predictor of Brownlie (1981). Brownlie found that his regression relation developed for laboratory data was modestly but consistently in discrepancy with his regression for field data. As a result the prediction for load is multiplied by a factor of 1.000 in applying the relation to flume data and a factor of 1.268 in applying the relation to the field.

The reason for this is not hard to decipher. The explanation provided here is adapted from the work of Paola and Seal (1995), Paola (1996) and Paola et al. (1999). Sediment transport predictors are invariably nonlinear in their primary driving parameter, e.g. Shields number. That is, a doubling of Shields number produces more than a doubling of the load. This effect is particularly strong at low transport rates.

To see this, consider a natural channel, with bars, bends and other elements of channel complexity. Local skin friction can be expected to vary spatially according to some probability distribution. The same holds true for local mean grain size, and thus for the Shields number based on skin friction itself. The more complex the channel is, the higher will be the standard deviations of these fluctuations. In a nonlinear transport relation, zones of high Shields number will magnify the transport rate far more than

zones of low Shields number depress it. The result is to elevate the overall transport rate. In addition, if the transport relation is grain size-specific and renders finer surface grains more mobile than coarser surface grains, the effect of nonlinearity can also act to bias the load toward the fine grains, especially in the case of relatively low boundary shear stress.

To see this, it is useful to begin with the case of uniform sediment. Consider a bed-load transport relation of the generic form

$$q = \sqrt{RgD}D\left[\frac{\tau_{bs}}{\rho RgD} - \tau_{sc}^{*}\right]^{n_L} \tag{3.89a}$$

where $\tau_{sc}^{*}$ denotes a critical Shields number and the exponent $n_L$ is expected to be greater than unity. In most applications of flume-derived sediment transport relations to the field, the parameters actually put into the equation are the spatial averages, i.e. in this case $\overline{\tau}_{bs}$ and $\overline{D}$ (the spatial averaging in the case of grain size being performed on the $\psi$ scale rather than directly on $D$). Because of the nonlinear dependencies in Eqs. (3.89a) and (3.1b) the input of these averaged parameters does not yield $\overline{q}$. Instead,

$$\overline{q} = \overline{\sqrt{RgD}D\left[\frac{\tau_{bs}}{\rho RgD} - \tau_{sc}^{*}\right]^{n_L}} = C_{comp}\sqrt{Rg\overline{D}}\,\overline{D}\left[\frac{\overline{\tau}_{bs}}{\rho Rg\overline{D}} - \tau_{sc}^{*}\right]^{n_L} \tag{3.89b}$$

where the overbar denotes averaging over a reach containing morphologic complexity and $C_{comp}$ is a dimensionless complexity coefficient. Abbreviating the functional relation of Eq. (3.89b), the above relation can be summarized as

$$\overline{q} = C_{comp}\,q\left(\overline{\tau}_{bs}, \overline{D}\right) \tag{3.89c}$$

where $q(x,y)$ denotes the functional relation, and $C_{comp} > 1$ is a dimensionless parameter that amplifies the sediment load.

Paola and Seal (1995), Paola (1996) and Paola et al. (1999) describe a way to implement the above calculation using probability densities for $\tau_{bs}$ and $D$. They find that C takes the value of 1 in a straight flume with no bedforms and no local sorting. This value increases with increasing complexity, becoming as large as 3 – 4 in braided streams. The above analysis provides a conceptual explanation for the multiplicative factor 1.268 in the Brownlie (1981) relation; it is none other than the complexity coefficient $C$. The fact that it is not larger than 1.268 is likely related to the fact that sediment transport measurements in natural streams are usually taken along the straightest reaches with the least variation possible, e.g. in a straight reach rather than at the apex of a bend. Brownlie (1981) himself was cognizant of this nonlinear amplification effect and explained the factor in terms of it.

The above framework receives further verification in terms of the flume experiments of Onishi et al. (1972). Onishi et al. studied sediment transport in two flumes, one straight and the other with meandering sidewalls, but with an average down-channel bed slope that was identical to that of the straight flume. For the same water discharge and sediment size, the sediment transport rate was measurably larger in the meandering flume.

Paola and Seal (1995) have extended the above analysis to sediment mixtures. Consider a generic model transport relation of the form

$$q_i = \sqrt{RgD_i}\, D_i F_i \left[ \frac{\tau_{bs}}{\rho RgD_i} - \tau^*_{scg} \left( \frac{D_i}{D_g} \right)^{-m} \right]^{n_L} \tag{3.90a}$$

where it is again expected that $n_L > 1$. Note that the above equation represents a direct generalization of Eq. (3.89a) to mixtures, with the term containing the exponent $m$ characterizing a hiding function. Again, the parameters actually input in field applications are usually the spatial averages $\overline{\tau}_{bs}$, $\overline{F_i}$ and $\overline{D}_g$. Again,

$$\overline{q_i} = \overline{\sqrt{RgD_i}\, D_i F_i \left[ \frac{\tau_{bs}}{\rho RgD_i} - \tau^*_{scg} \left( \frac{D_i}{D_g} \right)^{-m} \right]^{n_L}} = C_{comp,i} \sqrt{RgD_i}\, D_i \overline{F_i} \left[ \frac{\overline{\tau}_{bs}}{\rho RgD_i} - \tau^*_{scg} \left( \frac{D_i}{\overline{D}_g} \right)^{-m} \right]^{n_L} \tag{3.90b}$$

The above relation can be summarized as

$$\overline{q_i} = C_{comp,i}\, q_i \left( \overline{\tau}_{bs}, \overline{D}_g, \overline{F_i} \right) \tag{3.90c}$$

where $q_i(x,y,z)$ denotes the functional relation for bed-load transport and $C_{comp,i}$ are dimensionless grain size-specific complexity coefficients. Thus

$$\overline{q}_T = \sum_{i=1}^{n} C_{comp,i}\, q_i(\overline{\tau}_{bs}, \overline{D}_g, \overline{F_i}) > \sum_{i=1}^{n} q_i(\overline{\tau}_{bs}, \overline{D}_g, \overline{F_i}) = q_T(\overline{\tau}_{bs}, \overline{D}_g, \overline{F_i}) \tag{3.90d}$$

so that the total bed-load transport is amplified. In addition, the morphologically averaged grain size fractions $\overline{f}_{bi}$ of the bed-load differ from the ones that would be obtained using averaged parameters as input,

$$\overline{f}_{bi} = \frac{\overline{q}_i}{\overline{q}_T} \neq \frac{q_i(\overline{\tau}_{bs}, \overline{D}_g, \overline{F_i})}{q_T(\overline{\tau}_{bs}, \overline{D}_g, \overline{F_i})} \tag{3.90e}$$

and this bias is typically in the direction of a finer bed-load size distribution.

Paola and Seal (1995) found a notable enhancement of downstream fining in the North Fork Toutle River, Washington, USA due to the presence of "patches" and "lanes" of sediment mixtures with differing mean sizes. Two of these "patches" are visible in Figure 3.7. Paola (1996) outlines an algorithm for the adjustment of any sediment transport relation to account for channel complexity. In order to implement it, however, the probability distributions of spatial variation in boundary shear stress and grain size distribution must be known, measured or inferred.

The two-grain relation of Wilcock and Kenworthy (2002) is reconsidered in light of the above. Recall that the bed-load transport rates in field streams used by them to develop their relation tended to be consistently higher than in the laboratory by a factor that varied with transport rate but was close to 1.64. This difference is most likely not an expression of a fundamental difference in the physics of field streams compared to laboratory flumes, but rather an expression of the fact that field streams are more complex than flumes.

A second issue of particular interest for gravel-bed streams is partial transport. Partial transport may be defined as a condition in which a portion of the grains on the bed surface are actively transported, while the balance of the surface grains remain entirely immobile (Wilcock and McArdell, 1993). A case of particular interest is when the immobile grains are coarser than a threshold size.

The following thought experiment illustrates one of the dilemmas of partial transport. A flume is supplied with a modest, constant feed of heterogeneous sediment and allowed to develop to a macroscopic mobile-bed equilibrium, here called case A. At this equilibrium all sizes fed in must exit the flume at the same macroscopic rate. Now cut off the supply of the very coarsest grains from the feed, and, if necessary, slightly increase the feed rate of the remaining load so as to prevent bed degradation. Since the bed does not degrade, some of the coarsest grains will remain at least partially exposed on the bed. These exposed grains must, however, attain a configuration (by partial burial, the formation of stone clusters etc.) so as to eventually render them completely immobile. All the finer sizes continue to move through the system, so resulting in case B.

Now the hydraulic conditions have barely changed, but in case A the largest stones are mobile, whereas in case B they are not. At present there is no sediment transport relation that contains enough physics to discriminate between the two cases.

In recent years, however, there has been an increasing interest in partial transport, resulting in a data base that may help resolve this issue in the future (Wilcock and McArdell, 1993, 1997; Hassan and Church, 2000). Figure 3.39 illustrates three plots of the ratio of unit bed-load transport rate $q_i/F_i$ versus grain size $D_i$, one from Oak Creek, Oregon, USA (from Wilcock, 1997a), one for the experiments of Wilcock and McArdell (1997), and one from the Nahal Eshtemoa, Israel (Powell et al., 2001). Recalling that the fractions in the bed-load $f_{bi}$ are related to the fractional transport rates $q_i$ according to Eq.

(3.28), it is easily shown that if the ratio $q_i/F_i$ is constant for all grain sizes $D_i$ for a given flow, then

$$f_{bi} = F_i \tag{3.91}$$

so that the grain size distribution of the bed-load is identical to that of the bed surface. That is, a condition of perfect surface-based equal mobility prevails. A deviation from this constancy denotes size-selective transport. If $q_i/F_i$ drops to zero for any grain size range, partial transport prevails.

Figure 3.39a from Oak Creek reveals partial transport with an absence of the coarsest grains in the bed-load for the lowest flow in the diagram, size-selective transport biased toward the finer grains at somewhat higher flows, and near-equal mobility, or rather a slight bias toward the coarser grains at the highest flows, which transport the bulk of the sediment. Figure 3.39b reveals a much stronger tendency toward partial transport at the lower stages of the experiments of Wilcock and McArdell (1997) in a sediment-recirculating flume, with all sizes in motion and near-equal mobility only at the highest stage in the diagram. In the case of the Nahal Eshtemoa, Figure 3.39c shows possible partial transport at the two lowest stages, size-selective transport at the two next-highest stages and near-equal mobility at the seven higher stages.

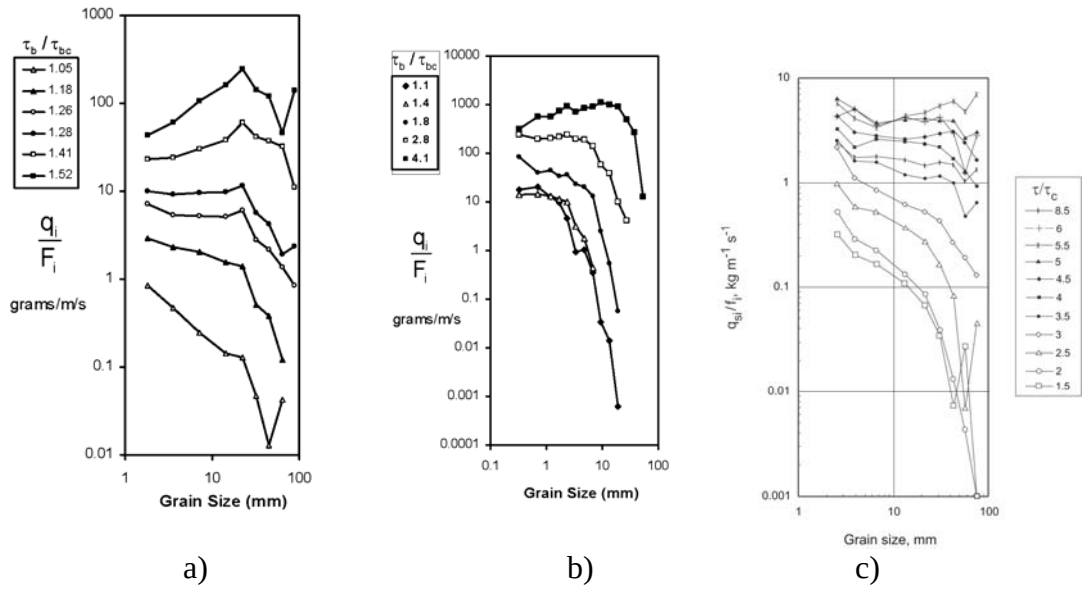


a) b) c)

Figure 3.39 Plots of $q_i/F_i$ versus $D_i$ for a) Oak Creek field data as presented by Wilcock (1997a); b) experiments of Wilcock and McArdell (1997); and c) Nahal Eshtemoa field data of Powell et al. (2001).

The issue of partial transport becomes particularly important when the diversion of floodwater from a gravel-bed river is considered. The loss of floodwater may impose a perennial condition of partial transport, with the coarser grains no longer participating in the load. As a result, the bed may no longer be reorganized and renewed by floods,

and habitat may degrade, as in the case of the Trinity River below Lewiston Dam (Kondolf and Wilcock, 1996).

### 3.7.17 Surface-based versus Substrate-based

A common objection to the use of surface-based formulations is that they require a knowledge of the composition of the surface, or active layer at any given time in order to compute the bed-load transport rate. The issue is important because the composition of the surface is free to respond to changes in the flow. Direct information on the composition of the surface is usually available, however, only at low flow when the bed can be sampled. So it would appear that there is no obvious way to know what surface grain size distribution to use in the model.

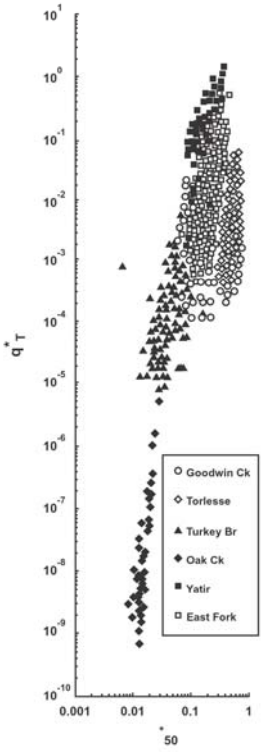


Figure 3.40 Dimensionless Einstein number based on total bedload transport rate $q_T^*$ versus Shields stress $\tau_{50}^*$ for six streams: Goodwin Creek, Mississippi, USA, East Fork River, Wyoming, USA, Oak Creek, Oregon, USA, Nahal Yatir, Israel, Turkey Brook, England, UK and Torlesse Stream, New Zealand. From Reid et al., (1995).

The above dilemma is easily resolved. Surface-based models are designed to be implemented in a numerical simulation of the flow and sediment transport. The low-flow composition of the surface is input as an initial condition. The calculation proceeds by solving a) the grain size-specific Exner equation of sediment continuity, b) a surface-based bed-load transport formula and c) an appropriate predictor of the flow, e.g. the St. Venant shallow water equations through a flood hydrograph. In this way the composition of the surface layer is computed along with other parameters such as bed elevation, bed-load transport rate, and bed-load grain size distribution, at every time step of the calculation. The issue is described in more detail in Section 3.9.

In some cases, however, it may not be feasible to implement a full numerical calculation; one may simply wish to estimate the bed-load yield and grain size distribution over one hydrograph or for a given flow duration curve. In such cases, a substrate-based formulation may be appropriate in that it requires a parameter, i.e. the grain size distribution of the substrate, which can be measured at low flow and which is unlikely to change too much in engineering time.

### 3.7.18 Comparison of Relations against Field Data: Future Developments

There have not been many comprehensive independent tests of predictive relations for bed-load transport of heterogeneous sediments against data, and in particular field data. Two attempts are outlined in Gomez and Church (1989) and van der Scheer et al. (2001). The results are not particularly encouraging. Gomez and Church state "No formula performs consistently well." In the case of van der Scheer et al., various formulas were compared with three experimental sets, each using a mix of sand and pea gravel and with well-developed dunes, as well as the data set due to Day (1980). The first three sets are likely to be outside the range of applicability of most relations developed for heterogeneous gravel-bed streams. Not surprisingly, most of the relations performed poorly; the Ackers and White (1973) relation with the Proffitt and Sutherland (1983) hiding correction performed the best.

In Figure 3.40 Reid et al. (1995) have plotted the Einstein number $q_T^*$ based on total bed-load transport rate summed over all grain sizes and on $D_{50}$ versus the Shields number $\tau_{50}^*$ based on average boundary shear stress and $D_{50}$ for six rivers; Goodwin Creek, Mississippi, USA, East Fork River, Wyoming, USA, Oak Creek, Oregon, USA, Nahal Yatir, Israel, Turkey Brook, England, UK and Torlesse Stream, New Zealand. The parameter $D_{50}$ was measured at low flow. The data from Oak Creek, Turkey Brook and Nahal Yatir appear to collapse into a single curve. The data from the East Fork, Goodwin Creek and Torlesse Stream are shifted to the right of this curve, and clearly do not collapse into a single curve. This same shift to the right can be seen in the data of Ashworth and Ferguson (1989) from three streams in Scotland and Norway. Reid et al. note, "Transport efficiency is shown to vary considerably for each stream and from one stream to another, suggesting that it may not be possible to incorporate it easily into bed-load equations in order to improve levels of prediction."

Their conclusion may be overly pessimistic. They themselves point out that Oak Creek, Turkey Brook and the Nahal Yatir define a relatively consistent relation, a point amplified upon by Almedeij and Diplas (2003). This issue is explored in more detail in Section 3.10. In addition, Wilcock and Kenworthy (2002) have developed a consistent relation for Oak Creek, Goodwin Creek and the East Fork River upon having accounted for the effect of sand content in the bed. A proper accounting of the relevant physics is thus likely to bring most of the disparities into concordance before the next time ASCE Manual No. 54 is revised. Considerations that might help bring about this concordance are given below.

1. As noted in Section 3.7.2, most transport relations for gravel-bed streams gloss over the issue of form drag (as opposed to sand-bed streams). Form drag may be more important than previously thought (Hey, 1989; Millar, 1999). Form drag associated with channel bars and bends may vary with channel width, slope, standard deviation of the parent sediment etc. The presence of large, immobile colluvial boulders in streams may contribute to form drag. A form drag predictor for gravel-bed streams needs to be developed.

2. As described in Section 3.7.16, channels with the same mean morphological characteristics may transport sediment differently due to differing levels of complexity. The methodology discussed in that section needs to be implemented for more field streams.

3. As noted in Section 3.7.16, gravel-bed streams with strong tendencies toward partial transport may behave differently from streams with only size-selective transport. Predictive methods specifically including partial transport need to be developed.

4. As illustrated by the relations of Wilcock and Kenworthy (2002) in Section 3.7.9 and Wilcock and Crowe (2003) in Section 3.7.10, variation in the sand content can in some cases dramatically affect the transport of gravel. The recent efforts to quantify this effect need to be redoubled.

5. If the composition of the surface layer changes with stage, the interaction of this variation with the bed-load transport may be intense. The few attempts to quantify this effect in the field (e.g. Andrews and Erman, 1986) need to be augmented.

6. Finally, as noted in Section 3.7.2, the fluid mechanics used to calculate primary parameters controlling bed-load transport, such as boundary shear stress, is often much too primitive. In many cases boundary shear stress $\tau_b$ is estimated from the simple depth-slope product rule for to steady, uniform (normal) flow in a wide, rectangular channel;

$$\tau_b = \rho g H S \tag{3.92}$$

where $S$ denotes mean bed slope and $H$ denotes mean depth. The technology presently exists to perform the computations needed to obtain more precise measurements of boundary shear stress, including the effects of hydrograph variation, spatial variation, secondary flow, convergences and divergences etc. This technology needs to be applied more consistently to the issue of bed-load transport in gravel-bed rivers.

## 3.8 FIELD DATA

Since ASCE Manual No. 54, "Sedimentation Engineering," was first published in 1975, a major expansion of the data base for the transport of heterogeneous sediments in rivers has taken place. This data base serves two roles. Firstly, it allows the engineer working on with a problem a particular stream to identify a similar stream for which the transport rate and grain size distribution have been measured in order to determine appropriate countermeasures. Secondly, it is an essential key to future advances in predictive technology. With this in mind, a partial accounting of this data base is provided in Table 3.2 below.

Wilcock (2001) has outlined a practical method for estimating sediment transport rates in gravel-bed streams. The importance of interaction between field-based and experimental research has been emphasized by Wilcock (2000). Kuhnle et al. (1989) and Kuhnle (1996) have pointed out the need to consider systematic temporal variation in flow and sediment transport rates, an effect that is likely to be more important in the field than in the laboratory.

In addition to the streams of Table 3.2, a research group in Colorado centered around K. Bundt (Bundt et al., 2004) has collected a substantial set of data for bedload transport in small gravel-bed streams, mostly in Colorado. When this database becomes public is should provide a most useful addition to the database represented by Table 3.2.

Table 3.2: Streams for which gravel/sand transport rate and grain size distribution have been measured; $S$ denotes slope and $D_{u50}$ denotes substrate or bulk median size.

| *STREAM* | *LOCATION* | *S* | $D_{u50}$, mm | *DATA SOURCE* |
|---|---|---|---|---|
| Allt Dubhaig | Scotland, UK | 0.0040 – 0.021 | 23-98 | Ashworth and Ferguson (1989) |
| Bambi Creek | Alaska, USA | 0.0082 | 14.7 | Sidle (1988); Smith et al. (1993); Lisle (1995) |
| Carl Beck | England, UK | 0.039 | 73 | Carling and Reader (1982), Carling (1989) |
| Clearwater River | Idaho, USA | 0.00048 | 18 | Emmett (1976) |
| Rio Cordon | Italy | 0.17 | 90* | Lenzi et al. (2000) |
| East Fork River | Wyoming, USA | 0.0007 | 6.4 | Emmett et al. (1980) |
| Elbow River | Alberta, Canada | 0.00745 | 28 | Hollingshead (1971) |
| Nahal Eshtemoa | Israel | 0.0075 | 18 | Powell et al. (2001) |
| Feshie River | Scotland, UK | 0.0086 – 0.0094 | 52 – 63 | Ashworth and Ferguson (1989) |
| Goodwin Creek | Mississippi, USA | 0.0033 | 14.2 | Kuhnle (1992) |
| Great Eggleshope Beck | England, UK | 0.010 | 67.7 | Carling and Reader (1982), Carling (1989) |
| Harris Creek | British Columbia, Canada | 0.013 | 20 | Hassan and Church (2001) |
| Jacoby Creek | California, USA | 0.0063 | 20.6 | Lisle (1989) |
| Las Vegas Wash | Nevada, USA | 0.003 – 0.004 | 5.2 | Duan and Chen (2003) |
| Lyngsdalselva | Norway | 0.020 – 0.028 | 69 | Ashworth and Ferguson (1989) |
| North Casper Creek | California, USA | 0.013 | 23.7 | Lisle (1989) |
| Oak Creek | Oregon, USA | 0.01 | 20 | Milhous (1973) |
| Nahal Og | Palestinian West Bank | 0.014 | 15 | Hassan and Egozi (2001) |
| Ohau River | New Zealand | 0.0065 | 19.2 | Thompson (1985) |
| Redwood Creek 1 | California, USA | 0.014 | 9.1 | Lisle and Madej (1992) |
| Redwood Creek 2 | California, USA | 0.026 | 18.1 | Lisle and Madej (1992) |
| Snake River | Idaho, USA | 0.0011 | 27 | Emmett (1976) |
| Tanana River | Alaska, USA | 0.0008 | 20.3 | Burrows et. al. (1981), Burrows and Harrold (1983) |
| Toklat River | Alaska, USA | 0.018 | 28.5 | pers. comm. to Lisle (1995) |
| Tom McDonald Creek | California, USA | 0.0060 | 10.8 | Smith (1990) |
| Torlesse Stream | New Zealand | 0.067 | 15* | Hayward (1980) |
| Turkey Brook | England, UK | 0.0086 | 16 | Reid et al. (1985), Reid and Frostick (1986) |
| Virginio Creek | Italy | 0.008 | 13 | Tacconi and Billi (1987) |
| Nahal Yatir | Israel | 0.0088 | 10 | Reid et al. (1995) |

*Denotes surface rather than substrate size.

## 3.9 ABRASION

In addition to sorting their sediment through selective transport, rivers can also modify their grains through abrasion. Gravels and sands that have been in a river for a sufficiently long time tend to be rounded as a consequence of abrasion. This effect is illustrated in Figure 3.13.

As noted in Section 3.1, many rivers show a clear pattern of downstream fining of characteristic grain size. An example is given in Figure 3.10. This decrease in characteristic grain size may be due to selective transport of finer grains, abrasion, a tendency for tributaries farther down in the drainage network to deliver finer sediment or some other cause. In order to help resolve this issue it is necessary to have some understanding of fluvial abrasion.

The issue can be of considerable engineering importance. Large amounts of fresh, and in many cases relatively weak sediment can enter river systems from natural or human-induced landslides (Figure 3.12) or from the disposal of waste sediment from e.g. a mine (Figure 3.16). This sediment often consists of a mixture of lithologies, each of which has a different resistance to wear. In addition, the sediment may be highly fractured and thus far easier to abrade than material that has been in the river system for some time. In this sense one may think of the gravel in rivers at points far downstream of the source area as the very tough residual of an input that has had all the weaker members ground out of it. Thus if abrasion plays a significant role in the reorganization of inputs of fresh sediment, the gravel bed-load transport rates at distances of 10's or 100's of km downstream of the source area may be considerably less than if abrasion had been neglected, because most of the gravel may be ground into sand and silt.

Mine waste in particular may contain such elements as copper, lead and cadmium, which in bioavailable form can lead to serious damage to riparian ecosystems. One step in the process by which these elements become bioavailable is the grinding of the stones that contain them into silt. The large ratio of surface area to volume of silt-sized grains as compared to e.g. gravel facilitates the desorption of toxic elements into the water column. In addition, elevated concentrations of suspended silt in rivers can damage stream habitat by clogging fish gills, reducing visibility, and drowning near-bank and floodplain habitat in mud.

### 3.9.1 Quantification of Abrasion

The focus here is on the abrasion of gravel. The most common sand lithology in rivers, i.e. quartz, is highly resistant to abrasion, and the process by which sand grains become rounded is evidently a very slow one. Maunsell and Partners (1982) have demonstrated the very subdued tendency for sand to abrade as compared to gravel.

In most cases the process of breakdown of a single clast (stone) consists of an initial period during which it may shatter, followed by a much longer period during

which it is gradually worn down by abrasion, producing silt and some sand as byproducts. There are several ways by which abrasion is accomplished.

1. In the case of rivers in cold regions, *in situ* freeze-thaw processes can play a role in abrasion.

2. In the case of meandering gravel-bed rivers with well-developed floodplains, channel migration can result in river gravels being stored under finer material in the floodplain for extended periods of time. This can result in the formation of a thin weathering rind. When the clast in question is re-introduced into the channel by migration or avulsion, the rind may be quickly shed, resulting on a one-time abrasion of the clast (Bradley, 1970).

3. As gravel clasts are carried downstream as bed-load, frequent collisions with other clasts in the bed result in a gradual wear, the main byproduct being silt (Shaw and Kellerhals, 1982). The exposition below focuses on this type of abrasion.

Abrasion by gradual wear due to fluvial transport is quantified in terms of an abrasion coefficient. The abrasion coefficient defined as the fractional volume loss (or equivalently mass loss) per unit distance traveled $\alpha_v$ is

$$\alpha_v = -\frac{1}{V_p}\frac{dV_p}{ds} \tag{3.93a}$$

where $V_p$ denotes particle volume and $s$ denotes distance of travel. The corresponding coefficient based on grain size $D$ is

$$\alpha_d = -\frac{1}{D}\frac{dD}{ds} \tag{3.93b}$$

Approximating grain shape as spherical so that $V_p \sim D^3$, it is found that

$$\alpha_v = 3\alpha_d \tag{3.94}$$

Substituting Eq. (3.1) into Eq. (3.93b),

$$\frac{d\psi}{ds} = -\frac{\alpha_d}{ln(2)} \tag{3.95}$$

For the case of an abrasion coefficient that varies with neither clast size nor downstream distance, Eqs. (3.94) and (3.95) can be solved to yield the results

$$D = D_u\, exp\left(-\alpha_d s\right), \quad \psi = \psi_u - \frac{\alpha_d}{ln(2)}s \tag{3.96a,b}$$

where $D_u$ and $\psi_u$ denote upstream values.

Eqs. (3.96a,b) are alternate expressions of Sternberg's law for grain size change in the downstream direction. The downstream variation in grain size in many rivers often approximates the exponential relation (3.96a), but this in and of itself is no guarantee that abrasion is the cause. A very similar pattern of downstream fining can be driven mainly or exclusively by selective transport of finer grains, as discussed in Section 3.12.

It is in general very difficult to measure abrasion directly in the field. As a result, researchers have resorted to rotating tumbling mills such as the Los Angeles abrasion mill, concrete mixers and circular flumes to quantify abrasion. The characteristics of the device are used to compute an equivalent distance traveled, and the resulting diminution in grain size is measured, allowing $\alpha_d$ to be computed from Eq. (3.93b).

Summaries of abrasion coefficients from such tests are given in Shaw and Kellerhals (1982), Kodama (1994a) and Rice (1999). Figure 3.41 provides a summary of experimentally-determined abrasion rates. It is seen that $\alpha_d$ has been found to vary from about $1x10^{-5}$ $km^{-1}$ to above $1x10^{-1}$ $km^{-1}$. The abrasion coefficient is partly a function of lithology, with quartz generally having a relatively low abrasion rate, limestone with a middling rate and some mudstones with a very high rate. In addition, it can vary with grain size itself. Finally, Mikoš (1993, 1994, 1995) has documented a tendency for the abrasion rate to decrease with increasing distance of travel, and for it to increase with increasing speed of a tumbling mill for the same travel distance.

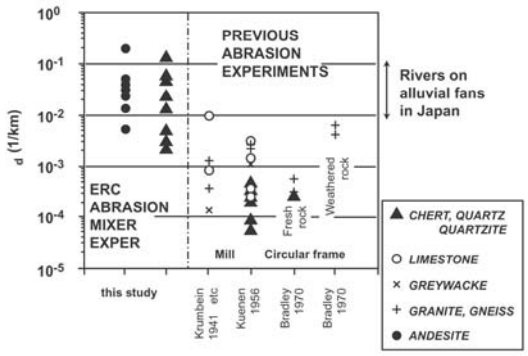


Figure 3.41 Abrasion coefficients $\alpha_d$ obtained from experiments by various researchers, as presented by Kodama (1994a).

In Figure 3.41 the abrasion rates reported by Kodama (1994a) are in the range $2x10^{-3}$ ~ $2x10^{-1}$ $km^{-1}$, and are generally substantially higher than those reported in earlier studies. Kodama is of the opinion that the earlier studies did not adequately replicate the violent grain-to-grain collisions during severe floods, and thus underestimated the abrasion rate. His experiments in a concrete mixer were designed to provide a better model of the process. The values reported by Mikoš (1995) are also higher than the earlier values, ranging from $3x10^{-3}$ ~ $2x10^{-2}$ $km^{-1}$.

### 3.9.2 Application to Rivers

Eq. (3.96a) can be used to define a "half-distance" $L_{1/2}$ for abrasion over which grain size is reduced by half;

$$L_{1/2} = \frac{0.693}{\alpha_d} \tag{3.97}$$

For a value of $\alpha_d$ of $1\text{x}10^{-5}$ km$^{-1}$ $L_{1/2}$ takes the value 69,300 km, and abrasion is likely to play a negligible role in the downstream change in grain size in a river. For a value of $\alpha_d$ of $1\text{x}10^{-1}$ km$^{-1}$ $L_{1/2}$ takes the value 6.93 km, and abrasion is likely to play a dominant role in downstream fining.

The application of abrasion coefficients to rivers is rather more complicated than simply plotting grain size as a function of distance using Eq. (3.96). There are two reasons for this. Eq. (3.96) does not account for grain size variation due to selective transport. In addition, when a moving grain strikes a non-moving grain on the bed, both can be expected to abrade, so that on the order of half of the abrasion is likely to be realized *in situ*.

To date there have not been many implementations of the abrasion term in the Exner equation of sediment continuity, Eq. (3.33). Parker (1991a,b) has, however, proposed a form. This form is most easily expressed in terms of the continuous probability densities $F(\psi)$, $f_I(\psi)$ and $f_b(\psi)$ for surface material, interfacial exchange material and bed-load material, respectively, rather than their discretized versions $F_i$, $F_{Ii}$ and $f_{bi}$. Let $\alpha_d(\psi)$ define the abrasion coefficient, which is specifically allowed to be a function of grain size. Eq. (3.33) takes the continuous form

$$(1-\lambda_p)\left[ f_I \frac{\partial \eta_b}{\partial t} + \frac{\partial}{\partial t}(L_a F) \right] = -\frac{\partial q}{\partial s} - A \tag{3.98a}$$

where $q(\psi)$ denotes the density of bed-load transport rate such that total gravel bed-load transport rate $q_T$ is given as

$$q_T = \int_1^\infty q(\psi)\, d\psi \tag{3.98b}$$

and $A(\psi)$, given by the relation

$$\begin{aligned} A &= q_T \left[ 3\alpha_d f_b - \frac{1}{ln(2)} \frac{\partial}{\partial \psi}(\alpha_d f_b) \right] \\ &+ q_T \left[ \int_1^\infty \alpha_d(\psi') f_b(\psi') d\psi' \right] \left[ 3F_{ae} - \frac{1}{ln(2)} \frac{\partial F_{ae}}{\partial \psi} \right] \end{aligned} \tag{3.98c}$$

denotes the density of the volume of material lost to abrasion per unit bed area per unit time, so that the total loss rate per unit area $A_T$ is given as

$$A_T = \int_1^\infty A(\psi)\, d\psi \tag{3.98d}$$

In Eq. (3.98c) the parameter $F_{ae}$ is defined as

$$F_{ae}(\psi) = \frac{F(\psi)2^{-0.5\psi}}{\int_1^\infty F(\psi)2^{-0.5\psi}} \tag{3.98e}$$

The lower limit of unity in the integral implies that only gravel is considered in the calculation; a value of $\psi$ of 1 corresponds to a grain size $D$ of 2 mm,

The first term on the right-hand side of Eq. (3.98c) denotes the abrasion density of bed-load particles, and the second term denotes the corresponding abrasion density of bed particles with which the bed-load particles collide. The derivative with respect to $\psi$ in the same equation describes the flux of sediment through grain size space as grains are ground ever finer.

The discretized version of Eq. (3.98c) is

$$\begin{aligned} A_i &= q_T\left[3\alpha_{d,i} f_{b,i} - \frac{1}{ln(2)}\frac{\left(\alpha_{d,i+1} f_{b,i+1} - \alpha_{d,i} f_{b,i}\right)}{\Delta\psi_i}\right] \\ &+ q_T\left[\sum_{j=1}^{n}\alpha_{d,j} f_{b,j}\right]\left[3F_{ae,i} - \frac{1}{ln(2)}\frac{\left(F_{ae,i+1} - F_{ae,i}\right)}{\Delta\psi_i}\right] \end{aligned} \tag{3.98f}$$

$$F_{ae,i} = \frac{F_i D_i^{-1/2}}{\sum_{i=1}^{n} F_i D_i^{-1/2}} \tag{3.98g}$$

where $\Delta\psi_i$ is given by Eq. (3.11c), $\alpha_{d,i}$ denotes the abrasion coefficient for the $i$th grain size range and $f_{b,i}$ is synonymous with $f_{bi}$. The total abrasion rate $A_T$ is given as

$$\begin{aligned} A_T &= A_{silt} + A_{sand} \\ A_{silt} &= 6q_T\sum_{i=1}^{n}\left(\alpha_{d,i} f_{b,i}\right) \\ A_{sand} &= \frac{q_T}{\Delta\psi_1 ln(2)}\left[\alpha_{d,1} f_{b,1} + \left(\sum_{j=1}^{n}\alpha_{d,j} f_{b,j}\right)F_{ae,1}\right] \end{aligned} \tag{3.98h-j}$$

where $A_{silt}$ and $A_{sand}$ are the associated volume rates of production per unit time per unit bed area of silt and sand, respectively. In the case of crystalline rock it is common that very little sand is produced until the grain size reaches the range 5 ~ 10 mm. In many crystalline rocks the crystal size is on the order of mm in size, and so the weak planes between crystals allow for a sudden shattering to sand-sized grains. This effect has been invoked as one possible explanation of the sharp gravel-sand transition evident in Figure 3.10 (Yatsu, 1955).

The above formulation is implemented in Parker (1991b) and the program ACRONYM4 in Parker (1990b). Parker (1991a) also provides the generalization to multiple lithologies. Results from an application to the disposal of mine waste in the Ok Tedi-Fly River system, Papua New Guinea are reported in Cui and Parker (1999).

## 3.10 NUMERICAL MODELING OF BED LEVEL VARIATION WITH SORTING

### 3.10.1 Elements of a Numerical Model

The active layer formulation of the grain size-specific Exner equation of bed-load continuity combined with an appropriate grain size-specific predictor for bed-load transport form the basis for the numerical modeling of the variation of bed level and grain size distribution in bed-load-dominated rivers. To this must be added a) an appropriate formulation of the fluid mechanics, usually realized through the St. Venant shallow water equations, and b) an appropriate methodology for the computation of hydraulic resistance (including skin friction and form drag). The simple versions of the 1-D shallow water St. Venant given in Section 3.7.2 are here restated as

$$\frac{\partial U}{\partial t}+U\frac{\partial U}{\partial s}=-g\frac{\partial H}{\partial s}-g\frac{\partial \eta}{\partial s}-gS_f$$
$$\frac{\partial H}{\partial t}+\frac{\partial UH}{\partial s}=0 \qquad (3.99a,b)$$

where $S_f$ denotes the friction slope, given by

$$S_f=\frac{C_fU^2}{gH}=\frac{n_m^2U^2}{k_{nuisance}H^{4/3}} \qquad (3.99c)$$

In the above relations $U$ denotes cross-sectionally averaged flow velocity, $H$ denotes cross-sectionally averaged flow depth (or hydraulic radius), $C_f$ is the dimensionless friction coefficient defined in Section 3.7.2, i.e.

$$C_f=\frac{\tau_b}{\rho U^2}=\frac{u_*^2}{U^2}=Cz^{-2} \qquad (3.99d)$$

where $Cz$ is the dimensionless Chezy resistance coefficient, $n_m$ is Manning's "n" and $k_{nuisance}$ takes a value of 1 using the MKS implementation of the SI system and 1.49 for an FPS implementation of "English" units.

It is possible to simplify the St. Venant equations depending upon the type of flow under consideration. When the channel is subject to a steady flow discharge, the classical quasi-steady approximation (de Vries, 1965) generally allows the neglect of the time terms in Eqs. (3.99a,b), while retaining them in the Exner equation of sediment

continuity, i.e. Eq. (3.23) or Eq. (3.33). In field streams in general, and gravel-bed rivers in particular, however, the characteristic time of a hydrograph may be so short that it is necessary to retain the time terms. Any simplified model of flood wave propagation based on the St. Venant equations must be capable of resolving the time variation in boundary shear stress necessary for the computation of the time variation of sediment transport rate and size distribution.

In executing engineering applications to field rivers, both the Exner equation of sediment continuity and the St. Venant formulation must be modified. A minimal modification is outlined below.

### 3.10.2 Minimal Form for Field Application to Engineering Problems

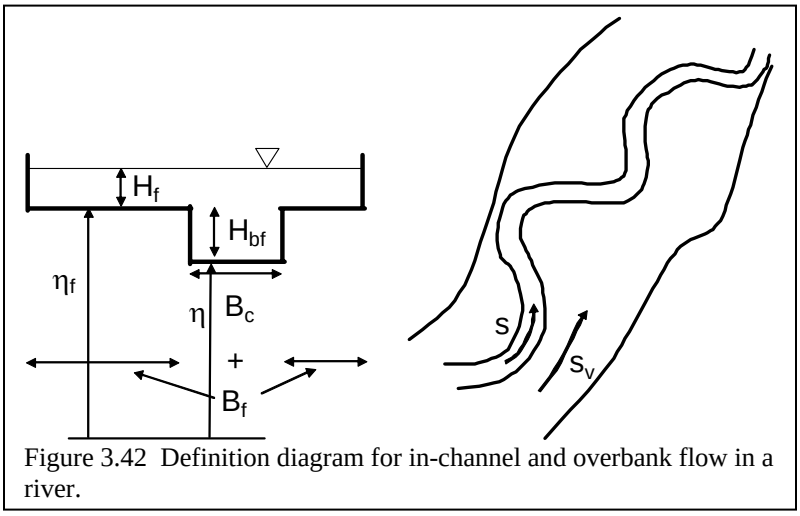

Figure 3.42 Definition diagram for in-channel and overbank flow in a river.

Modifications to the forms of Eq. (3.23) or (3.33) and Eqs. (3.99a,b) are required because a) rivers rarely have constant widths, b) they usually have floodplains, and c) they usually have some degree of sinuosity. Here the sinuosity $\Sigma_{sin}$ is defined as the average along-channel distance $s$ divided by the average along-valley distance $s_v$ (Figure 3.42); it commonly has a value between 1.0 and 2.5. The importance of the floodplain is as follows. Rivers transport the bulk of their sediment load during floods. Once river stage exceeds the bank-full stage, however, the water spreads out on the floodplain; further increases in stage increase water surface level very little. In the case of a vegetated floodplain, floodplain sediment is usually not mobilized, and a further increase in discharge does not result in substantially increased sediment transport. In the case of sufficiently sinuous channels, the sediment transport rate at above-bank-full stage can actually decline somewhat with increasing stage because the thread of high velocity no longer precisely follows the channel which constitutes the source of bed material load (Leopold, 1994). The failure to include the damping effect of the floodplain in numerical modeling of variation in river bed elevation can result in the spurious prediction of river bed degradation during floods.

With this in mind, a down-valley coordinate $s_v$ is defined in addition to the down-channel coordinate $s$. When averaged over several bends, the relation between these coordinates is

$$\frac{ds_v}{ds} = \frac{1}{\Sigma_{sin}} \tag{3.100}$$

This definition limits the spatial resolution of the model; cross-sections must be spaced by at least a bend or two. Channel width is denoted as $B_c$, which is here assumed to vary in the streamwise direction but not in time. The same holds true for floodplain width $B_f$, which here indicates the sum of the widths on both sides of the channel. In this simplest of implementations, the channel bed has elevation $\eta$, taken constant across the cross-section, and floodplain elevation $\eta_f$ is similarly held constant across the floodplain (Figure 3.41). Channel bank-full depth is denoted as $H_{bf}$, where

$$H_{bf} = \eta_f - \eta \tag{3.101}$$

For below-bank-full flow the St. Venant equations take the form

$$\begin{aligned} &\frac{\partial U_c}{\partial t} + U_c \frac{\partial U_c}{\partial s} = -g\frac{\partial H_c}{\partial s} - g\frac{\partial \eta}{\partial s} - gS_{fc} \\ &B_c \frac{\partial H_c}{\partial t} + \frac{\partial B_c U_c H_c}{\partial s} = 0 \end{aligned} \tag{3.102a,b}$$

where the subscript "*c*" denotes channel. For overbank flow the formulation is modified to

$$\begin{aligned} &\frac{\partial U_c}{\partial t} + U_c \frac{\partial U_c}{\partial s} = -g\frac{\partial (H_{bf} + H_f)}{\partial s} - g\frac{\partial \eta}{\partial s} - gS_{fc} \\ &\frac{\partial U_f}{\partial t} + \Sigma_{sin} U_f \frac{\partial U_f}{\partial s} = -\Sigma_{sin} g\frac{\partial H_f}{\partial s} - \Sigma_{sin} g\frac{\partial \eta_f}{\partial s} - gS_{ff} \\ &\frac{\partial}{\partial t}\left[ B_c(H_{bf} + H_f) + \frac{B_f H_f}{\Sigma_{sin}}) \right] + \frac{\partial}{\partial s}\left[ B_c(H_{bf} + H_f)U_c + B_f U_f H_f \right] = 0 \end{aligned} \tag{3.102c,d,e}$$

where the subscript *f* denotes floodplain, so that e.g. $S_{ff}$ denotes the friction slope of the floodplain. The corresponding form for the Exner equation of sediment continuity applied to sediment within the channel is

$$(1-\lambda_p)B_{ca}\left[ f_{Ii}\frac{\partial \eta_b}{\partial t} + \frac{\partial}{\partial t}(L_a F_i) \right] = -\frac{\partial B_{ca} q_i}{\partial s} - B_{ca} A_i \tag{3.103}$$

where the parameter $\eta_b$ is defined in Figure 3.32 and $B_{ca}$ denotes a channel width adjusted to describe sediment transport, as described below.

The above formulation must be augmented with relations for hydraulic resistance. In the case of the floodplain, it usually suffices to prescribe a floodplain value $n_f$ of Manning's "n"based on the calibration of backwater curves. In the case of the channel,

the resistance relation should include at the very least the effect of roughness due skin friction and bedforms. The resistance relations in Chapter 2 are formulated in terms of bed slope $S$ for the case of normal flow. In the case of flow that varies in time and space, the energy slope $S_e$, which may be defined as

$$S_e = \frac{\tau_b}{\rho g H} = -\frac{\partial \eta}{\partial s} - \frac{\partial H_c}{\partial s} - \frac{1}{g}\left( \frac{\partial U_c}{\partial t} + U_c \frac{\partial U_c}{\partial s} \right) \tag{3.104}$$

must be used instead. In the above relation, $\tau_b$ refers to channel bed stress and $H_c$ takes the value $H_b + H_f$ in the case of overbank flow. In addition, if the transport relation is based on skin friction $\tau_{bs}$ rather than total bed friction $\tau_b$, the hydraulic resistance relation must allow for such a decomposition.

The adjusted width $B_{ca}$ in the Exner equation (3.103) is in general a parameter that must be calibrated. It was seen in Section 3.7.16 that a complexity coefficient (or coefficients) must be introduced in order to account for the effects of channel complexity on sediment transport. One way to do this in a numerical model for a site-specific engineering application is to adjust the actual channel widths $B_c$ at each cross-section.

This adjustment can be accomplished by the process of zeroing the model. Natural rivers typically (but not always) undergo change only at a morphologic time scale that is large compared to engineering time scales. When the actual channel widths $B_c$ are input and the model run under natural conditions for which only minor morphologic change is expected, it usually turns out that spurious, unacceptable amounts of aggradation or degradation occur at specific nodes. Zeroing consists of modifying $B_c$ to the value $B_{ca}$ at each cross-section until such spurious bed level variation is reduced to an acceptable level. The model may be similarly zeroed by modest changes to the initial bed elevations. Without this process of zeroing the sediment transport and morphodynamic signals associated with engineering change such as flow diversion, dam removal or sediment dumping from a mine often cannot be seen through the spurious signals, much less accurately predicted.

In the case of a gravel-bed river, when the river aggrades to the point of filling its channel it can spread out on the floodplain. Any vegetation may be buried or ripped out, resulting in the formation of a braid plain over which the channel wanders. In such a case it is useful to compute the sediment transport within a channel of prescribed width and bank-full depth, but to spread the deposit out over the entire valley flat to as to simulate migration and avulsion. The form of the Exner equation for this case is

$$(1-\lambda_p) B_v \left[ f_{Ii} \frac{\partial \eta_b}{\partial t} + \frac{\partial}{\partial t}( L_a F_i ) \right] = -\frac{\partial B_c q_i}{\partial s} - B_{ca} A_i \tag{3.105a,b}$$
$$B_v = B_c + B_f$$

where $B_v$ denotes the width of the valley flat (including channel(s)).

It should be emphasized that the above treatment represents the simplest possible physically realistic engineering formulation for a field river. It nevertheless excludes myriad other important features of rivers and river flow, including transverse variation in floodplain elevation, dynamic channel-floodplain interaction and sorting due to 2-D and 3-D effects. One eventually reaches, however a point of vanishing returns; the repeated addition of poorly-constrained bells and whistles can degrade the predictive quality of a numerical model, in addition to making it difficult to use.

### 3.10.3 Examples of Numerical Models Using Grain Size Distributions

Several numerical models of bed level variation with sorting are described below. No attempt is made to be comprehensive. Rather, the goal is to provide the engineer with a brief summary of what kinds of models were available at the time of writing.

Belleudy and SOGREAH (2000) describe the latest developments of the model SEDICOUP. This model has been specifically designed to treat sediment mixtures. Earlier developments can be found in e.g. Holly and Rahuel (1990). SEDICOUP is a descendent of the model CARICHAR (Rahuel et al., 1989). Bezzola (1992) describes the application of the model MORMO to a flood in the Reuss River, Switzerland. Borah et al. (1982) present a numerical model designed for the study of the development of a static armor in rivers. The sediment transport equations used in the study are not grain size-specific; this feature is considered in terms of an adjustment for "residual transport capacity." Copeland and Thomas (1992) describe the dynamic sorting and armoring algorithm in the US Army Corps of Engineers TABS-1 model.

Cui et al. (1996) outline a model of grain sorting and aggradation verified against the experiments of Seal et al. (1997). This model is developed further in Cui and Parker (1997) for a shock-fitting of mobile gravel-sand transitions. Both models are descendants of ACRONYM 4 (Parker, 1990b). ACRONYM 4 was also adapted to study gravel transport, abrasion and change in bed elevation in the OKGRAV models applied to mine waste disposal in Papua New Guinea (Cui and Parker, 1999). Cui et al. (2003a, 2003b) develop the model further for the study of gravel pulses in rivers. See also Appendix A in this volume by Cui and Wilcox.

Hoey and Ferguson (1994) report on a model designed for and tested against downstream fining in the Allt Dubhaig, a river in Scotland, UK. Hoey and Ferguson (1997) use this model to study the controls on downstream fining. Ferguson et al. (2001) further develop this model and apply it to fluvial aggradation in the Vedder River, British Columbia, Canada. Van Niekerk et al. (1992) adapt the transport model of Bridge and Bennett (1992) to develop the numerical model MIDAS. Vogel et al. (1992) apply this model to the downstream sorting of heavy sediments such as placers in rivers. Robinson and Slingerland (1998) have expanded this work to the study of downstream sorting of bimodal sediment mixtures.

Armanini (1991/1992) defines the basis for a numerical model of mixed grain sizes that describes the evolution of various moments of the grain size distribution, rather than that of the distribution itself.

## 3.11 STATIC AND MOBILE ARMORING: OBSERVATIONS, EXPERIMENTS AND MODELING

The intense program of dam building in the United States and other countries in the period 1920 – 1950 led to a strong interest in the problem of static armor formation downstream of dams. The question of engineering relevance pertains to the elevation to which the bed would degrade downstream of a dam before coarsening sufficiently to stabilize and prevent further erosion. If this were not accounted for in designing the dam itself and the apron downstream of the spillway, the structure itself could be undermined.

It is important to realize in this regard that sand-bed streams often have at least a trace of gravel, which can accumulate as the sand is carried downstream and eventually form a stable armor layer. The evolution of such an armor is illustrated for the bed downstream of Hoover Dam in Figure 3.15.

### 3.11.1 Static Armor

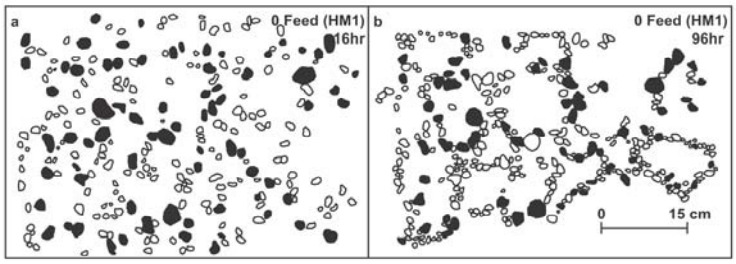


Figure 3.43 Evolution of stone cells on the bed surface of a laboratory flume as the bed evolves in response to the cutoff of sediment supply, as observed by Hassan and Church (2000). Hassan and Church also document the presence of these cells in the case of an equilibrium mobile-bed armor; the higher the sediment transport rate, the less developed are the cells.

The topic of static armoring remains of strong interest today. Ashida and Michiue (1971), Hirano (1971), Proffitt (1980), Gomez (1983), Egashira and Ashida (1990), Tsujimoto and Motohashi (1990), Tait et al. (1992), Marion et al. (1997), Willetts et al. (1998), Church et al. (1998) and Hassan and Church (2000) have studied the phenomenon. In all cases the bed surface is found to coarsen to a static armor as the sediment supply is cut off. Of recent interest is the tendency for the coarser grains to organize themselves into "clusters," "rings," and "stone cells" as the supply of gravel drops. Evidently armoring is not simply associated with the accumulation of coarser grains on the bed surface, but also with the organization of these grains into a pattern that increases the resistance to motion. An example of these structures is shown in Figure 3.43.

Full numerical models of the time evolution to static armor based on versions of the grain size-specific Exner equation of sediment continuity, Eq. (3.23) have been implemented by many researchers, including Park and Jain (1987), Vogel et al, (1992) and Tsujimoto and Motohashi (1990). An example of such a calculation and its comparison against data is shown in Figure 3.44.

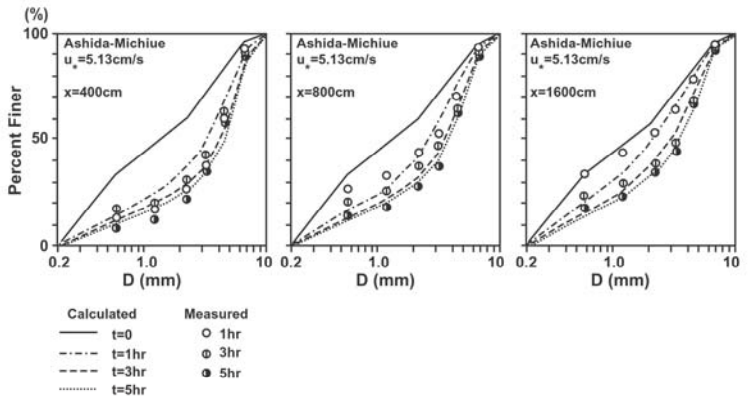


Figure 3.44 Examples of comparisons of a numerical model of evolution to static armor versus experimental data from a laboratory flume, in which x denotes distance downstream; from Tsujimoto (1999).

Ashida and Michiue (1971) devised a way to compute static armor in a much simpler way. This method was corrected by Proffitt (1980) and Sutherland (1987). The case of late-stage degradation is considered. By this time the active layer $L_a$ is assumed to have achieved a near-constant thickness. Assuming that the bed is degrading to a substrate with a spatially constant grain size distribution with fractions $\bar{f}_i$, Eq. (3.23) may be rearranged with the aid of Eqs. (3.26) and (3.28) to yield.

$$\frac{\partial F_i}{\partial t} = \frac{1}{L_a}\left[ ( f_{bi} - \bar{f}_i ) \frac{\partial \eta_b}{\partial t} - \frac{1}{1-\lambda_p} q_T \frac{\partial f_{bi}}{\partial s} \right] \tag{3.106}$$

As degradation progresses the term $\partial f_{bi} / \partial s$ can be expected to approach zero. Thus at late stage Eq. (3.106) simplifies with Eq. (3.24) to

$$\frac{dF_i}{d(\eta / L_a)} = f_{bi} - \bar{f}_i \tag{3.107}$$

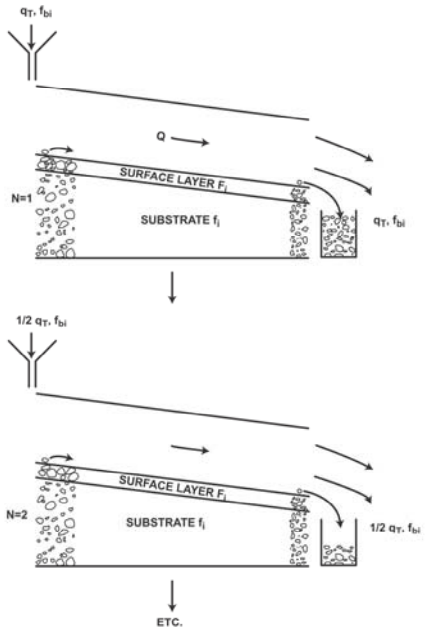


Figure 3.45 Conceptual diagram illustrating the evolution of a static armor from equilibrium mobile-bed conditions as the sediment feed rate is repeatedly halved.

In so far as the substrate fractions are given and the bed-load fractions can be computed from an appropriate sediment transport relation, the above equation can be solved iteratively until $f_{bi}$ approaches $\bar{f}_i$, after which

the bed will coarsen no more. Since the final state is the most important one to the engineer, Eq. (3.107) allows a considerable simplification over a full model.

Parker and Sutherland (1990) proposed an even simpler method. Consider Figure 3.45. The flume therein has a uniform substrate and is supplied with size fractions $\bar{f}_i$, constant water discharge and constant total sediment feed rate $q_T$ with constant size fractions $f_{bi}$. The flume is allowed to develop to a mobile-bed equilibrium. The experiment is then repeated keeping the substrate and feed fractions constant but halving the total feed rate $q_T$. The water discharge is adjusted from experiment to experiment to insure that each reaches a mobile-bed equilibrium at the same bed slope $S$ as the previous one. A static armor should be approached as $q_T$ approaches zero.

The surface-based bed-load relation of Parker (1990a), i.e. Eqs. (3.79a-g) is used here as an example. Eqs. (3.26) and (3.28) can be used to reduce these to

$$W_i^* = \frac{Rgq_T f_{bi}}{F_i u_{*s}^3} = G\left[\omega\phi_{sgo}\left(\frac{D_i}{D_g}\right)^{-0.0951}\right] \tag{3.108a}$$

Solving for surface fractions $F_i$, it is found that

$$F_i = \frac{\dfrac{f_{bi}}{G\left[\omega\phi_{sgo}\left(\dfrac{D_i}{D_g}\right)^{-0.0951}\right]}}{\displaystyle\sum_{i=1}^{n}\frac{f_{bi}}{G\left[\omega\phi_{sgo}\left(\dfrac{D_i}{D_g}\right)^{-0.0951}\right]}} \tag{3.108b}$$

The static armor size distribution $F_{ai}$ is then given as

$$F_{ai} = \lim_{q_T \to 0} F_i \tag{3.109}$$

This limit corresponds to extremely low transport rates, a range within which it is seen from Eq. (3.79f) that

$$G\left[\omega\phi_{sgo}\left(\frac{D_i}{D_g}\right)^{-0.0951}\right] \to \left[\omega\phi_{sgo}\left(\frac{D_i}{D_g}\right)^{-0.0951}\right]^{14.2} \tag{3.110}$$

Substituting Eqs. (3.108b) and (3.110) into Eq. (3.109), the following very simple relation for static armor is obtained;

$$F_{ai} = \frac{\bar{f}_i D_i^{1.35}}{\sum_{i=1}^{n} \bar{f}_i D_i^{1.35}} \tag{3.111}$$

This predictor requires nothing more complicated that a hand calculator or spreadsheet to implement. Parker and Sutherland (1990) found that the agreement with five sets of data from experiments on armoring and one set from Oak Creek could be optimized by lowering the exponent in Eq. (3.111) from 1.35 to 1.12. The agreement holds across the entire grain size distribution. Similar agreement was obtained with the Paintal (1971) bed-load transport model adapted for mixtures with the hiding function of Proffitt and Sutherland (1983). Any bed-load transport relation which satisfies a simple power law of the form of Eq. (3.51) at very low transport rates possesses such a simple limit for static armor.

### 3.11.2 Mobile Armor

The forms of Eqs. (3.108) and (3.109) raise another issue, however. In the thought experiment outlined above, the grain size distribution $F_i$ of the surface layer cannot be expected to suddenly jump to the distribution for static armor $F_{ai}$ as $q_T$ is lowered; instead the change should be gradual. That is, at conditions of relatively low transport rate, even when the all sizes participate in the bed-load due to the constant grain size distribution of the sediment feed, the bed surface should be coarser than the bed-load. If the bed-load material is the same material as that placed in the flume to make the substrate, then the bed surface should be coarser than the substrate as well. This state of an armored bed under equilibrium transport of all sizes may be called a mobile armor.

Until the concept of mobile armor was introduced, it was often thought that the armor layer in gravel bed rivers present at low flow was suddenly broken up by an appropriate threshold discharge, leading to an unarmored state during active bed-load transport. The armor was thought to reform by downstream and vertical winnowing as the flow declined.

The existence of an equilibrium mobile-bed armor was first demonstrated in a sediment feed flume by Parker et al. (1982b). Parker and Klingeman (1982) offered a simple explanation for it as follows. Consider a flume containing just two grain sizes, one coarse and one fine. The coarse and fine halves of the load are fed in at the same rate until a mobile-bed equilibrium is reached. The coarser grains are intrinsically less mobile than the finer grains, even after accounting for hiding effects. But once equilibrium is reached both halves must be transported at exactly the same rate. The way the model river in the flume accomplishes this is by overrepresenting the coarse material on the bed surface, so that the availability of coarse grains is increased, and that of fine grains decreased, until their effective mobility is equalized.

Parker and Toro-Escobar (2002) have termed this the weak form of the "equal mobility" hypothesis. Simply put, it says that no matter what the grain size distribution

of the sediment supply, in a stream that is locally in grade the bed surface must reorganize itself so that the coarse half of the feed moves through the system at the same rate as the fine half.

Mobile armor has been observed in laboratory sediment-feed flumes by Tsujimoto and Motohashi (1990), Egashira and Ashida (1990), Suzuki and Kato (1991), Suzuki and Hano (1992) and Hassan and Church (2000). Seal et al. (1997) documented the maintenance of a mobile armor under conditions of slow bed aggradation in a sediment feed flume. Parker et al. (2003) have documented the formation and maintenance of a mobile-bed armor under conditions of a repeated full hydrograph designed to model field gravel-bed rivers.

Mobile armor has also been observed in sediment recirculating flumes. The most comprehensive documentation in this configuration is outlined in Wilcock and Kenworthy (2002), but see also Marion and Fraccarollo (1997). The expression of mobile-bed armor in a recirculating flume is somewhat different from that in a sediment feed flume, in which all sizes in the feed are forced to move at mobile-bed equilibrium. As a result, partial transport with little transport of the coarsest grains, even when $D_{u50}$ is mobilized, is common. The reader is referred to Wilcock (2001b) for a discussion of the differences between the configurations.

### 3.11.3 The Variation of Mobile Armor with Bed-load Transport Rate

Now it is of use to consider the the limit of high transport rate. In the case of the relation of Parker (1990a), as $q_T$ ($\phi_{sgo}$) becomes large, $G(\phi_{sgo})$ approaches the constant limit 5474 in Eq. (3.77f). As a result, Eq. (3.108b) devolves to the result

$$\lim_{q_T \to \infty} F_i = f_{bi} \tag{3.112}$$

That is, at high transport rates the grain size distribution of the surface layer must approach that of the sediment supply. This same limit must be reached at high sediment

a) b)

Figure 3.46 Flash flood in the ephemeral Nahal Eshtemoa, Israel:
a) arrival of the flood wave (looking upstream); and b) passage of the flood wave (looking downstream). Images courtesy J. Laronne.

transport rates for any sediment transport relation for which $q_i^* \rightarrow \left(\tau_i^*\right)^{3/2}$ or equivalently $W_i^* \rightarrow const$. Relations satisfying this condition include those of Ashida and Michiue (1972), Hunziker and Jaeggi (2002), Wilcock and Crowe (2003) and Powell et al. (2001).

One may inquire as to whether or not mobile armor is observed in the field. It is difficult to sample a mobile gravel bed during a flood. This notwithstanding, Andrews and Erman (1986) report such a measurement. Sagehen Creek is a perennial stream in the Sierra Nevada of California. At low flow it has a well-armored bed, with a value of (surface) $D_{50}$ of 58 mm and a value of (substrate) $D_{u50}$ of 30 mm. In addition, it has a wel-defined self-constructed floodplain. The value of bank-full Shields number $\tau_{bf50}^*$, defined in Eq. (3.17e), is about 0.059, so that the stream fits in the center of the gravel-bed rivers of Figure 3.29, as is shown therein. The creek typically floods during snowmelt season. In 1983 the river went overbank during a snowmelt flood. Andrews and Erman sampled the surface layer both at low flow and near the flood peak, when particles as large as 86 mm were found to move. A mobile armor was found to be present during the flood, and the size distribution differed little from the static armor at low flow. The grain size distribution of the surface was sampled both at low flow and twice during the flood event. The surface grain size distribution at the peak of the flood had a median size of 46 mm. This value is somewhat finer than the low flow value of 58 mm, and considerably coarser than the substrate value of 30 mm. Evidently a mobile armor was present during an event that a) was above bank-full stage and b) mobilized grains larger than $D_{50}$. That is, the measured mobile armor had a median size that was coarser than that of the low-flow substrate but finer that that of the low-flow surface material.

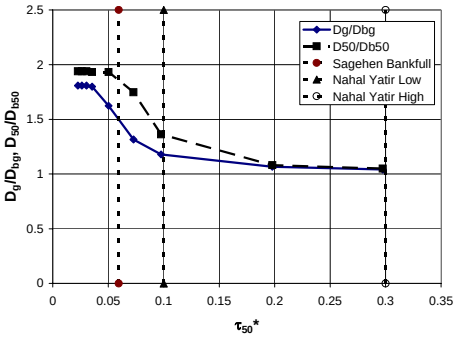


a)

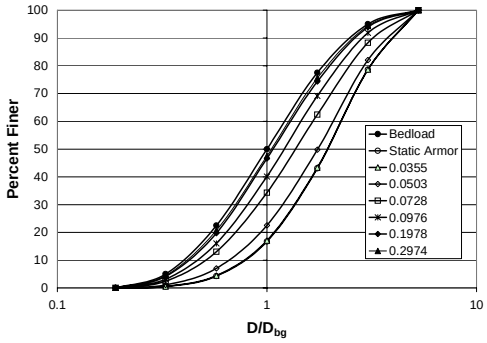


b)

Figure 3.47 a) Predicted variation of the ratios $D_g/D_{bg}$ and $D_{50}/D_{b50}$ in $\tau_{50}^*$, along with a bank-full value of $\tau_{50}^*$ for Sagehen Creek and two values of $\tau_{50}^*$ for the Nahal Yatir that bracket most of the bedload data.
b) Assumed normalized grain size distribution for bedload, along with predicted grain size distributions for static armor and mobile armor at the values of $\tau_{50}^*$ shown in the legend.

The Nahal Yatir is a desert wadi in Israel (Reid et al., 1995). It is subject to rare, intense flash floods. The arrival of a flash flood in a similar adjacent stream, the Nahal Eshtemoa, is documented in Figure 3.46. The floods subside so quickly that the bed has little time to reorganize itself. As a result, observations of the bed and substrate right after a flood more or less reflect the conditions at the

flood peak. As can be seen in Figure 3.1, the Nahal Yatir is essentially unarmored (Laronne et al., 1994). A substantial amount of the data in Reid et al. (1995) on bed-load transport in the Nahal Yatir pertains to values of $\tau_{50}^*$ (Shields number based on surface $D_{50}$) in the range 0.1 – 0.3, where in analogy to Eq. (3.18c)

$$\tau_{50}^* = \frac{HS}{RD_{50}} \tag{3.113}$$

These values are well above those reported for gravel-bed rivers in Figure 3.29. This is because the Nahal Yatir is incised into tough loess and older alluvium that resists erosion.

A juxtaposition of the field measurements for Sagehen Creek and the Nahal Yatir suggests that the surface grain size distribution changes systematically during floods. As $\tau_{50}^*$ increases above a threshold for significant gravel motion of about 0.03, the ratio $D_{50}/D_{u50}$ (surface median size to substrate median size), or alternatively the ratio $D_g/D_{ug}$ (surface geometric mean size to substrate geometric mean size) should gradually decrease toward unity, at which point no discernible armor is present.

A simple calculation using ACRONYM2 (Parker, 1990b) was implemented in an attempt to model this behavior. ACRONYM2 performs the calculation of Eq. (3.108b) using the Parker (1990a) relation. A reasonable approximation of the substrate size distribution of Sagehen Creek was constructed for this exercise. In the normalized form of $\bar{f}_i$ versus $D_i/D_{ug}$, it also serves as a crude approximation of the substrate size distribution in the Nahal Yatir. This normalized size distribution was used to approximate the size fractions $f_{bi}$ of the bed-load during transport events in both streams. A range of values of total bed-load transport rate $q_T$ were input into the program to simulate bed evolution as a function of transport rate. The results of the analysis are shown in Figure 3.47.

Figure 3.47a shows the ratios $D_{50}/D_{b50}$ and $D_g/D_{bg}$ versus $\tau_{50}^*$. ACRONYM2 predicts that in the case of bank-full flow in Sagehen Creek ($\tau_{50}^* = 0.059$), these ratios should decline only modestly from values at the low flow. In the case of the Nahal Yatir, these ratios have dropped dramatically at a value of $\tau_{50}^*$ of 0.1, and by the value 0.3 they are very close to unity. Figure 3.47b shows the size distribution of the bed-load, that of the static armor and that of the mobile armor at various values of $\tau_{50}^*$. The progressive approach of the surface grain size distribution to that of the bed-load as $\tau_{50}^*$ increases is evident.

In the above formulation, it has been assumed that the size distribution of the bed-load is always invariant and equal to that of the substrate, so that $D_{b50}$ is equal to $D_{u50}$ and $D_{bg}$ is always equal $D_{ug}$. If this were true, Figs. 3.47a,b would imply that the mobile armor would become progressively finer as $\tau_{50}^*$ increases, eventually approaching the grain size distribution of the substrate in the limit of large $\tau_{50}^*$. That is, the armor would vanish for sufficiently high values of $\tau_{50}^*$. This is in fact what is observed in the Nahal Yatir.

The above results needs to be qualified with the observation that the grain size distribution of the bed-load is typically not invariant with stage, but varies systematically such that $D_{b50}$ and $D_{bg}$ typically become coarser with increasing stage. This effect may tend to mute the approach of the surface grain size distribution toward that of the substrate as stage becomes progressively higher. This notwithstanding, it seems reasonable to infer that a) mobile armor is well-developed in gravel-bed streams of the type shown in Figure 3.29 even at bank-full conditions, but b) mobile armor is either poorly developed or absent in gravel-bed streams that can sustain substantially larger Shields numbers and transport orders of magnitude more gravel, such as the Nahal Yatir.

A second look at Figure 3.1 is instructive. Along with the unarmored Nahal Yatir, the well-armored River Wharfe is shown therein. It can be inferred from the photographs with some degree of reliability that the gravel supply to the River Wharfe is much lower than that to the Nahal Yatir. Dietrich et al. (1989) have quantified this concept in terms of a way to estimate the relative difference in gravel load between two streams based on the degree of armoring observed at low flow. The formulation may be used as a rough but accessible indicator of the gravel supply to the river.

### 3.11.4 The Hypothesis of Equal Mobility

A short discussion of the concept of "equal mobility" is in order. In addition to the weak form of Parker and Klingeman (1982), Parker et al. (1982a) advocated a "strong form" (Parker and Toro-Escobar, 2002), according to which the size distribution of the gravel bed-load averaged over many floods should be close to that of the gravel portion of the substrate layer immediately below the surface layer. That is, as an approximation

$$< f_{bi} >= \bar{f}_i \tag{3.114}$$

where the brackets denote values based on the size distribution of the mean annual gravel load. Lisle (1995) has performed a comprehensive test of this hypothesis. These results are shown in Figure 3.48 in terms of $<f_{bi}>$ versus $\bar{f}_i$. All grain size distributions have been truncated so as to remove material finer than 1 mm. Of the 14 stream reaches shown in the diagram, the strong form of equal mobility is rigorously or approximately satisfied in 8 cases, such that

$$1 < \frac{D_{u50}}{D_{b50}} < 1.5 \tag{3.115}$$

whereas in 6 cases it is not. The strongest discrepancy is in the East Fork River, which is not far upstream of a gravel-sand transition. In the other cases, Lisle associates the deviation from the strong form of equal mobility with low-order tributaries high up in a drainage basin. In addition, he also suggests that the prominent formation of patches of fine gravel may contribute to the preferential transport of these sizes in such streams.

Church et al. (1991) provide a test of the hypothesis of equal mobility in fluvial sediment transport, with a focus on the sand fraction of the load.

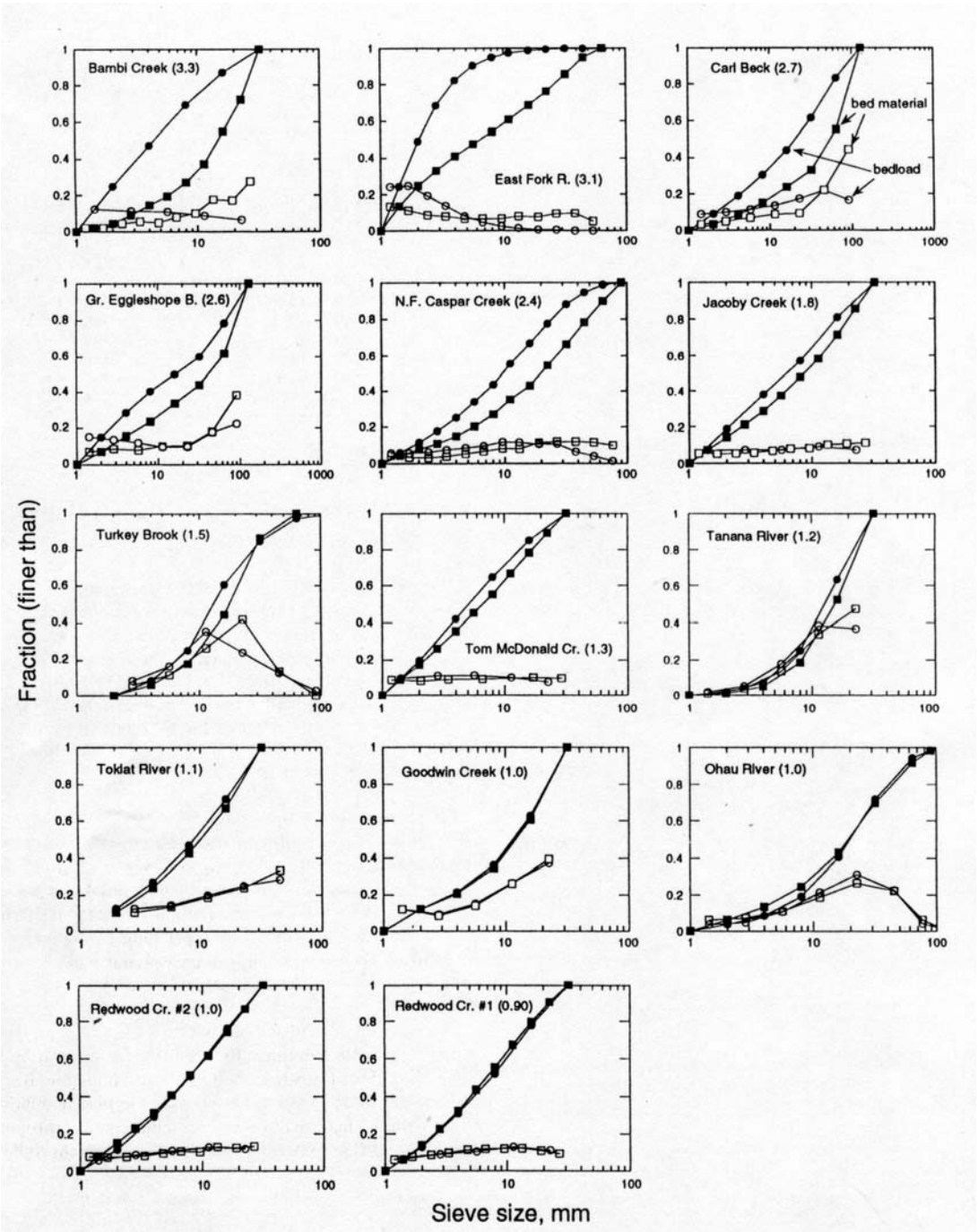


Figure 3.48 Normalized mean annual bedload (solid circles) and substrate (solid squares) grain size distributions for 14 gravel-bed rivers studied by Lisle (1995). The grain size distributions have been truncated at 1 mm. The hollow circles and squares pertain to fractions in each range.

## 3.12 DOWNSTREAM FINING: OBSERVATIONS, EXPERIMENTS AND MODELING

### 3.12.1 Abrasion or Selective Sorting?

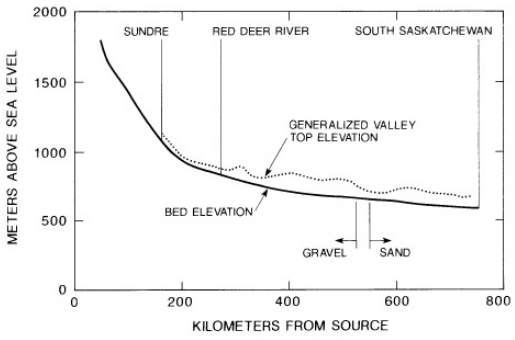


a)

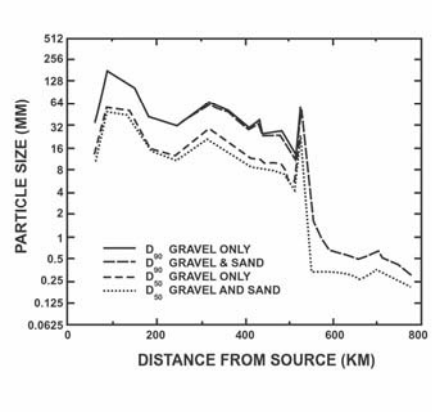


b)

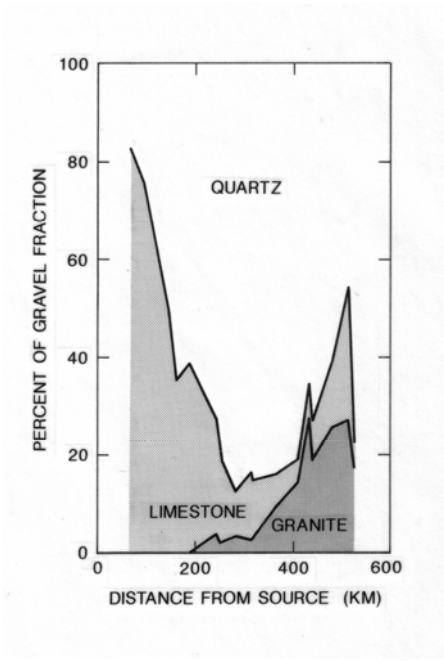


c)

Figure 3.49 Illustration of various aspects of downstream fining in the Red Deer River, Alberta, Canada. a) Long profile of the Red Deer River. b) Downstream variation in $D_{50}$ and $D_{90}$ in the Red Deer River. c) Downstream variation in three lithologies in the Red Deer River. From Shaw and Kellerhals (1982).

Most but not all rivers are characterized by a concave-upward long profile, so that slope declines downstream. Many gravel-bed rivers with such a concave-upward profile also show a systematic tendency for the grain size of the bed material to become finer in the downstream direction. An example already discussed is the Kinu River, Japan, shown in Figure 3.10. A second example, shown in Figure 3.49, is the Red Deer River, Alberta, Canada (Shaw and Kellerhals, 1982). The long profile is seen to be concave-upward in Figure 3.49a. The surface sizes $D_{50}$ and $D_{90}$ is seen in Figure 3.49b to decline in the downstream direction over most of the 500 km of the gravel-bed reach, and then drop quickly to sand at a gravel-sand transition.

As noted above, a downstream decrease in gravel size may be due to selective transport of the finer gravel, abrasion or some combination of the two. In the case of the Red Deer River, lithology provides a hint, as shown in Figure 3.49c. The relative composition of various rock types in the river gravels is seen to change systematically. In particular, the fraction of the bed that is limestone declines relative to quartz and granite, to the point of near-vanishing content some 450 km downstream of the stream source. Shaw and Kellerhals (1982) present evidence to the effect that the limestone clasts in the river are more easily abraded than the granite clasts, and much more so than the quartz clasts. The

implication is that the limestone is being ground out by abrasion, which thus may play an important or dominant role in the pattern of downstream fining.

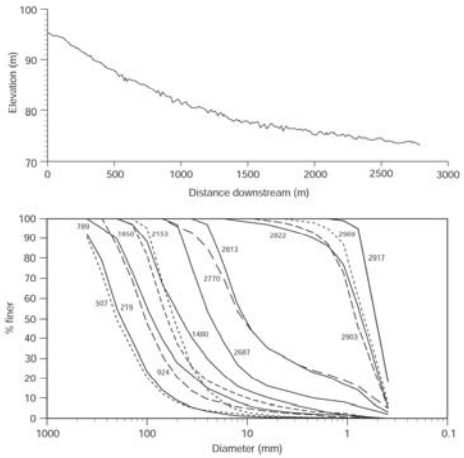


Figure 3.50 Illustration of downstream fining in the Allt Dubhaig, Scotland, UK, showing the long profile of the river (top) and grain size distributions of bulk surface samples taken at various points down the stream (bottom). From Ferguson et al. (1996).

Ferguson and Ashworth (1991) and Ferguson et al. (1996) provide another example of downstream fining that is very similar to the Red Deer River, yet very different from it. The Allt Dubhaig, Scotland, UK shows the same upward concave long profile and the same gravel-sand transition as the Red Deer (Figure 3.50). Yet in this case the amount of fining observed in the Red Deer River over hundreds of km is realized in the Allt Dubhaig over less than 4 km. In addition to the short distance, the durable nature of the rock types present in the river precludes an important role for abrasion. In this case, then, selective transport of the finer grains is the likely cause of the grain size variation.

Kodama (1994a,b) argues that the downstream fining observed in the Watarase River , Japan is primarily caused by abrasion. He argues that abrasion rates determined in mills and flumes severely underestimate the violent collisions associated with floods in the Watarase River, which are associated with typhoons. He used a concrete mixer to better approximate conditions in the Watarase River.

One might infer from the above that in a country such as Britain, which is geologically old, heavily glaciated and subject to a mild climatic regime, downstream fining might be wholly due to selective sorting, whereas a in geologically young, tectonically active country subject to violent storms such as Japan abrasion may tend to dominate. The picture is, however, not so simple. Seal and Paola (1995) observed rapid downstream fining over a 10 km reach upstream of a sediment retention dam on the North Fork Toutle River, Washington, USA (Figure 3.6). The sediment is largely derived from the Mount St. Helens eruption in 1980, and might be expected to abrade easily. Over the short distance of the deposit behind the dam, however, abrasion played a negligible role.

Gomez et al. (2001) have documented downstream fining over 90 km in the Waipaoa River, New Zealand. This example is of special interest because the median size of the substrate in the gravel-bed reach is in the pea gravel range. Rice (1998, 1999) has documented a pattern of "punctuated" downstream fining in British Columbia,

Canada, in which abrasion appears to play little role. That is, a pattern of downstream fining is set up by selective transport between major sediment sources, some of which can refresh the supply of coarse grains and interrupt the pattern of progressive downsream fining. These sources can include tributaries, glacial moraines and bedrock cliff exposures.

Gravel-bed rivers undergoing downstream fining often but not always end in a rather abrupt transition to a sand-bed reach over a few km. Yatsu (1955) documented these transitions on many Japanese streams. Recently Sambrook Smith and Ferguson (1995) have documented such transitions on 18 streams in Canada, England, Japan, Papua New Guinea, Romania and Scotland. The Waipaoa River discussed above also exhibits a gravel-sand transition. In most but not all cases the transition from gravel to sand is accompanied by a substantial drop in river bed slope. The reason for the transition is still a matter of debate, but it can often be ascribed to a bimodal grain size distribution with a gap or paucity somewhere near the interface between sand and gravel sizes. Fujita et al. (1998) document both downstream fining and gravel-sand transitions on a variety of Japanese streams, and present a conceptual model for the effect of engineering works on the location of the transition point.

Pizzuto (1995) has argued that downstream fining need be a consequence of neither abrasion nor downstream fining. Instead, it could be driven simply by a tendency for more distal tributaries to deliver finer sediment to the main stem of a river. His model underlines the importance of sediment provenance in considering the problem of downstream fining.

### 3.12.2 Laboratory Studies of Downstream Selective Sorting

Laboratory flumes are too short to allow modeling of downstream fining set up by abrasion, but they provide a useful venue for testing the process of selective sorting. An upward concave bed profile can usually be set up in a flume by forcing the bed to aggrade. The resulting downstream decrease in slope then ought to drive selective deposition of the coarser grains and transport of the finer grains. Curiously, however, one of the earliest documented studies of downstream sorting of heterogeneous sediments under aggradational conditions in the laboratory yielded the opposite result. Straub (1935) instead found a pattern of downstream coarsening caused by selective transport of the coarser grains. Kodama et al. (1992) specifically attempted to reproduce downstream fining in an aggrading channel and again obtained downstream coarsening. They describe this result as "quite contrary to common sense."

Paola et al. (1992b) and Seal et al. (1997) finally succeeded in reproducing downstream fining in the laboratory. Their channel was 0.3 m wide and over 50 m long; the sediment used in the study was a weakly bimodal mix of sand and gravel ranging from 0.125 mm to 90 mm. The sediment was fed in over an inerodible bed and allowed to prograde into standing water. The upward-concave profile of gravel ended in a distinct gravel front, downstream of which only sand prevailed. The height of this front was controlled by the base level of the standing water. Toro-Escobar et al. (2000) repeated

the experiments in a much wider channel, again obtaining unambiguous downstream fining driven by selective transport. The channel bed at the end of one of the experiments in Figure 3.51 serves to illustrate the pattern of downstream fining. This set of experiments revealed that an increased content of sand in the sediment feed caused more rapid downstream fining of the gravels, a result that might be explainable in terms of the new model of gravel-sand transport of Wilcock and Crowe (2003; see also Wilcock, 1998a and Wilcock et al., 2001).

The reason why downstream coarsening was obtained in some studies of aggrading deposits and downstream fining in others was identified by Solari and Parker (2000). They delineated a mobility reversal for bed slopes exceeding about two percent. At higher slopes the direct effect of gravity acting to pivot out the larger exposed grains is enough to disturb the delicate balance between grain weight and grain protrusion that renders finer grains somewhat more mobile in a mixture at lower slopes. The experiments of Straub (1935) and Kodama et al. (1992) were above the threshold, whereas the experiments of Seal et al. (1997) and Toro-Escobar et al. (2000) were below the threshold.

Brummer and Montgomery (2003) have documented a similar tendency for downstream coarsening in field channels near their headwaters. More specifically, downstream coarsening was observed for drainage areas less that 10 $km^3$, or slopes exceeding about eight percent.

Such a mobility reversal has been observed in other contexts. Everts (1973) reported on the phenomenon of overpassing, by which rare coarse grains can skim over a bed of much finer grains at relatively high speed. As opposed to slope-driven mobility reversal, overpassing appears to require a significant difference in size between the overriding coarse grains and the fine grains below.

Transitions similar to gravel-sand transitions have been modeled in the laboratory using density difference as a surrogate for size difference. In the experiments of Fujita et al. (1998) and Paola et al. (2001) the transition was produced in an aggrading

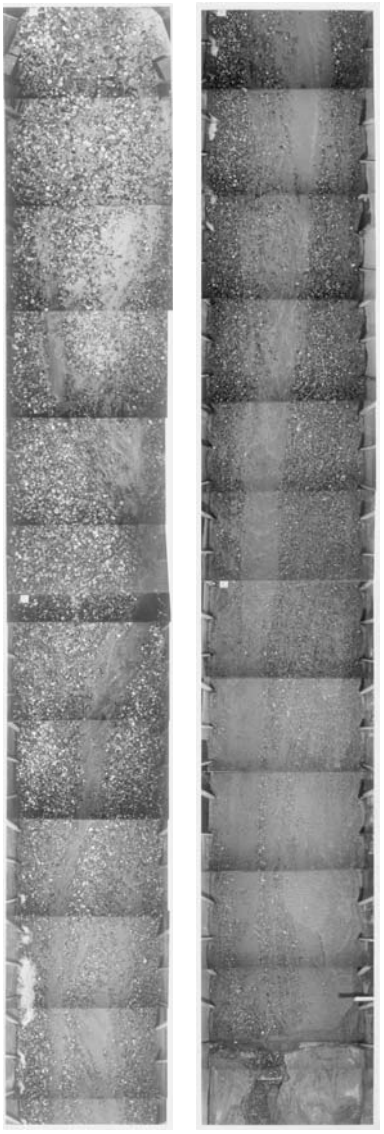

a) b)

Figure 3.51 Illustration of downstream fining produced in a laboratory channel; in Run 5 of Toro-Escobar et al. (2000). The channel width is 2.7 m. a) The upstream 20 m of the deposit. b) The downstream 20 m of the deposit. Flow was from top to bottom.

model river containing (heavy) sand and (light) crushed coal.

### 3.12.3 The Role of Tectonics and Base Level Variation

There are two ways to approach the phenomenon of downstream fining. Either one can take the initial long profile of the river as given and calculate downsteam change in grain size over it, or one may attempt to explain the shape of the long profile as well as the pattern of sorting.

The role of tectonics becomes important in the second case. The upward concave profile of a river is often set up as it flows from a zone of uplifting terrain to a zone of subsiding terrain. Indeed, rivers are attracted to zones of tectonic subsidence, as evidenced by the position of such major rivers as the Po and the Ganges. As a river migrates and avulses over the surface of such a zone, the accommodation space created by subsidence is gradually filled with sediment. While the process occurs over geomorphic rather than engineering time, engineering activities such as the disposal of mine waste in rivers can interrupt this slow, quasi-equilibrium process, and create major sedimentation problems. An inability to understand how a river establishes its long profile leads to an inability to predict the response of a river to such activities.

Not all rivers flow through depositional basins. Many of the streams on the west side of the northern Coast Range of California, such as the Mad River shown in Figure 3.14, are locked into place along synclines in an otherwise rapidly uplifting terrain. As a result, these streams show much less upward concavity in their profiles than rivers that flow into subsiding zones before reaching the sea. Before the advent of gravel mining, many of these rivers delivered gravel directly to the sea, with no gravel-sand transition. This balance, however, has been greatly altered by gravel mining.

Base level change can have a role analogous to tectonics. In particular, the 120 m rise in eustatic sea level since the end of the last glaciation has created accommodation space for the storage of sediment within the coastal plain and estuaries. Fujita et al. (1998) associate sea level rise with an upstream migration of gravel-sand transitions in Japan. Paola (2000) provides a comprehensive summary of numerical models of basin stratigraphy which include the effects of tectonics and base level variation.

### 3.12.4 Numerical Models of Downstream Fining

Abrasion, subsidence and delta progradation can all play a role in setting up the interaction between the long profile of the river and the heterogeneous bed sediment to produce downstream fining. In a numerical model, delta progradation can be handled with a migrating downstream boundary condition (e.g. Swenson et al., 2000; Kostic and Parker, 2003). Abrasion and subsidence (or uplift), however, must be incorporated directly into the Exner equation of sediment continuity.

The subsidence rate $\sigma_{sub}$ may be as high as a few mm per year depending upon setting. Negative subsidence corresponds to uplift. For the purpose of most engineering

models $\sigma_{sub}$ can be taken as constant in time, but may vary in space. In order to account for subsidence, the Exner equation of sediment continuity, Eq. (3.33) must be modified to the form

$$(1-\lambda_p)\left[ f_{Ii}\left( \frac{\partial \eta_b}{\partial t} + \sigma_{sub} \right) + \frac{\partial}{\partial t}( L_a F_i ) \right] = -\frac{\partial q_i}{\partial s} - A_i \tag{3.116}$$

It is easily shown that a constant speed of subsidence drives an upward-concave long profile in the same way as an aggradational profile driven by a downstream dam the height of which is raised at a constant speed. That is, subsidence can set up conditions for downstream fining.

Rana et al. (1973) provide the first hint of a mechanistic formulation of downstream fining. The first full numerical model of downstream fining in a river was developed by Deigaard (1980) in the context of an engineering project on the sand-bed Niger River, Africa. This pioneering work was nevertheless rather primitive in nature, in that no hiding effects were included in the sediment transport relation. Paola et al. (1992a) developed a simple two-grain model of downstream fining as rivers fill subsiding depositional basins. One grain size is in the gravel range and the other is in the sand range. They used the Meyer-Peter and Müller (1948) transport equation and a constraint on bank-full Shields number in rivers to reduce the Exner equation to diffusional form with the subsidence term acting as a sink. Both gravel and sand deposit out to balance subsidence, but the gravel does so at a higher rate. The gravel-sand transition occurs when the river runs out of gravel to carry. Paola and Seal (1995) developed a model capable of handling a full grain size distribution and applied it to the deposit on the North Fork Toutle River, Washington, USA shown in Figure 3.6. They showed that the morphologic complexity associated with local patches of sorted sediment acts to increase the rate of downstream fining, as described in Section 3.7.16.

Parker (1991a,b) developed a numerical model, ACRONYM3, for the study of the effects of both aggradation and abrasion on downstream fining. Profile concavity was driven by the assumption of a wave-like progradational profile of constant form. The model was further developed along with ACRONYM4 for the purpose of predicting the response of the gravel-bed Ok Tedi, Papua New Guinea, to sediment supplied from a mine (Cui and Parker, 1999). Cui et al. (1996) and Cui and Parker (1997) tested the model against the downstream fining experiments of Seal et al. (1997). Parker and Cui (1998) and Cui and Parker (1998) went on to develop a numerical model of downstream fining in rivers with gravel-sand transitions the locations of which are stabilized by subsidence. In the case of bimodal sediments with a gap in the pea gravel range, they identified three ways to drive a transition: a) the gravel runs out due to deposition upstream; b) the gravel is ground out by abrasion; and c) sand moving as throughput load eventually deposits on the bed as slope drops off and overwhelms the gravel. The model of Cui and Parker (1998) treats the throughput load of sand by filling the pores of the gravel to a prescribed porosity as it aggrades, and passing the rest of the sand down to the gravel-sand transition.

Hoey and Ferguson (1994, 1997) developed a numerical model of downstream fining in the Allt Dubhaig, a stream in which neither abrasion nor subsidence appear to be playing a role. Rather, the fining is set up by the progradation of the river into a lake. In such cases the gravel-sand transition cannot stabilize; as long as there is gravel and sand supplied to the river the transition must migrate downstream. The sediment supply is low in the case of the Allt Dubhaig, so that the transition migrates only slowly.

Robinson and Slingerland (1998) developed a numerical model for downstream fining in the case of bimodal sand-gravel mixtures. They applied it to the prediction of grain-size trends in a depositional foreland basin. The model is a descendant of MIDAS (van Niekerk et al., 1992).

## 3.13 MORPHODYNAMICS OF LOCAL PLANFORM SORTING

### 3.13.1 2D Bed-load Transport of Sediment Mixtures

Local sorting of bed-load sediment is often dominated by 2D effects, and thus must be described in terms of 2D formulations of bed-load transport of sediment mixtures. Such 2D relations have been presented for the case of uniform sediment with size $D$ in Chapter 2. Generalizations to mixtures are presented below.

Let

$$\vec{q}_i = (q_{i,s}, q_{i,n}), \quad \vec{\tau}_{bs} = (\tau_{bs,s}, \tau_{bs,n}) \tag{3.117a,b}$$

denote the 2D vectors of volume bed-load transport per unit width in the ith grain size range and boundary shear stress due to skin friction, respectively. Parker and Andrews (1985) have generalized the linearized Ikeda-Parker formulation (Parker, 1984) of Chapter 2 to the form

$$\vec{q}_i = |\vec{q}_i| \left[ \frac{\vec{\tau}_b}{|\vec{\tau}_b|} - \beta \left( \frac{\tau^*_{s,mag,i}}{\tau^*_{sci}} \right)^{-n_t} \vec{\nabla}\eta \right] \tag{3.118}$$

where $\vec{\nabla}\eta$ denotes the 2D vectorial gradient of bed elevation in the ($s$, $n$) directions,

$$\tau^*_{s,mag,i} = \frac{|\vec{\tau}_{bs}|}{\rho R g D_i}, \quad \beta = \frac{1 + r\mu_d}{\mu_d}, \quad n_t = \frac{1}{2} \tag{3.119a,b,c}$$

and values for $\mu_d$ and $r$ are given as Eqs. (2.112c,d) in Chapter 2. In addition, the parameters $\tau^*_{sci}$ are computed from the modified Egiazaroff hiding relation in the form of Eq. (3.73a). Under the condition $q_{i,n}/q_{i,s} << 1$ Eq. (3.118) further linearizes to the form

$$|\vec{q}_i| = q_{i,s}$$
$$q_{i,n} = q_{i,s}\left[\frac{\tau_{bs,n}}{\tau_{bs,s}} - \beta\left(\frac{\tau^*_{si}}{\tau^*_{sci}}\right)^{-n_t}\right]\frac{\partial\eta}{\partial n} \qquad (3.120a,b,c)$$
$$\tau^*_{si} = \frac{\tau_{bs}}{\rho RgD_i}$$

Parker and Andrews (1985) evaluated the streamwise bed-load transport rates $q_{si}$ in Eq. (3.120) using a generalization to mixtures of the Parker (1979) bed-load transport relation, also using the modified Egiazaroff hiding relation of Eq. (3.73a).

Recently Hasegawa et al. (2000) have similarly modified the 2D nonlinear bed-load transport relation of Kovacs and Parker (1994) to a 2D form for sediment mixtures. The linearized form of the relation is identical to Eq. (3.120) but

$$\beta = \sqrt{2} \qquad (3.121)$$

and $q_{i,s}$ is evaluated using the formulation of Ashida and Michiue (1972). Other relations for the 2D transport of bed-load mixtures can be found in Yamasaka et al. (1987) and Olesen (1987).

### 3.13.2 Manifestations of Local Planform Sorting

As noted in Section 3.1, rivers may also sort sediment from bend to bend and from dune to dune. These local sorting processes are only discussed briefly here; the interested reader may refer to the references quoted.

The flow in river bends drives a characteristic pattern of sorting, with coarser material at the outside of the bend, and on the upstream side of the point bar on the inside of the bend. This pattern can be seen in Figure 3.4. Bridge and Jarvis (1976) document bend sorting in the River South Esk, Scotland. Dietrich and Smith (1984) and Dietrich and Whiting (1989) document patterns of flow, topography, sediment transport and sediment sorting in a reach of the meandering Muddy Creek, Wyoming, USA. The latter study provides a complete set of data for testing numerical models.

The flow in river bends sets up a topography with strong transverse slopes. As bed-load is transported downstream across such slopes, the coarser grains tend to preferentially move down the transverse slope. This process is one of several that play a fundamental role in driving sorting in bends.

In order to treat sediment transport and sorting in bends it is necessary to generalize Eq. (3.23) to the 2D form

$$(1-\lambda_p)\left[ f_{Ii}\frac{\partial \eta_b}{\partial t}+\frac{\partial}{\partial t}(L_a F_i)\right]=-\frac{\partial q_{i,s}}{\partial s}-\frac{\partial q_{i,n}}{\partial n} \tag{3.122}$$

The form of Eq. (3.122) in conjunction with a 2D bed-load transport formulation of the form of Eq. (3.120b) allow for an intricate interplay between the depth-averaged flow in the *s* and *n* directions, the secondary flow set up by the bend and sorting of bed-load grains through the bend. Analytical and numerical models of bend sorting using the above formulation have been presented by Ikeda et al. (1987), Ikeda (1989), and Seminara et al. (1997) for the case of a bend of constant curvature; Parker and Andrews (1985) and Ashida et al. (1991) studied sorting in a meandering channel.

Rivers that are constrained from meandering or braiding by artificial, inerodible banks often develop a pattern of alternate bars instead. Lisle et al. (1997) have performed an experimental study of alternate bars in a steep channel containing heterogeneous sediment. Lanzoni and Tubino (1999) have developed a stability model of alternate bars in rivers that not only predicts realistic sorting pattern, with coarser grains accumulating toward the bar crests, but also demonstrates that the grain size distribution damps the growth of bar amplitude and reduces bar wavelength as well. A sorting model of the type of Eqs. (3.120b) and (3.122) is used to perform the analysis. Ashworth et al. (1991) describe sorting processes in braided streams. Predictive models for this case seem to be lacking.

Bed-load sheets are low sorting bedforms, the characteristics of which are shown in Figure 3.3. They have been observed in the laboratory by Iseya and Ikeda (1987) and Kuhnle and Southard (1988) and in the field by Whiting et al. (1988). It has been argued that bed-load sheets are simply immature dunes. This may be true of some bed-load sheets, but Seminara et al. (1996) have used stability analysis to delineate a nearly pure sorting wave that can propagate without evolving into a dune. The basis for the analysis is the Exner equation of sediment continuity, Eq. (3.23), the Parker (1990a) surface-based bed-load transport relation and a simplified $k$-$\varepsilon$ turbulence closure for the flow field. The handling of the exchange fractions $f_{Ii}$, however, proves difficult in a stability analysis due to the discontinuity in treatment between aggradation and degradation inherent in Eqs. (3.31) and (3.32). This points out the need for an improved Exner relation for sediment conservation that does not have this feature. Progress toward such a model is discussed in Section 3.15. Tsujimoto (1991, 1999) has approached the same problem from the point of view of bed-load entrainment rather than bed-load transport.

Figure 3.52 Side view of step-pool topography formed in the laboratory. Image courtesy K. Hasegawa.

Seminara (1998) provides an excellent summary of the application of stability analysis to river morphodynamics, including sediment mixtures in general and bed-load sheets in particular.

Tsujimoto (1991, 1999) and Colombini and Parker (1995) have developed stability theories to explain the longitudinal gravel-sand streaks of Figure 3.8. Colombini and Parker (1995) found that at least some variation in grain size is necessary to trigger the instability. The basis for their analysis is a) the Exner equation of sediment continuity (3.23), b) the Parker (1990a) formulation for bed-load transport and c) the Speziale (1987) turbulence closure for the flow. Tsujimoto posed the problem of longitudinal streaks in terms of bed-load entrainment rather than transport.

Whittaker and Jaeggi (1982) and Ashida et al. (1984) have explained the step-pool topography in steep streams shown in Figure 3.5 in terms of antidunes. The boulders tend to collect at the crest of antidunes during rare floods, and then stabilize into resistant steps as they are reworked by declining flows. Grant et al. (1990) suggest that these floods may have a recurrence interval on the order of 50 years. Removal of the boulders can lead to wholesale destabilization of the channel (Ikeda, 2001). Tatsuzawa et al. (1999a, 1999b) have performed parallel laboratory and field studies to illustrate the grain sorting processes that give rise to and maintain step-pool bedforms. An example of one of their laboratory step-pool morphologies is given in Figure 3.52.

Lisle et al. (1997) describe the fate of sudden sediment pulses in streams such as the landslide shown in Figure 3.12. Sutherland et al. (2002), Cui et al. (2003a, 2003b) and Cui and Parker (in press) describe a numerical model of the disposition of pulses in rivers that includes both selective transport and abrasion. The basis of the model is Eq. (3.33) for sediment conservation (but modified for multiple lithologies), the St. Venant equations and the Parker (1990a) formulation of bed-load transport. The model was tested in the laboratory and applied successfully to the landslide of Figure 3.12 (Lisle et al, 1997; Lisle et al., 2001; Cui and Parker, in press).

## 3.14 THE CASE OF SUSPENSION-DOMINATED SAND-BED RIVERS

### 3.14.1 Sorting in Suspension-Dominated Streams

As was shown in Section 3.4, sand-bed streams tend to a) be suspension-dominated and b) contain sediment that is much more uniform than gravel-bed streams. This rule is not universal. Muddy Creek (Dietrich and Whiting, 1989), for example, is an example of a small, relatively steep sand-bed stream in which bed-load and suspended load are both important. This observation notwithstanding, the larger the bank-full discharge and the lower the slope, the more likely a sand-bed stream is to be suspension-dominated.

Even though the bulk of the bed material load might be carried in suspension, one must not dismiss out of hand the possibility that the bed-load might do most of the sorting in such streams. To this end, consider as an example the bed-load equation of Ashida and Michiue (1972), Eq. (3.77a). As the Shields number becomes large compared to the critical Shields number, the relation reduces to

$$\frac{q_i}{F_i\sqrt{RgD_i}D_i} = 17\left(\frac{\tau_{bs}}{\rho RgD_i}\right)^{3/2} \tag{3.123a}$$

or reducing with Eq. (3.47),

$$\frac{q_i}{F_i} = \frac{17}{Rg}u_{*s}^3 \tag{3.123b}$$

That is, $q_i/F_i$ becomes independent of grain size. This result and Eq. (3.28) allow the conclusion that at Shields numbers sufficiently high to allow the neglect of the critical Shields numbers $\tau_{sci}^*$ in Eq. (3.77a) the bed-load size distribution becomes identical with that of the active layer, implying surface-based equal mobility and the absence of sorting.

The same result holds for the relations of Parker (1990a), Hunziker and Jaeggi (2002), Wilcock and Kenworthy (2002) and Powell et al. (2001) presented in Section 3.7. This is because in all these relations, for large values $\tau_i^*$ a) $q_i^*$ varies with $(\tau_i^*)^{3/2}$ and b) the critical or reference Shields number containing the hiding function drops out. The near-absence of armoring in the Nahal Yatir at Shields numbers based on surface $D_{50}$ between 0.1 and 0.3, as illustrated in Section 3.10.3, argues for the validity of this conclusion. In sand-bed streams of the type shown in Figure 3.29 the bank-full Shields number is on the order of 50 times the critical or reference value, with an average of 1.86. Even the assumption that as much as half of this is form drag does not change the conclusion that sorting due to bed-load should be rather minor in suspension-dominated sandbed streams. Some bed-load sorting may be caused topographically in accordance with Eq. (3.20b), however.

Before continuing with the issue of sediment sorting in suspension-dominated sand-bed streams, however, it is important to note that there is a class of streams which are bed-load-dominated but have beds with significant quantities of both sand and gravel and have median grain sizes falling in the ranges of coarse sand to fine gravel. These streams are seen in Figure 3.30 as the Japanese streams which fall in between the sand-bed and gravel-bed clusters of Figure 3.29. Kleinhans (2002) has described reaches of the Rhine, Allier and Meuse Rivers of Europe which fall into this range (see Figure 2.1 therein, which has the same format as Figures 3.30 and 3.31 here). Blom and Kleinhans (1999) and Kleinhans (2002) have modeled them experimentally, as have Wilcock et al. (2001). It is evident from Figure 3.2 that bedforms such as dunes play a major role in vertical sorting in such streams. The relations proposed by Wilcock and Kenworthy (2002) described in Section 3.7.9, Wilcock and Crowe (2003) described in Section 3.7.10 and Kleinhans and van Rijn (2002) mentioned in Section 3.7.14 may be used to predict grain size-specific bed-load transport in this type of river.

Sorting of suspended sediment arises from a rather different mechanism than that applying to bed-load. In turbulent suspensions of sediment, the finer particles tend to ride higher in the water column. This biases them toward a zone of higher velocity, and amplifies their downstream transport rate at the expense of the coarser grains. For the same reason finer particles are more likely to be carried overbank and deposited on the floodplain.

### 3.14.2 Modified Rouse-Vanoni Approach for Grain Size-Specific Suspended Load

The analysis of Chapter 2 is here modified for multiple grain sizes. The overbars below denote averages over turbulence. Let $\overline{c}_i(s, z, t)$ denote the volume concentration of suspended sediment of the *ith* grain size class at streamwise position *s*, normal distance above the bed *z* and time *t*. The grain size ranges are chosen so as to exclude wash load, which is conventionally (but not necessarily accurately) equated with the sediment in transport in the silt and clay sizes (< 0.0625 mm). The total concentration of bed material load in suspension is thus given as

$$\overline{c}_T = \sum_{i=1}^{n} \overline{c}_i \tag{3.124}$$

Eq. (3.23) is generalized to

$$(1-\lambda_p)\left[ f_{Ii}\frac{\partial \eta_b}{\partial t} + \frac{\partial}{\partial t}(L_a F_i) \right] = -\frac{\partial q_i}{\partial s} + v_{si}\left(\overline{c}_{bi} - E^*_{si}\right) \tag{3.125}$$

where

$$\overline{c}_{bi} = \overline{c}_i\big|_{z=z_b} \tag{3.126}$$

denotes a near-bed reference concentration at elevation $z = z_b$ and $v_{si}$ denotes the fall velocity of the *ith* grain size. In addition, $E_{si}^*$ denotes a dimensionless rate of entrainment of sediment from the bed such that $E_{si} = v_{si}E_{si}^*$ is the volume rate of entrainment of sediment from the *ith* grain size range per unit time per unit bed area, and $v_{si}\bar{c}_{bi}$ denotes the deposition rate of the *ith* class per unit time per unit bed area.

In the case of an equilibrium suspension, entrainment into suspension balances deposition from it, so that

$$E_{si}^* = \bar{c}_{bi} \tag{3.127}$$

In general, however, $\bar{c}_i$ must satisfy the advection-diffusion equation of conservation of suspended sediment. This is presented below in 2-D form in the *s*-*z* plane with *z* denoting the upward normal direction and the parameter $D_d$ denoting the kinematic eddy diffusivity of suspended sediment, here approximated by the corresponding value for momentum;

$$\frac{\partial \bar{c}_i}{\partial t} + \bar{u}\frac{\partial \bar{c}_i}{\partial s} + \left(\bar{w} - v_{si}\right)\frac{\partial \bar{c}_i}{\partial z} = \frac{\partial}{\partial z}D_d\frac{\partial \bar{c}_i}{\partial z} \tag{3.128}$$

This equation is in turn coupled to the equations of streamwise momentum balance and continuity of the flow;

$$\frac{\partial \bar{u}}{\partial t} + \bar{u}\frac{\partial \bar{u}}{\partial s} + \bar{w}\frac{\partial \bar{u}}{\partial z} = -g\frac{\partial H}{\partial s} - g\frac{\partial \eta}{\partial s} + \frac{\partial}{\partial z}D_d\frac{\partial \bar{u}}{\partial z} \tag{3.129}$$

$$\frac{\partial \bar{u}}{\partial s} + \frac{\partial \bar{w}}{\partial z} = 0 \tag{3.130}$$

In Eqs. (3.128) and (3.129) the slender flow approximation has been used to a) drop the streamwise turbulent diffusion terms, b) drop the upward normal equation of momentum balance and c) approximate the pressure distribution as hydrostatic. The above three relations easily generalize to 3-D flow.

The boundary conditions on Eq. (3.128) are

$$-D_d\frac{\partial \bar{c}_i}{\partial z}\bigg|_{z_b} = v_{si}E_{si}^*\ , \quad \left(v_{si}\bar{c}_i + D_d\frac{\partial \bar{c}_i}{\partial z}\right)\bigg|_{z=H} = 0 \tag{3.131a,b}$$

where $E_{si}^*$ is a specified function of the flow. The first of these specifies the near-bed rate of entrainment of sediment into suspension, and the second of these specifies the condition of vanishing upward normal sediment flux at the water surface. Eq. (3.131a) is sometimes replaced with a concentration boundary condition, according to which

$$\overline{c}_{bi} = \overline{c}_i\big|_{z=z_b} = \overline{c}_{bed,i} \tag{3.131c}$$

where $\overline{c}_{bed,i}$ is a specified function of the flow. In the case of equilibrium suspensions Eqs. (3.131a) and (3.131c) yield identical results in light of Eq. (3.127). In the case of disequilibrium suspensions Eq. (3.131a) is the preferred form, as outlined in e.g. Parker (1978a). The boundary conditions on the flow are

$$\frac{\overline{u}\big|_{z_b}}{u_*} = \frac{1}{\kappa} ln\left(30\frac{z_b}{k_s}\right), \quad D_d \frac{\partial \overline{u}}{\partial z}\bigg|_H = 0, \quad \overline{w}\big|_{z_b} = 0, \quad \left(\frac{\partial \overline{u}}{\partial t} + \overline{u}\frac{\partial \overline{u}}{\partial s} - \overline{w}\right)\bigg|_H = 0 \tag{3.132a-d}$$

i.e. that the streamwise flow velocity matches the logarithmic law near the bed, the water surface is free of shear stress, the normal velocity vanishes at the bed and the kinematic boundary condition is satisfied at the water surface. In Eq. (3.132a) $\kappa$ denotes the von Karman constant and $k_s$ is the roughness height of the bed.

As described in Chapter 2, density stratification effects induced by suspended sediment can interact with the flow. The net effect is to increase the flow velocity and reduce the concentrations of suspended sediment. Wright and Parker (2004a,b) have shown that this effect is particularly important in large, low-slope sand-bed rivers.

Extending the model of Smith and McLean (1977) outlined in Chapter 2 to sediment mixtures, the turbulent eddy viscosity $D_d$ is damped by a stratification effect mediated by the gradient Richardson number $RI_g$;

$$D_d = D_{do} F_{strat}\left(RI_g\right), \quad RI_g = \frac{-Rg\dfrac{\partial \overline{c}_T}{\partial z}}{\left(\dfrac{\partial \overline{u}}{\partial z}\right)^2} \tag{3.133a,b}$$

In the above relation $F_{strat}(RI_g)$ is a specified function of the gradient Richardson number that Smith and McLean (1977) equate to

$$F_{strat}\left(RI_g\right) = 1 - 4.7RI_g \tag{3.133c}$$

Note that according to Eq. (3.133c) the turbulence should be completely damped out for a gradient Richardson number of 0.21, a value that is fully in accord with the more advanced turbulence closure scheme of Mellor and Yamada (1974).

The above Eqs. (3.128) –(3.130) can be solved subject to Eq. (3.131a) or Eq. (3.131c), Eq. (3.131b), Eqs. (3.132), the above simple turbulence closure model and appropriate initial conditions to yield solutions for $\overline{c}_i(s,z,t)$ and $\overline{u}(s,z,t)$. The depth-

averaged flow velocity $U$ and concentrations $C_i$ and the bed material part of the volume suspended load per unit width per unit time $q_{si}$ are then computed as

$$UH = \int_{z_b}^{H} \overline{u}\, dz\ , \quad q_{si} = UC_i H = \int_{z_b}^{H} \overline{u}\,\overline{c}_i dz \tag{3.134a,b}$$

Eq. (3.128) can be depth-integrated subject to Eqs. (3.131a,b), yielding the relation

$$\frac{\partial C_i H}{\partial t} + \frac{\partial q_{si}}{\partial s} = v_{si}\left(\overline{c}_{bi} - E_{si}^{*}\right) \tag{3.135}$$

As long as the time rate of change of the volume of suspended sediment stored in the water column per unit bed area is small (as can be expected for nearly all fluvial suspensions), the first term on the left-hand side of Eq. (3.135) can be dropped, so that Eq. (3.125) reduces to

$$(1-\lambda_p)\left[ f_{Ii}\frac{\partial \eta_b}{\partial t} + \frac{\partial}{\partial t}(L_a F_i)\right] = -\frac{\partial q_i}{\partial s} - \frac{\partial q_{si}}{\partial s} = -\frac{\partial q_{bmi}}{\partial s} \tag{3.136}$$

where $q_{bmi}$ denotes the volume bed material load (bed-load + bed material suspended load) transport rate per unit time per unit width.

Let $U_{ch}$, $H_{ch}$ and $v_{sch}$ denote characteristic values for flow velocity, flow depth and sediment fall velocity. The parameter $(U_{ch}/v_{sch})H_{ch}$ defines an appropriate relaxation length for streamwise adjustment of the suspended sediment profile. When the length scale of interest for sorting due to suspension is smaller than this relaxation length the full 2D (or 3D) problem for the flow and suspended sediment profiles must be solved in order to determine the evolution of the bed elevation and sorting in accordance with Eq. (3.125). An example of this is the sorting of sediment over one bend or meander length of a suspension-dominated stream, in which case Eq. (3.125) must be amended to the 2D form

$$(1-\lambda_p)\left[ f_{Ii}\frac{\partial \eta_b}{\partial t} + \frac{\partial}{\partial t}(L_a F_i)\right] = -\frac{\partial q_{s,i}}{\partial s} - \frac{\partial q_{n,i}}{\partial n} + v_{si}\left(\overline{c}_{bi} - E_{si}^{*}\right) \tag{3.137}$$

in order to include transverse effects. In the above relation $(q_{s,i}, q_{n,i})$ denotes the volume bed-load transport rate per unit width in the *(s, n)* directions.

When the length scale of interest is, on the other hand, sufficiently long compared to the relaxation length it suffices to obtain $q_{si}$ from a quasi-equilibrium solution for suspension and flow and allow the bed to evolve and sort according to, e.g. in the case of a 1D formulation, Eq. (3.136). An example of such a problem is downstream fining in suspension-dominated sand-bed streams.

The case of an equilibrium or quasi-equilibrium suspension is considered below. As in Chapter 2, for simplicity the turbulent eddy diffusivity in the absence of stratification $D_{do}$ is chosen to be the one that yields the logarithmic profile;

$$D_{do} = \kappa u_* z\left(1-\frac{z}{H}\right) \tag{3.138}$$

For this case Eqs. (3.128) – (3.132) can be solved to yield

$$\bar{c}_i = E_{si}^* exp\int_{z_b}^{z}\left[-\frac{\nu_{si}}{\kappa u_* z\left(1-\frac{z}{H}\right)F_{strat}\left(RI_g\right)}dz\right] \tag{3.139a}$$

and

$$\bar{u} = \frac{u_*}{k}\left[ln\left(30\frac{z_b}{k_s}\right)+\int_{z_b}^{z}\frac{1}{zF_{strat}\left(RI_g\right)}dz\right] \tag{3.139b}$$

The above two equations do not in and of themselves constitute a solution to the problem, because $RI_g$ is a function of the concentration gradient $\partial\bar{c}_T/\partial z$ as specified by Eq. (3.133b). They can, however, be readily enough solved iteratively, starting with the Rouse-Vanoni concentration profile (Rouse, 1939) and logarithmic velocity profile that would prevail in the absence of stratification. These are obtained by setting $F_{strat}$ equal to unity in Eqs. (3.139a,b), yielding the respective forms

$$\bar{c}_i = E_{si}^*\left[\frac{\left(1-\frac{z}{H}\right)}{\left(1-\frac{z_b}{H}\right)}\right]^{\frac{\nu_{si}}{\kappa u_*}}$$
$$\bar{u} = \frac{u_*}{\kappa}ln\left(30\frac{z}{k_s}\right) \tag{3.140a,b}$$

Once the solutions for $\bar{c}_i$ and $\bar{u}$ are obtained the grain size-specific transport rates $q_{si}$ are evaluated as

$$q_{si} = \int_{z_b}^{H}\bar{u}\bar{c}_i dz \tag{3.141}$$

and bed evolution and sorting can be evaluated from Eq. (3.136).

### 3.14.3 Grain Size-Specific Relations for Sediment Entrainment or Near-bed Concentration

Few relations specifically designed for predicting the entrainment (bed concentration) of heterogeneous suspended sediment appear to be available. One of these is due to Garcia and Parker (1991). Along the lines of Section 3, the following general form is assumed;

$$\frac{E_{si}^*}{F_i} \equiv \hat{E}_{si} = T_{se}\left(\frac{u_{*s}}{v_{si}}, \frac{D_i}{D_{50}}, Re_{pi}, \sigma\right), \quad Re_{pi} = \frac{\sqrt{RgD_i}D_i}{\nu} \tag{3.142a,b}$$

Garcia and Parker (1991) used a similarity collapse of laboratory data, as well as field data from two small sand-bed streams, to obtain the following entrainment relation;

$$\hat{E}_{si} = \frac{AZ_{ui}^5}{1 + \frac{A}{0.3}Z_{ui}^5} \quad , \quad Z_{ui} = \lambda_m \frac{u_{*s}}{v_{si}} Re_{pi}^{0.6}\left(\frac{D_i}{D_{50}}\right)^{0.2} \tag{3.143a-d}$$
$$\lambda_m = 1 - 0.298\sigma \quad , \quad A = 1.3x10^{-7}$$

Recently Wright and Parker (2004b) found that the above relationship, while reasonably accurate for small to medium sand-bed streams, overpredicts the entrainment rate for large sand-bed streams. They have modified the relation as follows; $\hat{E}_{si}$ is still given Eq. (3.143a), but $Z_{ui}$ is now given by the relation

$$Z_{ui} = \lambda_m\left(\frac{u_{*s}}{v_{si}} Re_{pi}^{0.6}\right) S^{0.08}\left(\frac{D_i}{D_{50}}\right)^{0.02} \tag{3.143e}$$

where

$$A = 7.8x10^{-7} \tag{3.143f}$$

and $S$ denotes bed slope. In Eq. (3.143e), $\lambda_m$ is still given by Eq. (3.143c).

In either the original or amended Garcia-Parker relations the value $z_b$ at which the entrainment rate is evaluated is specified as

$$z_b = 0.05H \tag{3.143g}$$

This value was chosen because data were available at this elevation with which to develop the relation. Once the concentration profile is determined it can be extrapolated downward to find values closer to the bed.

McLean (1991, 1992) formulates the problem in terms of the concentration boundary condition of the form of Eq. (3.131c) rather than the entrainment boundary condition of Eq. (3.131a). McLean presents the following relation for near-bed concentration. Let $\bar{c}_{bT}$ denote the total near-bed concentration summed over all grain sizes. Recalling that $f_{bi}$ denotes the fractions in the bed-load, the computation for the near-bed concentrations $\bar{c}_{bi}$ proceeds as follows:

$$\bar{c}_{bi} = f_{sbi}\bar{c}_{bT} \tag{3.144a}$$

where $\bar{c}_{bT}$ denotes the total near-bed concentration summed over all grain sizes, $f_{sbi}$ denotes the fraction of the near-bed suspended sediment in the *i*th grain size range and

$$\bar{c}_{bT} = \frac{\gamma_o\left(\frac{\tau_{bs}}{\tau_{bsc}}-1\right)}{1+\gamma_o\left(\frac{\tau_{bs}}{\tau_{bsc}}-1\right)}\left(1-\lambda_p\right) \quad , \quad \gamma_o = 0.004$$

$$f_{sbi} = \frac{\varphi_i f_{bi}}{\sum_{i=1}^{n}\varphi_i f_{bi}} \quad , \quad \varphi_i = \begin{cases} 1 & for \quad u_{*s}/v_{si} > 1 \\ \dfrac{u_{*s}-u_{*sc}}{v_i - u_{*sc}} & for \quad u_{*s}/v_{si} < 1 \end{cases} \tag{3.144b-g}$$

$$u_{*s} = \sqrt{\frac{\tau_{bs}}{\rho}} \quad , \quad u_{*sc} = \sqrt{\frac{\tau_{bsc}}{\rho}}$$

The McLean relation uses a single critical shear stress $\tau_{bsc}$ evaluated using size $D_{50}$; this value is applied to all grain sizes. The relation for the point $z_b$ at which the near-bed concentrations are evaluated is

$$z_b = max\left(\begin{matrix} a_D D_{84} \\ a_o \delta_B(D_{84}) \end{matrix}\right) \quad , \quad \delta_B(D) = D\frac{A_1\left(\frac{\tau_{bs}}{\tau_{bsc}}-1\right)}{1+A_2\left(\frac{\tau_{bs}}{\tau_{bsc}}-1\right)} \tag{3.144h-i}$$

$$a_D = 0.12 \quad , \quad a_0 = 0.056 \quad , \quad A_1 = 0.68$$
$$A_2 = 0.0204(\ln D)^2 + 0.022(\ln D) + 0.0709 \tag{3.144j-m}$$

In the relation for $A_2$ the grain size must be in mm. The McLean formulation can also be used to specify the entrainment boundary condition, of Eq. (3.131a), in which case the functional form for $E_{si}^*$ is simply taken to be

$$E_{si}^* = f_{sbi}\bar{c}_{bT} \tag{3.144n}$$

### 3.14.4 Grain Size-Specific Bulk Predictors for Bed Material Load

The relation of Ackers and White (1980) as generalized for mixtures by Proffitt and Sutherland (1983) has been presented in Section 3.7.13. In this form it predicts the transport rate and grain size distribution of the bed material load, i.e. bed-load and bed material component of suspended load. As a predictor of total bed material load in its original form, which is not grain size-specific, the relation of Ackers and White has been shown to perform quite well for both laboratory and field streams (Brownlie, 1981; see also Chapter 2). The grain size-specific dependency was, however, introduced with the aid of a hiding function developed for coarse material. It remains to be seen how well the relation sorts sand.

The bed material load predictor of Yang (1973) has been presented in Chapter 2. That formulation uses only a single grain size. As discussed in Section 3.7.14, Yang and Wan (1991) have extended this formulation for sediment mixtures. The accuracy of the predictions of total bed material transport rate summed over all sizes has been tested against data with excellent agreement. The accuracy of the predicted grain size distributions of the bed-load has not similarly been subjected to a thorough test.

The bulk predictor for bed material transport rate of Karim and Kennedy (1981) was presented in Chapter 2. Karim (1998) has generalized the formulation for sediment mixtures. The generalization appears to apply specifically to sand-bed streams. Karim's relation takes the form

$$\frac{q_{bmi}}{F'_{ai}\sqrt{RgD_i}\,D_i} = 0.00139\left(\frac{U}{\sqrt{RgD_i}}\right)^{2.97}\left(\frac{u_*}{v_{si}}\right)^{1.47}\eta_i$$

$$\eta_i = C_1\left(\frac{D_i}{D_{50}}\right)^{C_2}, \quad C_1 = 1.15\left(\frac{v_{s50}}{u_*}\right), \quad C_2 = 0.60\left(\frac{v_{s50}}{u_*}\right) \qquad \text{(3.145a-d)}$$

In the above relations $F'_{ai}$ is computed from $F_i$ as

$$F'_{ai} = \frac{\left(F_i / D_i\right)}{\sum_{i=1}^{n}\left(F_i / D_i\right)} \qquad \text{(3.145e)}$$

Karim (1998) reports good agreement between the predicted load and grain size distribution and the observed values in three sand-bed streams; the Niobrara River, the Middle Loup River and Missouri River. The above formulation may be used in conjunction with the resistance formulation of Karim and Kennedy (1981), which was developed in tandem with the original bulk predictor of total bed material load of that document.

In addition to the grain size-specific bulk predictor for bed-load transport presented in Section 3.7.10, Wu et al. (2000) also present the following grain size-specific bulk predictor for the bed material part of the suspended load;

$$W^*_{sui} = \frac{Rgq_{si}}{\bar{f}_i u^3_{*s}} = 0.0000262 \frac{1}{\left(\tau^*_{si}\right)^{3/2}} \left[ \left( \frac{\tau^*_{si}}{\tau^*_{suri}} - 1 \right) \frac{U}{v_{si}} \right]^{1.74} \tag{3.146}$$

The relation has the advantage of simplicity. Wu et al. report excellent agreement with data when Eqs. (3.85) and (3.146) are used to predict grain size-specific bed material load, i.e. $q_{bmi} = q_i + q_{si}$.

Recently Wright and Parker (2004b) have used Eqs. (3.143a,e,f,g), Eqs. (2.177-2.181) of Chapter 2 and a consideration of flow stratification to develop a grain size-specific predictor of suspended load in sand-bed rivers. While the method is intended to be of general applicability, the formulation is specifically intended to capture flow stratification effects that can be significant in large, low-slope sand-bed streams.

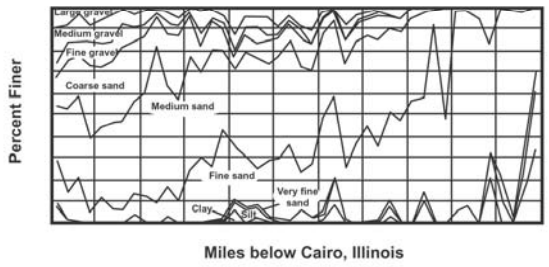


a)

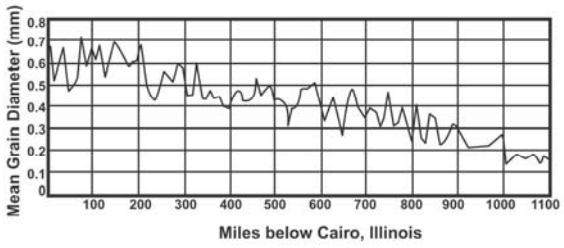


b)

Figure 3.53 Downstream fining in the bed material of the Mississippi River, USA. a) Downstream variation in grain size distribution. b) Downstream variation in mean grain size.

### 3.14.5 Downstream Fining in Sand-bed Streams

Downstream fining of bed sediment in a long reach of a large, low-slope sand-bed river is illustrated in Figure 3.53 for the Mississippi River between Cairo, Illinois and the Head of Passes, Louisiana, a reach nearly 1800 km long (Waterways Experiment Station, 1935, as quoted by Simons, 1971). Fig. 3.53a shows the streamwise variation of the complete grain size distribution and Fig. 3.53b shows the streamwise variation of the mean grain size of sand only. The former figure documents the pinch-out of the gravel, the coarse sand and then the medium sand as the bed fines. The latter figure documents a reduction in mean sand grain size from about 0.65 mm to under 0.20 mm over the reach.

Hydraulic sorting is only one cause of downstream fining. In the case of the Mississippi River, downstream fining may also be influcnece by the the delivery of successively finer sediment from tributaries farther downstream. In the case of the

pattern of downstream fining in the middle Fly River, Papua New Guinea illustrated in Figure 3.54 (Pickup et al., 1979; Dietrich et al., 1999), however, the cause is unambiguously hydraulic sorting. This is because no important tributaries enter the Fly over the reach extending from 50 km to 450 km in Figure 3.54, so that the input of both water and sediment from tributaries is small. Hydraulic sorting also appears to be the dominant mechanism of downstream fining on the reach of the Beni River, Bolivia studied by Aalto (2002).

The pattern of downstream fining given in Figure 3.54 characterizes conditions before the advent of sediment disposal from the Ok Tedi copper mine in 1985. Since then both the sediment balance of the river and the pattern of downstream fining in the middle Fly River has been greatly modified, with median size reduced by about half and the intensity of downstream fining suppressed (Dietrich et al., 1999; Cui and Parker, 1999).

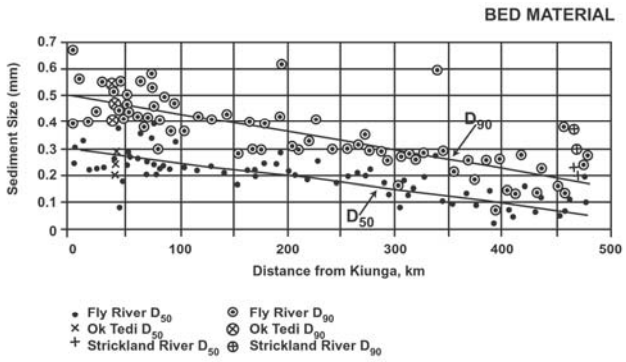


Figure 3.54 Downstream variation in $D_{50}$ and $D_{90}$ in the middle Fly River, Papua New Guinea in 1979, before the opening of the Ok Tedi copper mine in 1985.

The first attempt to numerically model downstream fining in any stream was the simple treatment of Deigaard (1980) applied to the sand-bed Niger River. Since that time the case of sand-bed streams has been neglected. Cui and Parker (1999), however, report on a model of downstream fining in the middle Fly River. The model uses water and sediment inputs specified on a daily basis, calculations of the flow based on a gradually-varied implementation of the St. Venant shallow water equation and a Rousean formulation neglecting stratification effects for $q_{si}$. Bed evolution is computed from an implementation of Eq. (3.136), with $L_a$ scaling with dune height and with the addition of the subsidence term in Eq. (3.116). The model also includes a simple formulation for overbank deposition, as outlined in the next section.

Wright and Parker (2004a,b) have demonstrated that stratification effects are usually negligible in sand-bed streams with medium to steep slopes. In large, low-slope sand bed streams, however, stratification can be sufficient to a) substantially suppress the bed material suspended load, and b) substantially reorganize the size distribution of this load toward the finer. Stratification may thus play an important role in the pattern of downstream fining in such streams.

### 3.14.6 Grain Size-specific Formulations for Floodplain Deposition of Suspended Sediment

The ability of a river to access its floodplain during floods is illustrated in Figure 3.55. The study of overbank deposition of sediment due to floods has been until recently the province of geographers and geologists rather than engineers. A summary of recent literature on floodplain processes can be found in Anderson et al. (1996).

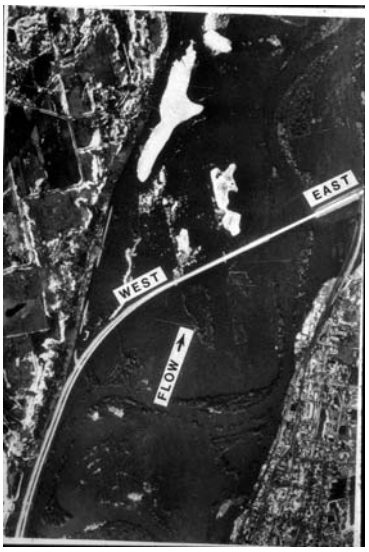

Figure 3.55 View of the floodplain of the Minnesota River, Minnesota, USA during the flood of record in 1965.

In recent years engineers have been drawn into the field of floodplain sedimentation in order to a) design river restoration projects, b) predict the deposition of anthropogenic sediment on floodplains and c) track the accumulation of toxic metals adsorbed onto the finest sediment grains as they deposit on the floodplain. Figure 3.56 illustrates a floodplain that has been heavily damaged by a flood which carried toxic sediments overbank in 1910.

The Exner equation of sediment continuity, Eq. (3.103) is here modified to the form

$$(1-\lambda_p)B_c\left(f_{Ii}\frac{\partial \eta_b}{\partial t}+L_a\frac{\partial F_i}{\partial t}\right)=-\frac{\partial B_c q_i}{\partial s}-\frac{\partial B_c q_{si}}{\partial s}-q_{obi} \qquad (3.147)$$

in order to include overbank deposition of sediment during floods. Here $q_{obi}$ denotes the volume rate of overbank deposition of sediment in the *ith* grain size range per unit time per unit channel length, including both banks. ($B_c$ in the above equation is modified to $B_{ca}$ only after zeroing of the model, as described in Section 3.10.2).


a) b)

Figure 3.56 a) View of a reach of Silver Bow Creek, Montana, USA in which the floodplain is so rich in toxic sediments that vegetation cannot take hold. The toxic sediment is derived from the Anaconda copper mine near Butte, Montana; the flood that deposited the sediment occurred in 1910. b) View of an uncontaminated, healthy tributary of Silver Bow Creek.

Narinesingh (1995), Narinesingh et al. (1999) and Parker et al. (1996) have independently devised very similar models for the computation of the parameter $q_{obi}$, one in the context of river restoration in the Netherlands, and the other in the context of floodplain deposition of mine-derived sediment. The basis of both models is convective rather than diffusive. Consider the meandering river of Figure 3.57. The total floodplain or meander belt width over which floodplain deposition takes place is denoted as $B_f$; the value includes both sides of the river. Overbank flow is followed along a characteristic floodplain streamtube of length $L_f$ from channel to channel. In the case of a vegetated floodplain, any sediment that deposits is unlikely to be resuspended. Let $C_{fi}$ denote the depth-averaged volume concentration of sediment in the *ith* grain size range in the water column over the floodplain, and let $H_f$ denote floodplain depth and $U_f$ denote depth-averaged floodplain velocity. Where $s_f$ denotes distance along the streamtube, then,

$$\frac{D}{Dt}\left(C_{fi}H_f\right)=U_f H_f\frac{dC_{fi}}{ds_f}=-v_{si}C_{fi} \quad (3.148)$$

Integrating along the streamtube from channel to channel, the volume deposition rate of the of material in the *ith* grain size range per unit time per unit distance normal to the coordinate $s_f$ is given as

$$v_{si}\int_0^{L_f} C_{fi}ds_f = v_{si}C_{ucfi}\frac{U_f H_f}{v_{si}}\left[1-exp\left(-\frac{v_{si}L_f}{U_f H_f}\right)\right]= \quad (3.149)$$
$$U_f H_f C_{ucfi}\left[1-exp\left(-\frac{v_{si}L_f}{U_f H_f}\right)\right]$$

where $C_{ucfi}$ denotes the concentration of sediment in the *ith* grain size range in the channel, averaged over that part of the channel flow that is above bank-full, i.e. over a layer with thickness $H_f$.

Now every such stream tube is of a different length, but one may reliably assume that $L_f$ scales with $B_f$ for most meandering streams. Assuming that the area of floodplain $A_b$ delineated by a single bend scales as

$$A_{pb}\approx B_f L_f \approx B_f^2 \quad (3.150)$$

and recalling that floodplain discharge $Q_f$ is given by

$$Q_f = U_f B_f H_f \quad (3.151)$$

the volume deposition rate per unit floodplain area per unit time $D_{fpi}$ scales as

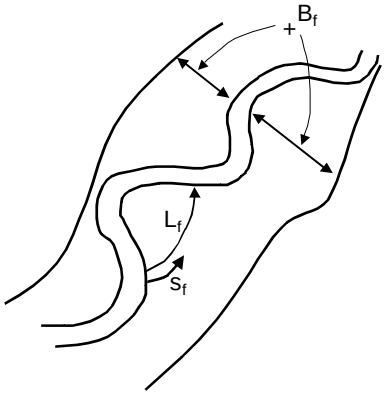

Figure 3.57 Diagram illustrating floodplain deposition.

$$D_{fpi} \approx \frac{C_{ucfi} Q_f}{B_f L_f}\left[1 - exp\left(-\frac{v_{si} L_f}{U_f H_f}\right)\right] \approx$$
$$\frac{C_{ucfi} Q_f}{B_f^2}\left[1 - exp\left(-\alpha_f \frac{v_{si} B_f^2}{Q_f}\right)\right] \equiv$$
$$Fl \frac{C_{ucfi} Q_f}{B_f^2}\left[1 - exp\left(-\alpha_f \frac{v_{si} B_f^2}{Q_f}\right)\right] \tag{3.152}$$

where $Fl$ is a dimensionless "floodplain number" and $\alpha_f$ is a dimensionless "attenuation coefficient," both of which might be expected to be of order unity. The parameter $q_{obi}$ in Eq. (3.147) is thus given as

$$q_{obi} = D_{fpi} B_f = Fl C_{ucfi} \frac{Q_f}{B_f}\left[1 - exp\left(-\alpha_f \frac{v_{si} B_f^2}{Q_f}\right)\right] \tag{3.153}$$

The parameter $C_{ucfi}$ can be computed from Eq. (3.132) as

$$C_{ucfi} = \frac{1}{H_f}\int_{H_{bf}}^{H_{bf}+H_f} \overline{c}_i dz = \frac{E_{si}}{H_f}\int_{H_{bf}}^{H_{bf}+H_f} exp\int_{z_b}^{z}\left[-\frac{v_{si}}{\kappa u_* z\left(1-\frac{z}{H}\right)F_{strat}\left(RI_g\right)} dz'\right] dz \tag{3.154}$$

where $H_b$ denotes bank-full depth. Eq. (3.146) can be coupled to a model of channel-floodplain flow such as that described in Section 3.10.2 in order to perform the calculation of floodplain deposition for each time step for which the channel is overbank. The parameters $Fl$ and $\alpha_f$ must at this point be calibrated for every application. Cui and Parker (1999), however, were able to obtain reasonable results with the values $0.2 < Fl < 0.72$ and $exp\left[-\alpha_f\left(v_{si} B_f^2\right)/Q_f\right] << 1$.

The above formulation of overbank deposition is both preliminary and incomplete. For example, it does not encompass splay deposits which provide a mechanism for bringing relatively coarse bed sediment onto the floodplain (e.g. Aalto, 2002).

### 3.14.7 Deposition of Fine Sediments in and Flushing from Gravels

As noted above, sand and silt often move through a gravel-bed river as throughput load during floods, with little interplay with the beds beyond partial filling of the interstices of newly-deposited gravels. When the concentrations of these "fines" are too

high, or when the flow velocities are too low to prevent excess accumulation of within the gravel framework, the gravels can become polluted with fines. This fines pollution degrades the gravel bed as both spawning grounds and habitat for anadromous fish. The discharge of relatively sediment-free flushing flows, often from an upstream reservoir, can at least partially remove the fines and renew the gravel.

Reiser (1998) provides a summary of the ecological and biological requirements of gravel-bed rivers, with emphasis on the quality of the bed sediments. Diplas and Parker (1992) have described experimentally the process of pollution of gravel beds by fines; Huang and Garcia (2000) provide a predictive model of fines pollution. Milhous (1998) describes a numerical model for designing flushing flows in gravel-bed streams. Wilcock et al. (1996) describe how flushing can be implemented on the Trinity River, California, and Wilcock (1998b) provides general criteria for the design of flushing flows.

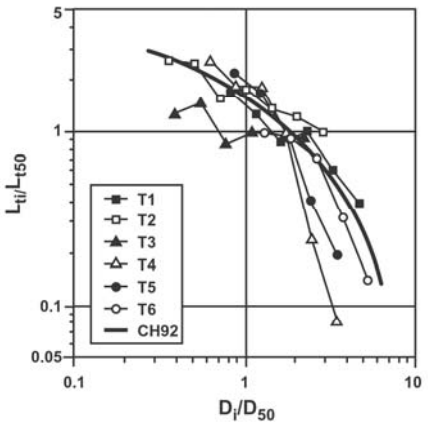


Figure 3.58 Relative travel distance of tracers in each size class as a function of relative grain size. From Ferguson and Wathen (1998).

## 3.15 TRACERS AND VERTICAL SORTING

### 3.15.1 Tracers

The use of tracer particles has a venerable history in the study of bed-load transport of mixed sizes in gravel-bed rivers (e.g. Leopold et al, 1966). In the early days of their use tracer particles were painted and placed on the bed of a stream during a dry period or at low flow. Recovery rates after a flood tended to be poor. More recently magnetically tagged particles have been used, much improving the recovery rates.

One way to characterize the relative mobility of grains of different sizes is to quantify the average distance $L_{ti}$ moved by tracers in each size class during a single flood as a function of grain size. Hassan et al. (1992), for example, found that the $L_{ti}$ tends to decrease only weakly with increasing grain size $D_i$ for the finer sizes in a mix, but declines notably with increasing grain size for sufficiently coarse grains. This result has been confirmed by Wilcock (1997b) and Ferguson and Wathen (1998). Field data for $L_{ti}/L_{t50}$ versus $D_i/D_{50}$, where $L_{t50}$ denotes the average distance moved by tracers with the surface median size $D_{50}$ are plotted in Figure 3.58. The data points are for the Allt Dubhaig (Ferguson and Wathen, 1998), and the solid line defines a relation determined by Church and Hassan (1992).

Tracers also provide an approximate method for characterizing the bed-load transport rate. The relation of Haschenburger and Church (1998) can be generalized to

estimate the volume bed-load transport rate per unit width $q_i$ for the *ith* grain size range as

$$q_i = (1-\lambda_p) v_{bi} L_a F_i \tag{3.155}$$

where $v_{bi}$ denotes the mean virtual velocity of the *ith* grain size and $L_a$ denotes the thickness of the active layer over which the grains are mixed during a transport event. The mean virtual velocity $v_{bi}$ is computed as the mean distance moved by tracers in the *ith* grain size range divided by the duration of the flood event during which they moved. It must be kept in mind that the value of $q_i$ determined from Eq. (3.148) represents an average over one flood, as the tracers cannot usually be recovered until the flood has subsided.

An implemention of Eq. (3.155) requires a knowledge of the thickness of the active layer $L_a$. This thickness has been inferred from the probability distribution of depth of burial of tracers as well as direct measurements of bed level variation in terms of scour and fill over one flood (e.g. Schick et al., 1987; Hassan, 1990, Hassan and Church, 1994; Wilcock, 1997b; Haschenburger, 1999). Figure 3.59 illustrates the use of "Leopold chains" to monitor scour and fill during a flood. Hassan and Church (1994), for example, have found that for single-peak floods the probability distribution associated with the depth of burial tends to follow an exponential curve, the exponent of which varies somewhat with grain size. The study indicates that a single flood is often sufficient to bury at least some tracers to a depth of 5 $D_{50}$ or more below the surface.

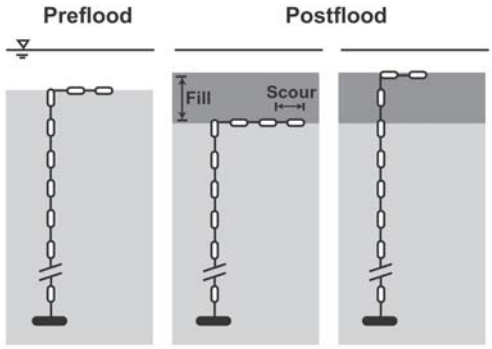


Figure 3.59 Diagram illustrating the use of "Leopold" scour chains to measure scour and fill associated with a flood. From Haschenburger (1999).

### 3.15.2 Extension of the Active Layer Model to Describe Vertical Sorting

The exponential curves for probability of depth of burial over a single flood are reminiscent of the curve for the probability of entrainment of a grain per unit time as a function of depth below the mean bed surface hypothesized in Figure 3.31c. That is, the exchange or active layer approximation of Figure 3.31d provides only the simplest possible description of the vertical exchange of particles of differing sizes associated with scour and fill. Schick et al. (1987), Hassan and Church (1994) and Haschenburger (1999) have devised

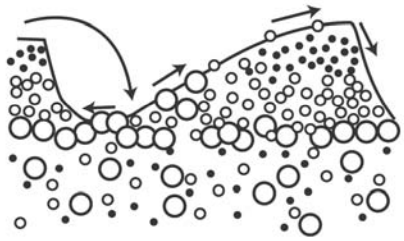

Figure 3.60 Schematization of the pattern of vertical sorting generated by the successive passage of dunes over a bed of heterogeneous sediment.

probabilistic models for vertical exchange of particles that use a probabilistic description with continuous variation in the vertical, rather than the simplification of a single, well-mixed layer underlain by a substrate that is never accessed in the absence of mean bed degradation.

The vertical exchange outlined in the papers above was likely accomplished in most cases by random scour and fill in the absence of well-developed dunes. Ribberink (1987) has investigated the case of vertical sorting of different sizes of sediment in a dune field, and has found a vertical structure of sorting that is too complex to explain in terms of the simple active layer model. This vertical sorting can be at least partially seen in Figure 3.2; a clearer schematization is given in Figure 3.60 (Blom et al., 2001). Blom and Ribberink (1999) and Blom and Kleinhans (1999) have found that as opposed to the typical case in gravel-bed streams, in the presence of dunes the coarser material tends to accumulate at the base of the dunes, creating a partial barrier between the somewhat finer substrate below and the considerably finer material in the migrating dunes above. Niño and Aracena (1999) have found a similar result for the case of ripples. Hooke (1968) describes an extreme case in which pebbles fed onto a sand bed covered with dunes migrated downward to form a one-grain thick immobile layer over which the dunes migrated.

In confirmation of the prediction of Suzuki and Michiue (1979), Blom and Ribberink (1999) and Blom and Kleinhans (1999) found that a wide grain size distribution tends to suppress dune amplitude. In addition, increasing stage of flow tends to mitigate the vertical sorting pattern.

The above observations have spurred the search for a formulation of the Exner equation for sediment continuity of size mixtures that is of more general validity than the active layer model of Section 3.5. Ribberink (1987), Ashida et al. (1989), Egashira and Ashida (1990) and Di Silvio (1991) introduced formulations with multiple layers in the vertical, each able to exchange with adjacent layers. Armanini (1995) went one step farther and developed a diffusion model for vertical mixing that is intrinsically continuous in nature.

Recently Parker et al. (2000) succeeded in developing a vertically continuous version of the Exner equation of sediment continuity for multiple grain sizes. The relation is based on a) the probability distribution associated with bed elevation fluctuations and b) structure functions for variation in the entrainment and deposition rates of sediment of various sizes with depth below the mean bed layer. The treatment draws heavily on the entrainment model of Tsujimoto (1991) for bed-load transport, as outlined in Section 3.5.5. The formulation can be briefly outlined as follows.

Let $\eta$ denote the local mean bed elevation averaged over fluctuations (see Fig. 3.31a) and let $y = z - \eta$ denote elevation relative to the mean bed elevation. The probability density function of elevation fluctuation is denoted as $p_e(y)$, and the parameter $P_s$ denoting the probability that the instantaneous bed is higher than elevation $y$ is defined as

$$P_s(y) = 1 - \int_{-\infty}^{y} p_e(y)dy \tag{3.156}$$

The bed-load entrainment and deposition rates $E_{bi}$ and $D_{bi}$ are those specified in Section 3.5.5. The local volume concentration of sediment in the bed $c_{bed}(y)$ is related to porosity as

$$c_{bed} = 1 - \lambda_p \tag{3.157}$$

and the mean value of $c_{bed}$ is given as

$$\bar{c}_{bed} = \int_{-\infty}^{\infty} c_{bed}(y) p_e(y)dy \tag{3.158}$$

Let $f_i(y)$ denote the grain size fractions of the bed at any relative elevation $y$ and $f_{bi}$ denote, as before, the grain size fractions in the bed-load. The conditions for grain size-specific sediment continuity then reduce to

$$\bar{c}_{bed}\frac{\partial \eta}{\partial t} = \sum_{i=1}^{n}\left(D_{bi} - E_{bi}\right)$$

$$c_{bed}P_s\frac{\partial f_i}{\partial t} = p_e\left[D_{bi}\left(\beta_{iD}f_{bi} - \frac{c_{bed}}{\bar{c}_{bed}}f_i\right) - E_{bi}\left(\beta_{iE} - \frac{c_{bed}}{\bar{c}_{bed}}\right)f_i\right] \tag{3.159a,b}$$

where $\beta_{iD}(y)$ and $\beta_{iE}(y)$ are bias functions determining the grain size-specific variation of deposition and entrainment rate with relative elevation $y$. Defining

$$\beta_D = \sum_{i=1}^{n}\beta_{Di}f_{bi}\ , \quad \beta_E = \sum_{i=1}^{n}\beta_{Ei}f_i\ , \tag{3.160}$$

it can be demonstrated that

$$\beta_D = \beta_E = \frac{c_{bed}}{\bar{c}_{bed}} \tag{3.161}$$

An appropriate integral in $y$ of Eqs. (3.159a,b) under simplifying assumptions recovers the active layer formulation of Eq. (3.40).

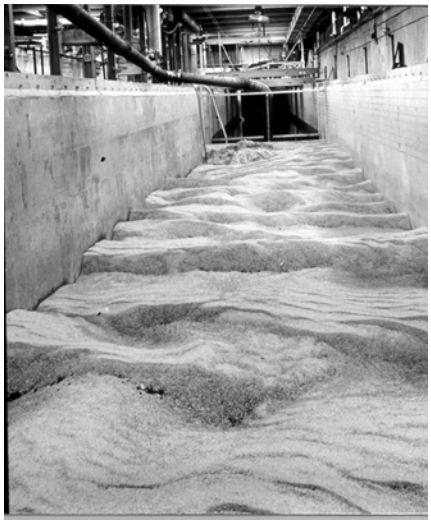

a)

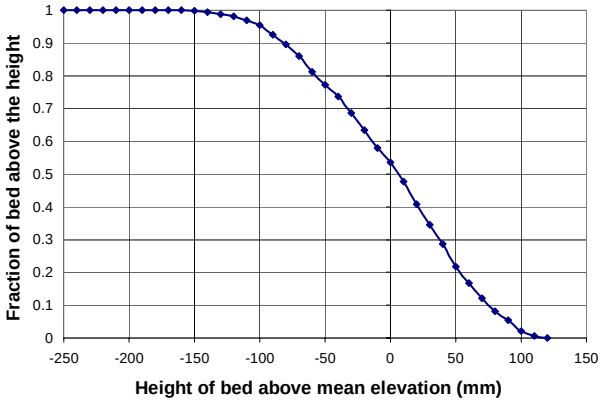


b)

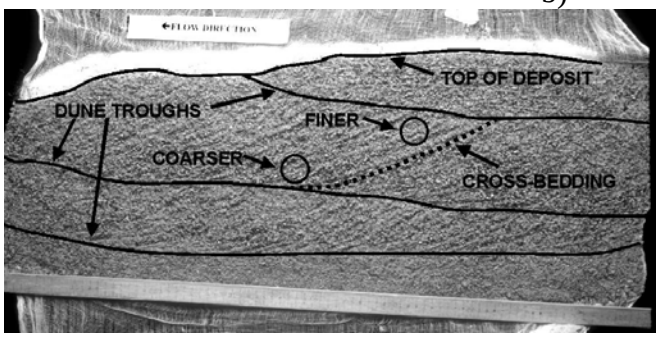


c)

Figure 3.61 a) Experimental dunes. b) $P_s(y)$ as a function of $y$ for the bed of part a). c) Pattern of stratification and sorting created by the passage of dunes in the flume illustrated in part a). From Parker et al. (2000).

Parker et al. (2000) did not specify general forms for the bias functions necessary to implement the model with confidence. Blom et al. (2001) have, however, implemented it in the case of the vertical dispersion of tracers in uniform material. In addition Blom (2003) has adapted the formulation for mixtures and specified bias functions for rivers which transport significant amounts of both gravel and sand as bed-load. Further development of such vertically continuous descriptions of grain size-specific sediment continuity holds the key to at least statistically describing the vertical structure of grain sorting in rivers. A case in point is the stratigraphy created by passing dunes illustrated in Figure 3.61.

## REFERENCES

Aalto, R., 2002, "Geomorphic form and process of sediment flux within an active orogen: denudation of the Bolivian Andes and sediment conveyance across the Beni Foreland," Doctoral thesis, University of Washington, Seattle, 365 p.

Ackers, P. and W. R. White, 1973, "Sediment transport: a new approach and analysis," *Journal of Hydraulic Engineering*, 99(11), 2041-2060.

Ackers, P. and W. R. White, 1980, "Bed material transport: a theory for total load and its verification," *Proceedings*, International Symposium on River Sedimentation, International Research and Training Center on Erosion and Sedimentation, Beijing, China.

Almedeij, J. H. and P. Diplas, 2003, "Bedload transport in gravel-bed streams with unimodal sediment," *Journal of Hydraulic Engineering*, 129(11), 896-904.

Anderson, M. G., D. E. Walling and P. D. Bates, eds., 1996, "Floodplain Processes," John Wiley & Sons.

Andrews, E. D., 1983, "Entrainment of gravel from naturally sorted riverbed materials," *Geological Society of America Bulletin*, 94: 1225-1231.

Andrews, E. D. and Erman, D. C., 1986, "Persistence in the size distribution of surficial bed material during an extreme snowmelt flood," *Water Resources Research*, 22: 191-197.

Armanini, A., 1991/1992, "A new formulation for modeling the transport of non uniform sediment mixtures," *Excerpta*, 6: 115-132.

Armanini, A, 1995, "Non-uniform sediment transport: dynamics of the active layer." *Journal of Hydraulic Research*, 33(5): 611-622.

Ashida, K. and M. Michiue, 1971, "An investigation of river bed degradation downstream of a dam," *Proceedings*, 14th Congress, International Association of Hydraulic Research, Société Hydrotechnique de France, Paris, France 3: 247-256.

Ashida, K. and M. Michiue, 1972, "Study on hydraulic resistance and bedload transport rate in alluvial streams, *Transactions*, Japan Society of Civil Engineering, 206: 59-69 (in Japanese).

Ashida, K., S. Egashira and N. Andou, 1984, "Origin and geometry of step-pool bed form," *Proceedings*, 28th Annual Hydraulics Conference, Japan Society of Civil Engineering, Tokyo, Japan, 743-749.

Ashida, K., S. Egashira, and Y. Takamura, 1989, "Mechanism for grain sorting in movable beds," *Annuals*, Disaster Prevention Research Institute, Kyoto University, Japan, 32(B-2), 517-526.

Ashida, K., S. Egashira and B. Liu, 1991, "Numerical method on sediment sorting and bed variation in meander channels," *Proceedings*, Annual Conference on Hydraulic Engineering, Japan Society for Civil Engineering, Tokyo, Japan, 35: 383-390.

Ashworth, P. J. and R. I. Ferguson, 1989, "Size-selective entrainment of bed-load in gravel bed streams," *Water Resources Research*, 25, 627-634.

Ashworth, P. J., R. I. Ferguson and M. D. Powell, 1991, "Bedload transport and sorting in braided channels," *Dynamics of Gravel-bed Rivers*, Billi, P., R. D. Hey, C. R. Thorne, and P. Tacconi, eds., John Wiley & Sons, 495-515.

Ashworth, P. J., R. I. Ferguson, P. E. Ashmore, C. Paola, D. M. Powell, and K. L. Prestegaard, 1992, "Measurements in a braided river chute and lobe, 2, sorting of bedload during entrainment, transport and deposition," *Water Resources Research*, 28: 1887-1896.

Bakke, P. D., P. O. Baskedas, D. R. Dawdy and P. C. Klingeman, 1999, "Calibrated Parker-Klingeman model for gravel transport," *Journal of Hydraulic Engineering*, 125(6), 657-660.

Belleudy, Ph., and SOGREAH, 2000, "Numerical simulation of sediment mixture deposition part 1: analysis of a flume experiment," *Journal of Hydraulic Research*, 38(6), 417-425.

Bezzola, G, R, 1992, "The effect of sediment transport during the 1987-flood in the Reuss River," *Proceedings*, International Seminar on Grain Sorting, Ascona, Switzerland," Mitteilungen 117 der Versuchsanstalt für Wasserbau, Hydrologie und Glaziologie, ETH Zurich, 331-344.

Blom, A. and J. S. Ribberink, 1999, "Non-uniform sediment in rivers: vertical sediment exchange between bed layers," *Proceedings*, IAHR Symposium on River, Coastal and Estuarine Morphodynamics, G. Seminara, ed., Springer, New York, 45-54.

Blom, A. and Kleinhans, M., 1999, "Non-uniform Sediment in Morphological Equilibrium Situations – Data Report Sand Flume Experiments 97/98," *Research Report* CiT 99R-002/MICS-001, Civil Engineering and Management, Twente University, the Netherlands.

Blom, A., G. Parker and J. S. Ribberink, 2001, "Vertical exchange of tracers and non-uniform sediment in dune situations," *Proceedings*, 2nd IAHR Symposium on River, Coastal and Estuarine Morphodynamics, Obihiro, Japan S. Ikeda, ed.,. Hokkaido River Disaster Prevention Research Center, Sapporo, Japan.

Blom, A., 2003, "A continuum vertical sorting model for rivers with non-uniform sediment and dunes," Doctoral thesis, University of Twente, the Netherlands.

Borah, D. K., C. V. Alonso, and S. N. Prasad, 1982, "Routing graded sediment in streams: formulations," *Journal of Hydraulic Research*, 108: 1486-1503.

Bradley, W. C., 1970, "Effect of weathering on abrasion of granitic gravel, Colorado River (Texas)," *Geological Society of America Bulletin*, 81: 61:80.

Bridge, J. S., and J. Jarvis, 1976, "Flow and sedimentary processes in the meandering river South Esk, Glen Cova, Scotland," *Earth Surface Processes*, 1, 303-336.

Bridge, J. S. and S. J. Bennett, 1992, "A model for the entrainment and transport of sediment grains of mixed sizes, shapes and densities," *Water Resources Research*, 28(2): 337-363.

Brownlie, W. R., 1981, "Prediction of flow depth and sediment discharge in open channels," *Report* No. KH-R-43A, W. M. Keck Laboratory of Hydraulics and Water Resources, California Institute of Technology, Pasadena, California, USA, 232 p.

Brummer, C. J. and D. R. Montgomery, 2003, "Downstream coarsening in headwater channels," *Water Resources Research*, 39(10), 1294, 14 p.

Buffington, J. M, and D. R. Montgomery, 1997, "A systematic analysis of eight decades of incipient motion studies, with specific reference to gravel-bedded rivers," *Water Resources Research*, 33(8), 1993-2029.

Bunte, K. and S. T. Abt, 2001, "Sampling surface and subsurface particle-size distributions in wadable gravel- and cobble-bed streams for analyses in sediment transport, hydraulics and streambed monitoring. *General Technical Report* RMRS-GTR-74, US Department of Agriculture, US Forest Service, Rocky Mountain Research Station, Fort Collins, CO, 428 p.

Bunte, K., Abt, S. R. and Potyondy, J. P., 2004, Measurement of coarse gravel and cobble transport using portable bedload traps," *Journal of Hydraulic Engineering*, 130(9), 879-893.

Burrows, R. L., W. W. Emmett, and B. Parks, 1981, "Sediment transport in the Tanana River near Fairbanks, Alaska, 1977-1979," *Water Resources Investigation Report* 81-20, U.S. Geological Survey, U.S. Government Printing Office, Washington, D.C., 56 p.

Burrows, R. L., and P. E. Harrold, 1983, "Sediment transport in the Tanana River near Fairbanks, Alaska, 1980-1981," *Water Resources Investigation Report* 83-4064, U.S. Geological Survey, U.S. Government Printing Office, Washington, D.C., 116 p.

Carling, P. A., 1989, "Bedload transport in two gravel-bedded streams," *Earth Surface Processes and Landforms*, 14: 27-39.

Carling, P. A. and N. A. Reader, 1982, "Structure, composition and bulk properties of upland stream gravels," *Earth Surface Processes and Landforms*, 7: 349-386.

Carson, M. A. and G. A. Griffiths, 1987, "Bedload transport in gravel channels," *Journal of Hydrology New Zealand*, 26(1), 1-151.

Church, M. and K. Rood, 1983, "Catalogue of alluvial river data," *Report*, Department of Geography, University of British Columbia, Vancouver, B. C., Canada.

Church, M. A., D. G. McLean and J. F. Wolcott, 1987, "River bed gravels: sampling and analysis," *Sediment Transport in Gravel-bed Rivers*, Thorne, C. R., J. C. Bathurst, and R. D. Hey, eds., John Wiley & Sons, 43-79.

Church, M., J. F. Wolcott, and W. K. Fletcher, 1991, "A test of equal mobility in fluvial sediment transport: behavior of the sand fraction," *Water Resources Research*, 27(11): 2941-2951

Church, M., and M. A. Hassan, 1992, "Size and distance of travel of unconstrained clasts on a streambed," *Water Resources Research*, 28: 299-303.

Church, M., M. A. Hassan, and J. F. Wolcott, 1998, "Stabilizing self-organized structures in gravel-bed stream channels: field and experimental observations," *Water Resources Research*, 34(11): 3169-3179.

Colombini, M. and G. Parker, 1995, "Longitudinal streaks," *Journal of Fluid Mechanics*, 304: 161-183.

Copeland, R. R. and W. A. Thomas, 1992, "Dynamic sorting and armoring algorithm in tabs-1 numerical sedimentation model," *Proceedings*, International Seminar on Grain Sorting, Ascona, Switzerland," Mitteilungen 117 der Versuchsanstalt für Wasserbau, Hydrologie und Glaziologie, ETH Zurich, 359-368.

Cui, Y., G. Parker, and C. Paola, 1996, "Numerical simulation of aggradation and downstream fining," *Journal of Hydraulic Research*, 34(2), 184-204.

Cui, Y., and G. Parker, 1997, "A quasi-normal simulation of aggradation and downstream fining with shock fitting," *International Journal of Sediment Research*, 12(2): 68-82.

Cui, Y., and G. Parker, 1998, "The arrested gravel front: stable gravel-sand transitions in rivers. Part 2: General numerical solution," *Journal of Hydraulic Research*, 36(2): 159-182.

Cui, Y., and G. Parker, 1999, "Sediment Transport and Deposition in the Ok Tedi-Fly River System, Papua New Guinea: Modeling of 1998-1999. *Report* No. 7, Environment Department, Ok Tedi Mining Ltd., downloadable at http://cee.uiuc.edu/people/parkerg/_private/Reports/ (August 13, 2005).

Cui, Y., and A. Wilcox, in press, "Development and application of numerical modeling of sediment transport associated with dam removal," *Sedimentation Engineering*, ASCE Manual No. 54, Appendix A.

Cui, Y., G. Parker, T. E. Lisle, J. Gott, M. E. Hansler, J. E. Pizzuto, N. E. Allmendinger, and J. M. Reid, 2003a, "Sediment pulses in mountain rivers. Part 1. Experiments," *Water Resources Research*, 39(9), 1239, doi:10.1029/2002WR001803.

Cui, Y., G. Parker, J. E. Pizzuto, and T. E. Lisle, 2003b , "Sediment Pulses in Mountain Rivers. Part 2. Comparison between Experiments and Numerical Predictions," *Water Resources Research*, 39(9), 1240, doi:10.1029/2002WR001805.

Cui, Y. and G. Parker, in press, "Numerical model of sediment pulses and sediment supply disturbances in mountain rivers," *Journal of Hydraulic Engineering*.

Day, T. J., 1980, A Study of the Transport of Graded Sediments, *Report* No. IT 190, HRS Wallingford, Wallingford, U.K.

Deigaard, R., 1980, "Longitudinal and transverse sorting of grain sizes in alluvial rivers," *Series Paper* 26, Institute of Hydrodynamics and Hydraulic Engineering, Technical University of Denmark, 108 p.

Di Silvio, G., 1991, "Sediment exchange between stream and bottom: a four layer model," *Proceedings*, *Proceedings*, International Seminar on Grain Sorting, Ascona, Switzerland, Mitteilungen Nr. 117 der Versuchsanstalt für Wasserbau, Hydrologie und Glaziologie, ETH Zurich, 163-192.

Dietrich, W. E. and J. D. Smith, 1984, "Bedload transport in a river meander," *Water Resources Research*, 20(10): 1355-1380.

Dietrich, W. E., and P. J. Whiting, 1989, "Boundary shear stress and sediment transport in river meanders of sand and gravel," *Water Resources Monograph* 12, River Meandering, American Geophysical Union, 1-50.

Dietrich, W. E., J. W. Kirchner, H. Ikeda and F. Iseya, 1989, "Sediment supply and the development of the coarse surface layer in gravel-bedded rivers," *Nature*, 340, 215-217.

Dietrich, W. E., G. Day, and G. Parker, 1999, "The Fly River, Papua New Guinea: inferences about river dynamics, floodplain sedimentation and fate of sediment," *Varieties of Fluvial Form*, Miller, A. J. and A. Gupta, eds., John Wiley & Sons, New York, 345-376.

Dinehart, R. L., 1992, "Evolution of coarse-gravel bedforms, field measurements at flood stage," *Water Resources Research*, 28(10): 2667-2689.

Diplas, P., 1987, "Bedload transport in gravel-bed streams," *Journal of Hydraulic Engineering*, 113: 277-292.

Diplas, P., and A. J. Sutherland, 1988, "Sampling techniques for gravel sized sediments," *Journal of Hydraulic Engineering*, 114(5): 484-501.

Diplas, P., and G. Parker, 1992, "Deposition and removal of fines in gravel-bed streams," *Dynamics of Gravel-bed Rivers*, Billi, P., R. D. Hey, C. R. Thorne, and P. Tacconi, eds, John Wiley & Sons, 314-326.

Duan, J.G. and L. Chen, 2003, "Sediment transport study in the Las Vegas Wash," *Technical Report*, Division of Hydrologic Sciences, Desert Research Institute, Las Vegas, Nevada USA.

Egashira, S. and Ashida, K., 1990, "Mechanism of armoring phenomena," *International Journal of Sediment Research*, 5(1), 49-55.

Egiazaroff, I. V., 1965, Calculation of non-uniform sediment concentrations, *Journal of Hydraulic Engineering*, 91(4), 225-248.

Einstein, H. A., 1950, "The Bed-load Function for Sediment Transportation in Open Channel Flows," *Technical Bulletin* 1026, U.S. Dept. of the Army, Soil Conservation Service, U.S. Department of Agriculture, Washington, D.C.

Emmett, W. W., 1976, "Bedload transport in two large, gravel-bed rivers, Idaho and Washington," *Proceedings*, Third Federal Inter-Agency Sedimentation Conference, Denver, Colorado, March 22-26, U.S. Government Printing Office, Washington, D.C..

Emmett, W. W., R. H. Myrick, and R. H. Meade, 1980, "Field Data Describing the Movement and Storage of Sediment in the East Fork River, Wyoming, Part 1. River Hydraulics and Sediment Transport," *Open-File Report* 80-1189, U. S. Geological Survey, U.S. Government Printing Office, Washington, D.C.

Everts, C. H., 1973, "Particle overpassing on flat granular boundaries," *Journal of the Waterways and Harbors Division*, 99: 425-438.

Ferguson, R., and P. Ashworth, 1991, "Slope-induced changes in the channel character along a gravel-bed stream: the Allt Dubhaig, Scotland," *Earth Surface Processes and Landforms*, 16: 65-82.

Ferguson, R., T. Hoey, S. Wathen, and A. Werrity, 1996, "Field evidence for rapid downstream fining of river gravels through selective transport." *Geology*, 24(2): 179-182.

Ferguson, R. I. and S. J. Wathen, 1998, "Tracer-pebble movement along a concave river profile: virtual velocity in relation to grain size and shear stress," *Water Resources Research*, 34(8), 2031-2038.

Ferguson, R. I., M. Church and H. Weatherley, 2001, "Fluvial aggradation in the Vedder River: testing a one-dimensional sedimentation model," *Water Resources Research*, 37(12), 3331-3348.

Fernandez Luque, R. and R. van Beek, 1976, "Erosion and transport of bedload sediment," *Journal of Hydraulic Research*, 14(2): 127-144.

Fripp, J. B. and P. Diplas, 1993, "Surface sampling in gravel streams," *Journal of Hydraulic Engineering*, 119(4): 473-490.

Fujita, K., K. Yamamoto and Y. Akabori, 1998, "Evolution mechanisms of the longitudinal bed profiles of major alluvial rivers in Japan and their implications for profile change prediction," *Transactions*, Japan Society of Civil Engineering, 600(II-44): 37–50 (in Japanese).

Galay, V. J., 1983, "Causes of river bed degradation," *Water Resources Research*, 19:1057-1090.

García, M., and G. Parker, 1991, "Entrainment of bed sediment into suspension," *Journal of Hydraulic Engineering*, 117(4): 414-435.

Gomez, B., 1983, "Temporal variations in bedload transport rates: the effect of progressive bed armoring," *Earth Surface Processes and Landforms*, 8: 41-54.

Gomez, B. and M. Church, 1989, "An assessment of bed load sediment transport formulae for gravel bed rivers," *Water Resources Research*, 25(6): 1161-1186.

Gomez, B., R. L. Naff and D. W. Hubbell, 1989, "Temporal variations in bedload transport rates associated with the migration of bedforms," *Earth Surface Processes and Landforms*, 14: 135-156.

Gomez, B., B. J. Rosser, D. H. Peacock, D. M. Hicks and J. A. Palmer, 2001, "Downstream fining in a rapidly aggrading gravel bed river," *Water Resources Research*, 37(6), 1813-1824.

Grant, G. E., F. J. Swanson and M. G. Wolman, 1990, "Pattern and origin of stepped-bed morphology in high-gradient streams, Western Cascades, Oregon," *Geological Society of America Bulletin*, 102: 340-352.

Günter, A. 1971, "Die kritische mittlere Sohlenschubspannung bei Gescheibemischungen unter Berücksichtigung der Deckschichtbildung und der turbulenzbedingten

Sohlenschubspannungsschwankungen ," *Mitt.* 3, Versuchsanstalt für Wasserbau, ETH, Zurich, Switzerland.

Hamamori, A, 1962, "A Theoretical Investigation on the fluctuations of bedload transport," *Report* R4, Delft Hydraulics Laboratory.

Haschenburger, J. K. and M. Church, 1998, "Bed material transport estimated from the virtual velocity of sediment," *Earth Surface Processes and Landforms*, 23: 791-808.

Haschenburger, J. K., 1999, "A probability model of scour and fill depths in gravel-bed channels," *Water Resources Research*, 35(9): 2857-2869.

Hasegawa, K,. T. Fujita, H. Meguro and H. Tatuzawa, 2000, "Bed forms in steep channels with heterogeneous bed materials induced by bottom elevation instability and sorting instability," *Suikougaku Ronbunshuu*, 44, 659-664 (in Japanese).

Hassan, M. A., 1990, "Scour, fill and burial depth of coarse material in gravel bed streams," *Earth Surface Processes and Landforms*, 15: 341-356.

Hassan, M. A., M. Church and P. J. Ashworth, 1992, "Virtual rate and mean distance of travel of individual clasts in gravel-bed channels," *Earth Surface Processes and Landforms*, 17: 617-627.

Hassan, M. A. and Church, M., 1994, "Vertical mixing of coarse particles in gravel bed rivers: a kinematic model," *Water Resources Research*, 30: 1173-1185.

Hassan, M. A. and Church, M., 2000, "Experiments on surface structure and partial sediment transport on a gravel bed," *Water Resources Research*, 36(7): 1885-1985.

Hassan, M. A., and Church, M. 2001, "Sensitivity of bed load transport in Harris Creek: Seasonal and spatial variation over a cobble-gravel bar," *Water Resources Research*, 37, 813-825.

Hassan. M. A. and R. Egozi, 2001, "Impact of wastewater on the channel morphology of ephemeral streams," *Earth Surface Processes and Landforms*, 26(12) 1285-1302.

Hay, D. F., ed., 1998, "Wetlands Engineering River Restoration Conference 1998, Engineering Approachs to Ecosystem Restoration," CD containing proceedings available from American Society of Civil Engineers.

Hayward, J. A., 1980, "Hydrology and Stream Sediment From Torlesse Stream Catchment," *Special Publication* 17, Tussock Grasslands and Mountain Lands Institute, Lincoln College, Canterbury, New Zealand.

Hey, R. D., 1979, "Flow resistance in gravel-bed rivers," *Journal of Hydraulic Engineering*, 105(4), 365-380.

Hey, R., 1989, "Bar form resistance in gravel-bed rivers," *Journal of Hydraulic Engineering*, 114(12): 1498-1508.

Hirano, M., 1971, "On riverbed variation with armoring," *Proceedings*, Japan Society of Civil Engineering, 195: 55-65 (in Japanese).

Hoey, T. B., and R. I. Ferguson, 1994, "Numerical simulation of downstream fining by selective transport in gravel bed rivers: Model development and illustration," *Water Resources Research*, 30, 2251-2260.

Hoey, T. B. and R. Ferguson, 1997, "Controls of strength and rate of downstream fining about a river base level," *Water Resources Research*, 33(11): 2601-2608.

Hollingshead, A. B., 1971, "Sediment transport measurements in a gravel river," *Journal of Hydraulic Engineering*, 97(11): 1817-1834.

Holly, F. M., and J. L. Rahuel, 1990, "New numerical/physical framework for mobile-bed modeling," *Journal of Hydraulic Research*, 28(5), 545-564.

Hooke, R. LeB., 1968, "Laboratory study of the influence of granules on flow over a sand bed," *Geological Society of America Bulletin*, 79: 495-500.

Hotchkiss, R. H. and M. Glade, eds., 2000, "Symposium on River Restoration," *Proceedings*, 2000 Joint Conference on Water Resources Engineering and Water Resources Planning and Management, CD available from American Society of Civil Engineers

Huang, X. and M. H. García, 2000, "Pollution of gravel spawning grounds by deposition of suspeneded sediment," *Journal of Environmental Engineering*, 126(10), 963-965.

Hubbell. D. W., 1987, "Bedload sampling and analysis," *Sediment Transport in Gravel-bed Rivers*, Thorne, C. R., J. C. Bathurst, and R. D. Hey, eds., John Wiley & Sons, 89-106.

Hunziker, R., and M. N. R. Jaeggi, 2002, "Grain sorting processes," *Journal of Hydraulic Engineering*, 128(12), 1060-1068.

Ikeda, H., 2001, "An Eye for Seeing Landforms," Kokon Shoin, Tokyo, Japan, 152 p. (in Japanese).

Ikeda, S., 1982, "Incipient motion of sand particles on side slopes," *Journal of Hydraulic Engineering*, 108: 95-114.

Ikeda, S., M. Yamasaka and M. Chiyoda, 1987, "Bed topography and sorting in bends," *Journal of Hydraulic Engineering*, 113(2): 190-205.

Ikeda, S., 1989, "Sediment transport and sorting at bends," *Water Resources Monograph* 12, River Meandering, American Geophysical Union, 103-126.

Iseya, F. and H. Ikeda, 1987, "Pulsations in bedload transport induced by a longitudinal sediment sorting; a flume study using sand gravel mixtures," *Geografiska Annaler*, 69: 15-27.

Kamphuis, J.W., 1974, "Determination of Sand Roughness for Fixed Beds," *Journal of Hydraulic Research*, 12(2), 193-202.

Keulegan, G. H., 1938, "Laws of turbulent flow in open channels," *National Bureau of Standards* Research Paper RP 1151, Washington, D.C..

Karim, F., 1998, "Bed material discharge prediction for nonuniform bed sediments," *Journal of Hydraulic Engineering*., 124(6): 597-604.

Karim, F., and J. F. Kennedy, 1981, "Computer-based predictors for sediment discharge and friction factor of alluvial streams," *Report* No. 242, Iowa Institute of Hydraulic Research, University of Iowa, Iowa City, Iowa.

Kellerhals, R. and D. I. Bray, 1971, "Sampling procedures for coarse fluvial sediments," *Journal of Hydraulic Engineering*, 98(8): 1165-1180.

Kellerhals, R., C. R. Neill, and D. I. Bray, 1972, "Hydraulic and geomorphic characteristics of rivers in Alberta," River Engineering and Surface Hydrology Report No. 72-1, Research Council of Alberta, Edmonton, Alberta, Canada.

Kellerhals, T. and D. Gill, 1973, "Observed and potential downstream effects of large storage projects in northern Canada," *Proceedings*, 12th Congress, International Commission on Large Dams, Madrid, 731-754.

Kelsey, A. R., 1996, "Modelling the sediment transport process," *Advances in Fluvial Dynamics and Stratigraphy*, Carling, P. A., and M. R. Dawson, eds., John Wiley and Sons, 229:262.

Kleinhans, M. G., 2002, "Sorting out sand and gravel: sediment transport and deposition in sand-gravel bed rivers", Doctoral thesis, Netherlands Geographical Studies 293, Faculty of Geographical Sciences, Utrecht, University, the Netherlands, 317 p.

Kleinhans, M. G. and van Rijn, L. C., 2002, "Stochastic prediction of sediment transport in sand-gravel bed rivers," *Journal of Hydraulic Engineering*, Special Issue on Stochastic Sediment Transport and Hydraulics, 128(4), 412-425.

Klingeman, P. C., C. J. Chaquette, and S. B. Hammond, 1979, "Bed Material Characteristics near Oak Creek Sediment Transport Research Facilities, 1978-1979," *Oak*

*Creek Sediment Transport Report No.* BM3, Water Resources Research Institute, Oregon State University, Corvallis, Oregon, June.

Kodama, Y., H. Ikeda, and H. Iijima, 1992, "Longitudinal sediment sorting along a concave upward stream profile in a large flume," *Report*, Hydraulic Experimental Center, Tsukuba University, 16: 119-123 (in Japanese).

Kodama, Y., 1994a, "Experimental study of abrasion and its role in producing downstream fining in gravel-bed rivers," *Journal of Sedimentary Research*, A64(1), 76-85.

Kodama, Y., 1994b, "Downstream changes in the lithology and grain size of fluvial gravels, the Watarase River, Japan: Evidence of the role of abrasion in downstream fining," *Journal of Sedimentary Research*, A64(1): 68-75.

Komar, P. D., 1987, "Selective gravel entrainment and the empirical evaluation of flow competence," *Sedimentology*, 34: 1165-1176

Komar, P. D., 1987, "Selective grain entrainment by a current from a bed of mixed sizes: a reanalysis," *Journal of Sedimentary Research*, 57: 203-211.

Komar, P. D. and P. A. Carling, 1991, "Grain sorting in gravel-bed streams and the choice of particle sizes for flow competence evaluations," *Sedimentology*, 38: 489-502.

Kondolf, G. M. and P. R. Wilcock, 1996, "The flushing flow problem: defining and evaluating objectives," *Water Resources Research*, 32(8): 2589-2599.

Kostic, S. and G Parker, 2003, "Progradational sand-mud deltas in lakes and reservoirs. Part 1: Theory and numerical model," *Journal of Hydraulic Research*, 41(2), 127-140.

Kovacs, A. and G. Parker, 1994, "A new vectorial bedload formulation and its application to the time evolution of straight river channels," *J. Fluid Mech.*, 267, 153-183.

Kuhnle, R. A. and J. B. Southard, 1988, "Bedload transport fluctuations in a gravel bed laboratory channel," *Water Resources Research*, 24: 247-260.

Kuhnle, R. A., J. C. Willis, and A. J. Bowie, 1989, "Variations in the transport of bed load sediment in a gravel-bed stream, Goodwin Creek, Mississippi, USA," *Proceedings*, 4th International Symposium on River Sedimentation, International Research and Training Center on Erosion and Sedimentation, Beijing, China, 539-546.

Kuhnle, R. A., 1992, "Fractional transport rates of bedload on Goodwin Creek," *Dynamics of Gravel-bed Rivers*, Billi, P., R. D. Hey, C. R. Thorne and P. Tacconi, eds., John Wiley & Sons, 141-155.

Kuhnle, R. A., 1993, "Fluvial transport of sand and gravel mixtures with bimodal size distributions," *Journal of Sedimentary Geology*, 85:17-24.

Kuhnle, R. A., 1996, "Unsteady transport of sand and gravel mixtures," *Advances in Fluvial Dynamics and Stratigraphy*, Carling, P. A. and M. R. Dawson, eds., John Wiley and Sons, 184-201.

Lanzoni, S. and M. Tubino, 1999, "Grain sorting and bar instability," *Journal of Fluid Mechanics*, 393: 149-174.

Laronne, J., I. Reid, Y. Yitshak, and L. E. Frostick, 1994, "The non-layering of gravel streambeds under ephemeral flood regimes," *Journal of Hydrology*, 159: 353-363.

Lenzi, M. A., V. D'Agostino, F. Comiti, G. R. Scussel, U. De Col., and G. Asti, 2000, "Bedload transport data from Rio Cordon torrent: comparison with sediment transport equations and field data from other Alpine streams," *In* Special Issue, Dynamics of Water and Sediments in Mountain Basins, Quaderni di Idronomia Montana, Editoriale Bios, Italy.

Leopold, L. B., 1994, "A View of the River," Harvard University Press, Cambridge, Massachusetts USA, 298 p.

Leopold, L. B., M. G. Wolman and J. P. Miller, 1964, "Fluvial Processes in Geomorphology," W. H. Freeman and Company, San Francisco, 522 p.

Leopold, L. B., W. W. Emmett and R. H. Myrick, 1966, "Channel and hillslope processes in a semiarid area, New Mexico," *Professional Paper* 352G, U.S. Geological Survey, U.S. Government Printing Office, Washington, D.C., .

Liu, X. L., 1986, "Nonuniform Bed Load Transport Rate and Coarsening Stabilization," M.S. Thesis, Chengdu University, China (in Chinese).

Lisle, T. E., 1989, "Sediment transport and resulting deposition in spawning gravels, north coastal California," *Water Resources Research*, 25(6): 1303-1319.

Lisle, T. E. and M. A. Madej, 1992, "Spatial variation in armoring in a channel with high sediment supply," *Dynamics of Gravel-bed Rivers*, Billi, P., R. D. Hey, C. R. Thorne, and P. Tacconi, eds., John Wiley & Sons, 277-296.

Lisle, T. E., 1995, "Particle size variations between bed load and bed material in natural gravel bed channels," *Water Resources Research*, 31(4), 1107-1118.

Lisle, T. E., J. E. Pizzuto, H. Ikeda, F. Iseya and Y. Kodama, 1997, "Evolution of a sediment wave in an experimental channel," *Water Resources Research*, 33(8): 1971-1981.

Lisle, T.E., Y. Cui, G. Parker, J. E. Pizzuto and A. M. Dodd, 2001, "The dominance of dispersion in the evolution of bed material waves in gravel-bed rivers," *Earth Surface Processes and Landforms*, 26, 1409-1420.

Marion, A., and L. Fraccarollo, 1997, "Experimental investigation of mobile armoring development," *Water Resources Research*, 33(6), 1447-1453.

Marion, A., I. McEwan and S. Tait, "On the competitive effects of particle re-arrangement and vertical sorting," *Proceedings*, 27th Congress of the International Association for Hydraulic Research, Volume 2, International Association of Hydraulic Engineering and Research, Madrid, Spain, 1493-1498.

Maunsell and Partners, 1982, "Waste rock and sedimentation methodology," *Ok Tedi Environmental Study*, Ok Tedi Mining Ltd., Tabubil, Papua New Guinea.

McLean, S. R., 1991, "Depth-integrated suspended-load calculations," *Journal of Hydraulic Engineering*, 117(11): 1440-1458.

McLean, S. R., 1992, "On the calculation of suspended load for non-cohesive sediments," 1992, *Journal of Geophysical Research*, 97(C4), 1-14.

Mellor, G.L., and T. Yamada, 1974. "A hierarchy of turbulence closure models for planetary boundary layers," *Journal of Atmospheric Science*: 31, 1791-1806.

Meyer-Peter, E., and R. Müller, 1948, "Formulas for bed-load transport," *Proceedings*, 2nd Congress International Association for Hydraulic Research, Stockholm, Sweden, 39-64.

Mikoš, M., 1993, "Fluvial Abrasion of Gravel Sediments," Mitteilungen 123 der Versuchsanstalt für Wasserbau, Hydrologie und Glaziologie, ETH Zurich, 322 p.

Mikoš, M., 1994, "The downstream fining of gravel-bed sediments in the alpine Rhine River," *Dynamics and Geomorphology of Mountain Rivers*, Ergenzinger, P. and K-H Schmidt, eds, Springer, 93-108.

Mikoš, M., 1995, "Fluvial abrasion: converting size reduction coefficients to weight reduction coefficients," *Journal of Sedimentary Research*, A65(3), 472-476.

Milhous, R. T., 1973, "Sediment Transport in a Gravel-bottomed Stream," *Ph.D. thesis*, Oregon State University, Corvallis, Oregon.

Milhous, R. T., 1998, "Numerical modeling of flushing flows in gravel-bed rivers," *Gravel-Bed Rivers in the Environment*, Klingeman, P. C., R. L. Beschta, P. D. Komar, and J. B. Bradley, eds., Water Resources Publications, Highlands Ranch, Colorado, USA, 579-602.

Millar, R. G., 1999, "Grain and form resistance in gravel-bed rivers," *Journal of Hydraulic Research*, 37(3): 303-312.

Misri, R. L, Garde, R. J., and Ranga Raju, K. G., 1984, "Bed load transport of nonuniform sediments," *Journal of Hydraulic Engineering*, 110(3): 312-328.

Nakagawa, H., T. Tsujimoto, and S. Nakano, 1982, "Characteristics of sediment motion for respective grain sizes of sand mixtures," *Bulletin*, Disaster Prevention Research Institute, Kyoto University, 32:1-32.

Narinesingh, P., 1995, "Nature Restoration and Floodplain Sedimentation," M.S. thesis, No. HH 218, IHE Delft, the Netherlands.

Narinesingh, P., G. J. Klaasen, and D. Ludikhuize, 1999, "Floodplain sedimentation along extended river reaches," *Journal of Hydraulic Research*, 37(6), 827-846.

van Niekerk, A., K. R. Vogel, R. L. Slingerland and J. S. Bridge, 1992, "Routing of heterogeneous sediments over mobile bed: model development," *Journal of Hydraulic Engineering*, 118(2): 246-252.

Neill, C. R., 1968, "A reexamination of the beginning of movement for coarse granular bed materials," *Report* INT 68, Hydraulics Research Station, Wallingford, England.

Niño, T. and D. Aracena, 1999, Experimental observations of ripple growth in non-uniform sediment," *Proceedings*, IAHR Symposium on River, Coastal and Estuarine Morphodynamics, G. Seminara, ed., Università degli Studi di Genova, Italy, 241-150.

Olesen, K. W., 1987, "Bed topography in shallow river bends," *Ph.D thesis*, University of Delft, the Netherlands, 265 p.

Onishi, Y., S. C. Jain and J. F. Kennedy, 1972, "Effects of meandering on sediment discharges and friction factors of alluvial streams," *Report* No. 141, Iowa Institute of Hydraulic Research, University of Iowa, Iowa City, Iowa USA.

Paintal, A. S., 1971, "Concept of critical shear stress in loose boundary open channels," *Journal of Hydraulic Research*, 9: 91-113.

Paola, C., P. L. Heller and C. L. Angevine, 1992a, "The large-scale dynamics of grain-size variation in alluvial basins. I: Theory," *Basin Research*, 4, 73-90.

Paola, C., G. Parker, R. Seal, S. K. Sinha, J. B. Southard, and P. R. Wilcock, 1992b, "Downstream fining by selective deposition in a laboratory flume," *Science*, 258: 1757-1760.

Paola, C. and R. Seal, 1995, "Grain size patchiness as a cause of selective deposition and downstream fining," *Water Resources Research*, 31(5), 1395-1407.

Paola, C., 1996, "Incoherent structure: turbulence as a metaphor for stream braiding," Coherent Flow Structures n Open Channels, Ashworth, P. J., S. J. Bennett, J. L. Best and S. J. McLelland, eds, John Wiley & Sons, 705-724.

Paola, C., G. Parker, D. C. Mohrig, and K. X. Whipple, 1999, "The influence of transport fluctuations on spatially averaged topography on a sandy, braided fluvial plain," *Numerical Experiments in Stratigraphy*, SEPM Special Publication 62, 211-218.

Paola, C., 2000, "Quantitative models of sedimentary basin filling," *Sedimentology*, 47(Supplement 1): 121-178.

Paola, C., J. Mullin, C. Ellis, D. C. Mohrig, J. Swenson, G. Parker, T. Hickson, P. L. Heller, L. Pratson, J. Syvitski, B. Sheets, and N. Strong, 2001, "Experimental stratigraphy," *GSA Today*, 11(7): 2-9.

Park, I. and S. C. Jain, 1987, "Numerical simulation of degradation of alluvial channel beds," *Journal of Hydraulic Engineering*, 113(7): 845-859.

Parker, G., 1978, Self-formed rivers with stable banks and mobile bed: Part I, the sand-silt river, *Journal of Fluid Mechanics*, 89(1), 109-126.

Parker, G, and A. G. Anderson, 1977, "Basic principles of river hydraulics," *Journal of Hydraulic Engineering*, 103(9): 1077-1087.

Parker, G., 1978, "Self-formed rivers with stable banks and mobile bed: Part I, the sand-silt river," *Journal of Fluid Mechanics*, 89(1), pp. 109-126.

Parker, G., 1978, "Self-formed rivers with equilibrium banks and mobile bed: Part II, the gravel river, "*Journal of Fluid Mechanics*, 89(1), 127-148.

Parker, G., 1979, "Hydraulic geometry of active gravel rivers," *Journal of Hydraulic Engineering*, 105(9), 1185-1201.

Parker, G. and A. W. Peterson, 1980, "Bar resistance of gravel-bed streams," *Journal of Hydraulic Engineering*, 106(10) 1559-1575.

Parker, G. and P. C. Klingeman, 1982, "On why gravel bed streams are paved," *Water Resources Research*, 18(5): 1409-1423.

Parker, G., P. C. Klingeman and D. G. McLean, 1982a, "Bedload and size distribution in paved gravel-bed streams," *Journal of Hydraulic Engineering*, 108(4): 544-571.

Parker, G., S. Dhamotharan, and S. Stefan, 1982b, "Model experiments on mobile, paved gravel bed streams," *Water Resources Research*, 18(5), 1395-1408.

Parker, G., 1984, "Discussion of 'Lateral bed load transport on side slopes'," *Journal of Hydraulic Research*, 110(2), 197-199.

Parker, G., and E. D. Andrews, 1985, "Sorting of bed load sediment by flow in meander bends," *Water Resources Research*, 21(9): 1361-1373.

Parker, G., 1990a, "Surface-based bedload transport relation for gravel rivers," *Journal of Hydraulic Research*, 28(4): 417-436.

Parker, G., 1990b, The ACRONYM Series of PASCAL Programs for Computing Bedload Transport in Gravel Rivers, *External Memorandum* M-200, St. Anthony Falls Laboratory, University of Minnesota, Minneapolis, Minnesota USA.

Parker, G. and A. J. Sutherland, 1990, "Fluvial armor," *Journal of Hydraulic Research*, 28(5), 529-544.

Parker, G., 1991a, "Selective sorting and abrasion of river gravel. I: Theory," *Journal of Hydraulic Engineering*, 117(2): 131-149.

Parker, G., 1991b, "Selective sorting and abrasion of river gravel. II: Application," *Journal of Hydraulic Engineering*, 117(2): 150-171.

Parker, G., 1992, "Some random notes on grain sorting," *Proceedings*, International Seminar on Grain Sorting, Ascona, Switzerland," Mitteilungen 117 der Versuchsanstalt für Wasserbau, Hydrologie und Glaziologie, ETH Zurich, 19-76.

Parker, G., Y. Cui, Imran, J. and W. Dietrich, 1996 "Flooding in the lower Ok Tedi, Papua New Guinea due to the disposal of mine tailings and its amelioration," *Proceedings* International Seminar on Recent Trends of Floods and their Preventive Measures, Hokkaido River Disaster Prevention Research Center, Sapporo, Japan, 21-48.

Parker. G., and Y. Cui, 1998, "The arrested gravel front: stable gravel-sand transitions in rivers. Part 1: Simplified analytical solution," *Journal of Hydraulic Research*, 36(1): 75-100.

Parker, G., C. Paola, and Leclair, S., 2000, "Probabilistic form of Exner equation of sediment continuity for mixtures with no active layer," *Journal of Hydraulic Engineering*, 126(11): 818-826.

Parker, G., and C. M. Toro-Escobar, 2002, "Equal mobility of gravel in streams: the remains of the day," *Water Resources Research*, 38(11), 1264, doi:10.1029/2001WR000669.

Parker, G., C. M. Toro-Escobar, M. Ramey and S. Beck, 2003, "The effect of floodwater extraction on the morphology of mountain streams," *Journal of Hydraulic Engineering*, 129(11), 885-895.

Pickup, G., R. J. Higgins, and R. F. Warner, 1979, "Impact of Waste Rock Disposal from the Proposed Ok Tedi Mine on Sedimentation Processes in the Fly River and its Tributaries, Papua New Guinea," *Report*, Dept. of Minerals and Energy and Office of Environment and Conservation, 138 pp.

Pizzuto, J. E., 1995, "Downstream fining in a network of gravel-bedded rivers," *Water Resources Research*, 31: 753-759.

Powell, D. M., 1998, Patterns and processes of sediment sorting in gravel-bed rivers," *Progress in Physical Geography*, 22(1): 1-32.

Powell, D. M., I. Reid and J. B. Laronne, 2001, "Evolution of bedload grain-size distribution with increasing flow strength and the effect of flow duration on the caliber of bedload sediment yield in ephemeral gravel-bed rivers," *Water Resources Research*, 37(5), 1463-1474.

Powell, D. M., Laronne, J. B. and Reid, I., 2003, "The dynamics of bedload sediment transport in low-order, upland, ephemeral gravel-bed rivers," *Advances in Environmental Monitoring and Modelling*, 1(2), http://www.kcl/ac/uk/advances/ .

Profitt, G. T., 1980, "Selective transport and armoring of non-uniform alluvial sediments," *Research Report* 80/22, Department of Civil Engineering, University of Canterbury, New Zealand, 203 p.

Proffitt, G. T. and A. J. Sutherland, 1983, "Transport of non-uniform sediments," *Journal of Hydraulic Research*, 21(1), 33-43.

Rahuel, J. L., F. M. Holly, J. P. Chollet, P. J. Belleudy, and G. Yang, 1989, "Modeling of riverbed evolution for bedload sediment mixtures," *Journal of Hydraulic Engineering*, 115(11): 1521-1542.

Rana, S. A., D. B. Simons, and K. Mahmood, 1973, "Analysis of sediment sorting in alluvial channels," *Journal of Hydraulic Engineering*, 99(11): 1967-1980.

Reid, I., L. E. Frostick, and J. T. Layman, 1985, "The incidence and nature of bedload transport during flood flows in coarse-grained alluvial channels," *Earth Surface Processes and Landforms*, 10: 33-44.

Reid, I. and L. E. Frostick, 1986, "Dynamics of bed load transport in Turkey Brook, a coarse-grained alluvial channel," *Earth Surface Processes and Landforms*, 11: 143-155.

Reid, I., J. B. Laronne, and D. M. Powell, 1995, "The Nahal Yatir bedload database: sediment dynamics in a gravel-bed ephemeral stream," *Earth Surface Processes and Landforms*, 20: 845-857.

Reiser, D. W., 1998, "Sediment in gravel bed rivers: ecological and biological considerations," *Gravel-Bed Rivers in the Environment*, Klingeman, P. C., R. L. Beschta, P. D. Komar, and J. B. Bradley, eds., Water Resources Publications, Highlands Ranch, Colorado, USA, 199-225.

Ribberink. J. S., 1987, Mathematical Modeling of One-dimensional Morphological Changes in Rivers with Non-uniform Sediment, *Ph.D. thesis*, Delft University of Technology, 200 p.

Rice, S., 1998, "Which tributaries disrupt fining along gravel-bed rivers?." *Geomorphology*, 22: 39-56.

Rice, S., 1999, "The nature and controls on downstream fining within sedimentary links," *Journal of Sedimentary Research*, 69(1): 32-39.

van Rijn, L. C., 1984, "Sediment transport. I: Bedload transport," *Journal of Hydraulic Engineering*, 110(10), 1613-1641.

Robinson, R. A. J., and R. L. Slingerland, 1998. "Origin of fluvial grain-size trends in a foreland basin: the Pocono formation on the Central Appalachian Basin," *Journal of Sedimentary Research* 68(3), 473-486.

Rood, K. and M. Church, 1994, "Modified freeze-core technique for sampling the permanently wetted streambed," *North American Journal of Fisheries Management*, 14, 852-861.

Rouse, H., 1939, "Experiments on the mechanics of sediment suspension," *Proceedings* 5th International Congress on Applied Mechanics, Cambridge, Mass,, 550-554.

Samaga, B. R., K. E. Ranga Raju, and R. J. Garde, 1986, "Suspended load transport of sediment mixtures," *Journal of Hydraulic Engineering*, 112(11): 1019-1035.

Sambrook Smith, G. H. and R. Ferguson, 1995, "The gravel-sand transition along river channels," *Journal of Sedimentary Research*, A65(2): 423-430.

van der Scheer, P., A. Blom and J. S. Ribberink, 2001, "Transport Formulas for Graded Sediment. Behavior of Transport Formulas and Verification with Experimental Data," *Research Report* 2001-R-004/MICS-023, University of Twente, the Netherlands, 12 p.

Schick, A. P., J. Lekach and Hassan, M. A., 1987, "Vertical exchange of coarse bedload in desert streams," *Desert Sediments: Ancient and Modern*, Frostick, L. E. and I. Reid, eds., Geological Society of London Special Publication No. 25, Blackwell Scientific, 7-16.

Seal, R. and C. Paola, 1995, "Observations of downstream fining on the North Fork Toutle River near Mount St. Helens, Washington," *Water Resources Research*, 31(5): 1409-1419.

Seal, R., C. Paola, G. Parker, J. B. Southard, and P. R. Wilcock, 1997, "Experiments on downstream fining of gravel: I. Narrow-channel runs," *Journal of Hydraulic Engineering*, 123(10): 874-888.

Seminara, G., M. Colombini, and G. Parker, 1996, "Nearly pure sorting waves and formation of bedload sheets," *Journal of Fluid Mechanics*, 312: 253-278.

Seminara, G., L. Solari and M. Tubino, 1997, "Finite amplitude scour and grain sorting in wide channel bends," *Proceedings*, 27th Congress of the International Association for Hydraulic Research, Volume 2, 1445-1450.

Seminara, G,. 1998. Stability and morphodynamics. *Meccanica*, 33: 59-99.

Shaw, J. and R. Kellerhals, 1982, "The Composition of Recent Alluvial Gravels in Alberta River Beds," *Bulletin* 41, Alberta Research Council, Edmonton, Alberta, Canada.

Shields, I. A., 1936, "Anwendung der ahnlichkeitmechanik und der turbulenzforschung auf die gescheibebewegung," *Mitt. Preuss Ver.-Anst*., 26, Berlin, Germany.

Shih, S.-H., and Komar, P. D., 1990, "Differential bedload transport rates in a gravel-bed stream: a grain-size distribution approach," *Earth Surface Processes and Landforms*, 15: 539-552.

Sidle, R. C., 1988, "Bed load transport regime of a small forest stream,"" *Water Resources Research*, 24(2): 207-218.

Simons, D., 1971, "River and canal morphology," *River Mechanics*, Shen, H. W., ed., publ., Water Resources Publications, LLC, Highlands Ranch, Colorado, Chapter 20: 20-1 – 20-60.

Smart, G. M. and M. N. R. Jaeggi, 1983, "Sediment transport on steep slopes," *Mitteilungen* 64 der Versuchsanstalt für Wasserbau, Hydrologie und Glaziologie, ETH Zurich, 19-76.

Smart, G. M., 1984, "Sediment transport formula for steep channels," *Journal of Hydraulic Engineering*, 110(3): 267-276.

Smith, J. D. and S. R. McLean, 1977, "Spatially averaged flow over a wavy surface," *Journal of Geophysical Research*, 82(12): 1735-1746.

Smith, R. D., 1990, "Streamflow and bedload transport in an obstruction-affected, gravel-bed stream," Ph.D. thesis, Oregon State University, Corvallis, Oregon, Colorado, 191 p.

Smith, R. D., R. C. Sidle and P. E. Porter, 1993, "Effects on bedload transport of experimental removal of woody debris from a forest gravel-bed stream," *Earth Surface Processes and Landforms*, 18: 455-468.

Solari, L., and G. Parker, 2000, "The curious case of mobility reversal in sediment mixtures," *Journal of Hydraulic Engineering*, 126(3): 198-208.

Speziale, C. G., 1987, "On nonlinear *k-l* and *k-ε* models of turbulence," *Journal of Fluid Mechanics*, 178: 459-475.

Straub, L. G., 1935, "Some observations of sorting of river sediments," *Transactions*, American Geophysical Union Annual Meeting, 16: 463-467.

Sutherland, A. J., 1987, "Static armor layers by selective erosion," *Sediment Transport in Gravel-bed Rivers*, Thorne, C. R. etc., eds., John Wiley & Sons, 343-267.

Sutherland, D. G., M. H. Ball, S. J. Hilton, and T. E. Lisle, 2002, "Evolution of a landslide-induced sediment wave in the Navarro River, California," *Bulletin Geological Society of America*,114(8), 1036-1048.

Suzuki, K, and M. Michiue, 1979, "On the dune height and the influence of sand mixture on its characteristics," *Proceedings*, 23rd Annual Conference on Hydraulic Engineering, Japan Society for Civil Engineering, Tokyo, Japan, 151-156.

Suzuki, K., and K. Kato, 1991, "Mobile bed armoring of bed surface in a steep slope river with gravel and sand mixture," *Proceedings*, International Workshop on Fluvial Hydraulics of Mountain Regions, Trento, Italy, Università degli Studi de Trento, Trento, Italy, 393-404.

Suzuki, K., and A. Hano, 1992, "Grain size change of bed surface layer and sediment discharge of an equilibrium river bed," *Proceedings*, International Seminar on Grain Sorting, Ascona, Switzerland," Mitteilungen 117 der Versuchsanstalt für Wasserbau, Hydrologie und Glaziologie, ETH Zurich, 151-156.

Swenson, J. B., V. R. Voller, C. Paola, G. Parker, and J. Marr, 2000, "Fluvio-Deltaic Sedimentation: A Generalized Stefan Problem," *Euro. J. Applied Math.*, 11, 433–452.

Tacconi, P., and P. Billi, 1987, "Bed load transport measurements by vortex-tube trap on Virginio Creek, Italy," *Sediment Transport in Gravel-bed Rivers*, Thorne, C. R., J. C. Bathurst, and R. D. Hey, eds., John Wiley & Sons, 583-606.

Tait, S. J., B. B. Willetts, and J. K. Maizels, 1992, "Laboratory observations of bed armoring and changes in bedload composition," *Dynamics of Gravel Bed Rivers*, Billi, P., etc., eds., John Wiley & Sons, 205-225.

Tatsuzawa, H., H. Hayashi and K. Hasegawa, 1999a, "Role of heterogeneous property of bed materials in the formation of step-pool systems in mountain rivers," *Journal of Hydroscience and Hydraulic Engineering*, 17(1), 37-45.

Tatsuzawa, H., H. Hayashi and K. Hasegawa, 1999b, "A study on small-scale bed topography in mountain streams," *Proceedings*, Japan Society for Civil Engineering, 656(II-52), 83-101 (in Japanese).

Thompson, S. M., 1985, "Transport of gravel by flows up to 500 $m^3/s$, Ohau River, Otago, N. Z.," *New Zealand Journal of Hydraulic Research*, 23(3): 285-303.

Toro-Escobar, C. M., G. Parker and C. Paola, 1996, "Transfer function for the deposition of poorly sorted gravel in response to streambed aggradation," *Journal of Hydraulic Research*, 34(1): 35-53.

Toro-Escobar, C. M., C. Paola, G. Parker, P. R. Wilcock, and J. B. Southard, 2000, "Experiments on downstream fining of gravel. II: Wide and sandy runs," *Journal of Hydraulic Engineering*, 126(3): 198-208.

Tsujimoto, T. and K. Motohashi, 1990, "Static armoring and dynamic pavement," *Journal of Hydroscience and Hydraulic Engineering*, 8(1): 55-67.

Tsujimoto. T., 1991, "Mechanics of Sediment Transport of Graded Materials and Fluvial Sorting," *Report*, Project 01550401, Kanazawa University, Japan, 126 p.

Tsujimoto, T, 1999, "Sediment transport processes and channel incision: mixed size sediment transport, degradation and armoring," *Incised River Channels*, Darby, S. E. and A. Simon, eds., John Wiley & Sons.

Vogel, K. R., A. van Niekerk, R. Slingerland, and J. S. Bridge, 1992, "Routing of heterogeneous sediments over movable bed: model verification," *Journal of Hydraulic Engineering*, 118(2): 263-279.

de Vries, M., 1965, "Considerations about non-steady bed-load transport in open channels," *Proceedings*, 11th Congress, International Association for Hydraulic Research, Leningrad, International Association of Hydraulic Engineering and Research, Madrid, Spain, 381-388.

Waterways Experiment Station, 1935 "Analysis of Mississippi River bed materials," *Paper* 17, Waterways Experiment Station, U. S. Army Corps of Engineers, Vicksburg, MS.

Wathen, S. J., R. I. Ferguson, T. B. Hoey, and A. Werrity, 1995, "Unequal mobility of gravel and sand in weakly bimodal river sediments," *Water Resources Research*, 31(8): 2087-2096.

White, W. R., E. Paris and R. Bettess, 1980, "The frictional characteristics of alluvial streams: a new approach,", *Proceedings* Institution of Civil Engineers, Part 2, 69:737-750.

White, W. R. and T. J. Day, 1982, "Transport of graded gravel bed material," *Gravel-bed Rivers*, Hey, R. D, C. Thorne, and J. Bathurst, eds., John Wiley & Sons, 181-223.

Wiberg, P. L. and J. D. Smith, 1987, "Calculations of the critical shear stress for motion of uniform and heterogeneous sediments," *Water Resources Research*, 23(8): 1471-1480.

Whiting, P. J., W. E. Dietrich, L. B. Leopold, T. G. Drake, and R. L. Shreve, 1988, "Bedload sheets in heterogeneous sediment," *Geology*, 16(2): 105-108.

Whiting, P. J., 1996, "Sediment sorting over bed topography," *Advances in Fluvial Dynamics and Stratigraphy*, Carling, P. A., and M. R. Dawson, eds., John Wiley & Sons, 203-228.

Whittaker, J.G. and M. N. R. Jaeggi, 1982, Origin of step-pool systems in mountain streams, *Journal of Hydraulic Engineering*, 108(6): 758-773.

Wiberg, P. L., and J. D. Smith, 1987, "Calculations of critical shear stress for motion of uniform and heterogeneous sediments," *Water Resources Research*, 23(8): 1471-1480.

Wilcock, P. R., 1988, "Methods for estimating the critical shear stress of individual fractions in mixed-size sediment," *Water Resources Research*, 24(7): 1127-1135. ✓

Wilcock, P. R. and J. B. Southard, 1988, "Experimental study of incipient motion in mixed-size sediment," *Water Resources Research*, 24(7): 1137-1151.

Wilcock, P. R., and B. W. McArdell, 1993, "Surface based fractional rates: mobilization thresholds and partial transport of a sand-gravel sediment," *Water Resources Research*, 25(7), 1629-1641.

Wilcock, P. R., G. M. Kondolf, W. V. G. Mathews and A. F. Barta, 1996, "Specification of sediment maintenance flows for a large gravel-bed river," *Water Resources Research*, 32(9), 2911-2921.

Wilcock, P. R., 1997a, "The components of fractional transport rate," *Water Resources Research*, 33(1): 247-258.

Wilcock, P. R., 1997b, "Entrainment, displacement and transport of tracer gravels," *Earth Surface Processes and Landforms*, 22: 1125-1138.

Wilcock, P. R. and B. W. McArdell, 1997, "Partial transport of a sand/gravel sediment," *Water Resources Research*, 33(1): 235-245.

Wilcock, P. R., 1998a, "Two-fraction model of initial sediment motion in gravel-bed rivers," *Science*, 280: 410-412.

Wilcock, P. R., 1998b, "Sediment maintenance flows: feasibility and basis for prescription," *Gravel-Bed Rivers in the Environment*, Klingeman, P. C., R. L. Beschta, P. D. Komar, and J. B. Bradley, eds., Water Resources Publications, Highlands Ranch, Colorado, USA, 609-633.

Wilcock, P. R., 2000, "The flow, the bed, and the transport: Interaction in flume and field," *Proceedings*, Fifth Gravel-Bed River Workshop, M. P. Mosley, ed., Water Resources Publications, LLC, Highlands Ranch, Colorado, 183-219.

Wilcock, P. R., 2001, "Toward a practical method for estimating sediment-transport rates in gravel-bed rivers," *Earth Surface Processes and Landforms,* 26, 1395-1408.

Wilcock, P. R., Kondolf, G. M., Mathews, W. V. G. and A. F. Bartha, 1996, "Specification of sediment maintenance flows for a large gravel-bed river," *Water Resources Research*, 32(9), 2911-2921.

Wilcock, P. R., S. T. Kenworthy and J. C. Crowe, 2001, "Experimental study of the transport of mixed sand and gravel," *Water Resources Research*, 37(12), 3349-3358.

Wilcock, P. R. and S. T. Kenworthy, 2002, "A two fraction model for the transport of sand-gravel mixtures," *Water Resources Research*, 38(10), 1194-2003.

Wilcock, P. R., and J. C. Crowe, 2003, "Surface-based transport model for mixed-size sediment," *Journal of Hydraulic Engineering*, 129(2), 120-128.

Williams, G. P. and M. G. Wolman, 1984, "Downstream effects of dams on alluvial rivers," *Professional Paper* 1286, US Geological Survey, U.S. Government Printing Office, Washington, D.C., 83 p.

Williams, G. P. and D. L. Rosgen, 1989, "Measured total sediment load (suspended load and bed load) for 93 United States streams," *Open-File Report* 89-67, USGS.

Willetts, B. B., G. Pender, and I. K. McEwan, 1998, "Experiments on the transport of graded sediment," *Proceedings Institution of Civil Engineers Waterways, Maritime and Energy*, 130: 217-225.

Wolman, M. G., 1954, "A method of sampling coarse riverbed material," *Eos Transactions* American Geophysical Union, 35: 951-956.

Wright, S. and G. Parker, 2004a, "Density stratification effects in sand-bed rivers," *Journal of Hydraulic Engineering*, 130(8), 783-795.

Wright, S. and G. Parker, 2004b, "Flow resistance and suspended load in sand-bed rivers: simplified stratification model," *Journal of Hydraulic Engineering*, 130(8), 796-805.

Wu, W., S. S. Y. Wang, and Y. Jia, 2000, "Nonuniform sediment transport in alluvial rivers," *Journal of Hydraulic Research*, 38(6), 427-434.

Yamasaka, M., S. Ikeda and S. Kizaki, 1987, "Lateral sediment transport of heterogeneous bed materials," *Proceedings*, Japan Society of Civil Engineering, 387(II-8): 105-114 (in Japanese).

Yamamoto, K., 1994, *The Study of Alluvial Rivers*," Sankaidou, Tokyo, Japan (in Japanese).

Yang, C. T., 1973, "Incipient motion and sediment transport," *Journal of Hydraulic Engineering*, 99(10), 1679-1704.

Yang, C. T., 1984, Unit stream power equation for gravel," *Journal of Hydraulic Engineering*, 110(12), 1783-1797.

Yang, C. T. and S. Wan, 1991, "Comparisons of selected bed-material load formulas," *Journal of Hydraulic Engineering*, 117(8), 973-990.

Yang, C. T., 1996, *Sediment Transport Theory and Practice*, Mc-Graw Hill, 396 p.

Yatsu, E., 1955, "On the longitudinal profile of the graded river," *Transactions*, American Geophysical Union, 36: 655-663.

**Notation for Chapter 3**

$A_i$ = volume rate per unit bed area per unit time at which material is lost from gravel in the *i*th grain size range due to abrasion [$LT^{-1}$];

$A_T$ = $\sum_{i=1}^{n} A_i$ [$LT^{-1}$];

$A_{sand}$ = volume rate per unit bed area per unit time at which sand is produced by abrasion of gravel in the *i*th grain size range [$LT^{-1}$];

$A_{silt}$ = volume rate per unit bed area per unit time at which silt is produced by abrasion of gravel in the *i*th grain size range [$LT^{-1}$];

$B_{bf}$ = bank-full channel width [L];

$\hat{B}$ = $B_{bf}/D_{50}$ = dimensionless bank-full width;

$B_c$ = channel width [L];

$B_{ca}$ = adjusted channel width for sediment transport calculations [L];

$B_f$ = floodplain width [L];

$B_v$ = width of valley flat [L];

$C_f$ = $\tau_b/(\rho U^2)$ = dimensionless bed friction coefficient;

$C_{fbf}$ = dimensionless bed friction coefficient at bank-full flow;

$Cz$ = $U/u_* = C_f^{-1/2}$ = dimensionless Chezy resistance coefficient;

$Cz_{bf}$ = estimate of bank-full value of dimensionless Chezy resistance coefficient;

$C_i$ = dimensionless depth-averaged volume concentration of sediment in the *i*th grain size range in the channel flow;

$C_{fi}$ = dimensionless depth-averaged volume concentration of sediment in the *i*th grain size range in the floodplain flow;

$C_{ucfi}$ = dimensionless depth-averaged volume concentration of sediment in the *i*th grain size range in the layer of channel flow above the level of the floodplain;

$\bar{c}_i$ = local dimensionless volume concentration of suspended sediment averaged over turbulence;

$\bar{c}_T$ = $\sum_{i=1}^{n} \bar{c}_i$ = local dimensionless total volume concentration of suspended sediment;

$\bar{c}_{bi}$ = local near-bed dimensionless volume concentration of suspended sediment averaged over turbulence;

$c_{bed}$ = $= 1-\lambda_p$ = dimensionless volume concentration of sediment in the bed deposit;

$\bar{c}_{bed}$ = dimensionless layer-averaged value of $c_{bed}$

$D$ = grain size in mm [L];

$D_i$ = characteristic grain size of the *i*th size range in mm [L];

$D_x$ = grain size such that *x* percent in a sample is finer [L];

$D_{50}$ = surface median surface grain size [L];

$D_{90}$ = grain size such that 90 percent in a surface sample is finer [L];

$D_{84}$ = grain size such that 84 percent in a surface sample is finer [L];

$D_{16}$ = grain size such that 16percent in a surface sample is finer [L];

$D_{u50}$ = substrate median grain size [L];
$D_g$ = surface geometric mean grain size [L];
$D_{ug}$ = substrate geometric mean grain size [L];
$D_m$ = surface arithmetic mean grain size [L];
$D_{um}$ = substrate arithmetic mean grain size [L];
$D_{bulk60}$ = size such that 60 percent of a bulk bed sample is finer [L];
$D_\sigma$ = $D_g\sigma_g$ [L];
$D_{bi}$ = volume rate per unit bed area at which sediment in the *i*th grain size range
= is deposited from bed-load transport [$LT^{-1}$];
$D_{bi}^*$ = $D_{bi}/\sqrt{RgD_i}$ = dimensionless bed-load deposition rate;
$D_d$ = turbulent kinematic eddy viscosity [$L^2T^{-1}$];
$D_{do}$ = value of $D_d$ for unstratified flow [$L^2T^{-1}$];
$E_{bi}$ = volume rate per unit bed area at which sediment in the *i*th grain size range is entrained into bed-load transport [$LT^{-1}$];
$E_{bi}^*$ = $E_{bi}/\sqrt{RgD_i}$ = dimensionless bed-load entrainment rate;
$E_{si}$ = volume rate per unit bed area at which sediment in the *i*th grain size range is entrained into suspension [$LT^{-1}$];
$E_{si}^*$ = $E_{si}/v_{si}$ = dimensionless entrainment rate into suspension;
$\hat{E}_{si}$ = $E_{si}^*/F_i$ = dimensionless entrainment rate into suspension normalized with content in the active layer of the bed;
$F_i$ = mass fraction of surface material in the *i*th grain size range;
$F_{ai}$ = mass fraction of material in the *i*th grain size range of a surface armor;
$F_1$ = mass fraction of surface material in the first grain size range;
$F_g$ = mass fraction of the surface material that is gravel;
$F_s$ = mass fraction of the surface material that is sand;
$F_{aei}$ = $= \left(F_iD_i^{-1/2}\right)\Big/\left(\sum_{i=1}^{n} F_iD_i^{-1/2}\right)$ = mass fraction of surface material in the *i*th grain size range adjusted for exposure in computing abrasion;
$F'_{ai}$ = $= \left(F_iD_i^{-1}\right)\Big/\left(\sum_{i=1}^{n} F_iD_i^{-1}\right)$ = adjusted mass fraction of surface material in the *i*th grain size range used in the formulation of Karim (1998);
$f_i$ = local mass fraction of material in the *i*th grain size range of the substrate;
$\bar{f}_i$ = mass fraction of material in the *i*th grain size range averaged over a thick layer of substrate just below the surface layer;
$f_{bi}$ = mass fraction of material in the *i*th grain size range of the bed-load;
$<f_{bi}>$ = mass fraction of material in the *i*th grain size range of the bed-load averaged over morphology;
$f_{bG}$ = mass fraction of bed-load that consists of gravel (rather than sand);
$f_{Ii}$ mass fraction of material in the *i*th grain size range that is interchanged across the surface-substrate interface as the bed aggrades or degrades;
$Fr_{bf}$ = $U_{bf}/\sqrt{gH_{bf}}$ = dimensionless Froude number of bank-full flow;
$Fl$ = dimensionless "floodplain" number in Eq. (3.153);

$g$ = acceleration of gravity [$LT^{-2}$];
$H$ = mean channel depth [L]
$H_{bf}$ = channel bank-full depth [L];
$\hat{H}$ = $H_{bf}/D_{50}$ = dimensionless bank-full depth;
$H_f$ = depth of flow over floodplain [L];
$k_s$ = roughness height of bed [L];
$L_a$ = thickness of active (surface) layer of the bed [L];
$L_{1/2}$ = distance of travel for abrasion to halve grain size [L];
$L_{ti}$ = mean distance of travel of a tracer particle in the *i*th size range [L];
$L_{t50}$ = mean distance of travel of a tracer particle with size $D_{50}$ [L];
$n$ = one of two parameters: a) number of grain size ranges used to discretize the grain size distribution, and b) cross-channel transverse coordinate [L];
$n_a$ = $L_a / D_{90}$ = dimensionless factor for active layer thickness;
$n_k$ = $k_s / D_{90}$ = dimensionless factor for roughness height;
$n_L$ = exponent in a generic bed-load transport relation;
$p(\psi)$ = volume probability density of of size $\psi$ in a sediment sample;
$p_f(\psi)$ = cumulative probability that the fraction of sediment in a sample is less than size $\psi$;
$P_s(y)$ = probability that the instantaneous bed is higher than relative elevation $y$;
$p_e(y)$ = probability density of bed elevation fluctuations;
$Q$ = water discharge [$L^3T^{-1}$];
$Q_{bf}$ = bank-full water discharge [$L^3T^{-1}$]
$\hat{Q}_{bf}$ = $Q_{bf} / \left( \sqrt{RgD_{50}}\ D_{50}^2 \right)$ = dimensionless bank-full water discharge;
$q$ = volume transport rate of bed-load per unit width [$L^2T^{-1}$];
$q^*$ = $q / \left( \sqrt{RgD}\ D \right)$ = a dimensionless Einstein number;
$q_i$ = volume transport rate of bed-load per unit width of *ith* size range [$L^2T^{-1}$];
$q_i^*$ = $q_i / \left( F_i \sqrt{RgD}\ D \right)$ = a surface-based dimensionless Einstein number;
$q_{s,i}$ volume transport rate of bed-load per unit width in the *s* (streamwise) direction [$L^2T^{-1}$];
$q_{n,i}$ volume transport rate of bed-load per unit width in the *n* (transverse) direction [$L^2T^{-1}$];
$q_{ui}^*$ = $q_i / \left( \bar{f}_i \sqrt{RgD}\ D \right)$ = a substrate-based dimensionless Einstein number;
$q_{si}$ = volume transport rate of suspended sediment per unit width of *ith* size range [$L^2T^{-1}$];
$q_{s,i}$ = volume transport rate of bed-load per unit width of *ith* size range in the *s* (streamwise) direction [$L^2T^{-1}$];
$q_{n,i}$ = volume transport rate of bed-load per unit width of *ith* size range in the *n* (transverse) direction [$L^2T^{-1}$];
$q_{bmi}$ = $q_i + q_{si}$ = volume transport rate per unit width of bed material load in the *i*th grain size range [$L^2T^{-1}$];
$q_{bmi}^*$ = $q_{bmi} / \left( F'_{ai} \sqrt{RgD_i}\ D_i \right)$ = a dimensionless Einstein number for total bed material load;

$q_T$ = $\sum_{i=1}^{n} q_i$ = total volume bed-load transport rate per unit width [$L^2T^{-1}$];

$q_{obi}$ = volume rate per unit streamwise distance at which sediment in the *i*th size range is delivered from the channel to the floodplain [$L^2T^{-1}$];

$R$ = $(\rho_s - \rho)/\rho$ = dimensionless submerged specific gravity of sediment;

$Re_p$, = $\left(\sqrt{RgD}\ D\right)/\nu$ = a dimensionless particle Reynolds number;

$Re_{pg}$, = $\left(\sqrt{RgD_g}\ D_g\right)/\nu$ = a dimensionless particle Reynolds number;

$Re_{pug}$ = $\left(\sqrt{RgD_{ug}}\ D_{ug}\right)/\nu$ = a dimensionless particle Reynolds number;

$Re_{p50}$ = $\left(\sqrt{RgD_{50}}\ D_{50}\right)/\nu$ = a dimensionless particle Reynolds number;

$Re_{pm}$ = $\left(\sqrt{RgD_m}\ D_m\right)/\nu$ = a dimensionless particle Reynolds number;

$Re_{pi}$ = $\left(\sqrt{RgD_i}\ D_i\right)/\nu$ = a dimensionless particle Reynolds number;

$RI_g$ = dimensionless gradient Richardson number defined by Eq. (3.133b);

$S$ = dimensionless downchannel bed slope;

$S_e$ = dimensionless downchannel energy slope;

$S_f$ = dimensionless downchannel friction slope;

$s$ = downchannel streamwise coordinate [L];

$s_v$ = downvalley streamwise coordinate [L]

$t$ = time [T];

$U$ = depth-averaged or cross-sectionally averaged streamwise flow velocity [$LT^{-1}$];

$U_{bf}$ = bank-full value of $U$ [$LT^{-1}$];

$\overline{u}$ = local streamwise flow velocity averaged over turbulence [$LT^{-1}$];

$u_*$ = $\sqrt{\tau_b/\rho}$ = shear velocity [$LT^{-1}$];

$u_{*bf}$ = $\sqrt{\tau_{bbf}/\rho}$ = estimate of shear velocity at bank-full flow [$LT^{-1}$];

$u_{*s}$ = $\sqrt{\tau_{bs}/\rho}$ = shear velocity due to skin friction [$LT^{-1}$];

$V_p$ = particle volume [$L^3$];

$v_{bi}$ = mean virtual velocity of transport of the *i*th grain size [$LT^{-1}$];

$v_{si}$ = fall velocity of size $D_i$ [$LT^{-1}$];

$W^*$ = $\left(Rgq\right)/u_{*s}^3$ = a dimensionless bed-load transport rate;

$W_i^*$ = $\left(Rgq_i\right)/\left(F_i u_{*s}^3\right)$ = a dimensionless bed-load transport rate;

$W_{ui}^*$ = $\left(Rgq_i\right)/\left(\bar{f}_i u_{*s}^3\right)$ = a dimensionless bed-load transport rate;

$W_{sui}^*$ = $\left(Rgq_{si}\right)/\left(\bar{f}_i u_{*s}^3\right)$ = a dimensionless suspended load transport rate;

$W_r^*$ = dimensionless reference value of $W^*$;

$\overline{w}$ = local upward normal flow velocity averaged over turbulence [$LT^{-1}$];

$y$ = $z - \eta$ = local bed elevation relative to mean bed elevation [L];

$z$ = upward normal coordinate from the bed in the water column; vertical coordinate within the bed deposit [L];

$z_b$ = reference value of $z$ above the bed for calculations of near-bed suspended sediment concentrations [L];

$\alpha_v$ = grain volume abrasion coefficient [$L^{-1}$];
$\alpha_d$ = grain size abrasion coefficient [$L^{-1}$];
$\alpha_{di}$ = grain size abrasion coefficient for *i*th grain size range [$L^{-1}$];
$\beta$ = dimensionless coefficient in Eq. (3.118) for transverse bed-load rate
$\beta_{iD}(y)$ = dimensionless grain size-specific bias function for bed-load deposition at level *y* relative to the mean position of the bed;
$\beta_{iE}(y)$ = dimensionless grain size-specific bias function for bed-load entrainment at level *y* relative to the mean position of the bed;
$\gamma$ = exponent in power hiding relations
$\phi$ = - $\psi$; grain size on base-2 logarithmic scale;
$\eta$ = bed elevation [L];
$\eta_b$ = elevation to base of the active layer of the bed [L];
$\eta_f$ = elevation of top of floodplain [L];
$\kappa$ = 0.4; dimensionless von Karman constant;
$\lambda_p$ = dimensionless porosity of bed deposit;
$\nu$ = kinematic viscosity of water [$L^2/T$]
$\rho$ = density of water [$ML^{-3}$];
$\rho_s$ = material density of sediment [$ML^{-3}$];
$\Sigma_{sin}$ = dimensionless channel sinuosity;
$\sigma$ = arithmetic standard deviation of surface grain size distribution on $\psi$ scale;
$\sigma_u$ = arithmetic standard deviation of substrate grain size distribution on $\psi$ scale;
$\sigma_g$ = geometric standard deviation of surface grain size distribution on $\psi$ scale;
$\sigma_{ug}$ = geometric standard deviation of substrate grain size distribution on $\psi$ scale;
$\sigma_{sub}$ = subsidence rate due to tectonism or other effects [$LT^{-1}$];
$\tau_b$ = boundary shear stress at bed [$ML^{-1}T^{-2}$];
$\tau_{bs}$ = boundary shear stress due to skin friction at bed [$ML^{-1}T^{-2}$];
$\vec{\tau}_{bs}$ = $(\tau_{bs,s}, \tau_{bs,n})$ = vectorial boundary shear stress due to skin friction with components in the *s* (streamwise) and *n* (transverse) direction, respectively [$ML^{-1}T^{-2}$];
$\tau_s^*$ = $\tau_{bs}/(\rho RgD)$ = a dimensionless Shields number;
$\tau_{bbf}$ = estimate of boundary shear stress at bed at bank-full flow according to Eq. (3.14a);
$\tau_{bf\,50}^*$ = $\tau_{bbf}/(\rho RgD_{50})$ = a dimensionless Shields number;
$\tau_{50}^*$ = $\tau_b/(\rho RgD_{50})$ = a dimensionless Shields number;
$\tau_{si}^*$ = $\tau_{bs}/(\rho RgD_i)$ = a dimensionless Shields number;
$\tau_{sg}^*$ = $\tau_{bs}/(\rho RgD_g)$ = a dimensionless Shields number;
$\tau_{sm}^*$ = $\tau_{bs}/(\rho RgD_m)$ = a dimensionless Shields number;
$\tau_{s50}^*$ = $\tau_{bs}/(\rho RgD_{50})$ = a dimensionless Shields number;
$\tau_{bsci}$ = critical value of $\tau_{bs}$ for the onset of motion for the *i*th grain size [$ML^{-1}T^{-2}$];

$\tau^*_{sci}$ = $\tau_{bsci}/(\rho RgD_i)$ = a dimensionless critical Shields number;

$\tau_{bscg}$ = critical value of $\tau_{bs}$ for the onset of motion for the size $D_g$ [$ML^{-1}T^{-2}$];

$\tau^*_{scg}$ = $\tau_{bscg}/(\rho RgD_g)$ = a dimensionless critical Shields number;

$\tau_{bscm}$ = critical value of $\tau_{bs}$ for the onset of motion for the size $D_m$ [$ML^{-1}T^{-2}$];

$\tau^*_{scm}$ = $\tau_{bscm}/(\rho RgD_m)$ = a dimensionless critical Shields number;

$\tau_{bssri}$ = surface-based reference value of $\tau_{bs}$ for the size $D_i$ [$ML^{-1}T^{-2}$];

$\tau^*_{ssri}$ = $\tau_{bssri}/(\rho RgD_i)$ = a dimensionless reference Shields number;

$\tau_{bssrg}$ = surface-based reference value of $\tau_{bs}$ for the size $D_g$ [$ML^{-1}T^{-2}$];

$\tau^*_{ssrg}$ = $\tau_{bssrg}/(\rho RgD_g)$ = a dimensionless reference Shields number;

$\tau_{bssr50}$ = surface-based reference value of $\tau_{bs}$ for the size $D_{50}$ [$ML^{-1}T^{-2}$];

$\tau^*_{ssr50}$ = $\tau_{bssr50}/(\rho RgD_{50})$ = a dimensionless reference Shields number;

$\tau_{bsuci}$ = substrate-based critical value of $\tau_{bs}$ for the size $D_i$ [$ML^{-1}T^{-2}$];

$\tau^*_{suci}$ = $\tau_{bsuci}/(\rho RgD_i)$ = a dimensionless critical Shields number;

$\tau_{bsucg}$ = substrate-based critical value of $\tau_{bs}$ for the size $D_{ug}$ [$ML^{-1}T^{-2}$];

$\tau^*_{sucg}$ = $(\tau_{bsucg}/\rho RgD_{ug})$ = a dimensionless critical Shields number;

$\tau_{bsuri}$ = substrate-based reference value of $\tau_{bs}$ for the size $D_i$ [$ML^{-1}T^{-2}$];

$\tau^*_{suri}$ = $\tau_{bsuri}/(\rho RgD_i)$ = a dimensionless reference Shields number;

$\tau_{bsurg}$ = substrate-based reference value of $\tau_{bs}$ for the size $D_{ug}$ [$ML^{-1}T^{-2}$];

$\tau^*_{surg}$ = $\tau_{bsurg}/(\rho RgD_{ug})$ = a dimensionless reference Shields number;

$\tau^*_{su50}$ = $\tau_{bs}/(\rho RgD_{u50})$ = a dimensionless Shields number;

$\tau_{bsur50}$ = substrate-based reference value of $\tau_{bs}$ for the size $D_{u50}$ [$ML^{-1}T^{-2}$];

$\tau^*_{sur50}$ = $\tau_{bsur50}/(\rho RgD_{u50})$ = a dimensionless reference Shields number;

$\tau_{bsuc50}$ = substrate-based critical value of $\tau_{bs}$ for the size $D_{u50}$ [$ML^{-1}T^{-2}$];

$\tau^*_{sc50}$ = $\tau_{bsuc50}/(\rho RgD_{u50})$ = a dimensionless critical Shields number;

$\xi$ water surface stage or elevation [L]

$\psi$ = grain size on base-2 logarithmic psi scale defined by Eq. (3.1);

$\psi_m$ = arithmetic mean size of surface material on psi scale;

$\psi_i$ = *i*th bounding grain size on psi scale defining ranges in size distribution;

$\overline{\psi}_i$ = $(\psi_i + \psi_{i+1})/2$ = characteristic size on phi scale of *i*th grain size range.

**Figure Captions**

Figure 3.1 Contrasts in surface armoring between a) the River Wharfe, UK, a perennial stream with a low sediment supply (left) and b) the Nahal Yatir, Israel, an ephemeral stream with a high rate of sediment supply (right). From Powell (1998).

Figure 3.2 Sediment sorting in the presence of a dune field. Flow was from top to bottom. Image courtesy A. Blom.

Figure 3.3 Pulsations associated with experimental bed-load sheets composed of a mixture of sand and gravel. a) Alternating arrangement of three bed states. b) Fluctuation in gravel transport rate. c) Fluctuation in sand transport rate. From Iseya and Ikeda (1987).

Figure 3.4 View of the Ooi River, Japan, showing sorting of gravel and sand on bars. From Ikeda (2001).

Figure 3.5 Step-pool topography in the Hiyamizu River, Japan. Image courtesy K. Hasegawa

Figure 3.6 View of sedimentation upstream of a sediment retention dam on the North Fork Toutle River, Washington, USA. Flow is from bottom to top. From Seal and Paola (1995).

Figure 3.7 Sorted sediment patches on the North Fork Toutle River, Washington, USA: a) coarse patch on fine sediment; b) fine patch on coarse sediment. From Paola and Seal (1995).

Figure 3.8 Streaks of sorted sediment in a) a laboratory flume (from Günter, 1971; courtesy A. Müller), and b) a river (image courtesy T. Tsujimoto).

Figure 3.9 Coarse static armor (dark grains) with a partial coverage of finer, mobile sediment (light grains) on the bed of the Trinity River, California, USA. The coarse grains are rendered immobile by the presence of the Lewiston Dam upstream. Image courtesy A. Bartha. a) View of the river. b) Closeup of the bed.

Figure 3.10 a) Long profile and b) downstream change in grain size of the Kinu River, Japan, illustrating downstream fining and a gravel-sand transition. Redrafted from an original in Yatsu (1955).

Figure 3.11 Grain size distribution of 174 samples of bed sediment from rivers in Alberta, Canada. From Shaw and Kellerhals (1982).

Figure 3.12 View of a landslide that blocked the Navarro River, California., USA in 1995. Image courtesy T. Lisle.

Figure 3.13 Four sediment samples from the Ok Tedi River system, Papua New Guinea. a) 1 km downstream of the Southern Dumps of the Ok Tedi Mine, and after having passed over a high waterfall, in the Harvey Creek debris flow fan as it enters the Ok Mani; b) 8 km downstream, at the fluvial fan of the Ok Mani where it enters the Ok Tedi; c) 27 km downstream on the Ok Tedi near the junction with the Ok Menga; and d) 90 km downstream on the Ok Tedi at Ningerum Flats. Note that the grains become progressively rounder as the distance from the source increases.

Figure 3.14 Evidence of channel degradation on the Mad River, California under the Highway 101 bridge.

Figure 3.15 Bed surface median grain size downstream of Hoover Dam on the Colorado River before and after closure. From Williams and Wolman (1984).

Figure 3.16 a) View of waste rock dump site at the Ok Tedi Mine, Papua New Guinea. b) View of the gravel-bed Ok Tedi downstream of the mine. The channel bed has aggraded and widened in response to disposal of mine sediment. c) View of the sand-bed Fly River downstream of its confluence with the Ok Tedi. Aggradation of bed sediment has exacerbated both flooding and the overbank deposition of fine sediment, resulting in the loss of riparian forest.

Figure 3.17 a) Diagram illustrating the probability density and distribution functions of a unimodal sediment sample. b) Diagram illustrating the probability density and distribution functions of a bimodal sediment sample. c) Plot of probability distribution function for a sand-gravel mix with constant content density as percent finer versus logarithmic grain size $\psi$. d) Plot of the same probability distribution function versus D in mm on a linear scale.

Figure 3.18 Plot of number of reaches for which characteristic grain size is within the specified grain size range for streams in Alberta, Canada and Japan.

Figure 3.19 Diagram illustrating the definition of bank-full discharge in terms of the stage-discharge ($\xi$ - Q) relation.

Figure 3.20 Dimensionless bank-full depth $\hat{H}$ versus dimensionless bank-full discharge $\hat{Q}$.

Figure 3.21 Dimensionless bank-full width $\hat{B}$ versus dimensionless bank-full discharge $\hat{Q}$.

Figure 3.22 Channel bed slope $S$ versus dimensionless bank-full discharge $\hat{Q}$.

Figure 3.23 Dimensionless Shields number $\tau_{bf50}^{*}$ based on bank-full flow and $D_{50}$ versus dimensionless bank-full discharge $\hat{Q}$.

Figure 3.24 Dimensionless Shields number $\tau_{bf50}^*$ based on bank-full flow and $D_{50}$ versus channel bed slope $S$.

Figure 3.25 Dimensionless Chezy friction coefficient $Cz_{bf}$ versus channel bed slope $S$.

Figure 3.26 Dimensionless Chezy friction coefficient $Cz_{bf}$ versus dimensionless depth $\hat{H}$.

Figure 3.27 Froude number at bank-full flow $Fr_{bf}$ versus channel bed slope $S$.

Figure 3.28 Bank-full width-depth ratio $B/H$ versus channel bed slope $S$.

Figure 3.29 Dimensionless Shields number based on bank-full flow $\tau_{bf50}^*$ versus particle Reynolds $Re_{p50}$ number based on $D_{50}$. Also included is a point from Sagehen Creek, California, USA.

Figure 3.30 Extended version of Figure 3.29 including data from Japanese streams and the empirical regime relation of Yamamoto (1994).

Figure 3.31 Definition diagram showing a) the spatial variation of bed elevation at a given time or temporal variation of bed elevation at a given location; b) the probability density of bed elevation; c) the probability of entrainment per unit time of a grain as a function of elevation in the bed; and d) the approximation of c) embodied in the active layer approximation.

Figure 3.32 Definition diagram for the active layer concept.

Figure 3.33 Plots illustrating the use of similarity. a) Plot of $W_i^*$ versus $\tau_{si}^*$ for a case for which similarity collapse is realized. b) Similarity plot of the data of the figure to the left which results in a perfect collapse. c) Plot of $W_i^*$ versus $\tau_{si}^*$ for a case for which similarity collapse is not realized. d) Similarity plot of the data of the figure to the left does not results in a collapse.

Figure 3.34 Plot of critical Shields number versus particle Reynolds number showing a) the Brownlie (1981) fit to the original Shields (1936) curve, b) the modified Brownlie fit of Eq. (3.71), c) the data of Buffington and Montgomery (1997) pertaining to $\tau_{cv50m}^*$ and d) the gravel-bed rivers of Figure 3.29.

Figure 3.35 Plots of a) hiding function obtained from Egiazaroff relation, the modified Egiazaroff relation, the condition of size-independence, the condition of equal-threshold, and the power relations of Eqs. (3.74a,b) using $\gamma_{subref} = 0.81$, $\gamma_{surfref} = 0.90$ and $\gamma_{surflarg} = 0.72$; and b) reduced hiding functions corresponding to a) above.

Figure 3.36 Plots of the functions $\sigma_O(\phi_{sgo})$ and $\omega_O(\phi_{sgo})$ for the Parker (1990a) relation.

Figure 3.37 Plot of $D_u/D_{50}$ as a function of $\tau_{50}^*$ for the hiding function of Proffitt and Sutherland (1983) as applied to the sediment transport relation of Ackers and White (1973).

Figure 3.38 Predictions of bed-load transport using the relations of Ashida and Michiue (1972) (A-M), Parker (1990a) (P(S)), Powell et al. (2001) (P-R-L), Hunziker and Jaeggi (2002) (H-J) and Wilcock and Crowe (2003) (W-C). a) Grain size distributions for bed-load calculations, b) total gravel bed-load transport rate, c) geometric mean size of gravel bed-load, d) gravel geometric standard deviation of gravel bed-load, and e) fraction of gravel in bed-load (the rest being sand).

Figure 3.39 Plots of $q_i/F_i$ versus $D_i$ for a) Oak Creek field data as presented by Wilcock (1997a); b) experiments of Wilcock and McArdell (1997); and c) Nahal Eshtemoa field data of Powell et al. (2001).

Figure 3.40 Dimensionless Einstein number based on total bed-load transport rate $q_T^*$ versus Shields number $\tau_{50}^*$ for six streams: Goodwin Creek, Mississippi, USA, East Fork River, Wyoming, USA, Oak Creek, Oregon, USA, Nahal Yatir, Israel, Turkey Brook, England, UK and Torlesse Stream, New Zealand. From Reid et al., (1995).

Figure 3.41 Abrasion coefficients $\alpha_d$ obtained from experiments by various researchers, as presented by Kodama (1994a).

Figure 3.42 Definition diagram for in-channel and overbank flow in a river.

Figure 3.43 Evolution of stone cells on the bed surface of a laboratory flume as the bed evolves in response to the cutoff of sediment supply, as observed by Hassan and Church (2000). Hassan and Church also document the presence of these cells in the case of an equilibrium mobile-bed armor; the higher the sediment transport rate, the less developed are the cells.

Figure 3.44 Figure 3.44 Examples of comparisons of a numerical model of evolution to static armor versus experimental data from a laboratory flume, in which x denotes distance downstream; from Tsujimoto (1999).

Figure 3.45 Conceptual diagram illustrating the evolution of a static armor from equilibrium mobile-bed conditions as the sediment feed rate is repeatedly halved.

Figure 3.46 Flash flood in the ephemeral Nahal Eshtemoa, Israel: a) arrival of the flood wave (looking upstream); and b) passage of the flood wave (looking downstream). Images courtesy J. Laronne.

Figure 3.47 a) Predicted variation of the ratios $D_g/D_{bg}$ and $D_{50}/D_{b50}$ in $\tau_{50}^*$, along with a bank-full value of $\tau_{50}^*$ for Sagehen Creek and two values of $\tau_{50}^*$ for the Nahal Yatir that bracket most of the bed-load data. b) Assumed normalized grain size distribution for

bed-load, along with predicted grain size distributions for static armor and mobile armor at the values of $\tau_{50}^*$ shown in the legend.

Figure 3.48 Normalized mean annual bed-load (solid circles) and substrate (solid squares) grain size distributions for 14 gravel-bed rivers studied by Lisle (1995). The grain size distributions have been truncated at 1 mm. The hollow circles and squares pertain to fractions in each range.

Figure 3.49 Illustration of various aspects of downstream fining in the Red Deer River, Alberta, Canada. a) Long profile of the Red Deer River. b) Downstream variation in $D_{50}$ and $D_{90}$ in the Red Deer River. c) Downstream variation in three lithologies in the Red Deer River. From Shaw and Kellerhals (1982).

Figure 3.50 Illustration of downstream fining in the Allt Dubhaig, Scotland, UK, showing the long profile of the river (top) and grain size distributions of bulk surface samples taken at various points down the stream (bottom). From Ferguson et al (1996).

Figure 3.51 Illustration of downstream fining produced in a laboratory channel; in Run 5 of Toro-Escobar et al. (2000). The channel width is 2.7 m. a) The upstream 20 m of the deposit. b) The downstream 20 m of the deposit. Flow was from top to bottom.

Figure 3.52 Side view of step-pool topography formed in the laboratory. Image courtesy K. Hasegawa.

Figure 3.53 Downstream fining in the Mississippi River, USA. a) Downstream variation in grain size distribution. b) Downstream variation in mean grain size.

Figure 3.54 Downstream variation in $D_{50}$ and $D_{90}$ in the middle Fly River, Papua New Guinea in 1979, before the opening of the Ok Tedi copper mine in 1985.

Figure 3.55 View of the floodplain of the Minnesota River, Minnesota, USA during the flood of record in 1965.

Figure 3.56 a) View of a reach of Silver Bow Creek, Montana, USA in which the floodplain is so rich in toxic sediments that vegetation cannot take hold. The toxic sediment is derived from the Anaconda copper mine near Butte, Montana; the flood that deposited the sediment occurred in 1910. b) View of an uncontaminated, healthy tributary of Silver Bow Creek.

Figure 3.57 Diagram illustrating floodplain deposition.

Figure 3.58 Relative travel distance of tracers in each size class as a function of relative grain size. From Ferguson and Wathen (1998).

Figure 3.59 Diagram illustrating the use of "Leopold" scour chains to measure scour and fill associated with a flood. From Haschenburger (1999).

Figure 3.60 Schematization of the pattern of vertical sorting generated by the successive passage of dunes over a bed of heterogeneous sediment.

Figure 3.61 a) Experimental dunes. b) $P_s(y)$ as a function of $y$ for the bed of part a). c) Pattern of stratification and sorting created by the passage of dunes in the flume illustrated in part a). From Parker et al. (2000).